THE UNIVERSITY
of EDINBURGH

THE UNIVERSITY
of EDINBURGH

A Role for Autophagy in Oncogenic Cell Signalling and Glioblastoma Multiforme

Jane Elizabeth Fraser

Thesis submitted for the degree of Doctor of Philosophy

The University of Edinburgh

2018

1 Contents

2 List of Figures and Tables

3 Abstract

The catabolic process of macroautophagy occurs constitutively in eukaryotic cells at a basal level and can become upregulated during periods of stress to recycle nutrients and promote cell survival. The role of this process in disease states is starting to be explored, particularly in cancers where the rapid growth and proliferation of cells generates a stressful environment. During the course of this study I investigated the role of autophagy in the aggressive brain cancer glioblastoma multiforme (GBM), focussing on the regulation of cellular signalling pathways that are known to drive oncogenesis. Specifically, I find that autophagy is required for tumour formation in an *in vivo* $KRas^{G12D}$-driven mouse model of GBM, correlating *in vitro* with the suppression of senescence and stimulation of pro-growth signalling pathways. Additionally, autophagy is seen to promote anchorage-independent growth in a panel of cell line models of GBM, as well as being required for maintenance of cell signalling activities upon anchorage loss. Further exploration of cellular signalling activities revealed that the knockout of autophagy gene expression significantly reduces ligand-induced signalling from receptor tyrosine kinases, such as the epidermal growth factor receptor (EGFR), which is frequently mutated in GBM. The endocytic trafficking of EGFR is found to be perturbed in autophagy-deficient cells, with the receptor accumulating in early endosomes rather than maturing into recycling endosomes and returning back to the plasma membrane for renewed activation. Mechanistically, autophagy players localise to endosomal structures, which appear morphologically disrupted upon loss of autophagy gene expression, thereby suggesting that autophagy may directly regulate endosomal homeostasis. Together, these results support a role for autophagy in facilitating the oncogenic cell signalling that drives GBM.

4 Lay Summary

Glioblastoma multiforme is a particularly aggressive brain cancer with a poor prognosis for patients. To develop better therapies there is an urgent need to understand more about the basic biology of these tumours. Previous work has shown that the aberrations that generate tumours increase the activity of signals in the cell that induce their uncontrollable division. Here we find that autophagy (literally meaning 'self eating'), a process traditionally believed to simply be a way to break down and recycle unwanted cell components, has a novel function of regulating these tumour-associated signals. Our findings demonstrate that autophagy is required for glioblastoma tumour formation in mice by maintaining the ability of cells to divide. Further investigations reveal that autophagy aids the proper movement of growth messages through the cell, which enhances their potency. If this knowledge can be utilised to halt tumourigenic signals then it may be possible to attack an Achilles heel of glioblastoma multiforme.

5 Acknowledgements

I would like to first and foremost thank my supervisor, Dr Noor Gammoh, for all her hard work; from helping me develop my hypotheses and supporting my experiments, to guiding me through writing my thesis. I sincerely appreciate your patience and faith in me.

Furthermore, I owe so much of the success of this work to my fellow group members, in particular Ainara González-Cabodevilla who has been with me every step of the way. Thank you.

To Gabi, Abby, and Zoe: thank you for helping my laugh my way through every day of these four years. It has been a blast!

Finally, I need to thank my parents and grandparents who have been a source of unwavering encouragement. I could never have done this without them.

6 Declaration

I declare that this thesis has been composed by myself and describes my own research unless where acknowledged in the text. No part of this thesis has been submitted for any other degree or professional qualification.

Signed…… Date…….

Jane Elizabeth Fraser

7 Abbreviations

3-MA	3-Methyladenine
AP-2	Adaptor protein 2
APPL1	Adaptor protein phosphotyrosine-interacting with PH domain and leucine zipper
ATG	Autophagy-related
BafA1	Bafilomycin A1
BSA	Bovine serum albumin
CDKN	Cyclin-dependent kinase inhibitor
CIE	Clathrin-independent endocytosis
CME	Clathrin-mediated endocytosis
CSC	Cancer stem cell
DAPI	4',6'-diamidino-2-phenylindole
DMEM	Dulbecco's modified Eagle's media
EEA1	Early endosome antigen 1
ECM	Extracellular matrix
EGF(R)	Epidermal growth factor (receptor)
ER	Endoplasmic reticulum
ErbB	Erythroblastic oncogene B
ERK	Extracellular signal-related kinase
ESCRT	Endosomal sorting complexes required for transport
FBS	Foetal bovine serum
FIP200	FAK-interacting protein of 200kDa
FGF(R)	Fibroblast growth factor (receptor)
Gal	Galectin
GAP	GTPase-activating protein
GBM	Glioblastoma multiforme
GEF	GTPase-effector protein
Grb2	Growth factor receptor bound 2
GTPase	Guanosine triphosphatase
HCQ	Hydroxychloroquine
HER2	Human epidermal growth factor receptor 2
HGF	Hepatocyte growth factor

hr	Hour
IF	Immunofluorescence
IL	Interleukin
IRS1	Insulin receptor substrate 1
IGF-1(R)	Insulin growth factor-1 (receptor)
KRas	Kirsten Ras
LAMP	Lysosomal-associated membrane proteins
LC3	Microtubule-associated protein 1A/1B-light chain 3
MAPK	Mitogen-activated protein kinase
min	Minute
mTOR(C1,C2)	Mammalian target of rapamycin (complex 1, complex2)
MVB	Multivesicular body
NDP52	Nuclear dot protein 52
NF-1	Neurofibromin 1
OIS	Oncogene-induced senescence
OPTN	Optineurin
PDK1	Protein-dependent kinase 1
PE	Phosphatidylethanolamine
PI	Propidium iodide
PI(3)P	Phosphatidylinositol-3-phosphate
PI3KC3	Phosphatidylinositol-3-kinase catalytic subunit type 3
pRb	Retinoblastoma protein
RCAS/*tv-a*	Replication-competent avian Sarcoma-leukosis LRT splice acceptor/*tumour virus A*
ROS	Reactive oxygen species
RTK	Receptor tyrosine kinase
SASP	Senescence-associated secretory phenotype
SEM	Standard error of the mean
sgRNA	Single guide RNA
siRNA	Small intefering RNA
SOS	Son-of-sevenless
STAT	Signal transducer and activator of transcription
TBC	Tre2-Bub2-Cdc16
TBK1	TANK-binding kinase 1

Tfn(R)	Transferrin (receptor)
Tp53	Tumour protein 53
ULK1	UNC51-like serine/threonine kinase 1
UVRAG	UV radiation resistance-associated gene
VEGF(R)	Vascular endothelial growth factor (receptor)
WIPI2	WD repeat domain phosphoinositide interacting 2
WT	Wild type

8 Introduction

8.1 The Autophagy Pathway

First coined by Christian de Duve fifty-five years ago, the term 'autophagy' finds its roots in Greek, roughly translating as 'self-eating'[1]. Since then, it has been revealed that autophagy can have far-reaching impacts on different organelles and cellular pathways and is finely tuned by a vast array of signals to tailor its rate to the specific needs of the cell. Several different modes of autophagy are known, although as much of the field focuses on macroautophagy this process has become synonymous as autophagy. Macroautophagy is the process of encapsulation of cellular components, such as proteins and organelles, in double-membrane vesicular structures, called autophagosomes, which can then fuse with the lysosome where the contents are degraded. Other forms include microautophagy (direct uptake of materials into the lysosome via membrane invaginations) and chaperone-mediated autophagy (assisted translocation of proteins through the lysosomal membrane)[2,3]. During the course of this study, I have focussed on the process of macroautophagy, which I shall hereafter refer to as autophagy.

On the organism level, autophagy has been seen to be critical during development and for tissue homeostasis, whilst its deregulation has been associated with a myriad of different pathologies. Mice deficient in autophagy cannot survive long after birth and loss of autophagy selectively in neurons results in the early onset of neurodegenerative disease[4–6]. Indeed, numerous studies of the the role of autophagy in neurodegeneration have suggested its function may be instrumental in preventing this disease[5]. Furthermore, a wealth of research has also focussed on the influence of autophagy on cancer, although the results are seemingly conflicting and certainly context-dependent[7]. To make sense of the findings from mouse models, however, we must look at the cellular level. Therefore, I shall begin by introducing the molecular machineries that mediate the process of autophagy.

8.1.1 Pathway Overview

Much of what is currently known regarding the essential components of autophagy was uncovered in a series of studies in yeast, with the earliest elegant experiments performed by Yoshinori Ohsumi, earning him the 2016 Nobel Prize for Medicine and Physiology[8–10]. He established that the products of autophagy-related (ATG) genes

co-ordinate a series of events that generate an autophagosome. Fortunately, autophagy is well conserved between yeast and mammalian cells and therefore much of this knowledge has been transferred between eukaryotes. Here I shall summarise what is known regarding key regulators of the mammalian autophagy pathway (Figure 8.1).

Autophagy occurs constitutively in cells but can be upregulated in situations of stress, such as amino acid depletion or low oxygen levels. The signals that sense these stressors are co-ordinated by the upstream UNC51 like serine/threonine kinase (ULK1) and phosphatidylinositol-3-kinase catalytic subunit type 3 (PIK3C3) complexes to stimulate autophagy.

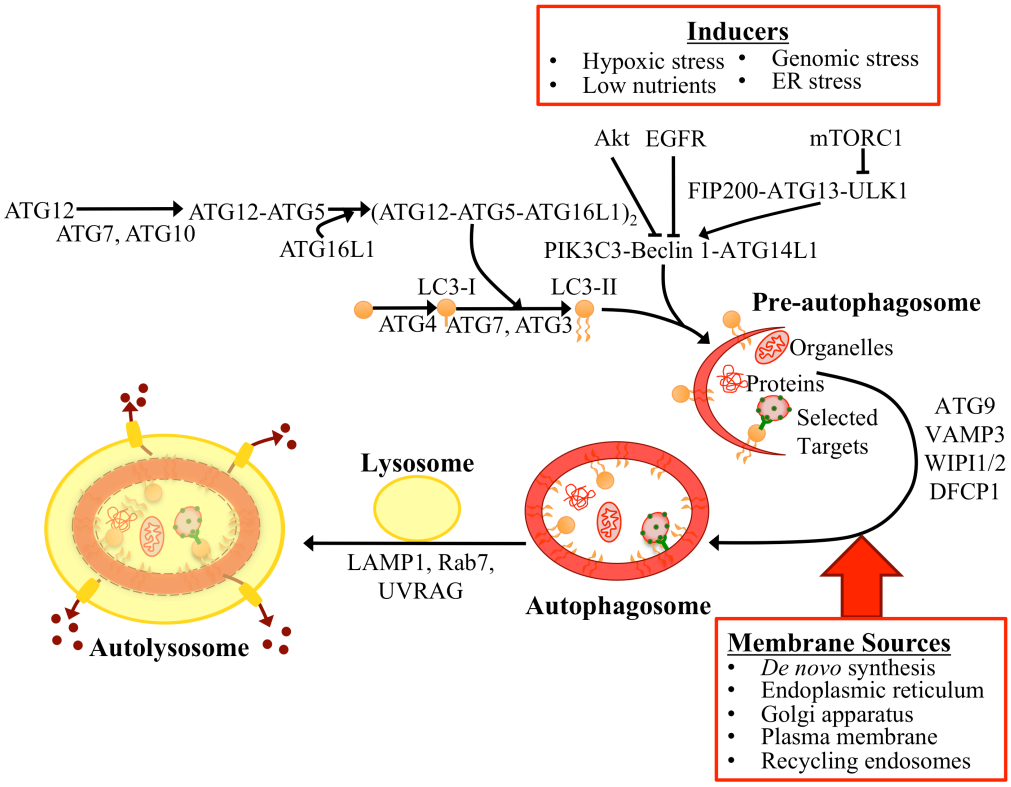

Figure 8.1 Overview of the Autophagy Pathway
ATG proteins catalyse the production of phosphatidylinositol-3-phosphate and the conjugation of LC3 to phosphatidylethanolamine. This facilitates the production of the pre-autophagosomal membrane that encapsulates cellular components. Following a membrane expansion step, the fully formed autophagosome vesicle can fuse with the lysosome, where contents are then degraded and recycled back into the cell.

These complexes can cross-activate each other by a series of post-translational modifications and result in the production of phosphatidylinositol-3-phosphate (PI(3)P), a lipid essential to recruit downstream autophagy players (as described in more detail section 8.1.3). Additionally, the mammalian ATG8 family members (gamma-aminobutyric acid receptor-associated proteins (GABARAP, GABARAPL1, and GABARAPL2) and microtubule-associated protein 1A/1B-light chain 3 proteins

(LC3A, LC3B, and LC3C)) are prepared for conjugation to the lipid phosphatidylethanolamine (PE) through proteolytic cleavage by ATG4 cysteine protease family members, which exposes a glycine at their C-termini. By pairing with ATG10, ATG7 can catalyse the ubiquitin-like conjugation of ATG12 to ATG5, which then binds to each molecule in a homodimer of ATG16L1, thereby producing the $(ATG12\text{-}ATG5\text{-}ATG16L1)_2$ complex. Next, ATG7 can function alongside ATG3 and the $(ATG12\text{-}ATG5\text{-}ATG16L1)_2$ complex to facilitate the enzymatic addition of ATG8 proteins to PE[11].

Following these initiation steps, $ATG8^{+}/PI(3)P^{+}$ membranes then undergo an expansion step enabled by membrane contributions from several sources. Electron microscopy has revealed that a wide variety of organelles can undergo some form of contact with autophagosomes, and therefore could be sources of membrane for autophagosome biogenesis[12]. However, the best-established site for autophagosome biogenesis is the 'omegasome' cradle that is formed by a highly curved branch from the endoplasmic reticulum (ER)[13]. Following completion of this expansion step, the fully formed autophagosome can then undergo fusion with the lysosome, where acidic hydrolases degrade the autophagosomal contents. In this manner, autophagosomes can act as shuttles to the lysosome.

8.1.2 The ULK1 Complex: Mediation of Autophagy by mTORC1 Signalling

The mammalian target of rapamycin complexes 1 and 2 (mTORC1 and mTORC2) are considered 'master regulators' of anabolic metabolism. mTORC1 is composed of mTOR, mLST8, and Raptor, whilst mTORC2 contains mTOR, mLST8, mSIN1, and Rictor[14]. mTORC1 can sense oxygen tension, mitogenic signalling, and the abundance of nutrients, such as amino acids, and subsequently co-ordinates the rates of synthetic and degradation processes according to the available resources[14,15]. For example, relinquishment of mTORC1-mediated inhibition ULK complex is required for the upregulation of autophagy during times of hypoxia or amino acid depletion[16]. ULK, originally identified in yeast as Atg1, functions in a complex consisting of: ATG13, FAK family kinase-Interacting Protein of 200 kDa (FIP200), ATG101, and a ULK family member (of which, ULK1 and ULK2 are apparently functionally redundant)[17]. Several reports concurrently described the regulation of this complex by mTORC1, which occurs via several residues on ULK1 and ATG13 that are targeted by the kinase activity of mTORC1[16,18,19]. Furthermore, mTORC1 prevents the TNF

receptor-associated factor 6 (TRAF6)-mediated addition of Lys^{63} ubiquitin chains to ULK1 by disrupting the autophagy and Beclin-1 regulator 1 (AMBRA1)-TRAF6 complex, thereby resulting in the destabilisation of ULK1.

It has been uncovered that mTORC1 is activated on the lysosomal membrane, in a mechanism that is mediated by the v-ATPase and the amino acid sensors Sestrin2, CASTOR1, and SLC38A9, as well as activation from Rheb and Rags 1 and 2, which are responsive to nutrient levels[15,20–22]. It is currently a point of active research how the mTOR complexes are spatially and temporally co-ordinated with downstream targets that are not themselves localised on the lysosome, such as ULK1[18,23,24].

The mechanism by which the ULK complex initiates autophagy is becoming increasingly understood. For example, studies have found that the complex that catalyses PI(3)P production at pre-autophagosomes, PIK3C3, is one of the targets for this kinase .

8.1.3 The PIK3C3 Complex: An Intersection for Autophagy Regulation

The core components of the PIK3C3 complexes are PIK3C3, also known as vacuolar protein sorting 34 (VPS34) (often used synonymously to refer to the holoenzyme), VPS15, and Beclin-1[25]. For its activity at autophagosomes it complexes with ATG14L1 (complex 1), whereas at endosomes it associates with UVRAG (complex 2)[25]. PIK3C3 can generate PI(3)P either on endosomal membranes or at sites of autophagosome biogenesis on the ER, such as at ER-mitochondria contact sites, by phosphorylating phosphoinositol (PI)[13,26,27]. Interestingly, the endocytic and autophagic PIK3C3 complexes have differing abilities to act on vesicles of different sizes: whilst both can act on smaller, more curved vesicles, only the endocytosis-specific complex can phosphorylate PI on less curved vesicles corresponding to the larger size of endosomes relative to pre-autophagosomal/omegasomal structures[28].

PI(3)P is essential for the formation of the autophagosome. Following the activity of PIK3C3 complex 1, downstream autophagy effectors are then recruited to PI(3)P, such as double-FYVE-containing protein 1 (DFCP1) and WD-repeat protein interacting with phosphoinoside family member 2 (WIPI2) [13,29,30]. Although current understanding of the process suggests that this primarily occurs from omegasome cradles at the ER, other membrane structures have also been seen to be involved in autophagosome nucleation[13,24,31,32]. The duality of PIK3C3 in these different complexes presents an opportunity to induce autophagy and endocytosis distinctly

according to upstream cues, such as mitogenic signalling (explored in greater detail in section 8.2.4)[33].

8.1.4 Regulation of LC3 Lipidation and Autophagosome Maturation

Once the ULK and PIK3C3 complexes have been stimulated to set the scene, LC3 lipidation is then undertaken. The conjugation of LC3/GABARAP proteins to the lipid PE is generally considered the hallmark of autophagosome formation. Therefore, autophagosome biogenesis relies not only on stimulation of the function of upstream players but also requires the activation of enzymes that facilitate the lipidation of LC3/GABARAP family proteins. As I frequently ablate the expression of players that mediate the lipidation of LC3B in the course of this study, here I shall describe what has been gleaned from studies that have primarily focussed on that isoform.

Parallels have been drawn between LC3 lipidation and the system of enzymes that catalyse the conjugation of ubiquitin to its targets. In autophagy, the enzymes that catalyse the conjugation of the ubiquitin-like ATG12 and LC3/GABARAP proteins to targets are comparable to E1, E2, and E3 ubiquitination enzymes. The regulation of this lipidation process is explored below.

8.1.4.1 Preparation of LC3

Lipidation of LC3B can only occur once the 22 amino acids from the C-terminus of pro-LC3B are cleaved off by an ATG4 family member, generating 'LC3-I', which exposes a glycine for conjugation to PE[34]. Current evidence suggests that there is some degree of redundancy between ATG4 A, B, C, and D isoforms, with ATG4B being the most broad-acting catalyst across the LC3/GABARAP families[35]. Additionally, ATG4 can catalyse LC3B deconjugation and so, when overexpressed, it can inhibit autophagosome formation[36,37]. Therefore, ATG4 has the intriguing ability to both promote and inhibit autophagic flux.

Post-translational modifications can modulate the activity of this protease. Firstly, oxidative conditions, sensed by a reactive cysteine residue at position 81, are required for ATG4 activity, whilst reducing conditions can inhibit the protein via a key disulphide bond between cysteines 338 and 394[38,39]. Therefore, oxidising conditions promote ATG4 function and autophagic flux. Furthermore, a recent paper has revealed that ATG4 is also modulated by the phosphorylation of serine 383 by Golgi resident protein mammalian STE20-like protein kinase 4 (MST4), which promotes its

activity[40]. These reports demonstrate that autophagosome biogenesis can be regulated by the cellular status at several different points, right down to the final catalytic steps.

8.1.4.2 The Lipidation of LC3

The lipidation of LC3 requires the same E1-like function of ATG7 at two distinct steps: it catalyses the link between ATG3 and the glycine in LC3-I as well as facilitating the coupling of ATG12 to ATG5, which binds ATG16L1.

The $(ATG12\text{-}ATG5\text{-}ATG16L1)_2$ complex can be recruited to PI(3)P-positive WIPI2-labelled pre-autophagosomal structures via interactions between ATG16L1 and WIPI2 as well as FIP200[29,41]. ATG12 can then recruit ATG3 to catalyse the bond between LC3 and PE, producing LC3-II, which facilitates the closure of the autophagosome. This step may be regulated by the physical properties ATG3 itself, which preferentially binds to highly curved membranes of the pre-autophagosome lipid bilayer[42].

Interestingly, ATG16L1 is dispensable for LC3 lipidation *in vitro* but is required in cells, thereby suggesting that ATG16L1 is required for targeting of the ATG12-ATG5 to pre-autophagosomal structures in the cell[43]. Although it has been reported that the localisation of ATG16L1 at pre-autophagosomes requires clathrin-mediated endocytosis from the plasma membrane, the molecular mechanism that mediates its trafficking is unknown[44]. Indeed, even the subcellular localisation of ATG16L1 is currently under dispute (see section 8.2.3.3).

Regulation of the LC3 lipidation machinery is suggested by observations that although ATG7 constitutively catalyses the formation of ATG12-ATG5 complexes in the cytoplasm, the conjugation of LC3 to PE occurs in a highly selective and controlled manner specifically at sites of autophagosome formation. This implies that either re-localisation or activation of these players must occur upon autophagy induction. Furthermore, whilst it is known that PI(3)P is important for the recruitment of upstream players, such as WIPI2, that then bind members of the LC3 lipidation machinery, it is not currently understood how certain PI(3)P pools are specified for autophagy. The majority of PI(3)P in the cell is found at early endosomes and yet it is a specific ER-localised PI(3)P pool that is generally believed to be responsible for the initiation of autophagy[13]. It is unknown how this spatial selectivity is achieved. These are exciting questions in the autophagy field, the answers to which may be enlightening in the search for a specific autophagy inhibitor.

8.1.4.3 Formation of the Autolysosome

Following its completion, the autophagosome is delivered to the lysosome, generating the autolysosome, where acidic hydrolases degrade its contents. Microtubule networks regulate trafficking to facilitate sorting nexin 17 (SNX17)/soluble n-ethylmaleimide sensitive factor attachment protein 29 (SNAP29)/vesicle associated membrane protein 8 (VAMP8)-regulated fusion of autophagosomal and lysosomal membranes[45,46]. Although this process is still incompletely understood, it is known that fusion requires the activity of the late endosomal regulator Rab7. Rab7 is regulated by its corresponding guanine nucleotide exchange factor (GEF) Mon1-Ccz1, as well as the homotypic vacuole fusion and protein sorting (HOPS) complex[47,48]. Further investigation has revealed that Pleckstrin homology domain containing protein family member 1 (PLEKHM1) plays a key role in this process by bringing LC3-containing structures into contact with the HOPS complex, Rab7, and SNX17[49]. It seems, therefore, that autophagosome-lysosome fusion involves many of the same players and regulators that are required in the endolysosomal pathway.

In addition to its role early in autophagosome biogenesis, ATG14L1 is also required for the final step of autophagosome-lysosome fusion, with homodimers of the protein engaging SNX17/SNARE19/VAMP8[50]. Furthermore, ATG14L1 facilitates production of the lipid PI(4,5)P_2 by type Iγ phosphatidylinositol phosphate kinase i5 (PIPKIγi5) at the interface between the ER and late endosomes[51]. This has the dual function of firstly significantly stabilising the PIK3C3 complex 1 and secondarily promoting fusion of autophagosomes with the lysosome by facilitating PI(4,5)P_2 production. Therefore, ATG14L1 has been seen to be key at both the very early embryonic stages of autophagosome biogenesis and the final fusion step with the lysosome to instigate degradation.

Intriguingly, a recent study from the Mizushima group observed that although LC3 lipid conjugation vastly increases the efficiency of degradation of autophagosomal structures, it is not strictly required for the process to occur[52]. This is indeed logical in terms of reaction kinetics and it demonstrates that LC3 lipidation is not necessarily the complete story of autophagy.

8.1.5 Specific Cargoes Are Targeted by Autophagy

For many years autophagy was thought to capture largely random sections of the cytoplasm and deliver them to the lysosome to regenerate cellular building blocks

under conditions of stress[53]. However, a considerable amount of recent evidence has revealed that autophagy actually utilises targeted cargo receptors to ensnare specific cargo. Some of these targeting mechanisms are outlined here.

8.1.5.1 Xenophagy

Autophagy targets can be marked out for degradation by post-translational modifications, such as ubiquitination. Ubiquitin-binding autophagy receptors such as sequestosome 1 (SQSTM1)/p62, nuclear dot protein 52 (NDP52), and Optineurin (OPTN) then recognise ubiquitinated cargoes and link them to the autophagy machinery[54–56].

These cargoes include bacteria, which are cleared from cytosolic and endosomal compartments of cells as part of the innate immune response to limit infection, in a process called xenophagy. Bacteria, such as *Shigella*, *Salmonella*, and *Listeria*, trigger the activation of nucleotide-binding oligomerisation domain (NOD)-like receptors and Toll-like receptors (TLRs) by recognition of pathogen-associated molecular patterns (PAMPs)[54,56,57]. The bacterium is then labelled with ubiquitin, which can be recognised by the autophagy machinery. In one example, ubiquitinated *Salmonella* is recognised by OPTN[56]. TANK-binding kinase 1 (TBK1), which is activated by TLR signalling, then phosphorylates OPTN and induces its binding to LC3 thereby facilitating the entrapment of the bacterium in the autophagosome.

The targeting of vesicular-resident bacteria for autophagic degradation is mediated upstream by galectins. Galectins are a family of proteins that recognise modified sugars found either on bacterial coats or on the inner face of endosomal membranes, which are exposed upon disruption of endomembranes by bacteria. Although galectins-3, -8, and -9 have all been described to localise to vesicles harbouring the *Salmonella* bacterium, galectin-8 is believed to be the primary means by which this bacterium is cleared[58]. This is mediated by the binding of galectin-8 to NDP52, which then binds LC3 on the autophagosome surrounding the bacterium. Interestingly, LC3C is the only Atg8 family member that can bind NDP52 and therefore may play a central role in xenophagy and immunity[59].

8.1.5.2 Organellar Autophagy

Due to common upstream autophagic targeting mechanisms, selective removal of the mitochondria by autophagy may parallel the clearance of bacteria during xenophagy. This is intriguing considering that current research suggests that both bacteria and

mitochondria evolved from similar prokaryotic ancestors. However, unlike xenophagy, 'mitophagy' is generally believed to maintain the health of the mitochondrial network rather than destroying it. Disruption of autophagy leads to the accumulation of damaged mitochondria that can leak reactive oxygen species causing significant damage to other cellular components, such as lipids, proteins, and DNA[60]. As a result, loss of mitophagy may promote mutagenesis, altered metabolism, or cell death.

Although it is now recognised that alternative mitophagy mechanisms may exist under basal conditions, inducing damage experimentally has revealed that a PINK1/Parkin-mediated process can target mitochondria for degradation by autophagy. Firstly, following depolarisation of its membrane, the ubiquitin kinase PINK1 binds to the mitochondrion[61]. The E3 ubiquitin ligase Parkin is then recruited and phosphorylated by PINK1. Parkin subsequently assembles ubiquitin chains on a variety of mitochondrial outer membrane proteins, which are themselves then subjected to phosphorylation by PINK1 at serine 65. These phospho-ubiquitin chains enhance Parkin binding and activity at the mitochondria, thereby acting as part of a positive feedback loop. TBK1 then acts in concert with OPTN, NDP52, and p62 to recognise phospho-ubiquitin, recruit LC3, and facilitate the sequestration of the mitochondrion into an autophagosome[55,61]. Defects in this process have been strongly linked to pathologies, such as Parkinson's disease and amyotrophic lateral sclerosis (ALS), although the precise causes and molecular mechanisms are still currently unknown[61,62].

Mitochondria are not the only organelle to be selectively degraded by autophagy, however; lysosomes, ribosomes, and the endoplasmic reticulum have all been shown to be targeted to autophagosomes. For example, leaking lysosomes can be cleared by autophagy to prevent the exposure of the cell to acidic conditions, cathepsins, and other such hydrolases[63–65]. These damaged membranes are recognised by galectins and are enriched in ubiquitin and p62[65]. Removal of such endo-lysosomal damage not only maintains lysosomal homeostasis to protect against cell death but also helps defend against invading pathogens that propagate in the lysosome[65,66].

Similarly, exciting data from the Sabatini group has shown that 'ribophagy' is also required for cell survival. This is facilitated by the recruitment of LC3B to ribosomes upon amino acid starvation by the cargo receptor nuclear fragile X mental retardation-interacting protein 1 (NUFIP1)[67]. The selective degradation of ribosomes during

starvation replenishes pools of arginine, lysine, and nucleosides in the cell. However, it is not currently known which cues induce the localisation of NUFIP1 to ribosomes upon amino acid depletion. It is possible that it is not an ubiquitin-mediated process, however, as these are not damaged or aberrant structures being degraded, but rather normal healthy organelles.

Additionally, further to its role in generating the omegasome autophagosome precursor, the ER network can itself be targeted by autophagy. The ER-resident proteins FAM134B, SEC62, cell cycle progression gene 1 (CCPG1), and reticulon 3 (RTN3) can act as receptors that mediate the degradation of the ER by binding to components of the autophagy machinery, including LC3B and FIP200[68–70]. In this way, 'ER-phagy' can conserve the gross structure and function of the organelle, as well as hastening the resolution of ER stress to maintain cell homeostasis. This is an emerging field and it is intriguing to consider what other key ER functions may rely its autophagic turnover.

8.1.5.3 Specific Proteins Can Be Targeted By Autophagy

In addition to organelles, specific proteins can also be targeted to autophagosomes for degradation. In this regard autophagy works hand-in-hand with the proteasome to mediate the degradation of ubiquitinated proteins. Some diverse examples of proteins that are degraded by autophagy include the tyrosine kinase Src, the naïve cytokine pro-interleukin (IL)-1β, and the redox regulator Keap1[71–73].

However, it is still unclear whether many other proteins could actually be regulated by autophagy under specific conditions. For example, Xu *et al.* showed that EGFR can be degraded by autophagy in an EGFR inhibitor-resistant lung cancer cells treated with the triterpene molecule celastrol[74]. The degradation of EGFR by autophagy promoted cell death in this instance; thereby suggesting that autophagy may be required to enhance the effects of some chemotherapeutic agents.

8.2 Endocytic Trafficking, Receptor Tyrosine Kinase Signalling, and Autophagy

During the course of research into the molecular regulation of autophagy, it has been found that autophagy and the endocytic pathway overlap at a multitude of points. These connections regulate autophagosome biogenesis and may also impact the

function of endosomes, such as the endocytic trafficking of receptor tyrosine kinases (RTKs). These concepts are explored in this section, although many open-ended questions remain, particularly with regards to the potential impact of autophagy on endosomes.

8.2.1 Introduction to the Endosomal Pathway

Cells can respond to extracellular conditions either by relaying signals from receptors on the membrane directly to intracellular networks or by taking up plasma membrane proteins or extracellular materials into single-membraned vesicles called endosomes. These vesicles can harbour diverse cargoes including invading bacteria and viruses, growth factor-RTK complexes, and nutrients such as glucose[75–77].

Endocytosis begins at the plasma membrane where different machineries can be engaged to create membrane invaginations that can bud off as endosomal vesicles. The uptake of targets in membrane-bound vesicles allows the internalisation of proteins with hydrophobic transmembrane domains and regulates their transport to specific intracellular compartments. Mechanisms for uptake include macropinocytosis, clathrin-mediated endocytosis (CME) or clathrin-independent endocytosis (CIE). Each of these three processes has specific sets of regulatory machineries and different triggers. For example, high doses of EGF ligand result in EGFR CIE whereas lower quantities of EGF engage CME[81]. Whilst CME promotes recycling of EGFR to the plasma membrane for continued activation, CIE directs the receptor to the lysosome, thereby ablating signalling. Therefore, protein activities can be differentially regulated by CME and CIE.

CME is considered a highly selective process and is the best characterised mechanism of endocytosis. Surrounding cargoes that undergo CME is a localised concentration of $PI(4,5)P_2$ that recruits lipid-binding adaptor proteins, such as adaptor protein 2 (AP-2). These membrane-targeted adaptor proteins, as well as other CME-regulators such as Epsin, induce the curvature of the pit structure[79,80]. Adaptor proteins also connect the target cargo to clathrin; a triskelion complex composed of heavy and light chains, which is assembled into a multimeric coat around cargoes (Figure 8.2A1,B1). Dynamin then acts around the neck of the bud to pinch it off and allow its entry into the cell as a clathrin-coated vesicle (Figure 8.2A2,B2). The coat complex then disassembles and adaptor protein phosphotyrosine interacting with PH domain and leucine zipper 1 (APPL1) is recruited to membranes containing active receptors and

$PI(4,5)P_2$. This is known as the pre-early endosome (Figure 8.2A3)[81]. The GTP-bound form of the small guanosine triphosphatase (GTPase) Rab5 is then recruited to the vesicle, following which the endocytosis-specific complex of PIK3C3 (PIK3C3-Beclin-1-UVRAG) generates PI(3)P[82]. The early endosome is then marked with early endosome antigen 1 (EEA1), which has binding domains for both Rab5 and PI(3)P[83].

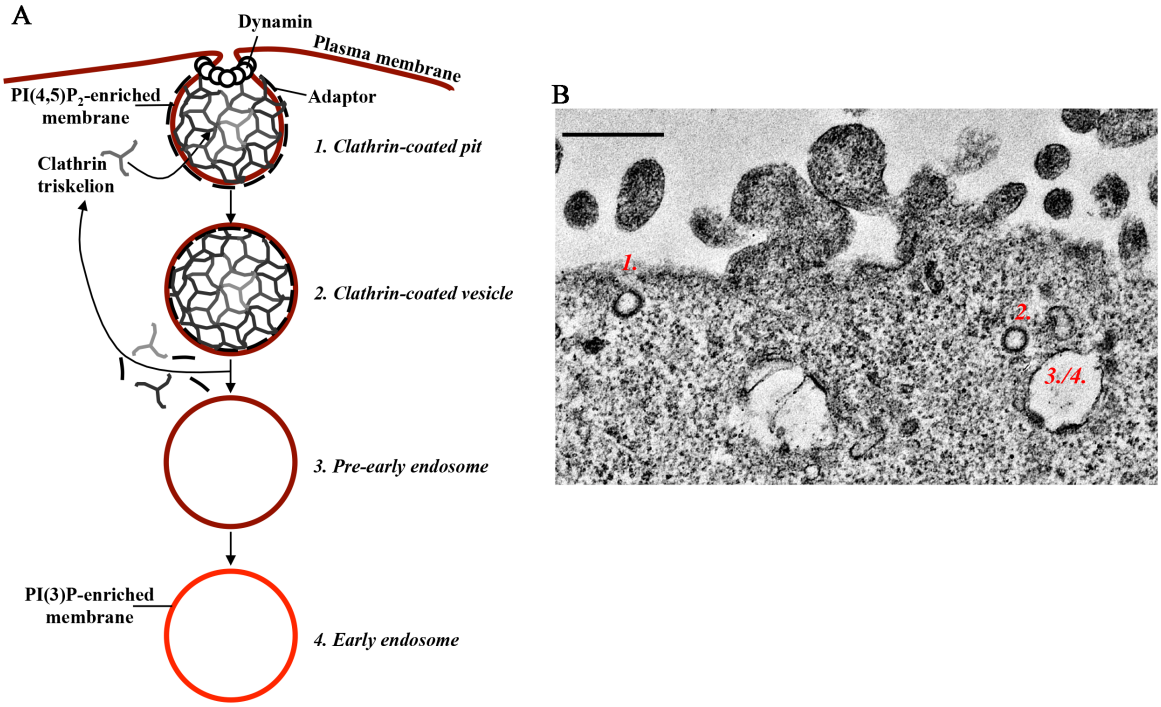

Figure 8.2 Clathrin-Mediated Endocytosis
A: A simplified diagram representing the process of clathrin-mediated endocytosis, from the formation of $PI(4,5)P_2$-containing pits at the plasma membrane that are coated in clathrin triskelions (*1*), to maturation into PI(3)P-positive early endosomes (*4*), **B:** Electron microscope image obtained by myself where different stages of clathrin-mediated endocytosis can be clearly seen and are labelled with numbers according to part **A**. Scale bar represents 500µm

Early endosomes mature into other endosomal classes (Figure 8.3). The regulation of endosomal maturation and trafficking are key to propagate or dampen the activity of a variety of different cargoes taken up from the plasma membrane and thereby influences a variety of cellular functions.

Whilst protein moieties that associate with different discrete endosomal compartments, such as members of the Rab superfamily, have been relatively well documented, the regulation of endosomal lipid composition has received sporadic attention. Whilst the synthesis and role of PI(3)P at early endosomes has been explored in some detail over more than two decades, phosphatidylinositol (PI) species at other endosomal compartments are only now starting to be elucidated[25,83]. These lipid moieties are important in facilitating the binding of the correct endosomal regulators, such as membrane remodelling proteins, to each compartment and

therefore the so-called 'phosphoinositol switch' is becoming recognised as a critical regulator of endosomes[84,85]. Therefore, during the ensuing sections, I shall describe both protein and PI markers of each endosomal compartment.

8.2.1.1 Late Endosome to Lysosome Trafficking

En route to the lysosome for degradation, cargos from the plasma membrane undergo transition through late endosomes that are marked by Rab7 and the lipid $PI(3,5)P_2$, which is generated by PIKfyve[86–89]. These late endosomes can either exist as a single vesicle or can undergo membrane invaginations, mediated by the endosomal sorting complexes required for transport (ESCRT) proteins, to form multivesicular bodies (MVBs)[90]. The ESCRT complex is recruited first by ESCRT 0, which binds PI(3)P on endosomes as well as their ubiquitinated cargo[91]. ESCRT I, which also has cargo-binding function, is then recruited to ESCRT 0[92]. ESCRT II then binds both ESCRT I and PI(3)P, thereby further anchoring the complex to the membrane. Finally, ESCRT III components assemble to induce membrane scission and pinch off the bud into the lumen of the endosome. Therefore, whilst the surface of MVBs is believed to be primarily decorated with $PI(3,5)P_2$, the intraluminal vesicles that are formed inside the body are PI(3)P -positive[93].

Late endosomes and MVBs then go on to fuse with the lysosome. The lysosomal vesicle is the final stop of the endolysosomal pathway and carries out the breakdown of cargoes, thereby terminating their signal. The lysosomal enzymes that catalyse these degradation reactions are hydrolases that function specifically in the acidic conditions that are found in this organelle (roughly pH 5)[94]. This prevents any inadvertent activity against cytosolic components, which, if left uncontrolled, could lead to cell death[63]. To achieve such a low pH, lysosomes employ vacuolar ATP-dependent proton pumps (v-ATPases) to transport protons against their concentration gradient into the lysosome[95]. The resulting vesicle can be recognised by the presence of lysosomal-associated membrane proteins 1 and 2 (LAMP1 and LAMP2), which are believed to make up approximately half of the membrane protein content of lysosomes[96].

8.2.1.2 Regulating Recycling to the Plasma Membrane

Instead of being degraded, some cargoes can be recycled back to the plasma membrane. The recycling of these cargoes can occur via either 'fast' or 'slow'

mechanisms. The more rapid system utilises Rab4 to return distal early endosomes directly back to the plasma membrane, whereas the slower Rab11-mediated system sends cargo via the perinuclear region, thereby providing a degree of spatial, temporal, and molecular regulation[97]. Rab11-positive recycling endosomes have been observed to form both from the Golgi apparatus, which is primarily localised near the nucleus, and from early/sorting endosomes[98]. The generation of these recycling endosomes relies on a dynamin-mediated tubulation and pinching off of membrane containing the specified cargoes[99,100]. Furthermore, recent work has elucidated that during the generation of recycling endosomes a characteristic PI conversion occurs: PI(3)P is dephosphorylated to PI, which is then phosphorylated to produce PI(4)P that can be further modified to PI(4,5)P_2[101,102].

The recycling of plasma membrane cargoes facilitates renewed activation of pathways without requiring additional protein synthesis, which is therefore faster and more energy-efficient for the cell.

8.2.1.3 Retrograde Endocytic Transport

Early endosomes can also undertake a retrograde route that sends cargo through the Golgi apparatus and ER. The cargo can then be exocytosed from the cell, returned to the plasma membrane, or delivered to a different cellular compartment, such as the lysosome. The transport of proteins through this route and controlled by the 'retromer' complex, composed of VPS26, VPS29, and VPS35, as well as a cargo-recognition complex[103,104]. Following the docking of the core retromer complex, SNX membrane remodelling proteins and the actin-polymerising WASH complex produce budding structures from PI(3)P-positive early endosomal membrane[105].

The retromer can be critical in the regulation of cell and organelle homeostasis. For example, the retromer mediates the endosome-Golgi retrieval of the cation-independent mannose-6-phosphate receptor (CI-M6PR)[103,106]. This is required for CI-M6PR function in delivering lysosomal proteins from the Golgi to the lysosome and thereby is critical for lysosomal function.

Further to these cytoplasmic trafficking events, it is now understood that the retrograde endocytic pathway can also be used to target proteins to the nucleus, in a mechanism that seems to require co-operation with nuclear pore proteins such as importin-β or members of the Sad1/unc-84 protein-like (SUN) family[107,108]. This therefore provides a mechanism to relay signals from the extracellular environment

directly to DNA regulation machinery in the nucleus (for details of this function see section 8.2.2.4). There is not much known regarding the exact mechanisms that regulate endosome-nucleus transport, but it is currently the subject of rigorous investigation, particularly with regards to cancer[109].

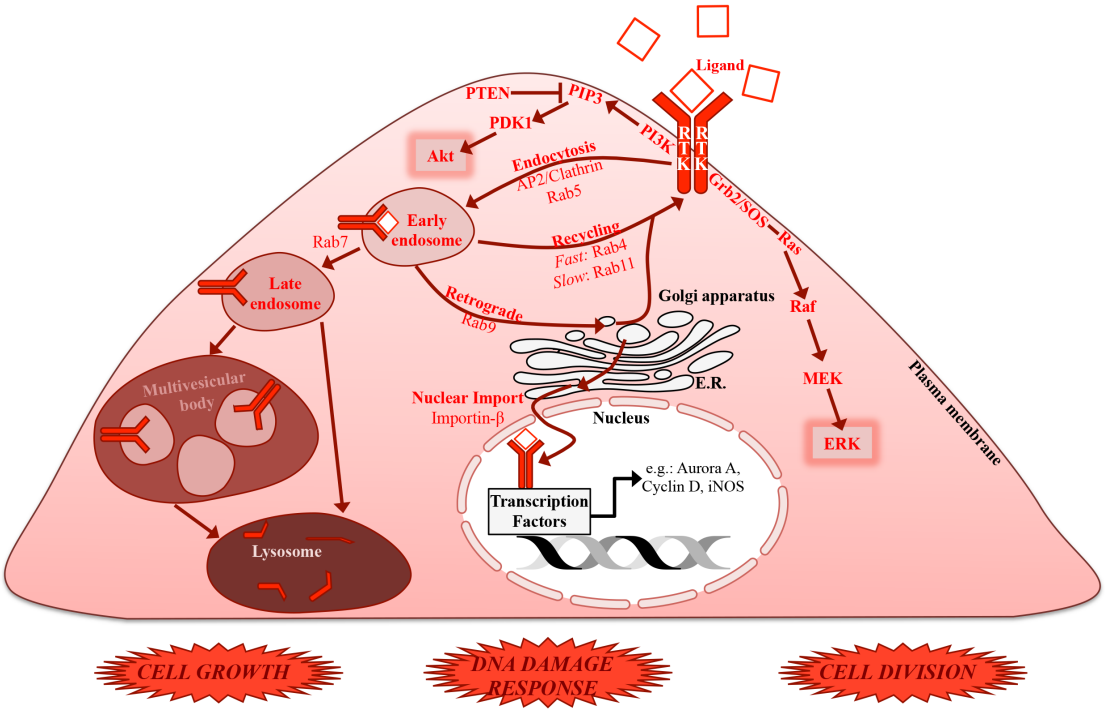

Figure 8.3 Summary of RTK Trafficking Through the Endolysosomal System
Following ligand binding at the plasma membrane, RTKs can be trafficked through different endosomal compartments or be transported to the nucleus. These events are mediated by different Rab family members, which can act as markers for each compartment, and generate a signalling response, a few of the key outputs of which (Akt and ERK) are summarised here.

8.2.2 Introduction to Receptor Tyrosine Kinase Signalling

One class of cargo that can be trafficked by endocytosis are the receptor tyrosine kinases (RTKs) transmembrane proteins. In this section, I will explain how these receptors are activated and endocytosed, then how they relay their activities to intracellular signalling cascades.

8.2.2.1 Receptor Tyrosine Ligand Binding

RTKs at the plasma membrane bind specific ligands from the extracellular milieu. Receptors then undergo conformational changes that result in asymmetric dimerization and cross-phosphorylation of the intracellular tyrosine kinase domains of the receptor (Figure 8.4). For example, phosphorylation of tyrosines 1,068 and 1,173 in the C-terminal domain of EGFR are reliably used as markers for its activation[110].

RTKs can be activated in response to growth factor ligands that induce a variety of cellular responses, including the stimulation of cell growth and anchorage-independence or the repression of cell death[77]. To prevent over-activation of tyrosine kinase signalling cascades the cell has developed a variety of regulatory mechanisms for RTKs. However, although extensively studied, detailed understanding of signalling pathways downstream from RTKs is considerably confounded by the regulatory complexities and capabilities for crosstalk between different components. Here I shall describe some example signalling pathways that are known to lie downstream of RTKs such as EGFR.

8.2.2.2 Ligand Binding Induces Post-Translational Modification of RTKs

It is known that RTK signalling is co-ordinated by the binding of adaptors containing Src homology (SH) or phospho-tyrosine-binding (PTB) domains to phosphorylated residues of activated receptors[77]. Several of these adaptors, such as growth factor receptor-bound protein-2 (GRB2) and insulin-receptor substrate 1 (IRS1), can simultaneously bind to the same activated receptors, providing multiplexing and synchronisation of downstream pathway activities. The particular domains present in each adaptor protein mediate the assembly of these complexes at RTKs. For example, in addition to a PTB domain, IRS1 also harbours a PH domain that anchors it to the plasma membrane at sites of $PI(4,5)P_2$ enrichment surrounding activated RTKs[111,112]. IRS1 is then phosphorylated, following which proteins containing SH2 and SH3 motifs, such as GRB2 and the p85 subunit of class I phosphatidylinositol-3 kinase (PI3K), are recruited to phospho-tyrosine residues[112,113].

It is known that certain protein tyrosine phosphatases (PTPs) can act on RTKs, thereby altering their protein conformation and inactivating their kinase activity. These phosphatases are themselves regulated both temporally and spatially. For example, induction of EGFR activity by EGF binding induces the inactivation of PTP1B by its oxidation[114,115]. This oxidation peaks at approximately ten minutes after EGF binding, then drops to baseline levels after approximately forty minutes, thereby allowing for a controlled window of EGFR signalling activity. PTPs are also regulated spatially to physically separate areas of RTK activation and inactivation. For example, PTP1B is constitutively localised to the endoplasmic reticulum where, at specific contact sites with endosomes, it can regulate the inactivation of most RTKs following their activation at the plasma membrane[116].

As well as phosphorylation, RTKs can be modified by ubiquitination, which induces their trafficking to lysosomes and therefore inhibits their signalling capacity[117,118].

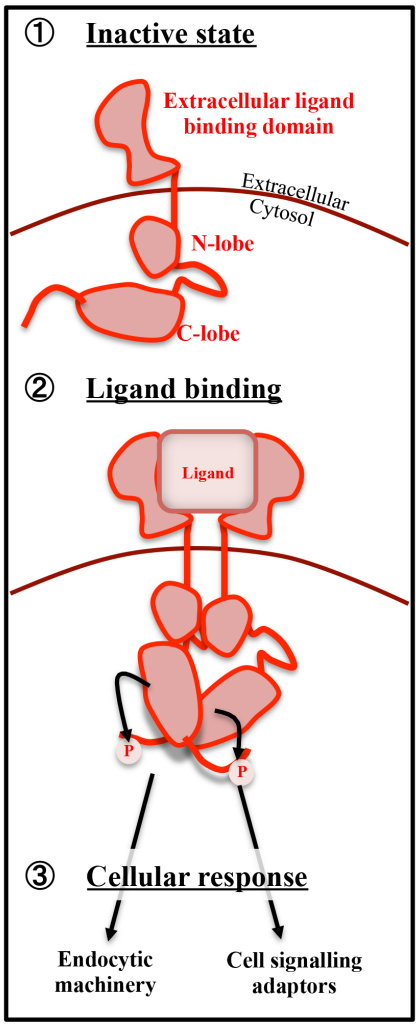

Figure 8.4 Schematic Diagram of Receptor Tyrosine Kinase Activation
1. Inactive RTK monomers reside in the plasma membrane. **2.** Ligand binds dimers of RTKs on their extracellular domains, causing a corresponding conformational change in the intracellular domains to activate the kinase and induce cross-phosphorylation in the C-termini. **3.** RTKs activate cellular signalling pathways and engage the endocytic machinery to facilitate their uptake.

Ubiquitin marks can act as binding sites for Hrs or ESCRT components, thereby promoting the sequestration of RTKs into MVBs that are destined for lysosomal delivery[92,118]. Interestingly, the degree RTK of ubiquitination, as mediated by the E3 ubiquitin ligase Cbl, appears to be conferred by the strength of ligand stimulation, as is the decision to be taken up by either CME or CIE[78,119]. Therefore, RTKs that are stimulated by a high concentration of ligand are prone to higher ubiquitination and CIE, and vice versa.

8.2.2.3 PI3K/Akt, mTOR, and MAPK Signalling Cascades

The assembly of adaptor proteins at RTKs nucleates the binding of cellular signalling factors. For example, through its interaction with IRS1, PI3K can then mediate the production of PI(3,4,5,)P_3 on the plasma membrane from PI(4,5)P_2 that then recruits the serine/threonine kinase Akt that can then be activated by phosphorylation. Phosphoinositide-dependent protein kinase-1 (PDK1) adds a phosphate group to threonine 308 of Akt, which is sufficient for low levels of activity but to achieve maximal activity serine 473 also needs to be phosphorylated, which can be catalysed by TORC2 or possibly by autophosphorylation[120–122]. Activated Akt then feeds into a variety of different pathways including nuclear factor-κB (NF-κB) signalling, glycogen synthase kinase-3β (GSK3β)-mediated glucose metabolism, repression of the cell cycle inhibitors Tp53 and p27, or activation of mTORC1 and 2 complexes. Furthermore, whilst mTORC2 can directly phosphorylate Akt, mTORC2 can be cross-activated by mTORC1 thereby feeding into Akt activity[123,124].

Alternatively to IRS1, GRB2 also sits at the top of an arm of RTK signalling. This RTK adaptor is one of the best characterised, primarily owing to its connection to Ras signalling, which has attracted much attention due to its frequent over-activity in cancers[125]. GRB2 is composed of a central SH2 domain and two SH3 domains, which facilitate its binding to Son of sevenless (SOS) at the plasma membrane. SOS is a guanine nucleotide exchange factor (GEF) for Ras, which is anchored in membranes by prenylation and palmitoylation[126]. Activated guanosine triphosphate (GTP)-bound Ras then triggers a series of kinase reactions from Raf to MEK and on to ERK[77]. This cascade, known as the mitogen-activated protein kinase (MAPK) pathway, is then capable of instigating pro-growth, pro-survival, and proliferation programmes[127].

There is a significant degree of crosstalk between the pathways downstream of active RTKs. For example, the MAPK pathway can directly feed into the PI3K/Akt/mTOR pathway by the phosphorylation and activation of the p110 subunit of PI3K by Ras[128].

Following their activation, RTKs become internalised into endosomes where they can be differentially trafficked according to a variety of factors, including receptor identity, cell type, and ligand potency and abundance (e.g. for EGFR: high EGF vs. low EGF vs. transforming growth factor α)[78,129]. As described above, endosomal trafficking can result in the transport of the receptor to late endosomes/the lysosome, the Golgi/ER, recycling endosomes/the plasma membrane, or the nucleus. Although there is a significant body of evidence showing that ligand-bound RTKs can signal

from early endosomal membranes, it is starting to become clear that this may be dependent on the pathway. For example, whilst MAPK constituents may be able to signal efficiently from either the plasma membrane or endosomes, Akt is considered to primarily signal from the plasma membrane, where PI3K is located, or potentially in APPL1-positive pre-early endosomes[130–134].

8.2.2.4 Nuclear Functions of RTKs

In addition to cytoplasmic signalling pathway activities, the nuclear functions of RTKs are also beginning to be investigated in greater detail. Many of these studies focussed on EGFR, which represents a good prototype on which to develop this model. In the nucleus it can act as a co-transcriptional activator in concert with transcription factors such as STAT proteins and E2F1, to induce the expression of genes such as *CYCLIN D1*, *C-MYC*, and *AURORA-A*[109]. The presence of RTKs like EGFR in the nucleus is therefore generally believed to be a positive stimulus for cell growth and survival, with obvious implications in pathologies like cancer[135–137]. However, the mechanism for nuclear translocation of RTKs is not yet completely understood; whilst some evidence supports a Golgi-ER-nucleus retrograde transport route, other studies suggest that early endosomes can directly fuse with the nuclear membrane[107,138–141]. What is clear from these studies, however, is that nuclear RTK translocation depends on its endocytosis and trafficking via functional early endosomes, rather than representing a population of receptors that directly enter the nucleus from the cytoplasm following synthesis. Interestingly, studies undertaken thus far have not addressed how these receptors are processed following their nuclear uptake: whilst we know that endosomal RTKs can be directed either back to the plasma membrane or degraded in the lysosome, it is unclear what the eventual fate of these nuclear receptors is.

8.2.3 Autophagy Players Functionally Localise to Different Endosomal Compartments

Numerous recent studies have described the localisation of autophagy proteins at endocytic compartments. Furthermore, autophagy and endocytosis are both vesicular processes that have been reported to rely on some common upstream regulators, such as certain Rab GTPase-activating proteins (GAPs). Here I shall outline what is currently known regarding the various endosomal localisations of different autophagy players and the resulting functional impact on autophagosome biogenesis.

8.2.3.1 ATG9 Trafficking

One of the most active areas of research in the autophagy field involves the investigation of the source of membrane during the expansion of the pre-autophagosome. Different groups have proposed that membranes from mitochondria, Golgi apparatus, ER, or endosomes can contribute to autophagosome biogenesis. ATG9 is the only known transmembrane autophagy player and so has been looked to by many as the dictator of autophagosome membrane source. Indeed, ATG9 has been seen to localise with several different compartments that can act as membrane sources during autophagosome biogenesis, including the Golgi and recycling endosomes[31,142–145]. Upon autophagy induction, ATG9 re-localises to sites of autophagosome formation, potentially mediated by the activity of the ULK1 complex[24,142,145].

Unexpectedly, the production of Golgi-derived ATG9 vesicles has been seen to rely on PI(3)P-binding capability of the endocytosis-specific PIK3C3 complex containing UVRAG[146]. Under untreated conditions UVRAG regulates transport between the Golgi and the ER to maintain Golgi morphology. Upon autophagy induction by rapamycin or nutrient depletion, UVRAG is required for ATG9 vesicle production and maximal LC3 lipidation. This contrasts to the established understanding of the PIK3C3 complexes as the UVRAG-containing complex is thought to function solely in early endosomal PI(3)P production whereas the ATG14-containing complex was believed to function at the ER for autophagosome biogenesis.

Furthermore, recently it has been shown that ATG9 and ATG16L1 traffic to sites of autophagosome biogenesis from recycling endosomes, mediated by membrane re-modellers SNX18 and Dynamin-2[147]. The importance of recycling endosomes is emphasised by the requirement for Rab11 activity to induce maximal autophagic flux in this context[24].

8.2.3.2 The Role of Tre2/Bub2/Cdc16 (TBC) Domain-Containing Proteins in Autophagy

The core autophagy player LC3 has been seen to interact with several Tre2/Bub2/Cdc16 (TBC) domain-containing Rab GAP proteins, most likely through LC3-interacting region (LIR) motifs[148]. Although the functional relevance of these associations has not yet been completely elucidated, several studies have yielded compelling results. For example, LC3 can interact with TBC1D25, which functions in autophagy by acting as a GAP for Rab33B, an ATG16L1 binding partner[149].

Additionally, LC3 binds TBC1D2 and co-ordinates Rab7 GTP binding, thereby regulating autophagosome-lysosome fusion steps, although the reciprocal influence on late endosomal function is unclear[150]. Interestingly, TBC1D2 has also seen to localise to Rab11-positive recycling endosomes[150].

Furthermore, it has been shown that the interaction of some TBCs with various autophagy players can impact both endocytic trafficking as well as the autophagy pathway. This has been shown in the case of TBC1D5, which interacts with and inhibits the function of the retromer complex at endosomes under fed conditions[148]. However, following autophagy induction LC3 displaces the retromer and instead targets TBC1D5 to autophagosomes. Therefore, autophagy induction can have a direct impact on endosomal processes. Moreover, as described in section 8.2.1.3, the retromer promotes the activity lysosomal hydrolases thereby providing an additional retromer-mediated interdependency between autophagy and endocytosis. The interplay between the retromer and autophagy was then further explored by Popovic and Dikic, who demonstrated that TBC1D5 is trafficked with AP-2 and ATG9 from clathrin coated pits at the plasma membrane through to early endosomes, where TBC1D5 inhibits the retromer complex[144]. Functionally, autophagic degradation of TBC1D5 is important to facilitate the proper trafficking of the glucose transporter GLUT1 from early endosomes back to the plasma membrane instead of being targeted to the lysosome[151].

Additionally, the ULK1 complex has been observed to interact with TBC1D14 at recycling endosomes, which inhibits its role in autophagy[24]. Following the induction of autophagy, TBC1D14 translocates to the Golgi complex, leaving ULK1 free to participate in autophagy. TBC1D14 also binds active Rab11 and mediates recycling endosomal tubulation, which negatively impacts autophagosome biogenesis.

Together these studies demonstrate that, similarly to other cellular vesicular pathways, autophagy relies on the regulation of certain Rab GTPases and it is now beginning to emerge that this may reciprocally influence endosomal trafficking.

8.2.3.3 The Localisation of ATG16L1

The localisation of ATG16L1 is proving to be somewhat contentious. On the one hand, the Rubinsztein and Simonsen laboratories have documented ATG16L1 co-localisation with Rab11-positive recycling endosomes and recycling transferrin receptor (TfnR)[31,44,152]. In these reports, ATG16L1 co-operates with ATG9 at

recycling endosomes to mediate autophagosome formation. Furthermore, ATG16L1 has been seen to tether to these recycling endosomes via PI(3)P-binding protein WIPI2, which co-immunoprecipitates with Rab11[153]. However, Li *et al.* found that although transiently overexpressed ATG16L1 co-localised with Rab11, its endogenous counterpart did not localise to recycling endosomes[154]. Further, this transiently overexpressed protein did not co-localise with its autophagy complex partner ATG12, and instead actually inhibited GFP-LC3 puncta formation. It remains to be seen how these observations of ATG16L1 and recycling endosome connections can be aligned, whether it be dependent on cell type, treatment conditions, or antibody variations.

Alternatively, ATG16L1 has been reported to interact with components of the CME machinery at the plasma membrane, which is required for its eventual delivery to sites of autophagosome biogenesis[44]. Additionally, ATG16L1 has been seen to bind the endosomal regulator Annexin A2; an interaction which facilitates the formation of autophagosomes[155]. However, whether the interaction between autophagy proteins and the CME components has an impact on CME endocytosis has not been explored.

Despite being documented at both the plasma membrane and at recycling endosomes, ATG16L1 has not been observed in the interim; i.e. at early endosomes[31,44]. One possibility is that ATG16L1 does not traffic through endosomes but instead independently localises at clathrin-coated pits and at recycling endosomes. Alternatively, there may just be a low level of ATG16L1 transport between the plasma membrane and recycling endosomes, or the localisation may be extremely transient. This option seems more feasible given that trafficking from the plasma membrane through early endosomes to recycling endosomes has previously been observed for ATG9[31].

Together, the studies described above draw attention to an intricate interplay between the processes of autophagy and endocytosis. However, explicit evidence documenting a reliance of endosomal homeostasis on autophagic flux remains elusive.

8.2.4 Receptor Tyrosine Kinase Signalling Can Regulate the Autophagy Machinery

Although some studies have shown that ligand activation of some RTKs (such as AXL, ERBB3/ERBB4, TRKA, Ephrin, and VEGFR) can promote autophagy,

stimulation of others (including EGFR, HER2, and FGFR1) can inhibit components of the autophagy machinery[156–162]. Crucially, mTORC1, mTORC2, and Akt lie downstream of RTK activation, and these kinases are known to directly phosphorylate and inhibit autophagy regulators, with the mTORC1-ULK1-PIK3C3 axis being perhaps the best known. Alternatively, Akt can phosphorylate serines 234 and 295 on Beclin-1, causing its association with the scaffold and cytoskeletal proteins 14-3-3 and Vimentin, and thereby preventing its localisation to sites of autophagosome biogenesis. This is likely to be reinforced by Akt-mTORC1 crosstalk that would also inhibit ULK1 (see section 8.1.2) and thereby prevent Beclin-1 activation. Moreover, mTOR, operating via Raptor and Rictor, has also been shown to influence Beclin-1 protein stability, although this mechanism has not been fully explored[163].

In addition to engaging mTOR and Akt, the RTK EGFR also directly phosphorylates Beclin-1 following EGF binding[33]. This displaces it from the PIK3C3 complex and recruits Rubicon thereby inhibiting the activity of the complex. On the other side of the coin, in the absence of ligand binding, inactive EGFR can act to promote Beclin-1/PIK3C3 activity by recruiting Rubicon, LAPTM4B, and the exocyst constituent Sec5, consequently promoting autophagy[164].

Overall, these regulatory interactions and modifications mediated by RTK/mTORC1/Akt signalling reduces the production of PI(3)P, which then ablates the recruitment of downstream autophagy players and autophagosome formation. In this way, mitogenic signalling pathways can limit cellular catabolism when conditions are permissive for growth and division.

Additionally, RTKs can modulate autophagic flux by the regulating the transcription of autophagy and lysosomal proteins, primarily via the forkhead transcription factors (FoxO), signal transducers and activators of transcription 3 (STAT3), and transcription factor EB (TFEB). Whilst FoxO and TFEB promote autophagy gene expression and are repressed by RTK signalling, STAT3 is activated by RTKs and acts to inhibit the expression of autophagy regulators[165–169].

8.2.5 The Putative Role of Autophagy in Receptor Tyrosine Kinase Signalling

The switch between the catabolism mediated by autophagy and the anabolism induced by mitogenic RTKs has attracted much attention in the past ten years. However, recent studies are also revealing an unexpected synergy between autophagy proteins and RTK signalling. These investigations are of particular interest with regards to

cancer where both autophagy and RTK activities are associated with increased malignancy and resistance to therapies.

8.2.5.1 Autophagy and the c-Met Receptor

Several groups have reported a co-operation between autophagy-related gene expression and the promotion of signalling from the HGF/c-Met receptor in cancer cell lines. Barrow-McGee and colleagues utilised a variety of cell lines in suspension to show that non-canonical ATG13-independent 'autophagy-related endomembranes' act as platforms for c-Met signalling to promote cell survival and ultimately tumourigenicity[170]. Additionally, as part of screen of RTK activities in autophagy-deficient colorectal cancer cells, c-Met appeared to be reliant on *ATG7* and *ATG5* expression to achieve maximal signalling[171]. These studies also found that c-Met localises to autophagy-related structures that are positive for LC3. Furthermore, autophagy has been seen to increase HGF expression and c-Met/JNK/STAT3 signalling, which promotes stemness in cirrhotic livers that increases hepatocarcinogenesis[172].

8.2.5.2 Autophagy and the Epidermal Growth Factor Receptor

With regards to EGFR signalling, there have been some conflicting reports of the effect of autophagy. Whilst several groups have shown that EGFR is not regulated by autophagy inhibition and that EGFR does not localise with autophagy proteins, others have shown that EGFR and LC3 can co-localise[24,51,52]. Additionally, although EGF-induced Akt and ERK phosphorylation were not influenced by autophagy loss in several studies, Martinez-Lopez *et al.* reported that autophagy-related structures assemble components of the MAPK cascade and facilitate their EGF-mediated activation[171,173,174].

In its capacity as an endosomal PI(3)P regulator, the autophagy-related protein Beclin-1 acts to dampen EGFR signalling by facilitating the switch from pre-early endosomes to early endosomes, where the tyrosine kinase activity is inhibited[82]. As Beclin-1 is re-distributed between its autophagosomal and endosomal PIK3C3 complexes during starved or fed conditions, respectively, the induction of autophagy may conversely sequester Beclin-1 from endosomes and thus enhance EGF-induced signalling[25].

Alternatively, the non-receptor tyrosine kinase Ack1 localises to autophagosomes under conditions of ligand withdrawal, thereby sequestering it from its function at

early endosomes where it acts to prevent EGFR lysosomal targeting[175]. Conversely, upon EGF treatment, Ack1 re-localises to early endosomes to support oncogenesis by promoting EGFR activity.

Additionally, autophagy has been suggested to be required for the mitochondrial delivery of EGFR, with autophagy stimuli inducing the translocation of EGFR to mitochondria[176]. This is dependent on the activity of the PIK3C3/Beclin-1 complex, as 3-methyladenine (3-MA) treatment or siRNAs knockdown of Beclin-1 inhibited the process. The mitochondrial load of EGFR correlated with increased survival and was depleted upon cell death induction by etoposide treatment. Interestingly, in a later study also by the Jiang group mitochondrially localised EGFR was shown to be independent of its endocytosis[177].

These emerging studies highlight an intriguing reliance of RTK signalling on the expression of key autophagy proteins and even on autophagosomal membranes themselves.

8.3 Autophagy and Cancer

Cancer is a particularly challenging disease to treat, not only due to the high variability between different tumour types but primarily because of its incredibly dynamic behaviour. Therefore, a major aim has become to understand whether cancer cells may have a targetable weak point. As a constitutive pathway that has been seen to promote several key hallmarks of cancer, such as elevated cell metabolism and survival, autophagy has garnered significant attention[178]. However, the current studies of autophagy in cancer have provided somewhat conflicting evidence, with both pro- and anti-tumourigenic properties described[7]. Here I shall explore some of these studies and how this knowledge has been applied so far in attempting to target autophagy for cancer treatment.

8.3.1 The Context-Dependent Role of Autophagy in Cancer

Autophagy has been implicated in processes such as cellular signalling, metabolism, and ROS production/DNA damage: all of which have been implicated in either cellular transformation and tumour maintenance. It is suggested that autophagy can act a double-edged sword with regards to cancer: whilst the lack of autophagy seems

to predispose cells to oncogenic transformation, the formation of a malignant tumour requires the metabolic support conferred by autophagy[7]. This is complicated by contradictory reports that rely on the use of non-autophagy-specific inhibitors such as hydroxychloroquine (HCQ) or 3-MA. In this section I aim to outline some of the data and hypotheses currently being put forward in this rapidly expanding field.

8.3.1.1 Autophagy Proteins Inhibit Cellular Transformation and Beclin-1 is an Archetypal Tumour Suppressor

A putative role for autophagy as a tumour suppressor pathway was heralded by early work carried out by the Levine group. A seminal study in 1999 revealed that the heterozygous loss of Beclin-1 resulted in the increased formation of tumours in a mouse model of breast cancer thereby suggesting a role as a tumour suppressor[179]. However, despite much further investigation since then, the impact of the PIK3C3 complex on cell transformation remains somewhat unclear.

In more recent work by the Levine group, both EGFR and Akt were shown to directly phosphorylate and inhibit Beclin-1[33,180]. This was substantiated by introducing acidic mutations into Beclin-1 to mimic its phosphorylation by EGFR resulting in autophagy suppression and enhanced tumourigenecity of transformed fibroblasts. Conversely, preventing the phosphorylation of Beclin-1 by Akt inhibited tumour formation. On the other side of the coin, enhanced binding between Beclin-1 and Rubicon during EGF stimulation may promote EGFR lysosomal degradation by relieving Rab7 from its inhibitory interaction with Rubicon[181].

Another intriguing study showed that the action of the Beclin-1/PIK3C3/UVRAG endocytosis-specific complex plays a key role as a tumour suppressor. This is conferred by its function in generating early endosomal PI(3)P, which then recruits effectors such as EEA1[182]. This facilitates the maturation of signalling receptors, like IGF-1R and EGFR, from signalling-competent to signalling-defective compartments, which limits oncogenic potential in a breast cancer cell line model. This highlights the possibility that the role of Beclin-1 in cancer may be at least partly attributable to its function in the endocytic pathway.

8.3.1.2 Autophagy Facilitates Progression from Benign Phenotypes

A variety of studies have demonstrated that ablating the expression of key autophagy players promotes tumourigenesis or tumour maintenance in several different cancers. This has been primarily attributed to the role of autophagy in supporting elevated

metabolic activity and resolving cell stresses that are induced by oncogenic transformation. In one example, the formation of tumours in a Polyoma Virus middle T-antigen mouse mammary model (MMTV-PyVT) was greatly inhibited when FIP200 was deleted[183]. Similarly, tumours in a Palb2 deletion-driven breast cancer model required Beclin-1 expression to form efficiently in Tp53 wild type but not Tp53-deficient background[184]. Autophagy has also been implicated in facilitating tumourigenesis driven by aberrant MAPK activity in the context of constitutively active BRaf. In a $BRaf^{V600E}$ melanoma model, mitophagy ablated oxidative stress and kept senescence at bay whereas $BRaf^{V600E}$-induced adenomas fail to progress into adenocarcinomas when ATG7 is lost[185,186].

Furthermore, several studies have investigated the connection between oncogenicity and *ATG* gene expression in different tumour types. In pancreatic cancer, increased *Atg* gene expression correlated with elevated autophagy/lysosomal gene expression signature[187]. Glioblastoma stem cells also exhibit elevated expression of autophagy regulators DNA damage regulated autophagy modulator 1 (DRAM1) and p62[188]. Additionally, in 2016 the Ketteler laboratory undertook a comprehensive analysis of the expression of autophagy genes across a variety of cancers[189]. The authors found that overall core autophagy player expression was not significantly changed in most cancers, although some mutations were observed in prostate cancers. Given that cancer cell genomes have a high mutagenic rate as a whole, this negative result may be suggestive of a requirement for autophagy gene function in tumourigenesis. However, the modulation of autophagy is believed to occur primarily at the protein level rather than by transcription regulation (see section 8.1). Therefore, the frequency of autophagy gene mutation rate in tumours is not necessarily an accurate read-out of the importance of autophagy in tumourigenesis.

8.3.1.3 Autophagy and Ras: A Special Relationship?

There are three main steps involved in tumour formation: firstly cells must acquire an oncogenic mutation that drives cell growth and proliferation, then they overcome their inherent cell cycle inhibition mechanisms that protect against cancer, and finally the transformed cells must maintain this phenotype in the face of any exogenous 'stop' signals or immune attack. Sitting atop the MAPK signalling cascade, overactive Ras can represent a strong first step, but then does autophagy help or hinder either of the consecutive steps required for transformation? Many cancer models using oncogenic

Ras as a driving mutation have documented a critical interplay with autophagy, particularly with regards to metabolism and senescence (also see section 8.3.1.2). The molecular mechanisms that underpin this have been investigated in some depth and shall be reviewed here.

Whilst there have been a multitude of studies regarding autophagy and Ras transformation, their cellular relationship still remains unclear. One study of Ras oncogene-induced senescence (OIS) in IMR90 primary fibroblasts showed that autophagy promotes OIS, with the knockdown of essential autophagy genes resulting in delayed senescence onset[190]. This observation was bolstered mechanistically by additional work showing that autophagy facilitates the degradation of components of the nuclear lamina during Ras OIS and preventing this promotes oncogenic transformation[191]. Furthermore, the autophagy-related protein ATG12 has been seen to repress the malignant growth of cells expressing oncogenic Ras by engaging BCL-2 family members and instigating cell death, although this appears to be independent of its function in autophagy[192,193].

However, in other contexts autophagy has been seen to promote Ras-induced transformation, such as in mouse embryonic fibroblasts (MEFs), where loss of ATG5 or ATG3 sensitises cells to senescence[194]. In this model, the authors found that cells can escape $HRas^{V12}$-induced senescence by expressing a high level of ATG5-ATG12 and that the exogenous expression of ATG5 increases the ability of cells to avoid senescence. These findings are supported by experiments undertaken by Lock and colleagues showing that autophagy promotes glycolytic metabolism that is required for the malignant growth of mammary epithelial cells[195].

From these studies we are starting to see that the influence of autophagy on *in vitro* transformation may be different according to the cellular context. However, in mouse models there appears to be a greater consensus that autophagy is required for the growth of a variety of Ras-driven tumours; including pancreatic, kidney and lung cancer models[196–200]. In these mouse models, mechanistic data has implicated autophagy in the deregulation of metabolic pathways[196–198,200]. For example, in a $KRas^{G12D}$ lung cancer model, autophagy was required for lipid fatty acid oxidation that promoted the formation of malignant adenomas and carcinomas rather than benign oncocytomas[200]. The disparities between mouse models and cell culture studies may be explained by the differing conditions that cells are exposed to. Oncogenic Ras-transformed cells may have an increased reliance on autophagy for

tumourigenic growth *in vivo* due to the sub-optimal growth conditions experienced, whereas cultured cells grow adhered in a monolayer with nutrients in excess. Alternatively, these opposing results may be due to the different cellular contexts, such as the presence of other mutations. Indeed, one elegant study by Rosenfeldt *et al*. was able to show that Tp53 status dictated the response to Ras transformation[201].

8.3.2 The Interplay of Autophagy, Senescence, and Cancer

The studies outlined above have revealed a conflicting array of data regarding the role of autophagy in cancer. This is similarly found with regards to the interplay of autophagy with senescence, where the use of different model systems has made comparison of variable results difficult to interpret. Below I shall summarise the findings of these studies and put them into the context of tumourigenesis.

8.3.2.1 Introduction to Senescence

The process of senescence is defined as an irreversible arrest of the cell cycle. This renders cells incapable of responding to mitogenic growth factors or replicating their DNA. Cell cycle arrest can instigate tissue re-modelling, prevent or promote malignant transformation, and mediate the clearance damaged aged cells by the immune system. A characteristic set of hallmarks is used to define senescence (Figure 8.5). This includes the increase in cell cycle arrest markers, such as p16 (cyclin-dependent kinase inhibitor (CDKN) 2A/p16^{INK4a}), p21 (CDKN1A), p27 (CDKN1B/KIP1), Tp53 (TP53), or Retinoblastoma protein-1 (pRb/RB1)[202–205]. Although previously understood to be separate pathways (p21/Tp53 or p16/pRb/p27), new research is showing that there is in fact an extensive cross-talk between the two pathways.

Tp53 was the earliest tumour suppressor protein to be characterised and has been dubbed ‘the guardian of the genome’ due to its ability to reduce DNA mutagenesis[206]. Since then, much has been elucidated regarding the cellular pathways that regulate or are regulated by Tp53. Engaging Tp53 can either halt cell growth or promote apoptosis, as well as influence other tumour-regulatory factors depending on cell status[207]. For example, DNA damaging agents, such as γ-radiation, activate Tp53/p21 and inhibit cell division, thereby preventing the propagation of cells with radiation-modified DNA, which might be tumourigenic[208].

First discovered in connection with the development of the eye cancer retinoblastoma, pRb represses the cell cycle by inhibiting E2F transcription factors and cyclin/cyclin-

dependent kinase 2 (CDK2) complexes that promote expression of key cell cycle progression regulators[205,209,210]. The retinoblastoma protein family, composed of pRb/p105, p107, and pRb2/p130, are characterised by a common 'small pocket' domain, but each family member can undertake several unique roles, particularly with regards to the establishment of senescence[209]. This is attributable to the fact that these pocket proteins appear to regulate different subsets of genes[211]. These proteins are active (i.e. replication repressive) when hypophosphorylated, with their phosphorylation mediated by CDKs during the cell cycle[210]. The activity of pRb is intimately connected with that of p27 as these proteins are able to activate one another in a positive feedback loop to reinforce cell cycle inhibition[204,205]. Interestingly, in addition to regulation by CDKs, it has been found that the pro-growth regulator Akt can phosphorylate and inhibit p27 activity, thereby blocking pRb/p27 cell cycle regulation[212–214]. Similarly, Akt inhibits Tp53 by phosphorylating and activating the Tp53 ubiquitin ligase MDM2, thereby destabilising Tp53[215].

In addition to these cell cycle regulators, other cellular markers are used to test for the establishment of senescence. The use of multiple markers of the senescent phenotype is important to rule out that alternative forms of cell cycle arrest may be occurring. One of the most frequently used hallmarks of senescence is the staining for β-galactosidase at pH 6.0[216]. This enzyme is elevated in senescent cells due to the presence of enlarged lysosomal compartments, where β-galactosidase activity is detected[217]. Additionally, senescent cells harbour regions of dense heterochromatin at proliferation-promoting genes, known as senescence-associated heterochromatic foci (SAHF)[218] as well as having significant increase in DNA damage markers, such as γH2AX[219,220]. In oncogene-induced senescence this damage is caused by the inability of DNA to efficiently replicate at the speed dictated by the signals from the oncogene, such as constitutively active Ras, whilst in replicative senescence it occurs at the ends of eroding telomeres. A more recently characterised feature of senescent cells is the secretion of a pro-inflammatory senescence-associated secretory phenotype (SASP)[221]. The SASP is composed of cytokines and chemokines, such as members of the interleukin family, which promote senescence in both a paracrine and autocrine manner. These factors can then recruit immune cells, which can either mediate senescent cell clearance or promote the growth of neighbouring cells.

8.3.2.2 Autophagy and Senescence

Autophagy has been connected to senescence in a variety of different contexts. Autophagy may regulate senescence through crosstalk with tumour suppressor pathways or maintaining cellular homeostasis. Observations by Young *et al.* demonstrated increased LC3-II generation during the initiation of senescence[190]. Additionally, Tp53 has been shown to upregulate the expression of ULK1 and ATG13, which promoted autophagic flux during DNA damage[222]. Furthermore, Kang *et al.* have found that autophagy is required for the generation of the SASP[223]. Specifically, autophagy degrades the transcription factor GATA4, and so ablates its action in promoting the expression of NF-κB effectors that induce the production of SASP factors such as IL-6, IL-8, and tumour necrosis factor α (TNFα).

Together, these studies highlight an interesting and possibly context-dependent effect of autophagy in the establishment and maintenance of senescence. Autophagy loss may make the cell more susceptible to senesce due to the accumulation of damaged components, such as mitochondria. Alternatively, autophagy can regulate senescence inducers by degradation. However, there is little known regarding the impact of autophagy loss on the induction of senescence outside the context of OIS, particularly with regards to the maintenance of tumours or their therapeutic targeting.

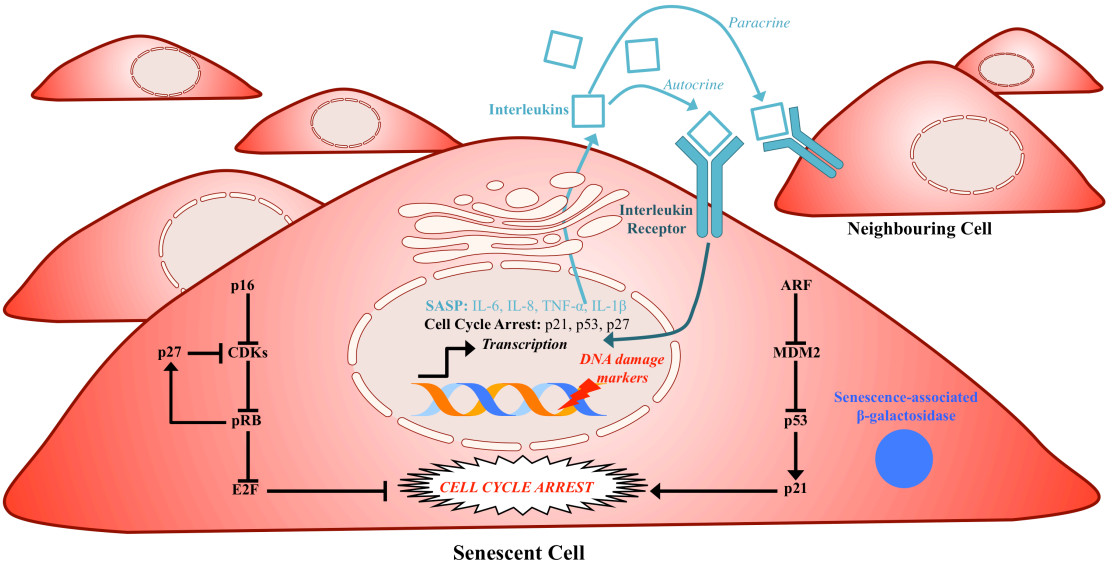

Figure 8.5 Diagram of the Cellular Hallmarks of Senescence
Engaging cell cycle inhibitors blocks cell replication, whilst SASP factors both reinforce the phenotype of the senescent cell and induce senescence in neighbouring cells. Senescence induction can be accompanied by DNA damage markers and senescence-associated β-galactosidase.

8.3.3 Autophagy Suppresses Anoikis During Anchorage-Independent Growth

As well as its role in cell cycle inhibition by senescence, the influence of autophagy on cell survival or death decisions has also been of particular interest in cancer biology. For some time the concept of 'autophagic cell death' garnered much interest but, as eloquently described in a review by Levine and Kroemer, the survival pathways that are promoted by autophagy mean it is more likely to be activated in a futile attempt to ablate cell death rather than being the causative mechanism[224]. Indeed, during oncogenic transformation, autophagy is primarily reported to support metabolism and cell survival[225]. From the extensive research undertaken in this field, I shall focus specifically on outlining the findings most pertinent to this study, which relate to ability of autophagy to prevent cancer cell death during anchorage loss.

To prevent inappropriate growth away from their intended niche, when normal cells detach from the extracellular matrix (ECM) they undergo a caspase-mediated form of cell death called 'anoikis' (a Greek derivation meaning 'homeless')[226]. A key property of cancer cells is to avoid anoikis and grow in conditions of anchorage loss[227]. Anoikis is evaded by a plethora of adaptations, including oncogenic transformation, an epithelial-to-mesenchymal transition (EMT), and acquisition of stemness by expressing transcription factors generally associated with a more developmentally naïve state[228–233]. However, overcoming initial cell death triggers is only the beginning for cancer cells- they must then maintain the activity of signalling and metabolic pathways to survive and proliferate during prolonged anchorage loss.

In order to compensate for the loss of integrin-mediated, anchorage-induced signalling, cancer cells employ oncogenic signalling cascades. The activation of receptors such as IGF1-R, EGFR, c-MET, NOTCH, or ERBB2 by their ligands or by oncogenic mutation can instigate a series of phosphorylation reactions that result in anchorage-independent growth[170,228,229,234,235]. The key kinases that relay these signals are Akt and ERK, the activities of which have been seen to be crucial for anchorage-independent growth in wide variety of contexts from breast, prostrate, and ovarian cancers to head and neck squamous cell carcinoma[228,229,235–237]. Additional reports show that alternative MAPK signalling axes may also be utilised to stimulate cell survival, such as TGFβ-activated kinase 1 (TAK1/MAP3K7), which induces non-canonical WNT signalling[238].

Detachment from the ECM and reduction in cell signalling causes a catastrophic disruption of glucose uptake and ATP production as well as an increase in reactive

oxygen species (ROS)[239,240]. The metabolism of non-anchored cells is particularly sensitive to ROS and their removal is therefore vital for anchorage-independent growth[239]. To override this, cancer cells can either upregulate the expression of detoxifying enzymes, such as superoxide dismutase 2 (SOD2)[241], or perturb metabolic pathways to generate reducing species that can quench ROS[242]. The deficit in ATP production caused by detachment can be overcome in cancer cells by increasing mitochondrial neobiogensis or upregulating metabolic programmes such as the pentose-phosphate pathway, for example by reducing pyruvate dehydrogenase kinase 4 (PDK4) expression[240,243].

One pathway that has been seen to both regulate cell signalling and supply additional metabolic demand in detached cells is autophagy. For the past decade, autophagic flux has been known to be important to avoid anoikis and promote cell proliferation following anchorage loss[244]. Induced by ROS and PERK signalling from the endoplasmic reticulum, detachment-induced autophagy is hypothesised to promote metabolism, via the supply of amino acids, as well as contributing to cell survival[170,245]. Furthermore, autophagy proteins are required for the recognition and lysosomal degradation of detached cells engulfed by the 'cell-in-cell' entosis phenomenon[246,247]. The outcome of entotic cell degradation is currently unclear, with some evidence suggesting that it may clear potentially tumourigenic detached cells, whilst others argue it can result in pro-oncogenic aneuploidy and provide a source of nutrients for a prospective cancerous host cell to survive[246,248].

8.4 Glioblastoma Multiforme

As described above, autophagy has been identified as a potential therapeutic target in several different cancer types, but perhaps one of the most promising opportunities is in the treatment of glioblastoma multiforme (GBM). These tumours exist in conditions that are known to strongly upregulate autophagy, such as hypoxia, and preliminary studies suggest that GBM cells require autophagy for rapid oncogenic growth and in the development of resistance against treatment strategies. To put this into context, I shall first introduce the defining features of GBM biology before discussing the role autophagy may play in its tumourigenesis.

8.4.1 Pathological Features

GBM is a devastating brain cancer that confers an extremely poor patient prognosis. These rapidly growing, high-grade tumours have a high lethality rate, even when treated with a combination of chemotherapy, radiotherapy, and surgery, with 1-, 2-, 3-, and 4-year survival estimated at 58%, 20%, 10%, and 7%, respectively[249]. The defining histological characteristics of glioblastoma include foci of necrotic cells surrounded by hypercellular zones, dubbed pseudopalisading necrosis, which illustrate the stressful nature of the tumour microenvironment generated by excessive cellular proliferation[250–252]. These tumours also exhibit elevated levels of microvasculogenesis, with the resulting naïve vessels unable to adequately supply the tissue with oxygen or nutrients.

Several different features of GBM tumours hinder the effective treatment of patients[251]. For example, the blood-brain barrier reduces the concentration of drugs, especially those based on antibodies, which can be delivered to tumour tissue. Furthermore, the highly invasive nature of GBM cells represents a significant challenge with regards to surgical resection. Given the delicacy and significance of the tissue surrounding the tumour, it is not possible to cut around the tumour, with cancerous cells remaining at the margins and spawning re-growth. Indeed, tumours that form during GBM relapse generally occur proximal to the site of primary tumour removal. GBM stem-like cells are believed to be the source of tumour recurrence as they are highly resistant to the current treatments, such as temozolomide and radiation (see section 8.5.1)[253–256]. Additionally, GBM tumours exhibit high degree of heterogeneity, not just between different tumours but also in the same tumour[251].

8.4.2 Subtypes and Mutational Landscape

The current poor patient survival rate of GBM necessitates the development of more rational therapeutic approaches. To do this, it is critical to understand the oncogenic processes that support glioblastoma growth. With the advent of advanced sequencing technology, frequently mutated genes in GBM patients have been identified, leading to the classification of GBM into four different molecular subtypes: proneural, neural, classical, and mesenchymal[250,251]. Furthermore, these analyses found that the most frequently mutated genes in GBM broadly fall into three pathways: aberrant RTK signalling, Tp53 loss of function, and pRb deregulation. By identifying the most common transforming aberrations in each subtype, the best means of applying

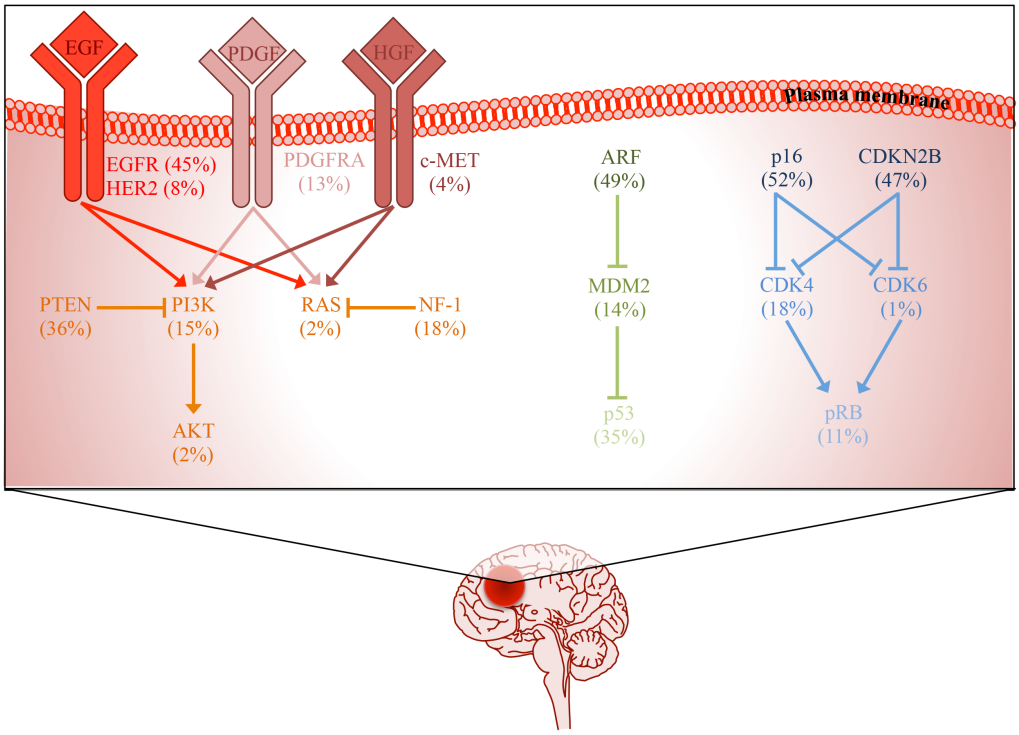

Figure 8.6 Summary of the Main Driving Mutations in Glioblastoma Multiforme
A select set of pathways are the focus of GBM oncogenic mutations: over-activity of RTK signalling (red/orange), loss of function of the Tp53 pathway (green), and deregulation of the pRb pathway (blue)[250].

Table 8.1 Summary of the Mutations Enriched in Glioblastoma Multiforme Subtypes
Analyses of genetic data gathered from patient tumours facilitated the definition that four 'subtypes' of GBM[250,251]

Subtype	Predominant Mutations	Frequency
Mesenchymal	*TP53*	32%
	NF-1	37%
	RB1	13%
	PTEN	32%
Neural	*TP53*	21%
	EGFR	26%
	NF-1	16%
	PTEN	21%
	ERBB2	16%
	PIK3R1	11%
Proneural	*EGFR*	16%
	TP53	54%
	PDGFRA	11%
	IDH1	30%
	PTEN	16%
	PIK3R1	19%
Classical	*EGFR*	32%
	EGFRvIII	23%
	PTEN	23%

targeted therapies may be clarified (Table 8.1)[250,257]. However, although these classifications may be useful in trying to generate efficient personalised medicines and understanding how resistance can develop, it is known that these subtypes are not completely distinct and several different subtypes can exist within one patient.

The efficacy of targeting specific signalling pathways with single-targeting agents has so far been poor in GBM[257]. For example, trials of the EGFR inhibitor erlotinib alongside the DNA alkylating agent temozolomide and radiotherapy exhibit only minor initial improvements, with no significant influence on progression-free survival[258,259]. Similar results were also seen with the PDGFR inhibitor imatinib[260]. The redundancy and cross talk that is known to exist between these RTK-mediated signalling pathways provides an opportunity for resistance to develop. Therefore, it is becoming increasingly clear that simultaneously treating with multiple targeting agents may be necessary to properly attenuate growth factor signalling or, alternatively, an agent that can target the activity of several processes simultaneously would be valuable[257].

8.5 Autophagy and Glioblastoma Multiforme

The rapid growth of GBM tumours outpaces the production of vasculature to deliver oxygen and nutrients to the proliferating tumour cells. Such a stressful environment requires the upregulation of survival pathways to maintain cell growth. One such pathway is autophagy and, indeed, several recent studies are starting to reveal a requirement for autophagy in GBM.

8.5.1 The Role of Autophagy in Glioblastoma Cancer Stem Cells

One hypothesis that may explain the heterogeneous oncogenic mutations found in GBM tumours is the generation of distinct populations of differentiated progeny from an oncogenic parental cancer stem cell (CSC) (Figure 8.7). CSCs are characterised by self-renewal, slow replication, and evasion of the Hayflick limit by the expression of telomerase[253,261–264]. Additionally, GBM recurrence may be attributable to the ability of CSCs to evade DNA damaging agents[253,256,265], although alternative reports suggest that there may be additional factors at play including the underlying mutational landscape[255].

CSCs are frequently observed in association with the hypoxic core of GBM tumours[266–271]. Hypoxia is a condition that upregulates autophagy and there is

increasing evidence that autophagy is required to regulate cell 'stemness' in a variety of different contexts, from normal haematopoietic stem cells to cancer stem cell maintenance[272–275]. Studies that have investigated the role of autophagy in GBM stemness have generated interesting results. For example, DRAM1 and p62, which are both implicated in autophagy induction, have been found to be important for the aggressive invasive qualities of GBM stem cells and their expression levels correlate negatively with patient survival[188].

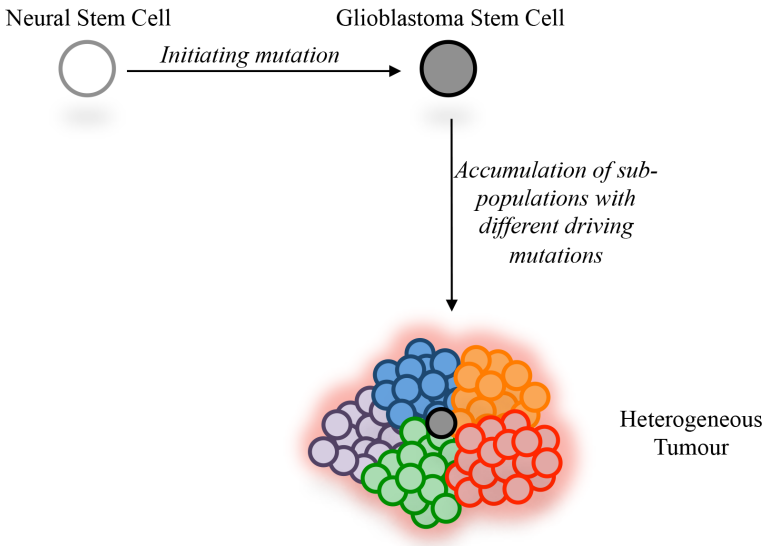

Figure 8.7 Schematic Model of a Potential Heterogeneous GBM Tumour Lineage Derived from a Single Glioblastoma Stem Cell

Conversely, CD133-positive GBM stem-like cells correlate with low levels of autophagy gene expression when treated with temozolomide, suggesting GBM CSCs have low levels of autophagy[254]. Moreover, Nager *et al*. revealed that Wnt/β-catenin signalling activity, which has been associated with stemness, inhibits autophagy in GBM cells[276,277]. By combining autophagy and Wnt signalling inhibitors the authors were able to significantly inhibit cell viability and tumourigenesis. This suggests a switch between autophagy and Wnt signalling that may represent the stemness state of GBM cells. When regarding non-drug treated cells, however, it seems that autophagy generally promotes cancer cell stem properties[278]. With such conflicting reports, it remains to be clarified how autophagy relates to GBM cancer stem cell states.

8.5.2 Modelling Glioblastoma Using the RCAS/*tv-a* System

The Replication-Competent Avian Sarcoma-leukosis virus LTR splice acceptor/Tumor Virus A (RCAS/*tv-a*) model of GBM been in use for over twenty years (Figure 8.8)[252,279]. This system uses avian virus-based vectors that can be propagated in chicken fibroblast cells ('DF-1'). Either the DF-1 cells or viral particles produced can be directly introduced into mouse brains. The somatic cell gene transfer system can specifically infect brain cells expressing the avian viral receptor tv-a. This receptor is expressed under the control of either *Nestin* promoter (*ntv-a*) in glial

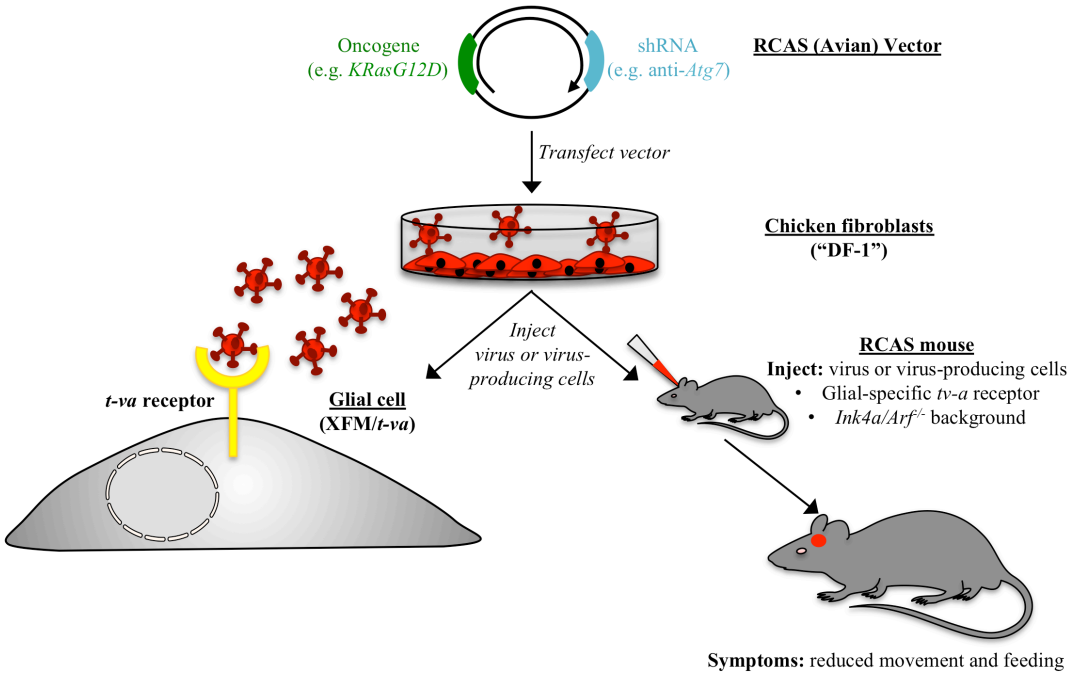

Figure 8.8 The RCAS/*tv-a in vitro* and *in vivo* Model Workflows
The RCAS vector harbouring oncogenic drivers and/or autophagy gene shRNA can be introduced into either mouse glial cells (XFM) or mice via the transgenic expression of the *tv-a* viral receptor under the control of a glial-specific promoter. DF-1 chicken fibroblast cells produce virus, and either this virus or the DF-1 cells can be introduced into the mouse brain to transform glial cells and induce GBM.

progenitors or the *Gfap* promoter in astrocyte progenitors (*gtv-a*) [279,280]. Chicken fibroblast cells produce high viral titres and thereby provide efficient vector delivery to target cells, following which they are then cleared from the mouse brain. RCAS viral vectors are extremely adaptable, making it possible to manipulate many of the genes that are commonly perturbed in glioblastoma. Vectors can be modified to concurrently express shRNA against genes of interest, (e.g. Atgs, Nf-1, or Tp53), and gene overexpression (e.g. KRas, Pdgf, or Cre recombinase)[280–283]. Studies utilising this system have reported a close resemblance to patient tumour histology[284]. By

inducing tumour formation *in situ* in the mouse brain the RCAS model is able to assay the influence of a particular process, such as autophagy, on tumourigenesis in the context of a fully functioning immune system.

Furthermore, this system can also be used to model GBM *in vitro*. Glial cells expressing the tv-a receptor are selected by puromycin from a mixed population of brain cells extracted from untreated mice[252]. These cells, called XFM/*tv-a*, can then be infected with viruses produced in DF-1 cells. Therefore, it is possible to carry out complementary studies in mice and cells using the RCAS/*tv-a* system.

8.5.3 Investigating Autophagy Inhibition as a GBM Treatment

Although autophagy has been identified as an attractive potential therapeutic target in glioblastoma, challenges remain regarding how to best study the impact of autophagy inhibition on GBM experimentally. Some of the approaches that have been employed to tackle this question are outlined below.

8.5.3.1 Genetically Engineered Mouse Models of Autophagy Inhibition

The genetic ablation of autophagy players is currently the only specific method to inhibit the pathway due to the non-specificity of inhibitors such as lysosome disrupting agents. Therefore, many researchers have chosen to prevent the expression of proteins by short-hairpin or small interfering RNA silencing, Cre-Lox gene deletion, or CRISPR/Cas9 gene modification.

The loss of autophagy gene expression in the whole-body of the mouse is preferably done by inducible means as autophagy is required for the survival of neonates[4]. Alternatively, by using tissue-specific promoters or xenografting of autophagy-deficient cell lines it is possible to achieve tumour-specific autophagy targeting, whilst retaining autophagy in the remainder of the animal and thereby maintaining its health. For example, some recent mouse xenograft studies have shown that autophagy promotes the growth of gliomas, with a particular focus on the employment of autophagy as a stress-response mechanism during hypoxia and therapeutic treatments[40,270,285]. However, a whole-body inhibition of autophagy is likely to be a more accurate representation of the application of a potential therapeutic that would be systemically introduced into patients. To make a whole-body *Atg5* knockout mouse viable, the Mizushima group expressed Atg5 specifically in neurons[286]. This rescued neurological functions such as neonatal suckling and therefore enabled

studies on the function of Atg5 in adult mice. However, this mouse is clearly not appropriate for studies in the brain, such as GBM modelling.

8.5.3.2 Chemical Inhibition of Autophagy in GBM

Although genetically engineered models offer a clean means of inhibiting autophagy, it is likely that a chemical inhibitor will be utilised in the clinic. With this in mind, several GBM studies have employed chemical inhibitors of autophagic flux that have yielded promising results. These are explored below.

8.5.3.2.1 Use of Lysosomal Disrupting Agents in GBM

Bafilomycin A1 and hydroxychloroquine (HCQ), both of which prevent the acidification of compartments such as autolysosomes, lysosomes, and endocytic vesicles, are the most common inhibitors used to inhibit autophagic flux *in vitro*. Of these, HCQ has been approved for human use and is routinely used as an anti-malarial drug. Clinical trials are currently on-going with the hope of re-purposing it to inhibit autophagy in cancer[225,287]. With regards to GBM, a phase I/II clinical trial of HCQ had mixed results[288]. Although LC3-II levels and autolysosomal numbers were increased in HCQ-treated patient blood cells, suggestive of successful lysosomal inhibition, the consistent and significant inhibition of autophagy was not achievable at the tolerated doses of the drug. Additionally, side-effects were reported in response to this drug in combination with other cytotoxic agents, including myelosuppression, and the pharmacokinetic variability lead the authors to suggest HCQ should not yet be utilised outside the clinical trial setting. These results suggest that a more specific autophagy inhibitor that could be specifically targeted to tumour tissue is needed to minimise toxicity.

Furthermore, we must take into consideration that these agents are far from specific to the autophagy pathway; they also inhibit of the acidification of the endolysosomal system. Inhibition of the endocytic pathway perturbs homeostasis and cellular function in both healthy and transformed cells. An example of one of the many processes that would be disrupted by this would be the detachment of ligands from receptor complexes (e.g. RTKs) that is required for the termination of their signalling[129]. Without this, the co-ordination of intracellular activities would be irresponsive to the extracellular conditions, whether that be adhesion or nutrient availability. Indeed, in contrast to studies that describe chloroquine synergising with RTK inhibitors, HCQ has also been seen to prolong endosomal signalling from RTKs

such as the insulin receptor[289]. Furthermore, reports are emerging that suggest that any potential efficacy of HCQ is in fact not attributable to autophagy inhibition[290,291]. Therefore, although several clinical trials are underway utilising HCQ in combination with traditional therapeutics[292], it is likely be beneficial to pursue other, more specific autophagy inhibitors.

8.5.3.2.2 Targeting Autophagy-Regulating Kinases

Kinase domains are generally considered appealing targets against which to develop inhibitors. The only kinase players that present a good opportunity to inhibit the autophagy pathway upstream are ULK1 and PIK3C3. To this end, inhibitors of ULK1 have recently been developed[293]. Unfortunately, these inhibitors also cross-react with other kinases, such as TBK1 and IKKϵ, making results more difficult to interpret and raising the possibility for side effects.

PIK3C3 inhibitors have also been developed, such as a highly specific compound called SAR405, which does indeed ablate LC3 lipidation[294]. This represents a significant advance from 3-MA, which also inhibits PIK3C1 activity[295]. However, as discussed above, PIK3C3 functions not only in autophagy but also in the endosomal pathway. Disruption of endosomal trafficking is likely to disrupt not just tumour cells but also normal cells and therefore side effects may be probable for patients.

8.5.3.2.3 Autophagy Inhibition as a Combination Therapy for GBM

Autophagy is frequently elevated following current GBM treatments. For example, treatment with the vascular endothelial growth factor (VEGF)-neutralizing antibody bevacizumab resulted in the upregulation of autophagy[270]. Here autophagy was seen to be important in tumour resistance to bevacizumab, with the knockdown of ATG7 reducing tumour burden in mouse xenografts in combination with this treatment. Additionally, autophagy is induced by both of the dual PI3K-mTOR inhibitors PI-103 or NVP-BEZ235 to promote resistance in xenografted cells[296].

Furthermore, upregulated autophagy correlates with GBM cell survival following temozolomide treatment, the most commonly used chemotherapy in GBM[297]. Mechanistically, high temozolomide doses have been seen to induce the autophagic targeting of aldehyde dehydrogenase 1A3 (ALDH1A3), an enzyme important in cancer cell 'stemness' and resistance to chemotherapies[298,299].

In addition to induction by chemotherapies, autophagy was also significantly induced by γ-radiation therapy in $CD133^+$ GBM stem-like cells, which was required for their

survival following exposure to this stress[300]. This was corroborated by a study by Huang *et al.*, who showed that expression of the serine/threonine kinase MST4 is upregulated in GBM cells following irradiation, which mediates the phosphorylation and activation of ATG4B thereby promoting LC3 lipidation[40]. Remarkably, using a specific inhibitor of ATG4B that was well tolerated in animals, NSC185058, the authors were able to demonstrate that this mechanism was important for *in vivo* tumourigenicity following exposure to radiation. This may well be the first step to the use of an autophagy-specific inhibitor to treat GBM. Overwhelmingly, these studies find autophagy to be a resistance mechanism against a wide variety of GBM treatment strategies, thereby representing exciting opportunity for advancing therapeutic efficacy.

There remains a lot to be resolved regarding autophagy inhibition as a GBM treatment. Firstly, HCQ may not be able to reach sufficient levels over the BBB to inhibit the lysosome in GBM tumours[288]. Moreover, although studies using the available autophagy inhibitors, including HCQ and SAR405, have suggested autophagy inhibition may be an efficacious cancer therapy, these come with caveats, such as lack of target or pathway specificity. In order to identify further 'druggable' targets that may be more specific to the autophagy pathway, it is necessary to better understand the regulation of the molecular machinery of autophagy. Furthermore, testing the impact of autophagy loss in an immune competent background is key to studying autophagy in GBM, particularly given that autophagy, senescence, immunity, and tumourigenicity are interconnected. Additionally, the reliance of different GBM molecular subtypes on autophagy has not been explored, although this is likely to produce significant variation in the efficacy of autophagy inhibition[201].

9 Aims and Objectives

As described above, interesting and unanticipated roles for autophagy in the cell are beginning to emerge that influence the development of pathologies such as cancer. In glioblastoma multiforme (GBM) there is strong suggestion that autophagy may promote properties that contribute to the aggressive phenotype that characterises these tumours. However, much of the research into the impact of autophagic flux on tumourigenesis in various models has relied on xenografts in immunocompromised animals and appears to produce highly context-dependent results. There is, therefore, a need for a study of autophagy in tumour formation in immunocompetent mice, particularly with regards to GBM.

The primary question at the commencement of this study therefore became: **'*Is autophagy able to drive pro-growth processes in GBM cells?*'**

To address this question, the following aims were proposed that were then challenged with a series of different experimental strategies.

Autophagy appears to play a context-dependent role in cancer. Is it required for gliomagenesis in an RCAS/*tv-a* mouse model? If so, what processes does it regulate? (*Chapter 11)*

As described above, there is currently a great deal of conflicting evidence regarding the influence of autophagy in cancer, which can be largely attributed to context-dependency. This extends to GBM, where it is unclear what impact autophagy has on tumour generation or maintenance, particularly in a host with a functional immune system. In an attempt to investigate this, constitutively active $KRas^{G12D}$ was used to drive the formation of tumours in the RCAS/*tv-a* mouse model alongside the concurrent knockdown of different autophagy players. To carry out a detailed molecular investigation of the phenotype, the oncogenic properties of transformed XFM/*tv-a* glial cells were assayed *in vitro*, using conditions akin to those experienced during GBM tumourigenesis.

Do the GBM subtypes experience differential reliance on autophagy for oncogenic transformation? (*Chapter 12)*

Disrupting autophagy in cells with different oncogenic mutations has been seen to cause varying outcomes in other cancer types, but how autophagy loss impacts

different glioblastoma subtypes is not known. To address this, here I used a set of cell lines derived from common parental XFM/*tv-a* cells and transformed them with different oncogenic perturbations. Autophagy was then inhibited and their capability for oncogenic anchorage-independent growth was assayed. In this way it was possible to directly compare the requirement for autophagy in models of different GBM subtypes.

Can autophagy influence the activity of receptor tyrosine kinase (RTK) signalling in glioblastoma? (*Chapter 13)*

Reports are emerging that autophagy proteins and autophagy-related endomembranes can have roles outside their canonical participation in autophagosome biogenesis, such as in the mediation of RTK signalling. However, the mechanistic details of this interplay are currently unclear. As aberrant RTK activity and downstream signalling is a key feature in GBM and is observed in the vast majority of tumours, I was interested to understand whether autophagy may regulate such signalling. To test this, transformed XFM/*tv-a* glial cells were stimulated with ligands for different RTKs and the signalling outputs were measured. I then set out to characterise the impact of autophagy on RTK signalling in this context.

How do autophagy proteins regulate RTK signalling? (*Chapter 14)*

Recent research has elucidated extensive connections between autophagy proteins, the endocytic pathway, and RTK signalling. Although studies have been able to show how autophagosome formation is facilitated by endosomes, little is known regarding how the presence of autophagy proteins in endosomal compartments impacts the homeostasis of the endocytic system and its function in regulating RTK signalling. In the XFM/*tv-a* glial cell model, the impact of autophagy loss on endosomal function was queried by its ability to properly traffic RTKs. Detailed molecular analyses ensued and revealed an intriguing novel role for autophagy.

10 Materials and Methods

10.1 Cell Culture

All cells were grown at 37°C with 5% CO_2, unless otherwise stated.

XFM/*tv-a* glial cells[280], DF-1 chicken fibroblasts (ATCC, CRL-12203), mouse embryonic fibroblasts (MEFs), and human embryonic kidney 293T (HEK293T) cells were cultured with Dulbecco's modified Eagle's media (DMEM) (Gibco) supplemented with 100 units/ml penicillin (Gibco) and 100 µg/ml streptomycin (Gibco), 2 mM L-glutamine (Gibco), and, unless otherwise specified, 10% fetal bovine serum (FBS) (Gibco). Transfection of DF-1 cells was achieved by culturing in Opti-MEM (Gibco) and application of DNA suspended in Lipofectamine 2000 (Life Technologies). XFM/*tv-a* cells were infected using 0.4 µm-filtered DF-1 virus-containing media, with the addition of 1 µg/ml polybrene (Sigma Aldrich).

Mouse neural stem cells (ANS4 and IENS) were kindly provided by Dr Steve Pollard (MRC Centre for Regenerative Medicine, University of Edinburgh) and have been described previously[301–304]. Cells were cultured with DMEM/Nutrient Mixture F-12 Ham (Sigma) supplemented with 1.45 g/L glucose (Sigma), 1% MEM non-essential amino acids (Gibco), 0.012% bovine serum albumin (Gibco), 100 µM beta-mercaptoethanol (Gibco), 0.5% B-27 supplement (Gibco), and 0.5% N-2 supplement (Gibco), with 10 ng/ml epidermal growth factor (EGF) and fibroblast growth factor (both Peprotech) and 1 µg/ml laminin (Sigma Aldrich) added to media immediately prior to plating cells. ANS4 and IENS cells were twice transfected with CRISPR/Cas9 vectors using the Amaxa Nucleofector kit (Lonza).

10.2 Vectors and Cloning

10.2.1 Transient gRNA Cloning Strategy

To target genes in ANS and IENS stem cells and MEF cells, transient non-selectable expression vectors for Cas9 and gRNAs were used (Table 10.1).

gRNAs were designed on http://crispr.mit.edu then inserted into the oligonucleotide sequences in Table 10.1 below.

For 50µl PCR: 0.5 µl Phusion polymerase and 10 µl HF Phusion Reaction Buffer (both New England Biolabs (NEB)), 2.5 mM dNTPs (Invitrogen), 2 µM forward

oligonucleotide and 2 μM reverse oligonucleotide. The resulting product was then gel purified.

PCR Cycles:	1X	98°C	30 sec
	30X	98°C	10 sec
		55°C	30 sec
		72°C	20 sec
	1X	72°C	20 sec

For 50 μl Digest: 2 μg vector, 2 μl Af1II, and 5 μl CutSmart buffer (both NEB).

For 4 μl Ligation: 4 ng PCR product, 30 ng linearised vector, 2 μl Gibson's Assembly Ligation Mix (Invitrogen). Incubated for 1 hr at 50°C.

Following transformation into DH5α cells, single colonies were selected from kanamycin-selection plates. These were tested for the presence of an insert using the 'transient gRNA sequencing primer' in Table 10.1.

10.2.2 RCAS-sgRNA Cloning Strategy

As described in introduction section 8.5.2, the RCAS vector can be used to generate viruses that efficiently infect XFM/*tv-a* cells to overexpress or knockdown proteins of interest. To develop this system further and generate CRISPR/Cas9-mediated knockout in XFM/*tv-a* cells, sgRNAs were cloned into the RCAS vector. These were then expressed alongside Cas9 delivered by lentivirus, which was selectable by blastocyodine (Sigma). The cloning strategy for this vector is described in further detail in results section 12.3.3 and briefly outlined below along with the sources of the reagents.

For 50 μl PCR: 0.5 μl Phusion polymerase and 10 μl HF Phusion Reaction Buffer (both New England Biolabs), 2.5 mM dNTPs (Invitrogen), 500 ng gRNA vector, 1.25 μM forward oligonucleotide and 1.25 μM reverse oligonucleotide to amplify gRNA sequence + U6 promoter + NotI digestion sites.

PCR Cycles:	1X	98°C	30 sec
	30X	98°C	10 sec
		55°C	45 sec
		72°C	45 sec
	1X	72°C	10 min

For 50 µl Vector NotI Digest: 3 µg RCAS empty vector, 3 µl NotI (NEB), 5 µl Buffer H. Followed by 5 min room temperature incubation with 2 µl calf alkaline phosphatase (NEB).

For 30 µl PCR Insert Digest: 400 ng purified PCR product, 0.5 µl NotI, 3 µl Buffer H.

For 10 µl Ligation: 90 ng digested PCR product, 30 ng digested vector, 0.5 µl T4 ligase and 1 µl T4 ligase buffer (both Promega). Incubated for 2 hr at room temperature.

Following transformation into DH5α cells, single colonies were selected from ampicillin-selection plates. These were tested for the presence of a correct insert firstly by KpnI digest (Promega) to determine correct orientation. As both the RCAS-Y vector and the U6 promoter sequence harbour one KpnI restriction site each, an excised product can only be generated from vectors where the PCR product was successfully inserted. The KpnI site lies upstream of the NotI cloning site in the RCAS-Y vector and at the start of the U6 promoter sequence. Therefore, a smaller digest product can distinguish between RCAS-Y vectors with a properly orientated gRNA insertion (6,035 bp+385 bp) from those with reversed insert (6,000 bp+420 bp). Secondly by sequencing with the 'RCAS-Y 5' sequencing primer' in Table 10.1 to ensure sequence fidelity was ensured.

10.2.3 Vectors

Vectors and sequencing primers used throughout this manuscript are summarised below in Table 10.1.

Table 10.1 Information on Vector Sequences, Derivations, and Cell Culture Usage

Backbone	Name	Source	Sequence Information	Bacterial/ Mammalian Resistance
RCAS (Addgene #11478)	RCAS-sh*LacZi*	Sub-cloned from corresponding $KRas^{G12D}$ vector	-	AMP
	RCAS-sh*Atg3*		shRNA target: GTACATCACTTA CGACAAA	
	RCAS-sh*Atg7*		shRNA target: CAGTTCAGAGCT AAATAAT	
	RCAS-sh*Atg13*		shRNA target: GAGAAGAATGTC CGAGAAT	
	RCAS-sh*Ulk1*		shRNA target: GAGCAAGAGCA CACGGAAA	
	RCAS-sh*Nf-1* #1	Cloned by PCR	shRNA target: CAAGGAGTGTCT GATCAAC	
	RCAS-sh*Nf-1* #2	Cloned by PCR	shRNA target: GGTTACAGGAGT TGACTGT	

	RCAS-sh*Tp53*	Cloned from KRas^{G12D} vector, which was a kind gift from Eric Holland[282–284]	shRNA target: GTACATGTGTAA TAGCTCC	
	RCAS-KRas^{G12D}-sh*LacZi*		shRNA targets as above	
	RCAS-KRas^{G12D}-sh*Atg3*			
	RCAS-KRas^{G12D}-sh*Atg7*			
	RCAS-KRas^{G12D}-sh*Atg13*			
	RCAS-KRas^{G12D}-sh*Ulk1*			
	RCAS-PDGFB		-	
	RCAS-CRE		-	
	RCAS-sg*Atg3* #1	Cloned by PCR from sgRNA vector	sgRNA target: AATGTGATCAAC ACGGTGAAGGG	
	RCAS-sg*Atg3* #3	Cloned by PCR from sgRNA vector	sgRNA target: TGTTTACACCGC TTGTAGCATGG	
	RCAS-sg*Atg7* #2	Cloned by PCR from sgRNA vector	sgRNA target: CTCACAGGTCCC CGGATTAGAGG	
	RCAS-sg*Atg7* #3	Cloned by PCR from sgRNA vector	sgRNA target: AGAAACTTGTTG AGGAGCATGGG	
	RCAS-sg*Atg16l1* #1	Cloned by PCR from sgRNA vector	sgRNA target: CCGAACTGCACA AGAAGCGTGGG	
	RCAS-sg*Atg16l1* #2	Cloned by PCR from sgRNA vector	sgRNA target: AAAAGCATGAC ATGCCAAATAGG	
	RCAS-sg*Atg16l1* #3	Cloned by PCR from sgRNA vector	sgRNA target: CCCACGCTTCTT GTGCAGTTCGG	
	RCAS-PDGFB	Kind gift from Eric Holland	-	
	RCAS-CRE	Kind gift from Eric Holland	-	
Transient sgRNA Vector (Addgene #41824)	sg*Atg3* #1	Cloned by PCR	sgRNA targets as above	KAN
	sg*Atg3* #3	Cloned by PCR		
	sg*Atg7* #2	Cloned by PCR		
	sg*Atg7* #3	Cloned by PCR Addgene #75228		
	sg*Atg16l* #1	Cloned by PCR		
	sg*Atg16l* #2	Cloned by PCR		
	sg*Atg16l* #3	Cloned by PCR		
Transient Cas9		Addgene #41815	-	AMP/Puro
Lentiviral Cas9		Addgene #52962	-	AMP/Blast
pBabe	FLAG-S-ATG16L1	Cloned by PCR	-	AMP/Puro
	GFP-ATG16L1	Cloned by PCR	-	AMP/Puro
	GFP-LC3	Cloned by PCR	-	AMP/Puro
	mCherry-Rab5	-	-	AMP/Puro
	mCherry-Rab7	-	-	AMP/Puro
	mCherry empty	-	-	AMP/Puro
mCherry-Rab4		Addgene #55125	-	KAN/Neo
mCherry-Rab11		Addgene #55124	-	KAN/Neo
pRetro	GFP-LAMP1	-	-	AMP/Puro
pEGFP C2	GFP-CD63	Addgene #62964	-	KAN/Neo
MSCV	EGFRvIII	Addgene #20737	-	AMP
sgRNA forward primer			TTTCTTGGCTTTA TATATCTTGTGG AAAGGACGAAA CACCG*_sgRNA_tar get_sequence*	-

sgRNA reverse primer	GACTAGCCTTATTTTAACTTGCTATTTCTAGCTCTAAAAC_*sgRNA_target_sequence_complement*_C	-
U6 promoter + sgRNA + NotI extension forward primer	ATAAGAATGCGGCCGCTGTACAAAAAAGCAGGCTTTAAAG	-
U6 promoter + sgRNA + NotI extension reverse primer	ATAGTTTAGCGGCCGCTAATGCCAACTTTGTACAAGAAAG	-
RCAS-Y 5' sequencing primer	CTCTGCTGGTGGCCTCGCGTACCACTG	-
Transient gRNA sequencing primer	GCAGGCTTTAAAGGAACCAATTCAGTC	-

10.3 Cell Treatments

10.3.1 Low Serum

XFM/tv-a cells were seeded under normal culture conditions with 10% FBS-supplemented DMEM 24 hr prior to changing to DMEM with 0.1% FBS for the indicated periods of time.

10.3.2 Hypoxia

Cells incubated for specified time prior to lysis on ice in Whitley H35 Hypoxystation set to 37°C, with 0.5% O_2.

10.3.3 Growth Factor Stimulation

Following 4 hr of serum starvation, the following factors were added for the durations specified at the following concentrations (unless otherwise stated): 20 ng/ml EGF (Peprotech #100-18b), 20 ng/ml FGF (Peprotech #100-18b), 10 ng/ml HGF (R&D Systems #2207-HG-025), and 10 ng/ml insulin (Sigma #I9278).

10.3.4 Soft Agar

10,000 cells were suspended in DMEM containing 0.4% agar (Sigma Aldrich) and plated on DMEM containing 0.8% agar in 6-well plates and grown for 3 weeks, replenished weekly with 0.4% agar DMEM. To stain colonies, 0.02% iodonitrotetrazolium (Sigma Aldrich) in PBS was applied overnight. Images of plates taken using Epson Perfection V750 Pro scanner and colonies quantified using ImageJ.

10.3.5 Culture on Low-Adherence Alvetex Scaffolds

5,000 cells were seeded per Alvetex 12-well insert (AVP005-12) that were then filled with each cell type's respective medium. Media was changed every 2-3 days for 14 days, before staining with 0.02% iodonitrotetrazolium (Sigma Aldrich) in PBS overnight. Images were then taken using Leica DM IL LED microscope using the Qimaging Retiga EXi Fast1394 Camera and quantified using ImageJ.

10.3.6 Acute Cell Suspension Assay

90% confluent 10 cm diameter plates of cultured cells were trypsinised then spun down. Cells were then re-suspended in media without FBS (XFM/*tv-a*) or without growth factors (IENS) and seeded onto plates without tissue culture treatment. Cells were incubated at 37°C for the indicated number of hours before harvesting cells for Western blot or addition of propidium iodide (images taken using Leica DM IL LED microscope using the Qimaging Retiga EXi Fast1394 Camera then quantified using ImageJ).

10.3.7 Inhibitors

The following inhibitors were used at the indicated final concentration: 20 nM bafilomycin (Sigma), 25 μM erlotinib (LKT labs, E6846), 10 μM PIK3C3 inhibitor (kind gift from Ian Ganley, PPU, University of Dundee), 10 μg/ml 3-MA (Sigma), 100 μM monensin, and 30 μM Dynasore (Sigma).

10.3.8 Autophagic Flux Assay

Autophagic function was measured by culturing cells in Hank's buffered salt solution (Gibco) for 2 hr with 20 μM bafilomycin (Sigma Aldrich).

10.4 Western Blotting and Antibodies

Cells were washed twice in ice cold PBS before lysis in RIPA buffer, as previously[305], with protease and phosphatase inhibitors (both Fisher Scientific: 1287-1640 and 1284-1650, respectively). Lysates were run on 8, 10, or 15% acrylamide gels then transferred onto nitrocellulose membranes. Membranes were blocked with 5% non-fat milk before probing with primary antibodies at room temperature for 2-4 hours or at 4°C overnight. The antibodies used throughout this manuscript for Western blotting are summarised in Table 10.2.

Table 10.2 Antibodies and beads used for Western blotting, immunofluorescence/immunohistochemistry (IF/IHC)), and immunoprecipitation (IP)

Epitope	Species	Company	Catalogue Number	Clone	Western Blotting Dilution	IF/IHC Dilution	Per IP
β-Actin	Mouse	Sigma	A5316	AC-74	1:3000	-	-
Akt	Rabbit	CST	9272	-	1:1000	-	-
Akt p- Ser473	Rabbit	CST	4060	-	1:3000	-	-
AP-2	Mouse	Thermo Fisher	MA1-064	AP6	1:500	-	-
Atg3	Mouse	MBL	M133-3	3E8	1:3000	-	-
Atg7	Rabbit	Sigma	A2856	-	1:3000	-	-
Atg13	Rabbit	Sigma	SAB4200100	-	1:2000	-	-
Atg14l1	Rabbit	MBL	PD026	-	1:1000	-	-
Atg16l1	Rabbit	MBL	PM040	-	1:3000	1:200	2 µl
Atg16l1	Mouse	MBL	M150-3	1F12	1:2000	-	1 µl
Beclin-1	Rabbit	MBL	PD017	-	1:2000	-	2 µl
BrdU	Mouse	BD Biosci	555627	3D4	-	1:200	-
Caspase-3	Rabbit	CST	9665	-	1:1000	-	-
EEA1	Rabbit	CST	3288	C45B10	1:2000	1:200	-
EEA1	Mouse	BD Biosci	410456	-	-	1:200	-
EGFR	Rabbit	Santa Cruz	sc-03	-	1:3000	1:500	2 µl
EGFR	Mouse	Millipore	04-290	13G8	1:2000	-	2.5 µl
EGFR p-Tyr1068	Rabbit	CST	2234	-	1:500	-	-
ERK	Rabbit	CST	9102	-	1:1000	-	-
ERK p-Thr202/ Tyr204	Rabbit	CST	4370	D13.14.4E	1:3000	-	-
GFP	Rabbit	CST	2956	D5.1	1:2000	-	-
HIF-1α	Mouse	R&D Systems	MAB1536	241809	1:500	-	-
IL-1β	Mouse	R&D Systems	AF-301-NA	-	1:500	-	-
IL-6	Mouse	R&D Systems	BAF-406	-	1:500	-	-
β1-Integrin	Rabbit	CST	4706	-	1:1000	-	-
Ki67	Rabbit	Vector Labs	VP-K451	-	-	1:200	-
KRas^{G12D}	Rabbit	CST	14429	-	1:1000	-	-
LC3B	Rabbit	Sigma	L7543	-	1:3000	-	-
Nestin	Mouse	BD Biosci	556309	RAT401	-	1:200	-
Nf-1	Rabbit	Bethyl Labs	A300-140A	-	1:1000	-	-
p27	Rabbit	CST	2552	-	1:1000	-	-
PCAF	Mouse	Santa Cruz	E-08	-	1:1000	-	-
PIK3C3	Rabbit	CST	4263	D9A5	1:3000	-	2 µl
Rab4	Rabbit	CST	2167	-	1:2000	1:100	-
Rab5	Rabbit	CST	3547	C8B1	1:1000	1:200	-
Rab5-GTP	Mouse	New East Biosciences	26911	-	-	-	1 µl
Rab7	Rabbit	CST	9367	D95F2	1:1000	1:200	-
Rab11	Rabbit	CST	5589	D4F5	1:1000	1:200	-
Rab11-GTP	Mouse	New East Biosciences	26919	-	-	-	1 µl
Ras	Mouse	Calbiochem	OP40	RAS10	1:1000	-	-
Ras^{G12D}	Rabbit	CST	14429	D8H7	1:3000	-	-
pRb/p105	Mouse	BD Biosci	554136	G3-245	1:1000	-	-

Rubicon	Rabbit	MBL	PD027	-	1:1000	-	-
S6	Rabbit	CST	2217	-	1:3000	-	-
S6 p-Ser235/236	Rabbit	CST	4858	-	1:3000	-	-
TBK1 p-Ser172	Rabbit	CST	5483	D52C2	-	1:200	
Tp53	Mouse	CST	2524	1C12	1:1000	-	-
α-Tubulin	Rabbit	CST	2144	-	1:3000	-	-
ϒ-Tubulin	Mouse	Sigma	T6557	GTU-88	1:2000	-	-
ULK1	Rabbit	Sigma	A7481	-	1:2000	-	-
UVRAG	Mouse	MBL	M160-3B	Clone 1H4	1:2000	-	-
FLAG Tag	Mouse	Sigma	F1804	M2	-	1:200	-
HA Tag	Mouse	Thermo Scientific	26183-HRP	-	1:1000	-	-
S Tag	Rabbit	Bethyl Labs	A190-135A	-	-	1:200	1 µl
Normal Rabbit IgG	Rabbit	Millipore	12-370	-	-	-	0.5-1 µl
Rabbit (HRP Secondary)	Goat	CST	7074	-	1:5000	-	-
Mouse (HRP Secondary)	Goat	CST	7076	-	1:5000	-	-
Rabbit (Alexa488 Secondary)	Goat	Invitrogen	A11008	-	-	1:500	-
Rabbit (Alexa594 Secondary)	Goat	Invitrogen	A11012	-	-	1:500	-
Mouse (Alexa488 Secondary)	Goat	Invitrogen	A1101	-	-	1:500	-
Mouse (Alexa594 Secondary)	Goat	Invitrogen	A11032	-	-	1:500	-
Mouse (Alexa647 Secondary)	Goat	Invitrogen	A28181	-	-	1:500	-
Protein G4 Sepharose FastFlow Beads	-	GE Healthcare	17-0618-01	-	-	-	7.5 µl
GFP-Trap Beads	-	Chromotek	gta-20	-	-	-	5 µl
Streptavidin-Sepharose High Performance Beads	-	GE Healthcare	17-5113-01	-	-	-	7.5 µl

10.5 Reverse Phase Protein Array

Protein analysis by RPPA was carried out as previously described[306]. Cells were either untreated (10% FBS) or starved of serum for 4hr then stimulated with 20 ng/ml EGF or 1% FBS for the indicated length of time. Cells were then lysed with MD Anderson lysis buffer (1% Triton X-100, 50 mM HEPES (pH 7.4), 150 mM sodium chloride, 1.5 mM magnesium chloride, 1 mM EGTA, 100 mM sodium fluoride, 10

mM sodium pyrophosphate, 1 mM sodium vanadate, 10% glycerol, supplemented with Complete ULTRA protease inhibitor and PhosSTOP phosphatase inhibitor cocktails). Following normalisation of protein concentration using the Bradford assay, samples were dotted on nitrocellulose-coated slides (Grace Bio-Labs) in serial dilution using Aushon Biosystems 2470 array platform. Slides were probed with an array of different validated antibodies (Table 10.3) that were detected using anti-rabbit and –mouse DyLight800-conjugated secondary antibody (New England BioLabs) and read by the InnoScan 710-IR scanner (Innopsys). Relative fluorescence was determined using Mapix software (Innopsys). Values presented represent the mean of technical triplicates ± SEM.

Table 10.3: Antibodies Used In Reverse Phase Protein Array Assay

Epitope	Company	Catalogue Number	Species
4E-BP1 P Ser65	CST	9451	Rabbit
4E-BP1 P Thr37,Thr46	CST	2855	Rabbit
Akt	CST	9272	Rabbit
Akt P Ser473	CST	4060	Rabbit
Akt P Ser473	CST	9271	Rabbit
Akt P Thr308	CST	2965	Rabbit
AMPK alpha	CST	2532	Rabbit
AMPK alpha P Thr172	CST	2535	Rabbit
ATM	Merck (Calbiochem)	PC116	Rabbit
ATM/ATR Substrate P Ser/Thr	CST	2851	Rabbit
Aurora A/B/C P Thr288/Thr232/Thr198	CST	2914	Rabbit
Bad P Ser112	CST	9291	Rabbit
Bad P Ser136	CST	9295	Rabbit
Bak	Epitomics	1542-1	Rabbit
Bax	Epitomics	1063	Rabbit
Bcl-2	Epitomics	1017-1	Rabbit
Bcl-x	Epitomics	1018	Rabbit
beta-actin	CST	4970	Rabbit
beta-Catenin	CST	9562	Rabbit
beta-Catenin P Ser33,Ser37,Thr41	CST	9561	Rabbit
beta-Catenin P Thr41,Ser45	CST	9565	Rabbit
beta-Tubulin	Abcam	ab6046	Rabbit
Bid	Epitomics	1008	Rabbit
Bim	Epitomics	1036	Rabbit
Bim P Ser69	CST	4585	Rabbit
BRCA1	CST	9010	Rabbit
Calmodulin	Calbiochem	-	-
Calpain2	CST	2539	Rabbit
Calpastatin	CST	4146	Rabbit
CamKII alpha (22B1) P Thr286	Abcam	ab2724	MouseIgG1
CamKII P Thr286	CST	3361	Rabbit

Caspase 3	CST	9662	Rabbit
Caspase 3 cleaved	CST	9664	Rabbit
cdc25A	CST	3652	Rabbit
cdc25c P Ser216	CST	4901	Rabbit
CDK1 (p34cdc2) P Tyr15	CST	9111	Rabbit
CDK2	Epitomics	1134-1	Rabbit
Chk1 P Ser345	CST	2348	Rabbit
Chk2 P Thr68	CST	2661	Rabbit
c-Jun N-term	Epitomics	1254-1	Rabbit
c-Jun P Ser73	CST	9164	Rabbit
c-Myc	CST	5605	Rabbit
c-Myc P Thr58,Ser62	Epitomics	1203-1	Rabbit
CREB	CST	9197	Rabbit
CREB P Ser133	Millipore (Upstate)	06-519	Rabbit
CrkL	CST	3182	MouseIgG1
CrkL P Tyr207	CST	3181	Rabbit
Cyclin D1	CST	2926	MouseIgG2a
Cyclin D1 P Thr286	CST	3300	Rabbit
E-Cadherin	CST	3195	Rabbit
eEF2	CST	2332	Rabbit
EGFR P Tyr1068	Invitrogen (Biosource)	44-788G	Rabbit
EGFR P Tyr1173	CST	4407	Rabbit
ErbB-1/EGFR	CST	2232	Rabbit
ErbB-2/Her2/EGFR	Dako	A0485	Rabbit
ErbB-2/Her2/EGFR P Tyr1248/Tyr1173	CST	2244	Rabbit
ErbB-3/Her3/EGFR	CST	4754	Rabbit
ErbB-3/Her3/EGFR P Tyr1289	CST	4791	Rabbit
FAK1	CST	3285	Rabbit
FAK1 P Y397	CST	3283	Rabbit
FLT3 P Tyr591 P Tyr591	CST	3461	Rabbit
FRA1 (R20)	Santa Cruz	sc-605	Rabbit
GAPDH	Abcam	ab9484	MouseIgG2b
GFAP	Abcam	ab7260	Rabbit
GSK 3 B	CST	9315	Rabbit
GSK-3-alpha/beta P Ser21/Ser9	CST	9331	Rabbit
GSK-3-beta	CST	9315	Rabbit
GSK-3-beta P Ser9	CST	9336	Rabbit
Hexokinase	CST	2867	Rabbit
Histone H2A.X P Ser139	Millipore (Upstate)	05-636	MouseIgG1
HSP27 (HSPB1)	CST	2402	MouseIgG1
HSP27 (HSPB1) P Ser78	CST	2405	Rabbit
IGF-1R beta P Tyr1162,Tyr1163	Invitrogen (Biosource)	44-804G	Rabbit
IkB-alpha	CST	4812	Rabbit
IkB-alpha P Ser32	CST	2859	Rabbit
IKK alpha/beta P Ser176/Ser177	CST	2078	Rabbit
IRS-1	CST	2382	Rabbit
IRS-1 P S636/639	CST	2388	Rabbit
JAK1	CST	3332	Rabbit

JAK1 P Tyr1022,Thr1023	Invitrogen (Biosource)	44-422G	Rabbit
Ki-67 (Annexin II, p36)	Beckton Dickinson	610968	MouseIgG1
LKB1	CST	3047	Rabbit
MAPKAPK-2	Epitomics	1497-1	Rabbit
MAPKAPK-2 P Thr334	CST	3041	Rabbit
M-CSF P Tyr723	CST	3155	Rabbit
MEK1/2	CST	9122	Rabbit
MEK1/2 P Ser217/221	CST	9154	Rabbit
Met	CST	4560	Rabbit
Met P	Signalway	11238	Rabbit
Met P Tyr1234	Signalway	11227-1	Rabbit
MNK1 (MKNK) P Thr197,Thr202	CST	2111	Rabbit
MSK1 P Ser376	CST	9591	Rabbit
mTOR	CST	2972	Rabbit
mTOR P Ser2448	CST	2971	Rabbit
mTOR P Ser2448	CST	2971	Rabbit
mTOR P Ser2481	Millipore (Upstate)	09-343SP	Rabbit
NFkB p105/p50	GeneTex	GTX110585	Rabbit
NFkB p65 Ser536	CST	3033	Rabbit
P Myosin light chain	CST	3761	Rabbit
p21 CIP/WAF1	CST	2946	MouseIgG2a
p21 CIP/WAF1 p Thr145	Santa Cruz	20220-R	Rabbit
p38 MAPK	CST	9212	Rabbit
p38 MAPK PThr180,Tyr182	CST	9211	Rabbit
p44/42 MAPK (ERK1/2)	CST	9102	Rabbit
p44/42 MAPK (ERK1/2) P Thr202/Thr185,Tyr204/Tyr187	CST	4370	Rabbit
p53	CST	9282	Rabbit
p53 P Ser15	CST	9284	Rabbit
p70 S6 Kinase	CST	9202	Rabbit
p70 S6 Kinase P Thr389	Epitomics	1175-1	Rabbit
p70 S6 Kinase P Thr421,Ser424	CST	9204	Rabbit
p90 S6 kinase (Rsk1-3)	Santa Cruz	sc-231	Rabbit
p90 S6 kinase (Rsk1-3) P Thr359,Ser363	CST	9344	Rabbit
PABP1	CST	4992	Rabbit
PARP	CST	9542	Rabbit
PARP cleaved Asp214	CST	9541	Rabbit
PDGFR P Tyr751	CST	4549	Rabbit
PDGFR P Tyr1021	CST	2227	Rabbit
PDK-1	CST	3062	Rabbit
PDK-1 P Ser241	CST	3061	Rabbit
PI3 Kinase p110-alpha	CST	4249	Rabbit
PKA	Abcam	ab26322	Rabbit
PKA RII P Ser96	Epitomics	1151-1	Rabbit
PKC (pan) P Ser660 (beta-2)	CST	9371	Rabbit
PKC substrate P (R/K)X(S*)(Hyd)(R/k)	CST	2261	Rabbit
PKC-alpha	Beckton Dickinson	610108	MouseIgG2b
PKC-alpha P Thr638	Abcam	ab32502	Rabbit

PKC-gamma P Thr514	GeneTex	GTX25778	Rabbit
PKC-zeta	CST	9372	Rabbit
PKC-zeta/lambda P Thr410/403	CST	9378	Rabbit
PKM2 XP(R)	CST	4053	Rabbit
PLC-gamma1	CST	2822	Rabbit
PLC-gamma1 P Tyr783	CST	2821	Rabbit
Prohibitin	Santa Cruz	sc-28259	Rabbit
PTEN	CST	9552	Rabbit
PTEN P Ser380,Thr382,Thr383	CST	9554	Rabbit
Puma	CST	4976	Rabbit
Raf P Ser259	CST	9421	Rabbit
Raf P Ser338	CST	9427	Rabbit
Raf1 (C-12)	Santa Cruz	sc-133	Rabbit
Rap1	CST	4938	Rabbit
Ras	Beckton Dickinson	8100001	Mouse
Rb	Epitomics	2655-1	Rabbit
Rb P Ser807,Ser811	CST	9308	Rabbit
Rb P Ser780	CST	9307	Rabbit
Rsk2 Pser 227	CST	3556	Rabbit
S6 Ribosomal Protein	CST	2217	Rabbit
S6 Ribosomal Protein	CST	2217	Rabbit
S6 Ribosomal Protein	CST	2211	Rabbit
S6 Ribosomal protein P Ser235,Ser236	CST	2211	Rabbit
S6 Ribosomal protein p Ser240,Ser244	CST	2215	Rabbit
SAPK/JNK	CST	9258	Rabbit
SAPK/JNK P	CST	4668	
SAPK/JNK P Thr182,Tyr185	CST	4668	Rabbit
SAPK/JNK P Thr183,Tyr185	CST	9251	Rabbit
SHP2 P Tyr542	CST	3751	Rabbit
SirT1 (IF3)	CST	8469	Mouse
Smad1/5 P Ser463/Ser465	CST	9516	Rabbit
Smad2 P Ser465,Ser467	CST	3108	Rabbit
Smad2/3 P Ser465/Ser423,Ser467/Ser425	CST	9510	Rabbit
Smad3 P Ser423,Ser425	CST	9520	Rabbit
SQSTM1	CST	8205	Rabbit
Src	CST	2109	Rabbit
Src (family) P Tyr416	CST	2101	Rabbit
Stat1	CST	9176	MouseIgG1
Stat1 P Ser727	Invitrogen (Biosource)	44-382G	Rabbit
Stat1 P Tyr701	CST	9171	Rabbit
Stat3	CST	9132	Rabbit
Stat3 P Tyr705	CST	9131	Rabbit
Stat3 P Tyr705	CST	9138	MouseIgG1
Stat5	Invitrogen (Biosource)	44-368G	Rabbit
Stat5	CST	9351	Rabbit
Stat6	CST	9362	Rabbit
Stat6 P Tyr641	CST	9361	Rabbit
Survivin	CST	2808	Rabbit

Tau	Epitomics	2368-1	Rabbit
Tau P Ser396	Epitomics	1178-1	Rabbit
Tsc-2 (Tuberin)	CST	3612	Rabbit
Tsc-2 (Tuberin) P Thr1462	CST	3617	Rabbit
Tuberin P S1387	CST	5584	Rabbit
Tyk2 P Tyr1054,Tyr1055	CST	9321	Rabbit
Ubiquitin (P4D1)	CST	3936	MouseIgG1
VEGFR P Tyr1059	CST	3817	Rabbit
VEGFR P Tyr1175	CST	3770	Rabbit
VEGFR P Tyr951	CST	4991	Rabbit
VEGFRP Tyr1175	CST	2478	Rabbit
XIAP	CST	2045	Rabbit
YB1	CST	4202	Rabbit
Zap70	CST	2705	Rabbit
cdc2	CST	9112	Rabbit
BCL2 P	CST	2827	Rabbit
FOX01 P	CST	9461	Rabbit
HDAC 4/5/7 P	CST	3443	Rabbit
EZRIN P	CST	3149	Rabbit
FAK P Y397	Invitrogen (Biosource)	44624G	Rabbit
Stat 5	CST	9363	Rabbit
TBK1/NAK	CST	3504	Rabbit
P44/P42	CST	4696	Rabbit
PLK1	CST	3472	Rabbit

10.6 Immunohistochemistry

Mouse brains harvested from animals were fixed in 10% formalin for 24–72 h and then transferred to 70% ethanol. Samples were then paraffin-embedded, sectioned and stained with H&E by Histoserv Inc., Maryland. Similarly, MEFs derived from wildtype or atg7 knockout cells were pelleted and processed for paraffin embedding. For immunocytochemistry staining, paraffin-embedded sections were treated with xylene twice for 10 min each before being sequentially hydrated in decreasing concentrations of ethanol. Epitope retrieval was performed by incubating slides in 10 mM sodium citrate buffer, pH 6 for 15 min at 95°C then allowed to cool for 20–45 min. Subsequently, slides were blocked with TBST (150 mM NaCl and 10 mM Tris pH 7.5, 0.1% Tween 20 [Sigma, P5927] + 5% BSA [Thermo Fisher Scientific, BP1605-100]) for 45 min, and incubated with primary antibodies overnight at 4°C. Subsequently, slides were incubated with Alexa-conjugated secondary antibodies and images acquired using a Nikon Eclipse Ti-U Confocal Microscope.

10.7 Beta-Galactosidase Assay for Senescence

Cellular senescence was measured using an SA-GLB1 assay[221]. Briefly, cells were fixed with 0.5% glutaraldehyde then incubated with X-gal staining solution, pH 6.0 (1 mM $MgCl_2$ phosphate-buffered saline [Fisher BioReagents, BP399], X-gal [Thermo Fisher Scientific, R0941], 0.12 mM $K3Fe[CN]_6$ [Sigma, 60299], 0.12 mM $K4Fe[CN]_6$ [Sigma, 60279]) overnight at 37°C. Images of cells were taken using a Nikon Digital Sight DS-L3.

10.8 BrdU Proliferation Assay

For the BrdU incorporation assay, cells were pulsed with 50 μM BrdU (Sigma, B5002) for 18 h followed by fixation with 3.7% paraformaldehyde and permeabilization with 0.2% Triton-X100. Cells were blocked with 0.2% gelatin-fish (Sigma, G7765) in 5% BSA-phosphate-buffered saline and incubated with anti-BrdU primary antibody, 0.5 U/L DNase (Sigma, D4527), and 1 mM $MgCl_2$ in blocking solution. Subsequently, slides were incubated with Alexa-conjugated antibodies and 1 μg/ml DAPI; images were acquired using ImageXpress and analyzed using MetaXpress software.

10.9 Cell Fractionation

The fractionation buffer base was made of 150 mM NaCl (Sigma), 25 mM HEPES pH 7.5 (ThermoFisher), 1 mM β-mercaptoethanol (Sigma), 0.2 mM $CaCl_2$ (Sigma), 0.5 mM $MgCl_2$ (ThermoFisher) +1:100 phosphatase and protease inhibitors (both Fisher Scientific: 1287-1640 and 1284-1650, respectively). This was supplemented with 1 μg/ml digitonin (Sigma, D141) for 30 min at 4°C before spinning 1 min 13,000 rpm to obtain the '*cytosolic fraction'*. The resulting pellet was washed three times with the fractionation buffer then 0.5% NP-40 (Source Bioscience, ABE5465) was added, the pellet was vortexed, then the lysate was spun 1 min 13,000 rpm leaving the *'membrane fraction'* in the supernatant. The pellet was again washed then the *'nuclear fraction'* was re-suspended in 1X SDS loading buffer.

10.10 Immunoprecipitation

Detergent-free buffer: 150 mM NaCl (Sigma), 25 mM HEPES pH 7.5 (Fisher), 1 mM β-mercaptoethanol (Sigma), 0.2 mM $CaCl_2$ (Sigma), 0.5 mM $MgCl_2$ (Fisher) +1:100 phosphatase and protease inhibitors (both Fisher Scientific: 1287-1640 and 1284-

1650, respectively). To this buffer was added either 1 µg/µl digitonin (for fractionation: Sigma, D141), 0.5% NP-40 (for fractionation: Source Bioscience, ABE5465), or 0.8% CHAPS (for Beclin-1 and PIK3C3 IPs: Sigma). IPs were also supplemented with Mg132 (Sigma).

Rab-GTP IP buffer: 25 mM Tris pH 7.5, 30 mM $MgCl_2$, 150 mM NaCl, 1% NP-40 +1:100 phosphatase and protease inhibitors (both Fisher Scientific: 1287-1640 and 1284-1650, respectively) and Mg132 (Sigma).

10.11 Cell Surface Biotinylation Endocytosis/Recycling Assay

Cells were seeded 1 day in advance. Then, to accumulate receptors on the plasma membrane, cells were starved of serum for 4 hr. After washing twice with ice-cold PBS, cells were incubated with 0.2 mg/ml biotin (EZ-Link sulfo-NHS-SS-biotin Pierce, ThermoFisher) 30 min 4°C. Excess biotin was washed off with PBS then quenched with 20 mM glycine (Alfa Aesar, J61855) in PBS 15 min 4°C. Endocytosis was induced with serum-free media supplemented with 2 ng/ml EGF 15 min 37°C. Plates were then returned to ice and washed with ice-cold PBS. To remove un-endocytosed biotin, cells were incubated with stripping buffer (37.5 mM NaOH (Sigma), 37.5 mM NaCl (Fisher), 25 mM L-glutathione (Sigma), 25 mM MesNA (Sigma), 0.5% BSA (Fisher)) 30 min 4°C, washed, then quenched with 20 mM iodoacetamide (Sigma) in PBS 20 min 4°C. To allow recycling, cells were returned to 37°C with EGF media for a further 15 min. The stripping procedure was then repeated. Thus, both endocytosis and recycling rates can be measured according to the quantity of protein (e.g. EGFR) that is biotinylated, as measured by pulling down overnight 4°C with streptavidin-sepharose beads following cell lysis with RIPA. Beads were then washed three times with RIPA and 300 mM NaCl RIPA, followed by 2 washes with PBS, then resuspended in 2X SDS loading buffer and subjected to Western blotting.

10.12 *in vitro* EGFR Kinase Assay

Cells were serum-starved for 4 hr before they were lysed in kinase assay buffer (1% NP-40 (Source Bioscience, ABE5465, 20 mM HEPES pH 7.5 (Fisher), 150 mM NaCl (Fisher), 10 mM $MgCl_2$(Fisher), 1 mM EDTA (Sigma), 1 mM DTT (Sigma), 1:50 phosphatase inhibitors, 1:100 protease inhibitors) and spun 13,000 rpm 1 min. In a total reaction volume of 60 µl, 4.2 µl of phosphocreatine (Sigma), 1 mM ATP

(Sigma) and 50 ng EGF were added on ice, before incubation at 30°C for 15 min before the addition of 4X SDS loading buffer and incubation at 95°C.

10.13 Microscopy Analyses

10.13.1 Cell Culture Imaging

Images of cells in culture were taken on a Leica DM IL LED microscope using the Qimaging Retiga EXi Fast1394 Camera.

10.13.2 Fixed Sample Preparation

Cells were plated on glass coverslips in a 6-well plate 24 hr prior to experiment, then were treated as indicated for each experiment. Cells were washed twice with ice-cold PBS then fixed with PFA (3.7% PFA (Sigma) 200 mM HEPES pH 7.4 (ThermoFisher) in PBS (ThermoFisher)) 10 min on ice and 20 min RT. Either 0.1% Triton X-100 (Sigma, T9284) 5 min or, in the case of Atg16l1 staining, methanol (ThermoFisher) 3 min were used to permeabilise cells. 1% BSA in PBS was used to block for 15 min. Coverslips were then incubated with 1:200 primary antibodies (Table 10.2) in blocking buffer either 4°C overnight or 37°C 3 hr. Following washing, cells were incubated 1 hr RT with 1:500 dilution of appropriate secondary antibody conjugated to Alexa fluorophores (Table 10.2). Finally, nuclei were stained with 1 µg/µl DAPI (Sigma) 5 min RT then coverslips were mounted with Prolong Gold Anti-fade (Invitrogen).

10.13.3 Confocal Microscopy Analysis

Leica SP5 confocal microscope was used for fixed samples. The 488 nm and 594 nm laser lines were used as well as the UV line for DAPI. 63X objective was used for the majority of experiments, except for Alexa555-Transferrin recycling analyses. For the majority of experiments, Pearson's correlation coefficient was obtained using the unbiased ImageJ Coloc2 plugin. However, to calculate the Pearson's correlation coefficient for 555-EGF colocalisation with EEA1, Rab5, and Rab7 it was necessary to use Imaris Coloc software was used to identify EGF vesicles due to their low fluorescence intensity that was incompatible with the use of Coloc2.

Where co-localisation is given as a percentage of total vesicles that are co-localised, vesicle quantification was undertaken manually.

10.13.4 Perinuclear EGFR Quantification

Using ImageJ software, circles were drawn around the nucleus with diameter 30 μm. The quantity of EGFR inside these parameters was measured and classed as 'perinuclear'.

10.13.5 Transferrin Recycling Analysis

Following 4 hr serum starvation, serum-free media with 20 ng/ml Alexa555-Transferrin (Tfn) (Invitrogen T35352) was applied for 15 min. Cells were then either fixed with 3.7% PFA or chased with serum- and Tfn-free media for 5 or 15 min before fixation to allow recycling of the Tfn receptor and expulsion of fluorescent Tfn. The Tfn levels in cells following these treatments were imaged by confocal microscopy at 20X magnification and quantified using ImageJ.

10.13.6 EGF Uptake Quantification

20 ng/ml Alexa555-EGF was applied to cells plated in a 12-well plate for the specified length of time following 4 hr serum starvation. Cells were then fixed using 3.7% PFA and stained for DAPI. Fluorescence readings were taken using the ImageXpress plate reader and analysed using ImageJ software.

10.13.7 Live Cell Imaging and Analysis

Cells were plated on glass-bottom plates (World Precision Instruments, FluoroDish FD35-100) and starved of serum for four hours before the addition of Alexa555-EGF. Live cell imaging was performed using the Andor Dragonfly spinning disc confocal microscope. Images were captured using 63X objective lens and the 488 and 594 nm laser lines. Vesicle speed, direction, and duration were analysed using Imaris Cell and Tracking software.

10.13.8 Super-Resolution Microscopy and Analysis

Samples were prepared on Zeiss High-Performance coverslips (thickness no. 1.5, 18x18 mm) and incubated with antibodies as described above. The Nikon NSIM structured-illumination microscope was used to capture images with a 100X objective and the 488, 594, 647, and UV laser lines. Images were then reconstructed using the NIS Elements software.

10.13.9 PI(3)P Probe Levels and Detection

The FYVE-Alexa488 probe used to detect PI(3)P was kindly donated by Ian Ganley (PPU, University of Dundee) and cells were stained for PI(3)P as previously described[1]. Briefly, cells plated on coverslips were treated with serum starvation for 4 hr before 15 min EGF stimulation (2 ng/ml). Cells were washed with PBS and placed in glutamate buffer (25 mM HEPES pH 7.4, 25 mM KCl, 2.5 mM MgAc, 5 mM EGTA, 150 mM potassium glutamate). Coverslips were then briefly submerged in liquid nitrogen, brought back to room temperature then returned to glutamate buffer. Following washing with glutamate, cells were then fixed with PFA (3.7% PFA, 200 mM HEPES pH 7.4) for 30 min. PFA was quenched using two washes and 10 min incubation in DMEM with 10 mM HEPES pH 7.4. After blocking in 1% BSA in PBS, cells were incubated with 1:200 primary antibody against EEA1 3 hr 37°C. Then they were incubated with 1:300 FYVE-Alexa488 and 1:500 anti-mouse-Alexa594 for 1 hr RT. Cells were then washed, stained with 1 µg/µl DAPI (Sigma) 5 min RT, then mounted with Prolong Gold Anti-fade (Invitrogen).

10.13.10 Electron Microscopy Analysis

Cells were starved for 4 hr before they were trypsinised and pelleted. Cells were then washed twice with PBS and fixed with glutaraldehyde. Sections were then cut using a diamond knife by the University of Edinburgh electron microscopy facility.

10.13.11 Serum Starvation Cell Death Assay Analysis

To induce cell death, cells plated in a 12-well plate were starved of serum for 24 hr in the presence or absence of 20 ng/ml EGF or 10 ng/ml HGF. 1 µg/ml of propidium iodide dye (Caymen Chemical Company, #10008351) was added to cells and measured using the Tecan Spark20M plate reader. Cells were then fixed with 3.7% PFA and stained for DAPI, which was also measured using the Tecan reader. The ratio of propidium iodide/DAPI relative fluorescence signals was then calculated and made relative to RCAS-Y control cells. Representative images were taken on a Leica DM IL LED microscope using Qimaging Retiga EXi Fast1394.

10.13.12 Statistical Analyses

Experiments were repeated a minimum of three times and represented in all cases as mean ± S.E.M. Statistical significance was calculated using two-tailed unpaired *t*-tests with *<0.05, ** <0.01, ***<0.005.

11 Autophagy is Required for KRASG12D-driven Glioblastoma

11.1 Introduction

11.1.1 Modelling GBM Using Constitutively Active KRasG12D

The overwhelming plethora of mutations exhibited in glioblastoma multiforme (GBM) makes it challenging to choose an accurate model system in which to best test the relevance of select cellular processes in gliomagenesis. Lying at the heart of the aberrant mutational landscape, however, is the proto-oncogene and key signalling integrator, Ras (Figure 11.1). Therefore, Ras is a good candidate to manipulate in a model of GBM.

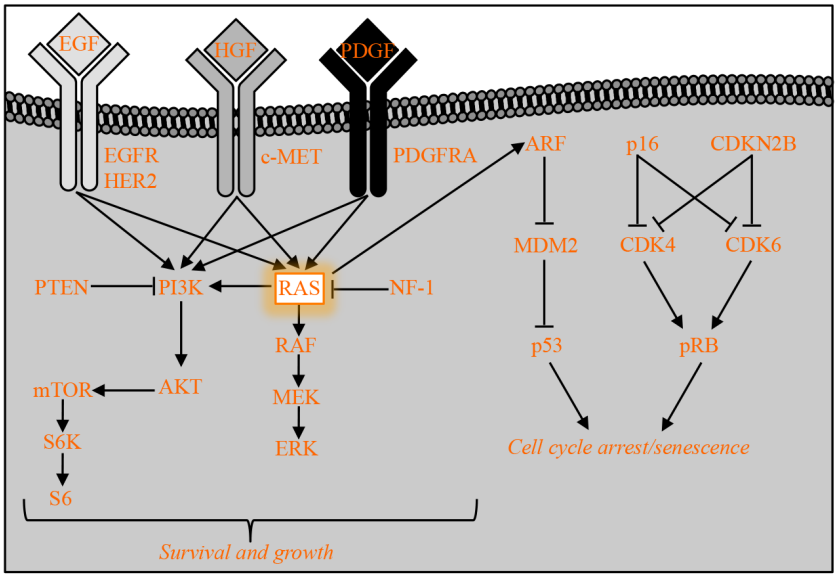

Figure 11.1 A simplified cartoon depicting the major pathways mutated in GBM
Signalling from receptor tyrosine kinases (EGFR, HER2, c-MET, PDGFRA) through PI3K-AKT and MAPK cascades is found in 88% of GBM tumours. These can feed into the regulation of DNA damage and cell-cycle mediators, such as p53 and p16, which are themselves frequently found to be mutated in GBM. At the centre of many of these signalling and regulatory networks is Ras (highlighted box).

Furthermore, Ras is seen to have high activation in all glioblastoma lines that have been tested and previous models utilising KRas as a driving mutation have developed features which closely represent the human disease[281,307,308]. It must be considered, however, that although the upstream regulators and downstream targets of Ras are frequently seen to be mutated in GBM, mutations in Ras itself are rarely seen[251]. Consequently, although elegant in its simplicity, a model using Ras as its one driving mutation can be considered as a preliminary basis for future studies. Nonetheless, given the considerable inter-patient mutational variations and that the aetiology of

GBM is still unknown, generating a completely accurate representation of GBM is impossible, even if a vast array of genes were to be perturbed in a single model.

To introduce this oncogene *in vivo* and *in vitro* the RCAS/*tv-a* system was employed (see introduction section 8.5.2)[252,279,281]. Briefly, the RCAS vector can contain both overexpression of a target protein (e.g.$KRas^{G12D}$) and shRNA against the target of choice (e.g. Atg7). This vector is then transfected into DF-1 chicken fibroblast cells, which produce 'RCAS viruses'. The viruses or virus-producing cells are then used to infect either the cultured XFM/*tv-a* glial cell line or *N/TVA;cdkn2a/ink4a-arf*$^{-/-}$*;Pten*$^{fl/fl}$ mouse pups. This mouse line expresses the avian virus receptor '*tv-a*' under the control of the Nestin promoter and has deletion of the *Ink4a/Arf*$^{-/-}$ locus. Therefore, whilst cultured cells have constitutive expression of *tv-a*, *in vivo* this receptor is only expressed in neural progenitor cells[309]. Following the infection of these cells with RCAS viruses, mice undergo a period of latency before gliomagenesis occurs.

My supervisor, Dr Noor Gammoh, performed all experiments involving the direct handling mice and the harvesting and sectioning of tumours as well as some of the immunocytochemistry.

11.1.2 Autophagy and Ras-induced Tumourigenesis

What hypothesis might we draw regarding the role of autophagy in this $KRas^{G12D}$-driven model of gliomagenesis? In previous studies, the loss of autophagy in Ras-driven cancer has produced varying results. The function of autophagy in cultured cells expressing oncogenic Ras has been conflictingly described as either pro-cell death[192] and pro-senescence[191,310], or pro-malignant[195] and anti-senescence[194,223]. However, upon mining the literature one finds that studies from mouse tumour models point to a more conclusive result: Ras-driven cancers seem to rely on autophagy for malignant transformation[196–200]. With these studies in mind, how a $KRas^{G12D}$ gliomagenesis mouse model might respond to the loss of autophagy was unknown, but it was possible to hypothesise that tumourigenic growth may inhibited.

11.1.3 The Function of Autophagy In Low Nutrient and Hypoxic Conditions

Autophagic flux occurs constitutively at basal levels in cells then can be amplified further by certain stress stimuli[311]. Conditions like hypoxia and low nutrients that induce autophagy are often found in rapidly growing tumours where the generation of vasculature lags behind cellular proliferation and occurs in an erratic and disorganised fashion[178]. The function of autophagy under such conditions has traditionally been

considered to produce additional metabolites and nutrients for the cell to survive. However, others have argued that these stressors can initiate autophagy to such an extent that the eventually the cell actually degrades itself, thereby causing so-called 'autophagic cell death', although this concept remains controversial in the field[312–314]. Alternatively, under such conditions autophagy has been seen to mediate a diverse array of other cellular processes, such as mitophagy to prevent the errant production of reactive oxygen species, 'ER-phagy' to maintain the function and integrity of the endoplasmic reticulum, or the regulation of cytokine secretion[69,70,315,316]. The cellular outcome of autophagy loss during conditions of low nutrients or oxygen therefore appears to be varied. This can be additionally confounded in the context of cancer where oncogenic mutations can perturb normal pathways and generate additional metabolic demand. Therefore, the role of autophagy in regulating vascular-deficient tumourigenic growth can be complex.

11.1.4 Senescence: What Is It and How Does It Relate to Autophagy?

Senescence is a state of irreversible cellular proliferation arrest that can be induced when a cell is exposed to certain stressors, such as DNA damage, oncogene activation, or replicative exhaustion[202,317–319]. This phenotype can be defined experimentally by a set of molecular and cellular hallmarks including increased cell-cycle arrest markers, such as p21, p27, Tp53, and Rb, a non-responsiveness to growth factors, positive staining for β-galactosidase, or expression of pro-inflammatory senescence-associated secretory phenotype (SASP) factors[216].

Apparently opposing functions have been proposed for autophagy in the establishment and maintenance of senescence. On the one hand, autophagy is seen to be activated upon the induction of oncogene-induced senescence (OIS), with some reports suggesting that autophagy actually facilitates this switch[310,320]. Autophagy proteins have also been implicated in the generation of the SASP, which can act to promote senescence in both an autocrine and paracrine manner[223,316]. Furthermore, autophagy has been shown to degrade the nuclear lamina, a phenomenon found in several types of senescence[191]. Additionally, in mouse cancer models the loss of autophagy is associated with DNA damage and senescence, resulting in either a lack of tumourigenesis or failed progression from neoplastic to malignant phenotype[196,201,321]. However, conflicting evidence shows that autophagy proteins can protect cells against senescence and maintain them in a proliferation-competent

state[192,223,322]. Given these disparities in reports, I was interested to understand whether autophagy might regulate senescence in a $KRas^{G12D}$-driven model of glioblastoma.

11.2 Aims

Research question: Is autophagy important in regulating $KRas^{G12D}$-driven gliomagenesis *in vivo* and, if so, why?

To address this question, two objectives must be undertaken:

1. Test the impact of autophagy on $KRas^{G12D}$-driven glioblastoma *in vivo*
2. Measure the activity of key pro- and anti-proliferative regulators in autophagy-competent and -deficient $KRas^{G12D}$-transformed XFM/*tv-a* cell lines when exposed to tumour-like conditions *in vitro*

11.3 $KRas^{G12D}$-Driven Gliomagenesis Relies on the Expression of Key Autophagy Players

To investigate the role of autophagy in KRas-driven gliomagenesis, *N/TVA;cdkn2a/ink4a-arf*$^{-/-}$ mice were generated by Dr Gammoh with $KRas^{G12D}$ expression and shRNA against either *LacZi* or the autophagy players *Atg7*, *Atg13*, and *Ulk1*. Animals injected with control sh*LacZi* had a short latency period (4-6 weeks) before the onset of symptoms suggestive of GBM formation (macrocephaly, lethargy, dehydration, weight loss, or poor grooming) and the culling of the animals. However, when autophagy genes were concurrently lost there was a striking reduction in gliomagenesis (Figure 11.2A). shRNA against *Ulk1* and *Atg13* resulted in the complete loss of tumourigenesis and only a small number of *KRas*^{G12D}:sh*Atg7* mice developed GBM. As Ulk1 and Atg13 are upstream signalling regulators of autophagy initiation and Atg7 acts in the final stages of autophagosome biogenesis, we can conclude that it is the process of autophagy rather than individual players that is important in the formation of these tumours. However, these results raise the question of why tumours were able to form when Atg7 is knocked-down but not when Ulk1 or Atg13 were lost? And were the resulting gliomas any different to their control counterparts?

Dr Gammoh assessed the efficiency of the virus-producing DF-1 cells used during this experiment and confirmed all shRNAs were equally able to reduce expression levels of their target autophagy genes *in vitro*, thereby discounting the possibility of poor shRNA targeting by *KRas*^{G12D}:sh*Atg7* RCAS vectors (Figure 11.2B). It has previously been shown that autophagy-deficient tumours are unable to progress to a malignant phenotype (for example, Karsli-Uzunbas *et al*.[198]). Therefore, Dr Gammoh undertook haematoxylin and eosin staining of the tumours formed in *KRas*^{G12D}:sh*LacZi* and *KRas*^{G12D}:sh*Atg7* mice, which revealed an apparently similarly high grade of aggressive GBM in both cases (Figure 11.2C). Both control and knockdown tumours exhibited high cellularity and the formation of micro-vasculature characteristic of high-grade gliomas[250]. To confirm the active growth and tumourigenic status molecularly, I performed immunohistological staining of the stem cell and GBM cell marker Nestin and the proliferation marker Ki67. Both of these proteins were exhibited to a similar degree in *KRas*^{G12D}:sh*LacZi* and *KRas*^{G12D}:sh*Atg7* mouse tumours (Figure 11.2D). These results suggest that the tumours from these mice were of a similar grade and both were still actively growing at the time their hosts were sacrificed.

Finally, Dr Gammoh tested the expression of Atg7 in the GBM mass itself by immunohistological staining, which revealed that *KRas*^{G12D}:sh*LacZi* and *KRas*^{G12D}:sh*Atg7* tumours were expressing the Atg7 protein to similar levels, or, indeed, elevated levels in tumours where *Atg7* was supposed to be knocked-down (Figure 11.2E). The Atg7 antibody was then applied using a similar protocol to Atg7-/- mouse embryonic fibroblasts (MEFs), which were negative for staining by this antibody thereby confirming its specificity (Figure 11.2F). *KRas*^{G12D}:sh*Atg7* tumours must therefore have adapted in some way to counteract the shRNA, such as acquisition of mutations in the targeted region of *Atg7* or silencing of the shRNA or its processing machinery. Consequently, all KRas^{G12D}-driven GBM tumours formed in the course of this experiment were actually autophagy-competent. I was then interested to understand what pathways autophagy was promoting in the cell that conferred tumourigenicity.

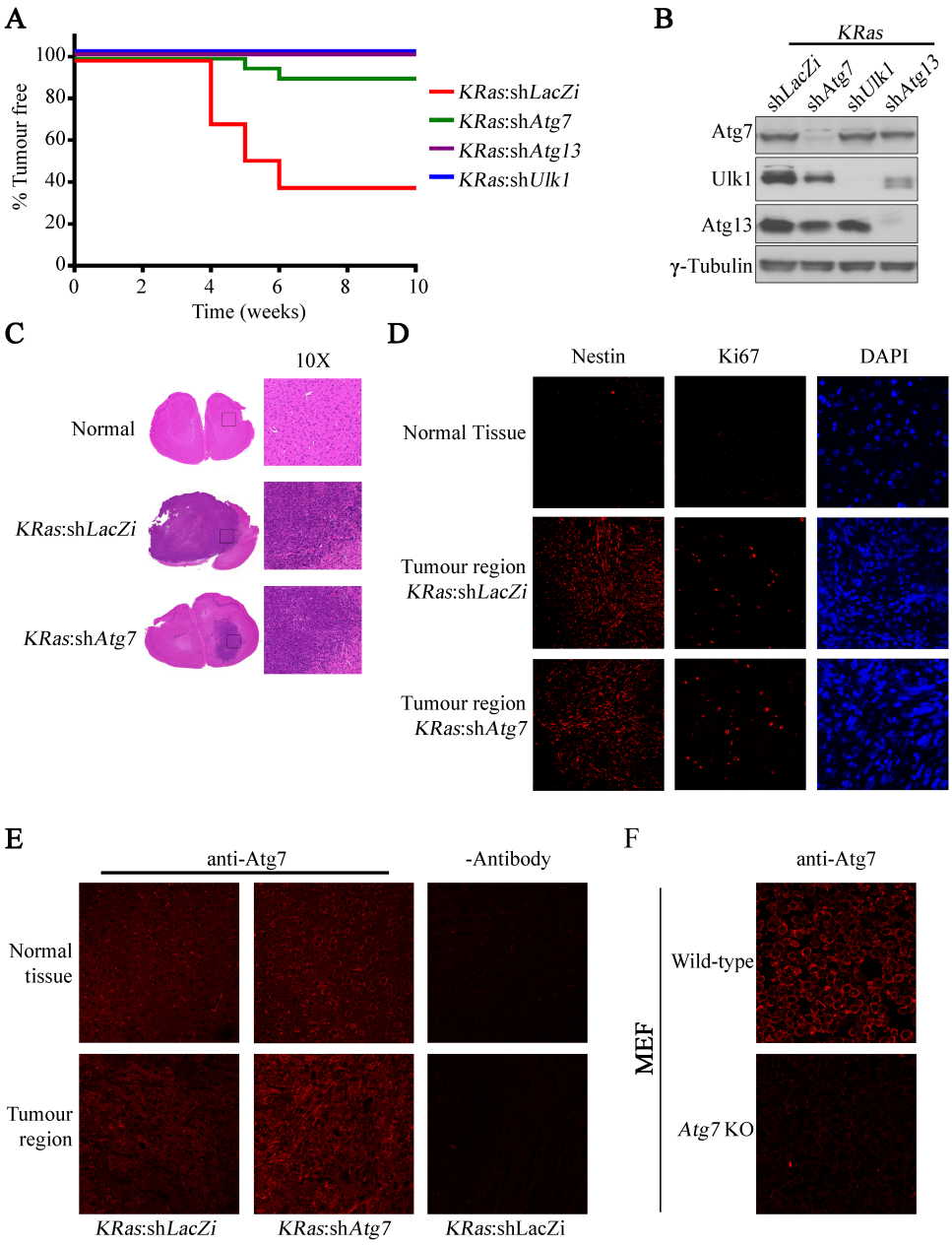

Figure 11.2 Expression of key autophagy players is required for KRas^{G12D}-driven gliomagenesis
A: Kaplan Meier curve of tumour-free survival in *N/TVA;cdkn2a/ink4a-arf*$^{-/-}$;*KRas*^{G12D} mice with or without shRNA against different autophagy players, **B:** Western blot confirms that autophagy protein expression is suppressed efficiently by RCAS *KRas*^{G12D}:sh*Atg7*, *Atg13*, and *Ulk1* in XFM/*tv-a* glial cells, **C:** Haematoxylin and eosin staining in untreated and *KRas*^{G12D}-induced GBM tumours, revealing similar histological features in sh*LacZi* and sh*Atg7* tumours, **D, E:** Immunocytochemical staining against Nestin, Ki67, and Atg7 in sections taken from normal brain tissue or tumour regions from *KRas*^{G12D}:sh*LacZi* or *KRas*^{G12D}:sh*Atg7* animals, **F:** Immunofluorescence against Atg7 in wild-type or *Atg7* knockout mouse embryonic fibroblasts (MEFs). Each experiment was performed at least 3 times. **A-C, E, F:** Data generated by Dr Gammoh, **D:** Data generated by the author.

11.4 Molecular Characterisation of XFM/*tv-a* KRas^{G12D} Cells Exposed to Hypoxic and Low Nutrient Stress

11.4.1 Pro-Growth Signalling Activity Under Tumour-Like Stress Conditions Requires Autophagy

To investigate how autophagy might play a role in malignant transformation and gliomagenesis in this mouse model, cells were assayed with conditions akin to those cancer cells are exposed to during the rapid proliferation that generates tumours. Deficient and disorganised vasculature is a well-established hallmark of cancer that results in areas of poor nutrient supply and low oxygen tension[250]. To mimic these conditions, cells were grown either in media with low serum content (1% foetal bovine serum (FBS)) or in a cell culture chamber where oxygen levels were reduced to 0.5%. The mechanisms that sense oxygen and nutrient availability are intimately linked with the activities of PI3K/Akt, mTOR, and MAPK pro-growth signalling pathways that promote cell proliferation and survival (represented in a simplified format in Figure 11.1)[323–327]. Therefore, the activities of these pathways were tested to assess the impact of autophagy on cells exposed to low oxygen and serum.

Cells were exposed to hypoxia (0.5% oxygen) for seventy-two hours, following which they were lysed for Western blotting analysis. In agreement with previous reports, hypoxia dramatically increased autophagic flux in autophagy-competent cells, as shown by an increase in the LC3-II:LC3-I ratio (Figure 11.3A)[328–330]. Additionally, blotting revealed a novel role for autophagy in promoting the activities of the key pro-growth signalling proteins Akt and ERK during hypoxia. Whilst comparable under untreated conditions, phosphorylation levels were significantly reduced in autophagy-deficient cells relative to sh*LacZi* controls when grown in hypoxia. Several papers have suggested that HIF-1α lies downstream of PI3K/Akt and ERK signalling cascades[324,327,331] and, interestingly, HIF-1α expression was significantly lower in *Atg7* knockdown cells (Figure 11.3A). Therefore, autophagy appears to facilitate the activities of Akt and ERK under hypoxia, which then induce the expression of HIF-1α. HIF-1α expression is then known to initiate a variety of cellular adaptations that can stimulate cell survival and proliferation and promote tumourigenesis in hypoxic conditions[332]. However, on the cellular level, the morphology and growth of sh*LacZi* and sh*Atg7* cells was similar and cell death did not appear to be induced in hypoxia (Figure 11.3B). Together, these data show that autophagy is required for hypoxia-

induced signalling but observation of cell morphology and confluency suggests it may be dispensable for proliferation and survival in hypoxia.

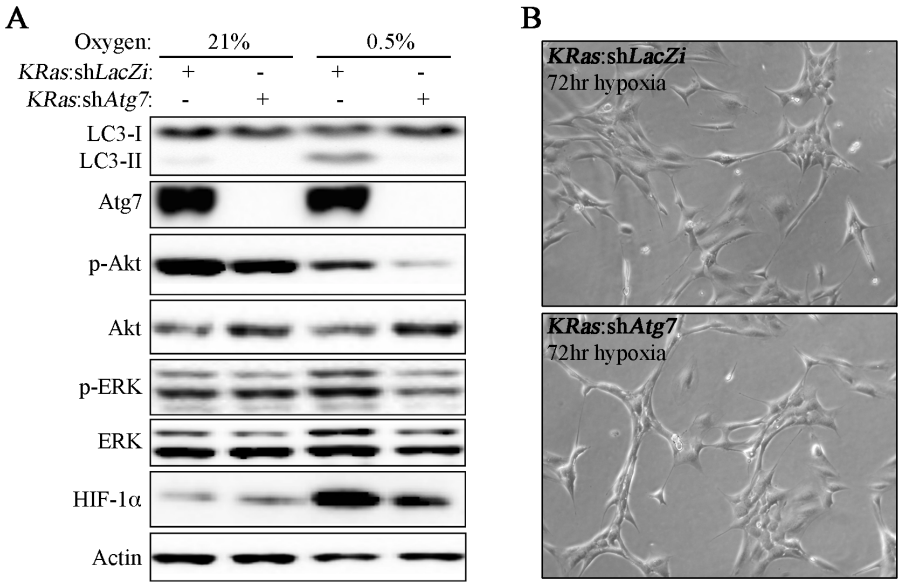

Figure 11.3 Autophagy promotes hypoxia-induced cell signalling through Akt and MAPK pathways
A: Western blotting analysis of key pro-growth signalling pathway activities and levels of HIF-1α of XFM/*tv-a* cells transformed with $KRas^{G12D}$ cultured in normoxia (21% oxygen) or hypoxia (0.5% oxygen) for 72 hr, **B:** Images of $KRas^{G12D}$-transformed cells grown in hypoxia for 72 hr, showing that cells exhibit a similar morphology when autophagy-deficient. Experiment was repeated 3 times.

Poorly-vascularised tumours not only have reduced oxygen availability, they also have a restricted supply of nutrients. When the vast majority of differentiated cell types are grown *in vitro* serum is the principle source for nutrients, so by restricting serum we can mimic the conditions found in a tumour with characteristically insufficient vasculature. Here, $KRas^{G12D}$-transformed XFM/*tv-a* cells were grown in DMEM with a low percentage of serum (0.1% FBS) for four or eight hours, or left untreated (10% FBS). As has been seen in a variety of cell types previously, LC3 lipidation was induced following serum starvation[333] (Figure 11.4).

Furthermore, whilst autophagy-competent cells were able to prevent significant loss of Akt and S6 activity following serum restriction, cells with *Atg7* knockdown experienced a dramatic reduction in the phosphorylation of these key pro-growth signalling proteins (Figure 11.4). During these short treatment time-points there was no change in cell morphology in either cell type (data not shown). However, with the reduction in these signalling pathways being so striking, a prolonged serum starvation was undertaken in which to test the eventual outcome of this treatment on cells. Equal numbers of $KRas^{G12D}$:sh*LacZi* and $KRas^{G12D}$:sh*Atg7* cells were plated then grown in

low serum (1% FBS) for fourteen days, at which time there appeared to be similar numbers of each cell type. However, the enlarged and flattened morphology exhibited

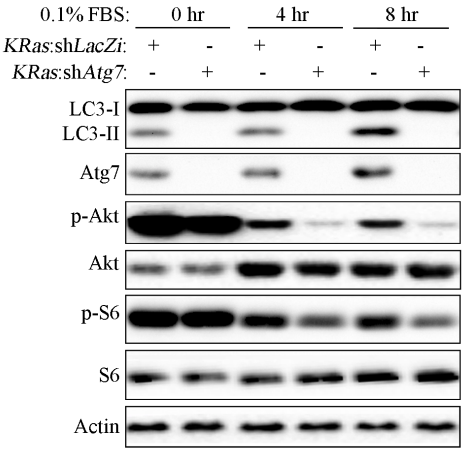

Figure 11.4 Autophagy promotes cell signalling under conditions of restricted nutrients
XFM/*tv-a* cells expressing either *KRas*^{G12D}:sh*LacZi* or *KRas*^{G12D}:sh*Atg7* were grown in low serum for 0, 4, or 8 hr before lysis and analysis by Western blotting. Experiment repeated at least 3 times.

by *Atg7* knockdown cells highly resembled that of senescent cells (Figure 11.5). Senescent cells are insensitive to mitogens and growth factors so to test whether these cells had undergone irreversible growth arrest, full growth media (10% FBS DMEM) was re-applied to cells for one week. At that time it was apparent that whilst a sub-population of control cells were able to re-expand following a period of serum depletion, autophagy-deficient cells were unable to do so (Figure 11.5).

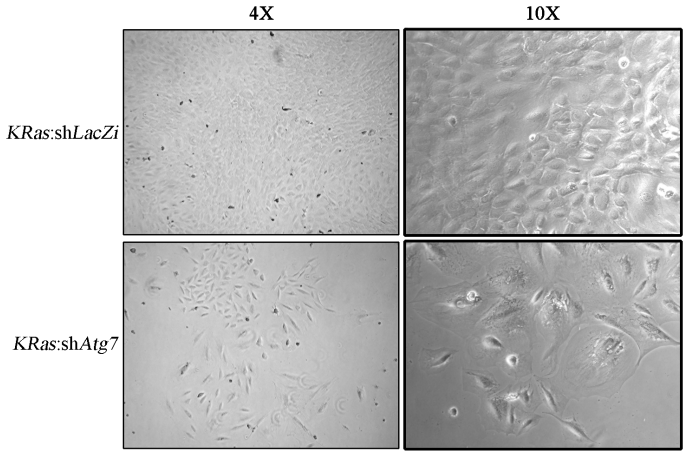

Figure 11.5 Autophagy is required to maintain the proliferation potential of KRas^{G12D}-transformed cells exposed to prolonged serum starvation
KRas^{G12D}:sh*LacZi* and *KRas*^{G12D}:sh*Atg7* XFM/*tv-a* cells were grown in 0.1% FBS for 14 days then medium was changed to 10% FBS for 7 days. Each medium was changed every 2-3 days. Cell images taken at the end of the re-feeding experiment at 4X (left) and 10X (right) magnification. Experiment was performed at least 3 times.

Therefore, autophagy is required to sustain the proliferative capacity of $KRas^{G12D}$-transformed cells during prolonged nutrient deprivation, potentially by maintaining the activity of key pro-growth signalling pathways.

11.4.2 Investigation of the Senescent Phenotype Established In *KRas^{G12D}*:sh*Atg7* Cells Following Prolonged Serum Starvation

Figure 11.5 shows that after 14 days of culture in low serum conditions, *KRas^{G12D}*-transformed cells lacking Atg7 expression enter an irreversible growth arrest. However, several hallmarks must be confirmed before a cell can truly be deemed senescent (see section 8.3.2.2). The following studies were therefore carried out in order to clarify whether this halt in cell cycle was actually senescence and to determine how this senescence was established.

The most widely used marker of senescence is the up-regulation of senescence-associated (SA) β-galactosidase, which is caused by an expanded perinuclear lysosomal compartment[217]. Staining for this enzyme involves its reaction with X-gal and potassium ferricyanide that generates a characteristic electric blue product. Here, the culture of cells with low serum for seven days induced staining for SA β-galactosidase in a subset of *KRas^{G12D}*-expressing XFM/*tv-a* control cells (29%) (Figure 11.6A, B). However, the number of SA β-galactosidase-positive cells was almost double that amount when Atg7 expression was lost (54%). Upon growing for a further seven days, SA β-galactosidase staining was increased further for both cell types (65% and 78%, respectively), with Atg7-deficient cells again exhibiting significantly higher numbers than controls.

To assess the influence of serum depletion of the rate of cell division, BrdU incorporation was measured. When the synthetic nucleoside BrdU is incubated with cells overnight it becomes incorporated into any newly synthesised DNA. Subsequent immunofluorescence against BrdU then reveals which cells have passed through S-phase in that period. As senescent cells do not go through the cell cycle they do not integrate BrdU and are therefore negative for the stain. Following seven days growth in low serum conditions 37% of control cells were positive for BrdU (Figure 11.6C). Under normal growth conditions, *KRas^{G12D}*-transformed XFM/*tv-a* glial cells divide approximately once every 16 hours, therefore these nutrient restricted conditions appeared to have a deleterious impact on normal cell division. However, when autophagy was prevented by Atg7 loss there was a further reduction in cell division,

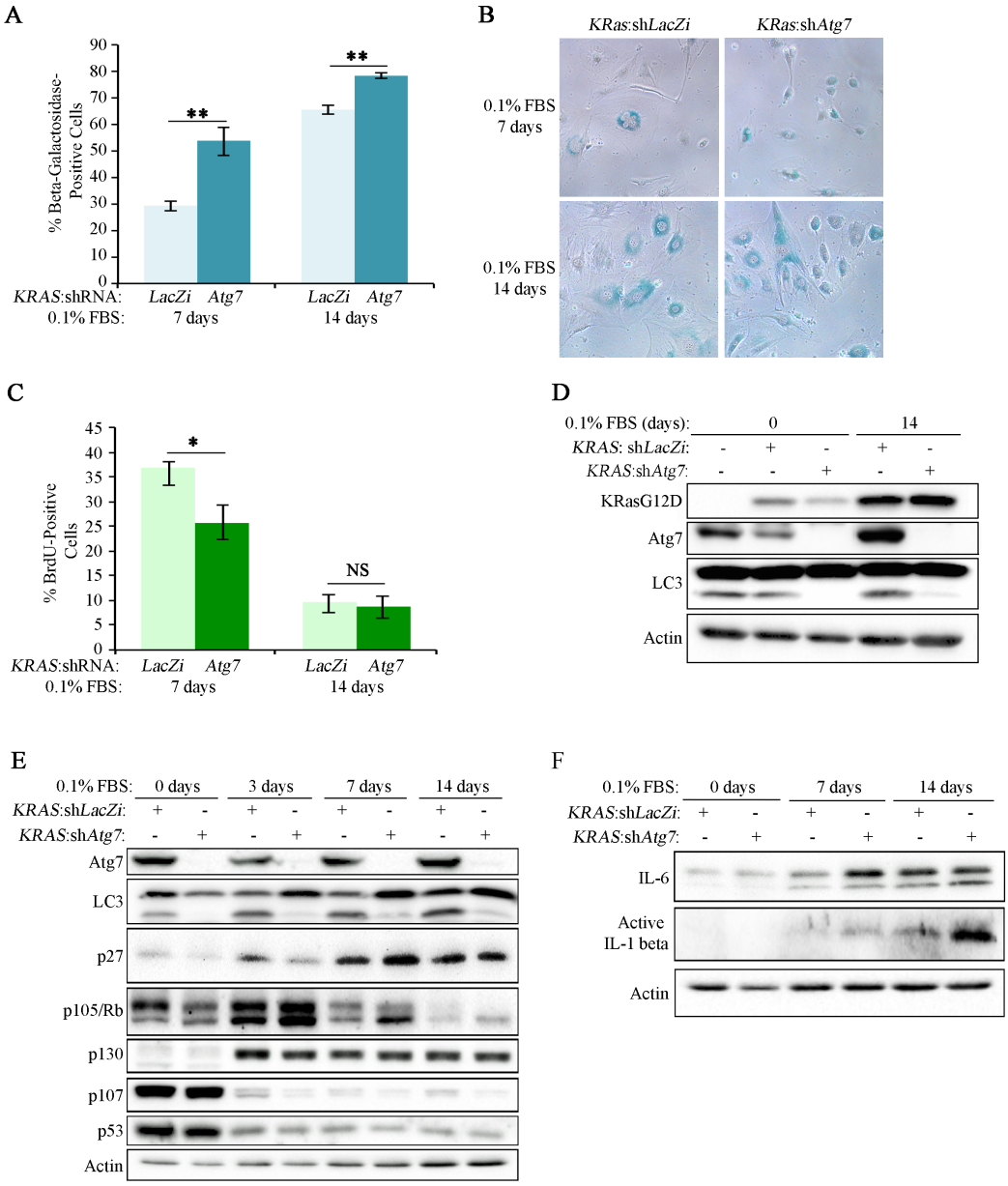

Figure 11.6 Prolonged serum starvation requires autophagy to maintain quiescence and prevent senescence in KRas^{G12D}-transformed cells
A-F: Assays performed in XFM/*tv-a KRas^{G12D}* cells. **A, B:** Senescence-associated (SA) β-galactosidase activity is significantly higher in Atg7-deficient cells following 7 and 14 days cultured in 0.1% FBS, **A:** Percentage of cells stained positive for SA β-galactosidase, **B:** Representative images of SA β-galactosidase staining, **C:** Percentage of actively dividing cells, as measured by BrdU incorporation, is reduced in sh*Atg7* cells relative to sh*LacZi* following 7 days cultured in 0.1% FBS, but both are similarly reduced by 14 days of treatment, **D:** Western blotting demonstrating the efficacy of the RCAS vector is maintained during establishment of senescence, **E:** Western blotting showing the upregulated expression of certain senescence markers in *Atg7* knockdown cells after growth in 0.1% FBS for 0, 3, 7, or 14 days (Rb family members: Rb/p105, p130, and p107), **F:** Expression of senescence-associated secretory phenotype markers in autophagy-deficient cells after culture in 0.1% FBS for 0, 7, or 14 days. n=3, error bars represent SEM, * p<0.05, ** p<0.01, *** p<0.001.

with only 25% of cells labelled with BrdU. After fourteen days growth in 0.1% FBS sh*LacZi* and sh*Atg7* cells experienced similar cell cycle repression (both ~10% BrdU-positive). In combination with SA β-galactosidase and starvation/re-feed data, this

suggests that whilst sh*Atg7* cells become senescent, some sh*LacZi* cells are able to adopt a non-dividing yet proliferation-competent quiescent state.

During the experiments in mice, cells infected with *KRas*^{G12D}:sh*Atg7* eventually evolved a response to overcome Atg7 shRNA targeting and thereby facilitate Atg7 expression, autophagy, and tumour formation. To investigate whether such selection pressure was exhibited under these conditions, following fourteen days of growth in low serum the expression of KRas^{G12D} and Atg7 were examined as well as LC3 to measure autophagic flux. As expected, nutrient deprivation-induced stress increased the ratio of LC3-II:LC3-I in control cells, suggesting increased autophagic activity (Figure 11.6D, E). Furthermore, Atg7 expression was upregulated by serum depletion in control cells. Although there was no evident re-expression of Atg7 in sh*Atg7* cells over this period, there was a detectable amount of LC3-II, implying that at least some cells were expressing Atg7 (Figure 11.6D, E). Interestingly, both autophagy-competent and -deficient cells also exhibited increased stabilisation of KRas^{G12D} when serum was restricted for two weeks (Figure 11.6D). Therefore, autophagy was upregulated and KRas^{G12D} was stabilised by prolonged serum deprivation. The importance of autophagy in maintaining cell fitness over this period is highlighted by the attempt of *Atg7* knockdown cells to re-activate the autophagy pathway.

The focus then turned to examining which molecular pathways were utilised to establish this senescent phenotype. Following three, seven, or fourteen days of growth in low serum media, cells were lysed and expression of cell-cycle regulators were analysed. Despite previous associations observed between autophagy and Tp53[201,322], there was no stabilisation of either Tp53 or its transcriptional target p21 observed in Atg7-deficient cells following prolonged serum depletion (Figure 11.6E). Indeed, in both sh*LacZi* and sh*Atg7* cells Tp53 levels decreased during culture in low serum.

Alternatively, cell cycle arrest can be induced via the pRb/p27 pathway that inhibits cyclin/cyclin-dependent kinase 2 complexes as well as E2F transcription factors, which promote expression of key cell-cycle regulators. The retinoblastoma protein family is composed of pRb/p105, p107, and pRb2/p130 and is characterised by a common 'small pocket' transcriptional repressor domain. pRb undertakes several unique roles in cells, particularly with regards to the establishment of senescence, whereas pRb2 and p107 are believed to be associated with cycling or quiescent cells, respectively, by regulating different subsets of E2F complexes[209,334]. The activity of these proteins is regulated both by expression levels and phosphorylation by cyclin-

dependent kinases, such that hyper-phosphorylated Rbs are inactive and hypo-phosphorylated Rbs are active, which can be detected by an downward shift in migration on Western blots when the protein is active[210]. Here, serum depletion quickly resulted in a reduction of p107 expression and increase of p130 expression that was similar between sh*LacZi* and sh*Atg7* cells. These levels were then unchanged during the course of the experiment, during which time senescence had become established (Figure 11.6E). Therefore, we can rule-out that p107 or p130 were influencing cell-cycle regulation in the induction of this senescent phenotype. The levels of pRb/p105, however, were more dynamic. pRb/p105 experienced a transient elevation in expression level in control and autophagy-deficient cells after three days growth in 0.1% FBS media, with this increase being more marked when *Atg7* was knocked-down. Therefore, there is more pRb/p105 present to inhibit E2Fs and inhibit cell cycle. Following this early peak, control cells then reduced pRb/p105 expression back to levels similar to that of untreated cells. Conversely, hypo-phosphorylated active pRb/p105 remained high in Atg7-deficient cells after seven days cultured in low serum, suggestive of sustained cell cycle inhibition associated with senescence. Indeed, at this time-point there was also an increase in p27, the downstream transcriptional target of pRb/p105, in *Atg7* knockdown cells. By fourteen days of serum starvation, the levels of pRb/p105 were lower than those found in untreated conditions for both cell lines, but hypo-phosphorylated pRb/p105 was still higher in autophagy-deficient cells relative to controls. Together, these results suggest that autophagy-deficient cells activate the pRb-p27 cell cycle inhibition pathway to arrest cells in the G1 phase.

Autophagy has previously been implicated in the production of the senescence-associated secretory phenotype (SASP), a phenomenon that reinforces the senescent state in both an autocrine and paracrine manner thereby helping to lock them into permanent growth arrest[221,223,310]. To identify whether the senescent phenotype observed here in autophagy-deficient cells instigated the production of key SASP regulators, $KRas^{G12D}$-transformed cells were grown in serum-depleted media before lysis and Western blotting analysis. This revealed that the levels of the cleaved active form of the SASP member interleukin-1β (IL-1β) were consistently higher in *Atg7* knockdown cells following seven and fourteen days of nutrient-restricted growth, with production increasing exponentially over this time (Figure 11.6F). Contrastingly, whilst *Atg7* knockdown cells have a greatly increased production of the SASP

member interleukin-6 (IL-6) after seven days cultured in 0.1% FBS, relative to control cells, by fourteen days culture in low serum there was elevated production of IL-6 in both control and knockdown cells. As all other markers firmly point towards Atg7-deficient cells exhibiting a senescent phenotype following fourteen days of serum starvation but control cells remaining in largely proliferation-competent state, the equal IL-6 production after fourteen days of treatment implies that this cytokine is either not important in establishing this form of senescence, or it is only functional when found in conjunction with other senescence regulators. Alternatively, the few senescent cells that are observed in control cells at this time-point may be particularly active in IL-6 production.

Together, these data demonstrate that autophagy-deficient $KRas^{G12D}$-transformed cells are particularly sensitive to prolonged nutrient restriction, resulting in an increased propensity to senesce relative to their autophagy-competent controls. This senescence is instigated by the pRb-p27 pathway and reinforced by the production of a pro-inflammatory SASP, thereby inhibiting the expansion of cells following nutrient deprivation.

11.5 Discussion

The above studies illustrate an important role for autophagy in $KRas^{G12D}$ glial cell transformation and tumourigenicity. In a mouse model for gliomagenesis, autophagy was seen to be essential for tumour formation, potentially as a result of reduced pro-growth signalling capacity during nutrient and oxygen restriction- conditions that are inherent in a rapidly expanding tumour. The prolonged exposure of cells to low nutrient conditions reveals that autophagy-deficient cells are more prone to senescence, thereby potentially putting a halt to cell proliferation in a vasculature-defective tumour. But how representative are these results of the potential situation in patients? And how do these results fit into what is currently known about autophagy in the field of GBM as a whole?

Firstly, regarding the $KRas^{G12D}$-driven mouse model, this potent inducer of malignant transformation generated aggressive tumours with histological and proliferative markers resembling the human situation, as had previously been observed in this model[281,308]. Although over-active Ras is often observed in glioblastoma tumours, this mutation is not frequently observed in patients[307]. Therefore, $KRas^{G12D}$ may be predictive for the majority of cases but some mutations found in glioblastoma may not

have the same response when perturbed by autophagy inhibition. In this model we see that autophagy loss completely abrogates gliomagenesis, with cells even developing adaptations against shRNA knockdown in order to carryout autophagy and generate tumours. This therefore raises the question, would autophagy be similarly required for transformation with all the different driving mutations in GBM? I attempt to address this point in the next chapter utilising cell line models representing the four subtypes of GBM.

The RCAS mouse model of GBM has advantages and disadvantages. The somatic cell gene transfer viral infection from DF-1 fibroblasts to the developing mouse's Nestin-expressing glial cells results in the transformation of the host's own cells and the development of a tumour *de novo*. It is becoming increasingly clear that the immune system has a complex relationsip with tumours and studying tumour formation in the absence of a competent immune system is likely not to be representative[335]. In terms of tumour formation, therefore, the RCAS system is closer to how the pathology actually develops in patients, compared to a xenograft system that has to be performed in an immunocompromised animal and involves the introduction of a large number of foreign cells into the host[336]. In terms of autophagy, the interplay with the immune system is likely to play a large role given what has been seen previously, as well as in this study, with regards to the regulation of inflammatory signalling by autophagy.

Xenograft experiments are beginning to become more sophisticated, however, with the cells introduced into the mouse that are derived directly from patients and carrying all their associated acquired mutations. Nonetheless, these cells are expanded in culture before xenografting into mice and therefore tend to have been passaged. These cells have therefore had time to acquire a number of mutations and adapt to a tissue culture environment. Contrastingly, the RCAS model is initiated with select perturbations and then can acquire further mutations with selection pressures similar to those that would occur in a patient tumour. Therefore, it can be argued that human tumours developing in patients could be more accurately modelled by: a) *ex vivo* human tumour cells xenografted into mice, b) mouse tumours developing in mice.

These arguments consider the properties and pitfalls of different models of tumour formation but the more clinically relevant matter is how to mirror the application of potential pharmaceutical inhibitor to a tumour. Patients will not be treated with an anti-GBM agent prior to tumour formation; rather they will receive therapeutics to

target an already established tumour. In this regard, the RCAS model is not the ideal setting in which to test the role of autophagy. Whilst it can be used to investigate whether autophagy is required for malignant growth, the constitutive expression of shRNA against autophagy targets is unable to represent the application of a putative inhibitor against a pre-existing tumour. To develop this model further, a system to induce ablation of autophagy gene expression would be of greater value and potentially be more predictive of clinical outcome. Currently, inhibition of autophagy is most cleanly achieved by genetic means, as although there are a variety of known compounds that inhibit autophagy, none are specific to the pathway of autophagy alone.

In order to better understand the results gleaned from the RCAS mouse model, cells were cultured under the stressful conditions which GBM cells experience *in vivo* that occur as a result of their poor vascularity and rapid growth. Specifically, cells were cultured in low oxygen and low nutrient levels and the activities of pro-growth and pro-survival pathways were analysed. The results showed that autophagy was required to maintain the phosphorylation and activation of Akt, ERK, and S6 following exposure to these cell stressors. In the course of this study it was not possible to delve into the exact mechanisms by which autophagy maintained these signalling pathways, and it is also not something that has been previously documented in the field. Given what is known, however, one can hypothesise that there are a few possible mechanistic options. Firstly, the cellular building blocks generated by autophagic catabolism may promote the activity of metabolic pathways that then signal to proteins such as Akt to convey that the energy status in the cell is permissive for growth. Alternatively, it is known that hypoxia and low nutrients exert additional demand on the mitochondria to produce energy and endoplasmic reticulum to synthesise new proteins. The piecemeal degradation of mitochondria (mitophagy) or the endoplasmic reticulum (ER-phagy) by autophagy may help sustain the health of these organelles during such stress, thereby dampening stress signals that inhibit these pro-growth signalling pathways[60,69,70,337]. Finally, when the cell is stressed, upregulated autophagy may directly regulate a signalling player that is required for the activation of these cascades and maintains cell growth.

Upon finding that signalling from Akt and S6 were reduced in autophagy-deficient cells following culture in low serum conditions for acute time-points, it was interesting to discover what the fate of cells were after sustained growth in low serum

media. We found that whilst autophagy-competent control cells were able to re-expand in full-serum media after a period of starvation, autophagy-deficient cells had acquired a senescent phenotype. This halt in cell cycle correlated with the stabilisation of active, hypo-phosphorylated pRb and its downstream target p27, as well as the induction of a pro-inflammatory senescence-associated secretory phenotype (SASP). Others have previously documented connections between autophagy and the generation of a SASP. For example, the secretion of IL-1β has been reported to rely on the expression of key autophagy proteins[316]. However, others have seen that basal autophagy actually suppresses IL-1β inflammatory signal generation by the clearance of damaged mitochondria[338]. Furthermore, by means of degrading the NFκB regulator GATA4, autophagy is able to suppress the generation of SASP components until cells are assaulted with different senescence-inducers[223]. In support of this theory, here we see that autophagy loss promotes the production of SASP components IL-6 and cleaved, active IL-1β.

But how might autophagy loss engage the pRb-p27 pathway? An interesting flurry of corroboratory papers in 2002 might provide the key to connecting the experiments undertaken here[212–214]. These papers show that Akt is able to directly bind and phosphorylate p27, which holds it in the cytoplasm thereby preventing its nuclear functions that inhibit the cell cycle. Here we have seen that the genetic ablation of autophagy reduces the activity of Akt during serum starvation, through mechanisms unknown, which may have the result of allowing the translocation of p27 to the nucleus and priming the cell for the induction of senescence. As well as lying downstream of pRb, p27 can feed back to stabilise and promote pRb activity[205,339]. Therefore, we can start to build up a model whereby: autophagy → Akt ⊣ p27 → pRb. To test such a hypothesis, a constitutively active myristoylated Akt mutant could be introduced into autophagy-deficient cells to test whether this is able to inhibit the induction of senescence[340]. Alternatively, Akt could be knocked-down in autophagy-competent cells that could be then tested for a senescent phenotype following prolonged serum depletion.

Senescence has been suggested to be paradoxically pro- and anti-tumourigenic according to the context. Early reports suggested that senescence is the brake on proliferation utilised by multicellular organisms to prevent the formation of cancers, whether this be following DNA damage, ageing (which highly correlates with a likelihood for DNA damage), or oncogene activation[202,341]. Then, key to the role of

senescence as an anti-tumour pathway, oncogene-induced senescent cancer cells could be actively cleared by the immune system[342,343]. The elimination of senescence regulators, such as Tp53 and p16, are some of the most frequently observed mutations in cancers, highlighting their importance as tumour suppressors. However, current research is showing that in an established tumour the influence of senescence can be conflicting, particularly with regards to the SASP. Whilst SASP does confer autocrine and paracrine senescence to cells, these pro-inflammatory factors can contrastingly promote the aggressive stem properties of cancer cells as well as inducing angiogenesis and the pro-metastasis epithelial to mesenchymal transition[344]. The study carried out here has drawn correlations between autophagy loss, induction of senescence, and inhibited tumourigenesis. As discussed above, the RCAS system provides a model for studying autophagy GBM formation but not maintenance. Therefore, it is not possible to assess whether autophagy inhibition might induce senescence and the SASP production in established tumours *in vivo* by this method, or what the consequences of this would be in the context of treatment. It would be interesting to use an inducible autophagy genetic ablation to test whether the poor vasculature and nutrient scarcity of GBM would cause a senescent phenotype in established tumours in mice and what the consequences of that would be. Previous reports have shown that senescence in GBM can either support stemness and tumour growth[345], or halt cell proliferation and induce tumour cell clearance resulting in tumour regression[346].

Taken as a whole, this work utilising a $KRas^{G12D}$ GBM model presents a picture where autophagy can regulate the activity of key signalling cascades and cell cycle regulators during periods of stress *in vitro*, and is completely depended upon for gliomagenesis *in vivo*. The results gleaned here raise important questions regarding the role of autophagy in GBM and cell signalling, some of which I shall begin to address in the ensuing chapters.

12 GBM Cell Line Models Require Autophagy for Detachment-Induced Signalling and Anchorage-Independent Growth

12.1 Introduction

12.1.1 Modelling Glioblastoma Multiforme

Although the underlying epidemiology of glioblastoma multiforme (GBM) remains elusive it is generally considered to arise from an accumulation of sporadic mutations. GBM tumours exhibit a high degree of heterogeneity not only between different patients but also within a single patient's tumour, thereby representing a significant challenge in developing effective treatment strategies. Such heterogeneity also hinders our ability to model this disease accurately in researching the fundamental biology underpinning the aggressive growth of GBM *in vitro* and using mouse models.

The constitutively active $KRas^{G12D}$ mutant used in the previous chapter, whilst representative of MAPK pathway over-activity observed in the majority of glioblastomas, is not itself commonly observed in patients. Instead, the loss of the tumour suppressors such as NF-1 or TP53 and the over-expression and over-activity of receptor tyrosine kinases are observed most frequently in the clinic[250,251]. For example, one mutant of EGFR found in approximately 23% of tumours harbours a deletion of exons 2-7, generating a constitutively active variant called EGFRvIII[347]. GBM mutations can be grouped according to the genes that are most frequently found to be concurrently mutated and are designated 'classical', 'proneural', 'neural', and 'mesenchymal'. In order to study the role of autophagy in glioblastoma more accurately it was therefore necessary to develop a panel of cell lines with mutations more akin to those found in the clinic. Furthermore, in a different cancer type the reliance on autophagy for tumourigenic growth has been seen to be dependent on the mutational status[201]. Therefore, in modelling the different subtypes of GBM we can begin to tease apart whether certain mutations confer more dependence on autophagy.

A mounting body of research suggests that GBM tumours may derive from a sub-population of so-called 'cancer stem cells'[348–351]. However, the importance of

autophagy in maintaining the oncogenic tumour-initiating properties of a glioblastoma stem cell model system remains unclear[188,352].

Mouse neural stem cells were transformed with constitutively active EGFRvIII mutant and *Ink4a/Arf* knockout to model the classical GBM subtype in a stem-like context, whilst mouse glial cell lines with *Ink4a/Arf* knockout, *Nf-1* and *Tp53* knockdown, or the overexpression of *Pdgfa* ligand were used to model proneural, neural, and mesenchymal subtypes. CRISPR/Cas9 gene modification technology and shRNAs were then utilised to ablate the expression of essential autophagy players and therefore study the impact of autophagy loss on oncogenicity in glioblastoma model cell lines. The tumourigenic potential of cell lines could then be assayed in a variety of ways, including testing the ability of cells to grow independent of adhesion to basement matrices.

12.1.2 Anoikis, Anchorage-Independence, and Autophagy

A key step in cellular oncogenic transformation is acquisition of the ability to proliferate independent of anchorage, thereby facilitating their growth in a tumour[227]. To prevent this event, normal cells engage a form of caspase-mediated cell death called anoikis. Anoikis can be evaded by oncogenic transformation, epithelial-to-mesenchymal transition (EMT), and exhibition of stem-like properties (see introduction section 8.3.3)[228–233]. In a wide variety of cancers, these perturbations have been seen to facilitate anchorage-independent growth by engaging the activities of signalling kinases Akt and ERK[228,229,235–237].

Once cell death is overcome, cancer cells must then upregulate certain metabolic and signalling pathways in order to proliferate without anchorage[239,240]. One means by which these processes can be fuelled is by upregulated autophagic flux[170,244,245]. Although several cell lines are known to rely on autophagy for anchorage-independent growth, it is not known whether this is true for the four GBM subtypes or whether they have differential dependencies on autophagy in this regard. I therefore wanted to assess the influence of autophagy on the ability of different GBM model cell lines to grow without adherence. Further to this, I was interested to investigate the molecular mechanisms by which autophagy is able to influence cell fate following anchorage loss.

12.2 Aims

Research question: Is there a reliance of specific GBM subtypes on autophagy for malignant transformation?

1. Generate cell models of glioblastoma multiforme subtypes with autophagy gene expression ablation
2. Assay the oncogenicity of these cell lines by testing their capability for anchorage-independent growth in different settings:
    a. Soft agar assay
    b. Low-adhesion plates
    c. Acute suspension
3. Explore the molecular role of autophagy in anchorage loss in cell models of glioblastoma

12.3 Generating Cell Lines

12.3.1 Knockout of Key Autophagy Genes in Transformed Neural Stem Cells and Mouse Embryonic Fibroblasts

CRISPR/Cas9 gene modification technology is finding a multitude of exciting applications from the bench to the clinic with the full potential of this technique still to be uncovered. To introduce CRISPR/Cas9 into our laboratory, single-guide RNAs (sgRNAs) targeting essential autophagy genes *Atg3*, *Atg7*, and *Atg16l1* were cloned into a transient expression vector (sequence information summarised in section 10.2.1). The efficacy of these 'sgRNA vectors' was then trialled by transfecting them into a mouse embryonic fibroblast (MEF) cell line using Lipofectamine 2000 and then cells were assayed for gene expression by Western blot. Whilst all guides were functional in reducing expression in a pool of transfected cells, single-guides against *Atg16l1* were unexpectedly inefficient relative to the other genes (Figure 12.1A-C). Single colonies picked from these pools by my colleague Ainara González-Cabodevilla were indeed knockout for *Atg16l1*, however, validating the use of these sgRNAs in further studies (Figure 12.1D). Alas, sg*Atg7* #1 resulted in the rapid proliferation of transfected cells, which is highly suggestive of an off-target effect,

and therefore its use was discontinued during this study. This should be considered a reminder that CRISPR/Cas9 is not infallible and that multiple sgRNAs need to be used against one gene in order to discount the possibility of off-target effects.

Having confirmed the functionality of these sgRNA vectors in MEFs, they were then transfected by Nucleofection into IENS cells kindly gifted by Dr Steve Pollard, which have been described elsewhere[302–304]. The IENS glioma-initiating mouse neural stem cell line has been transformed to model a 'classical' GBM subtype by the knockout of the *Ink4a*/*Arf* locus and the expression of the constitutively active EGFRvIII mutant. Fortunately, in these cells all guides were able to yield a good reduction in Atg gene expression without the necessity to select single clones, thereby avoiding clonogenic effects (Figure 12.1E-G).

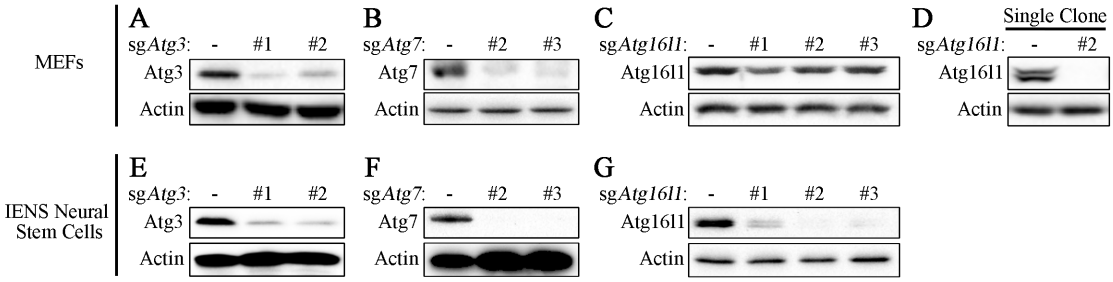

Figure 12.1 CRISPR/Cas9 knockout of essential autophagy genes
A-G: Western blotting for expression of autophagy players following CRISPR/Cas9 modification. **A-D:** sgRNAs against *Atg3* (**A**), *Atg7* (**B**), and *Atg16l1* (**C**) were transiently transfected into mouse embryonic fibroblasts (MEFs), then single clones were selected of either Cas9 only control or sg*Atg16l1*#2 knockout cells (**D**), **E-G**: Glioma-inducing Neural Stem Cells (IENS) were Nucleofected with sgRNAs against *Atg3* (**E**), *Atg7* (**F**), and *Atg16l1* (**G**).

12.3.2 Modelling GBM Subtypes in XFM/*tv-a* Glial Cells

The RCAS-XFM/*tv-a* system provides a highly adaptable and rapid method by which to knockdown genes or express exogenous proteins. Its use with $KRas^{G12D}$ expression proved to be a powerful tool with which to carry out our initial experiments and it was used again here to develop differently transformed glial cell lines. With a constitutive knockout of *Ink4a/Arf*, the XFM/*tv-a* glial cell line is immortalised and poised for transformation to an oncogenic phenotype with the addition of other drivers.

In an effort to model both mesenchymal and neural classifications simply, cells were given a combined knockdown of *Nf-1* and *Tp53*. To model the proneural subtype I used shRNA against *Tp53* and overexpressed HA polypeptide-tagged PDGFA ligand, which over-stimulates the PDGFRA receptor to mimic its oncogenic amplification.

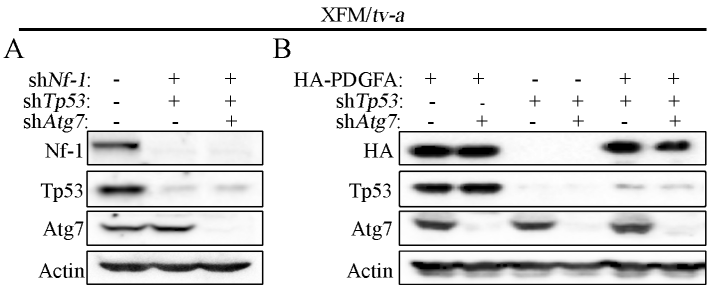

Figure 12.2 Generation of XFM/*tv-a* GBM cell line models with Atg7 knockdown
A: A Mesenchymal/Neural model with combined knockdown of *Nf-1* and *Tp53*, **B:** A Proneural model with *Tp53* knockdown and overexpression of HA-tagged PDGFA ligand.

Following the generation of these XFM/*tv-a* cell lines, either control RCAS-sh*LacZi* or RCAS-sh*Atg7* was applied to cells to knockdown expression of this essential autophagy player (Figure 12.2).

12.3.3 Development of the RCAS-sgRNA System

Whilst using XFM/*tv-a* cells with a combination of shRNAs against *Nf-1* and *Tp53*, the shRNA against the key autophagy gene *Atg7* was consistently selected against, with cells re-expressing the Atg7 protein at significant levels after just a few passages (Figure 12.3A). Whilst this evolution was interesting in its implication of *Atg7* as an important mediator of cell fitness in this context, it made consistent and reliable experimentation challenging. In order to overcome this difficulty, the gene was suppressed by CRISPR/Cas9 knockout rather than knockdown with shRNA. However, XFM/*tv-a* cells do not transfect efficiently by either Lipofectamine 2000 or Nucleofection techniques to be able to use transiently expressing vectors. To overcome this, I developed a method by which the single guide RNAs could be extracted from the 'sgRNA vector' (previously used in the neural stem cell transfection) and then cloned into the 'RCAS-Y vector' so the sgRNA could be introduced virally, as described in the Material and Methods chapter (Figure 12.3B). This strategy combines the efficiency of the RCAS-XFM/*tv-a* system with the irreversibility of CRISPR/Cas9 modification.

Successful cloning was confirmed by Sanger sequencing performed by the IGMM's technical services team using a primer against a RCAS-Y sequence upstream of the NotI cloning site (e.g. RCAS-sg*Atg7* #3 vector sequencing in Figure 12.3C). RCAS-sgRNA viruses could then be produced in DF-1 chicken fibroblasts and used to infect XFM/*tv-a* cells. Three infections were sufficient to significantly reduce the expression of all the genes trialled (Figure 12.3D). This system therefore represents an efficient,

rapid, and adaptable system by which genes can be knocked-out from a pool of XFM/*tv-a* cells.

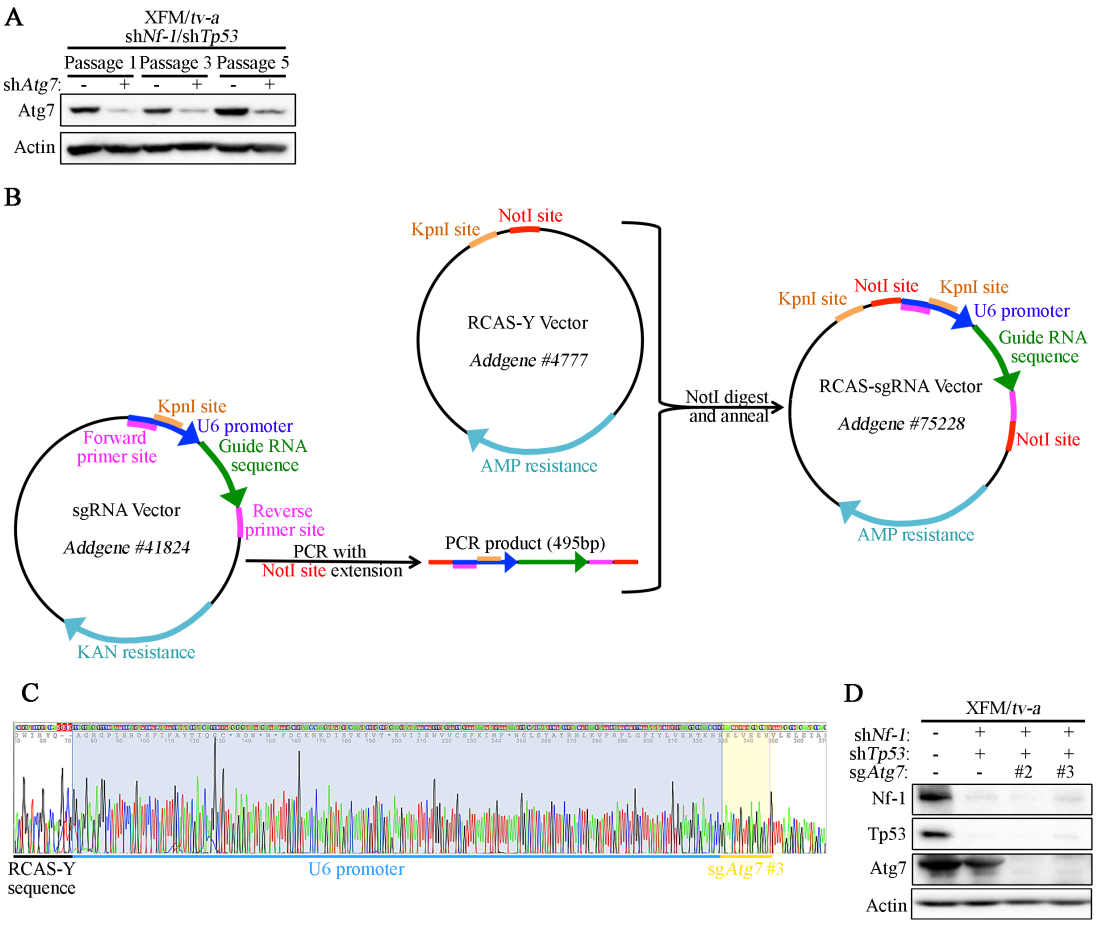

Figure 12.3 Development of the RCAS-sgRNA vector
A: Western blotting demonstrating the re-emergence of Atg7 expression over time in XFM/*tv-a* cells with Nf-1 and Tp53 loss, **B:** Agarose gel of the PCR product of U6 promoter – sg*Atg7*#3 – NotI restriction site, which was amplified from the sgRNA vector, **C:** KpnI digestion products following cultivation of RCAS-Y vectors annealed with PCR products from B (properly orientated inserts generate a product of 6,000 bp and incorrectly orientated inserts give a product of 420 bp), **D:** Cloning strategy to insert single-guide RNAs into the RCAS-Y vector, **E:** Sanger sequencing file of the U6 promoter and sg*Atg7*#3 sequences correctly inserted into the RCAS-Y vector, **F:** XFM/*tv-a* cells are tested for the successful knockdowns of *Nf-1* and *Tp53* and knockout of *Atg7* using by Western blotting.

12.4 Autophagy Gene Expression is Necessary for Anchorage-Independent and Low-Adhesion Growth

With these models in place, it was then possible to test the reliance of their oncogenicity on the expression of essential autophagy player Atg7 using the soft agar assay for anchorage-independent growth. The basis of this technique is to suspend cells in a low-agar semi-solid layer on top of a base layer of with a higher composition of agar, thereby sequestering cells from the bottom of the plate where they could adhere. Therefore, if a cell cannot resist anoikis or maintain its metabolism

and pro-growth signalling, it will not be able to proliferate to form a colony in the agar. This represents the capability of cancer cells to grow independently from the basement layer of their tissue of origin and form neoplastic groups of cells that can develop into a tumour.

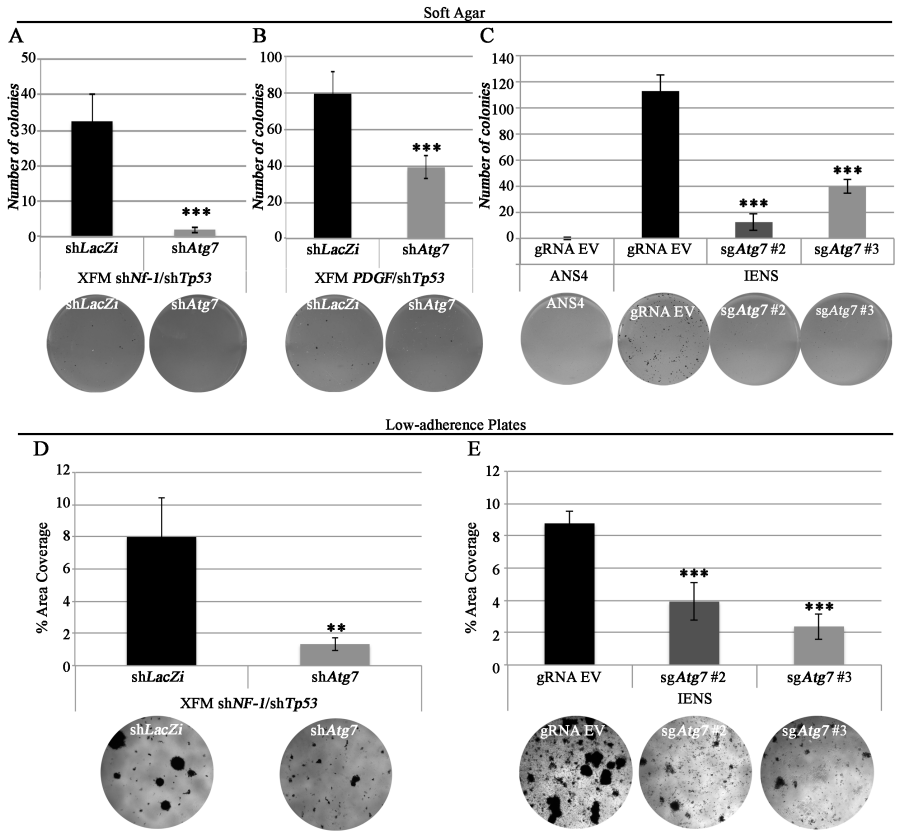

Figure 12.4 Growth of GBM subtype cell models under adhesion-restricted conditions
A-C: Soft agar colony formation assay, **D-E:** Low-adhesion plates. **A, B, D:** *Atg7* knockdown in XFM/*tv-a* cells transformed by a combined knockout of *Ink4a/Arf* and knockdown of *Tp53* and *Nf-1* (**A, D**) or PDGF-A ligand overexpression and knockdown of *Tp53* (**B**). **C, E:** ANS4 (untransformed) and IENS (*Ink4a/Arf*$^{-/-}$, *EGFRvIII*-expressing) neural stem cells with CRISPR/Cas9-mediated *Atg7* loss. n=3, error bars represent SEM, * $p<0.05$, ** $p<0.01$, *** $p<0.001$.

The GBM subtype models that I had developed here were all able to form colonies when harbouring the control empty vector, demonstrating that they were indeed transformed to a malignant phenotype. However, when expressing shRNA or sgRNA against *Atg7* the formation of colonies was significantly inhibited in all cases (Figure 12.4A-C).

The soft agar assay establishes a complete loss of anchorage and I was interested to know whether Atg7 would be required for colony formation under a less stringent condition, where a small quantity of surface is available for a minority of the cells to adhere to. The mesenchymal/neural subtype (XFM/*tv-a*: *Ink4a*/*Arf*-/-, sh*Nf-1*, sh*Tp53*) and classical subtype (IENS: *Ink4a/Arf*-/-, *EGFRvIII*) were therefore cultured on low-

adherence Alvatex scaffolds. These 200μm-deep honeycomb structures are made of polystyrene formed with ~40μm pores that allow cells to be cultured in 3 dimensions[353]. Therefore, these scaffolds foster the growth of spheroids of cells; the efficient formation of which requires the capability for anchorage-independent growth. Equal numbers of sh*Nf-1*/sh*Tp53* XFM/*tv-a* cells and IENS glioblastoma-initiating neural stem cells, with or without Atg7 expression, were plated on these scaffolds in their respective growth media and cultured for 14 days. In both cell lines the loss of Atg7 expression correlated with a significant reduction in the formation of 3D cell spheres (Figure 12.4D, E). Interestingly, IENS cells formed colonies with a much higher efficiency than XFM/*tv-a* cells in both the soft agar and low-adhesion assays (Figure 12.4). This could either be due to the expression of the constitutively active mutant EGFRvIII or the properties associated with their stemness, both of which are factors associated with colony formation[354–358].

Together, these results show that autophagy is required to support the proliferation of colonies of cells under both conditions of complete and partial anchorage restriction.

12.5 Autophagy Supports Detachment-Induced Signalling But Does Not Influence Anoikis

The soft agar assay is recognised to be a highly predictive model in cancer biology research[227], but it simultaneously evaluates the initial oncogenic mutation, evasion of anoikis, as well as the secondary stimulation of metabolic and signalling activity required for prolonged anchorage-independent growth. To try to understand which of these stages relies on autophagy, a crude acute suspension method was used. Cells were seeded on plates with or without normal tissue-culture treatment in media without growth factors. When plates are not treated with a plasma gas to make the polystyrene surface negatively charged, cells are not able to adhere to the plates and so are kept in suspension. Cells can then be harvested for Western blot or stained with propidium iodide to measure anoikis cell death.

Again, the IENS neural stem cell classical GBM subtype model (*Ink4a/Arf*-/-, *EGFRvIII*-expressing) and XFM/*tv-a* mesenchymal/neural subtype model (*Ink4a/Arf*-/-, sh*Tp53*, sh*Nf-1*) were used to investigate the potential influence of autophagy in these adhesion studies. Upon suspending cells for four hours on plates not ionised for tissue culture use, there was a slight induction of cell death in IENS cells (~3%), which was slightly, but not significantly, increased by the knockout of *Atg7* (~5%)

(Figure 12.5A). This was increased to ~8% and ~9%, respectively, after eight hours. However, the sh*Nf-1*/sh*Tp53* cells had a dramatic stimulation of anoikis after just four hours, with approximately 30% of cells positive for P.I. staining, which was not influenced by Atg7 loss (Figure 12.5C). This supports the observations from the soft agar and low-adhesion assays that IENS transformed neural stem cells exhibit increased growth in comparison to XFM/*tv-a* glial cells following anchorage loss.

As the initial induction of anoikis was not influenced by autophagy, I was interested to know whether a defect in cell signalling may contribute to the reduction in anchorage-independent growth observed in the soft agar assay caused by Atg7 loss. To assess signalling in this setting, the phosphorylation statuses of the key pro-growth, anti-anoikis proteins ERK and Akt were tested. In both IENS and XFM/*tv-a* sh*Nf-1*/sh*Tp53* cells there was an induction in ERK phosphorylation following detachment, relative to adhered cells cultured in serum-/growth factor-free medium (Figure 12.5B, D). However, there was only an induction of Akt phosphorylation, relative to adhered starved conditions, in XFM/*tv-a* sh*Nf-1*/sh*Tp53* cells. Following IENS cell suspension for either two or four hours there was significantly less phosphorylation of Akt and ERK in cells with Atg7 knockout, although this was equalised to the level observed in control cells after sixteen hours in suspension (Figure 12.5B). XFM/*tv-a* sh*Nf-1*/sh*Tp53* cells, similarly, have reduced Akt phosphorylation in Atg7-deficient cells following four hours of suspension (Figure 12.5D). However, ERK phosphorylation was not influenced by Atg7 loss in this cell type. ERK remained active after sixteen hours in suspension, but both control and sg*Atg7* #3 cells were defective in Akt phosphorylation after this time. In line with low cell death measurements in Figure 12.5A, following four and eight hours of suspension, anchorage loss did not induce any detectable cleavage and activation of caspase-3 in IENS cells (Figure 12.5B). Following sixteen hours of suspension, however, cells with and without Atg7 expression both had detectable levels of caspase-3 cleavage. Previous reports have shown that high EGFR levels facilitate anchorage-independent growth and that a reduction in EGFR levels following detachment results in anoikis[229,237]. To investigate whether EGFR may play a role in this context, its levels were measured during anchorage loss. Whilst EGFR expression decreased in XFM/*tv-a* sh*Nf-1*/sh*Tp53* cells upon suspension, it remained stable and then increased in IENS cells (Figure 12.5B, D). This is likely to be mediated by the expression of EGFRvIII in these cells, which is known to be stably localised to the

plasma membrane where it avoids endocytic regulation and co-operates with the wild-type receptor[359–361]. Indeed, I found that the exogenous expression of EGFRvIII stabilises wild-type EGFR in XFM/*tv-a* parental cells and in IENS cells, relative to ANS4 adult mouse neural stem cells, under untreated conditions (Figure 12.6). As EGFR signalling, via Akt/ERK activation, can facilitate anchorage-independence, this result may explain the disparities in growth rate between the two GBM model cell lines in soft agar and low-adherence assay. There was not, however, any influence of Atg7 on EGFR levels and, therefore, the influence of autophagy on Akt/ERK signalling and anchorage-independent growth are not due to the regulation of EGFR expression.

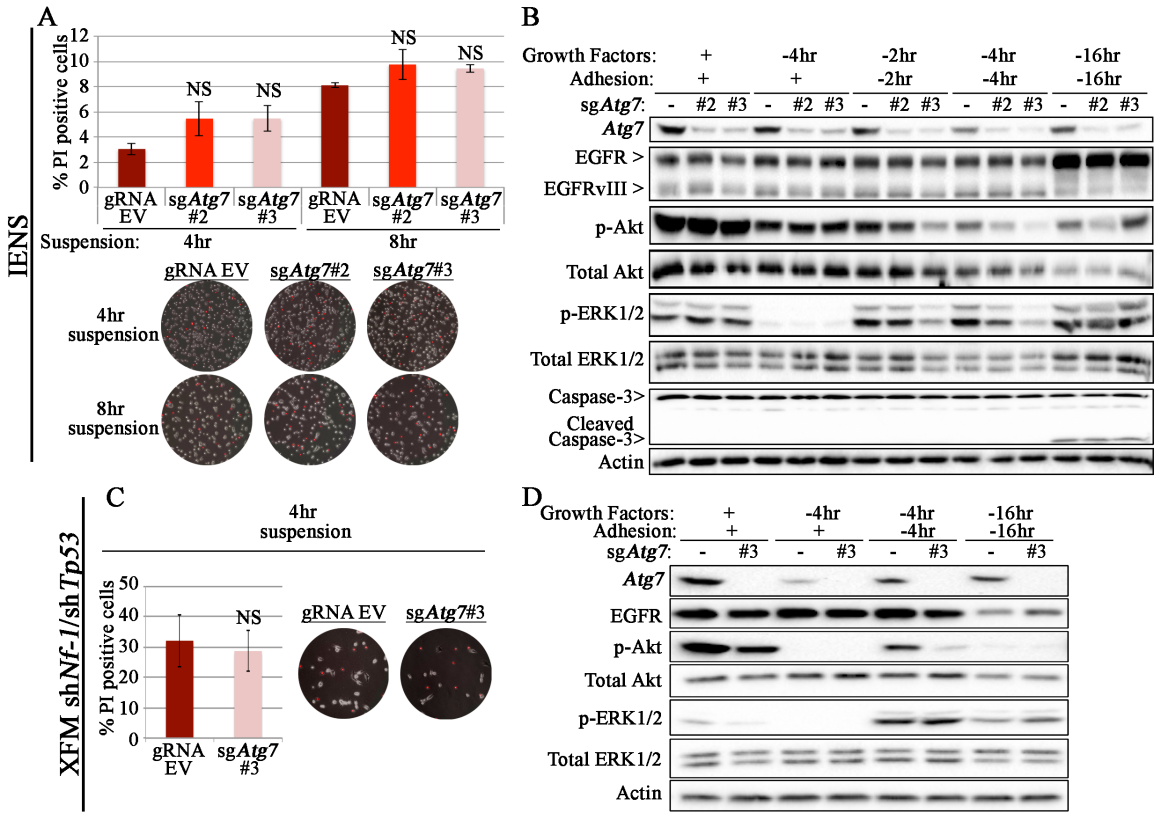

Figure 12.5 Assaying the influence of Atg7 on anoikis and cell signalling following acute suspension

A, C: Anoikis was measured by propidium iodide (red) staining of cells cultured on non-tissue culture treated plates in serum-/growth factor-free media for the indicated times (n=2 experiments), **B, D:** The activity of pro-growth signalling cascades was measured during either normal adhered growth, serum starvation, or serum starvation in suspension. **A, B:** IENS (*Ink4a/Arf*-/-, *EGFRvIII*-expressing) neural stem cells with CRISPR/Cas9-mediated *Atg7* loss. **C, D:** XFM/*tv-a* cells transformed by a combined knockout of *Ink4a/Arf* and knockdown of *Tp53* and *Nf-1* with CRISPR/Cas9-mediated *Atg7* knockout. n=3, error bars represent SEM, * p<0.05, ** p<0.01, *** p<0.001.

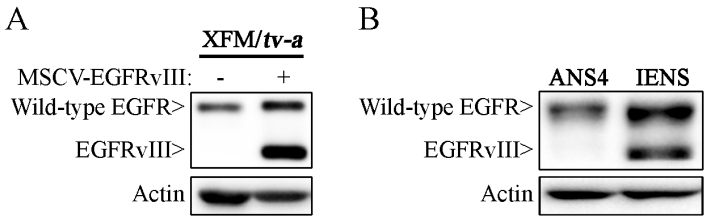

Figure 12.6 EGFRvIII expression stabilises wild type EGFR expression
A: Expression EGFRvIII in the MSCV vector in XFM/*tv-a* glial cells increases the levels of wild-type EGFR, **B:** IENS transformed neural stem cells expressing EGFRvIII have higher wild-type EGFR levels than untransformed ANS4 adult neural stem cells.

12.6 Discussion

Anchorage-independence is a key step in the malignant transformation of cancer cells, but much of its regulation remains incompletely understood. Whilst it is known that oncogenic signalling pathways can prevent anoikis, it is becoming clear that more than the initial evasion of cell death is required to sustain anchorage-independent growth; cells must sustain pro-growth and pro-survival signalling as well as alter their metabolic configuration. The loss of attachment to ECM eliminates signalling from integrins and their cofactors, and this needs to be replaced by oncogenic signalling from pathways such as PI3K-Akt and ERK. These cascades prevent the activation of cell death players and stimulate metabolic programmes that promote ATP production and quench ROS.

Whilst autophagy is known to be required for the anchorage-independent growth of a variety of cell lines, its influence on specific subtypes of GBM is unknown. Here I have shown that the essential autophagy player Atg7 is required for soft agar colony formation and the growth of 3D spheroid cultures on low-anchorage scaffolds in cell line models of different GBM subtypes (Table 12.1). Further investigation of two of these GBM subtype model lines reveals that the activity of Akt and ERK signalling pathways is significantly reduced in Atg7-deficient cells following acute anchorage loss. However, the phosphorylation levels of Akt and ERK did not correlate with induction of anoikis in these cell lines, which was unaffected by autophagy status. Crucially, all of the subtypes modelled here had a similar reliance on autophagy for anchorage-independent growth and detachment-induced pro-survival signalling. This is of interest in terms of a potential GBM therapeutic, where it is important to target an oncogenic pathway that is common between the different mutations exhibited across a tumour and between patients. However, producing a sufficient concentration

of an autophagy inhibitor in GBM tumours is challenging due the low permeability of the blood-brain barrier and the difficulty in penetrating completely through the tumour mass. Therefore, an autophagy inhibitor may be more closely mimicked genetically by an shRNA against autophagy genes than by CRISRP/Cas9-mediated knockout. Results gleaned where autophagy genes were knocked out, such as the signalling studies in Figure 12.5, may not reflect how a tumour might respond to a putative pharmacological agent. However, as we find new ways to exploit CRISPR/Cas9 gene editing technology we may be able to develop a way in which autophagy genes can indeed be removed completely from patient tumours[362].

Table 12.1 Summary of the results of studies in different cell lines investigating the role of autophagy in anchorage-independent growth

Cell Line	Oncogenic Drivers	GBM Subtype	Method of autophagy ablation	Autophagy Required for Anchorage-Independent Growth?	Results of Further Studies
XFM	Ink4a/Arf$^{-/-}$ PDGF/sh*Tp53*	Proneural	shRNA	✓	-
	Ink4a/Arf$^{-/-}$ sh*Nf-1*/sh*Tp53*	Mesenchymal/ Neural	shRNA	✓	• Growth on low-adhesion plates supported by Atg7
			CRISPR /Cas9	Not studied	• Autophagy promotes cell signalling following detachment loss • Autophagy loss does not influence anoikis
IENS	Ink4a/Arf$^{-/-}$ EGFRvIII	Classical	CRISPR /Cas9	✓	• Growth on low-adhesion plates supported by Atg7 • Autophagy promotes cell signalling following detachment loss • Autophagy loss does not influence anoikis

Furthermore, these results are confounded by studies that have described Atg5- and Atg7-independent means of autophagosome biogenesis, thereby suggesting that targeting these proteins may not prevent the degradation of autophagy substrates[363]. Moreover, although LC3 lipidation and completion of the autophagosome does expedite the fusion of autophagosomes with lysosomal compartment, the delivery of pre-autophagosomal structures to the lysosome can also occur in the absence of the ubiquitin-like LC3 conjugation players[52]. These means of bypassing the need for LC3 lipidation machinery raise questions regarding the efficacy of ablating the expression of these players as selected cargoes may still find a way to be degraded in an autophagy-like manner. Therefore, the most comprehensive means of preventing the

degradation of targets selected by autophagy cargo receptors would be inhibiting the fusion of autophagosomal and lysosomal membranes. These studies exploring the alternative forms of autophagy are important to understand if we believe autophagic degradation to be important in the development of different diseases, such as cancer, as we may need to target them all.

Although autophagy was seen to be similarly essential in all the differently transformed cells assayed in these studies, the variety of oncogenes/tumour suppressors that were manipulated were by no means exhaustive of the combinations that have been documented in the clinic. However, in terms of preliminary basic research, the number of perturbations that are used to transform cells to a malignant GBM subtype will always be limited and a degree of prioritisation must be employed according to the most frequently observed mutations.

Also, here we have used a combination of studies in XFM/*tv-a* glial cells and IENS glioma-initiating stem cells to model different GBM subtypes but it is difficult to directly compare results obtained in these two cell lines. Firstly, they are cultured in media of differing compositions: whilst XFM/*tv-a* are grown in 10% FBS media, IENS require stem cell culture-like conditions with serum-free media supplemented with EGF, FGF, laminin, and B27/N2 supplements (see chapter 10 for full details). Therefore, the activity of the signalling pathways is likely to be significantly different between these cell types. Generally, modelling GBM in serum-free conditions is considered to be closer to the *in vivo* situation. Therefore, it would be more accurate to compare the influence of autophagy on GBM subtype models derived from glioma-initiating cells transformed with driving mutations that are cultured in such serum-free media.

Furthermore, it is important to consider that whilst generally believed good ways to assess the potential of a cell line to form tumours *in vivo*, the soft agar assay and other such techniques of anchorage-independent growth are only simple *in vitro* models. These conditions are unable to include all of the factors that GBM cells are exposed to in the human brain. The conditions of cell culture are highly favourable for cell growth, with abundant nutrients and growth factors and, crucially, lack the contribution of cross talk from resident brain cells, such as the microglia. Therefore, these assays cannot definitively show that autophagy would be required for tumourigenesis *in vivo*.

The results of the experiments described above, however, do lay the foundation for a range of future studies that might clarify the role of autophagy in anchorage-independent growth. For example, whilst here it has been shown that detachment-induced phosphorylation of Akt and ERK is hindered by autophagy loss, it is not known whether this is the cause of the reduced anchorage-independent growth capacity observed in autophagy-deficient cells. To address this, constitutively active mutants of these proteins (such as a construct of ERK2 fused to its upstream regulator MEK1 that confers constant activation[364]) could be expressed in *Atg7*-knockdown cells to test whether soft agar colony formation can be rescued, for example.

It was also not explored here how autophagy regulates Akt and ERK phosphorylation following detachment. One possibility is that autophagic flux generates amino acids that stimulate mTORC1, thereby facilitating mTORC2 activation, and inducing Akt phosphorylation[365,366]. In this scenario, the activation of mTORC1 by amino acids would then exert feedback inhibition on autophagy via the inhibition of ULK1 activity, preventing excessive activation of this cascade. Alternatively, autophagy may directly influence of activity of signalling pathways, via modulation of an upstream signalling molecule, such as has been proposed previously regarding c-Met/β-integrin-ERK signalling[170]. On the other hand, the maintenance of mitochondrial and endoplasmic reticulum homeostasis by autophagy may reduce the production of ROS and PERK signalling; thereby helping prevent repression of Akt and ERK activity. The mechanism by which autophagy induces pro-growth signalling and anchorage-independent growth is important to understand before considering the use of an anti-autophagy pharmaceutical agent in patients in order to anticipate any potential side effects.

Given the caveats outlined above, this study of autophagy function in anchorage-independent growth can be considered as promising preliminary work that warrants further investigation. Together, these data demonstrate that, in the context of glioblastoma cell models, autophagy does not regulate anoikis but is important in promoting malignancy-related cellular signalling pathways that are required for anchorage-independent growth.

13 Autophagy Supports Signalling from the Epidermal Growth Factor Receptor

13.1 Introduction

13.1.1 Receptor Tyrosine Kinase Signalling Cascades

Receptor tyrosine kinase (RTK) signalling pathways are highly oncogenic and are elevated in 88% of glioblastoma multiforme (GBM) cases[250,251]. Moreover, the aberrant over-activation of RTKs is observed in a wide variety of cancers, leading to great interest in studying RTK signalling. However, much of their regulation is still unknown, largely owing to its highly context-dependent nature. Expression levels of different RTKs can differ between different tissue types and extra layers of

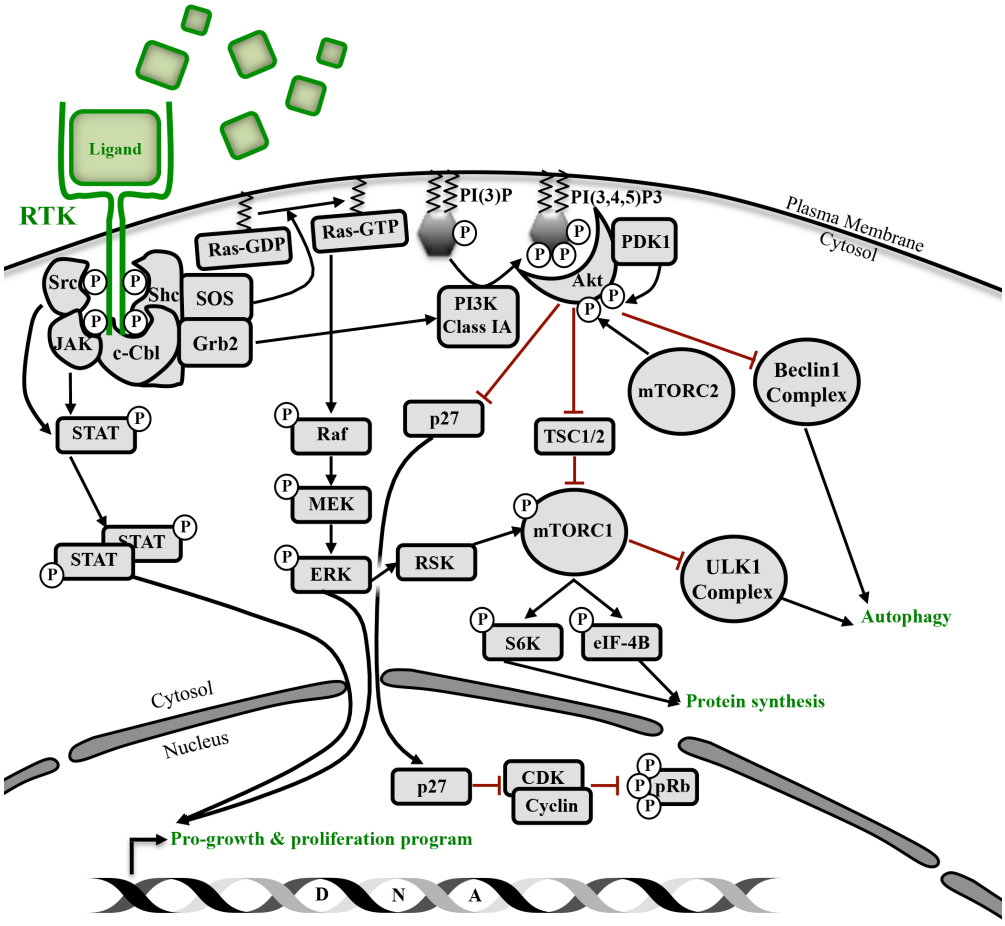

Figure 13.1 A simplified diagram of signalling cascades downstream of RTK activation

complexity are added once one begins to consider pathological specificities and crosstalk between different pathways[367].

We do know, however, that a non-discrete set of interconnected signalling cascades can be induced upon activation of the kinase domains of different RTKs. These can be

roughly grouped as: PI3K/Akt, mTOR, MAPK, and JAK/STAT (Figure 13.1)[77]. Adaptor proteins, such as Grb2/SOS, initiate the transmission of signalling from RTKs into these different pathways before the endocytic machinery is recruited and receptors are internalised and their activities moderated. The signalling pathways initiated by RTK activity generally result in the activation of pro-growth and pro-survival pathways as well as the suppression of cell-death activators and cell-cycle repressors.

It is interesting to note that RTKs, such as members of the HER family, can crosstalk with other each other as well as with other families of receptors (e.g. EGFR and VEGFR[368]). Furthermore, the same pathways can be activated by different RTKs. This represents a significant problem therapeutically, as pharmacological inhibition of one pathway can result in the compensatory activation of another. Understanding the regulatory mechanisms that are common between RTKs might lead us to uncovering a target that might prevent these adaptations.

But how can we measure the activity of these pathways? The traditional, most frequently used method is using SDS-Page Western blotting, but this method is relatively low throughput, as only a select number samples can be run per membrane and only a few proteins can be probed for, thereby leaving much of the pathway untested. One method by which these limitations can be overcome is the the reverse phase protein array (RPPA) (Figure 13.2)[369,370]. This technique uses protein lysates applied to nitrocellulose membranes in a serial dilution of triplicate spots, which then can be probed for different protein abundances using small quantities of diluted primary and HRP-conjugated secondary antibodies. The HRP signal is then detected

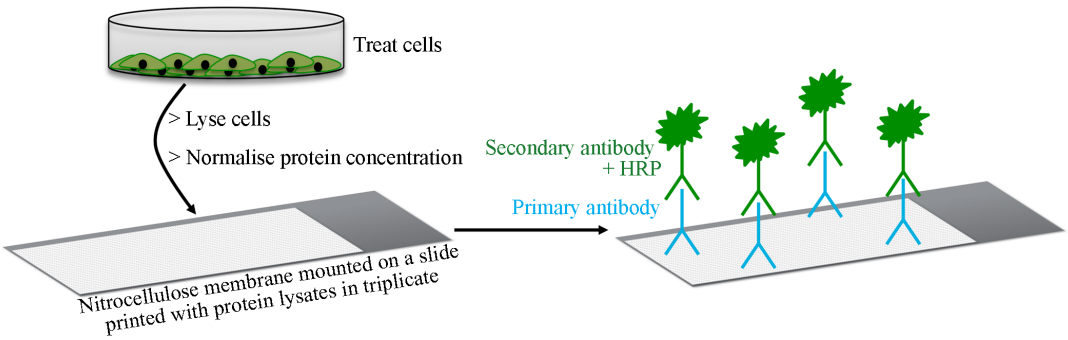

Figure 13.2 Workflow of the high-throughput reverse phase protein array

and can be normalised to housekeeping genes, such as β-actin, and thus the levels of a large number of proteins and protein modifications can be measured. This is

particularly suited to cell signalling studies where the phosphorylation of known proteins in certain cascades can be measured relative to their expression.

13.1.2 Regulation of Signalling From RTKs

Although the majority of the downstream signalling pathways are relatively well characterised, the regulation of the RTKs themselves remains more elusive. Although the seminal review by Ullrich and Schlessinger outlined much of what is known regarding the activation mechanism of the RTK kinase domain nearly thirty years ago, how this signal is terminated is the subject of continued study[371].

Further to catalytic inhibition by the action of protein tyrosine phosphatases (PTPs), the primary method by which RTK signalling is regulated is by its endocytosis and subsequent endocytic trafficking. Briefly, following ligand binding and receptor activation, phospho-tyrosine residues in the cytoplasmic domains of the protein are recognised by adaptor proteins that tag the protein with ubiquitin and recruit endocytic machinery[77,117]. The receptor then becomes internalised into pre-early endosomes that mature into early endosomes. Receptors can then be sorted into either recycling or late endosomes, which are destined for return the plasma membrane or trafficking to the lysosome, respectively.

13.1.3 Autophagy Influences RTK Signalling- The Current Evidence

A recent review composed by my colleagues and myself has outlined much of the current evidence connecting autophagy and RTK signalling, with a particular focus on the role of autophagy in regulating RTK activity, which I shall summarise briefly here[372].

The majority of studies considering RTKs and autophagy focus on the regulation of autophagy by signalling cascades downstream of RTKs, such as EGFR[33]. However, some recent reports are revealing that autophagy can be just as influential in the modulation of RTK activity. For example, it has been shown that expression of autophagy proteins ATG5 and ATG7 is required for the phosphorylation and downstream activity of a variety of RTKs, including the c-Met receptor[170,171,373]. Autophagy proteins also mediate the trafficking of EGFR to the mitochondrion, where it can regulate cell fate decisions[176]. Alternatively, the Beclin-1 complex, which is involved in autophagy initiation, is also required for the maturation of RTK signalling-competent pre-early endosomes to signalling-repressed early endosomes[182].

Moreover, RTKs and downstream MAPK signalling players have actually been directly localised on autophagy-related vesicles[170,171,374].

Together, these studies are starting to unfurl an interesting role for autophagy in promoting oncogenic RTK activity. However, there is currently no consensus regarding the underlying mechanism of this phenomenon.

13.2 Aims

Research question: What role does autophagy play in modulating signalling from RTKs, such as EGFR?

This question represents an important detail not just in understanding normal cell homeostasis but also in terms of how cancers such as GBM regulate oncogenic signalling pathways to facilitate their malignant growth. To begin to answer it, a series of experiments were undertaken:

1. Determine whether autophagy regulates signalling from different receptor tyrosine kinases (RTKs) in response to their cognate ligands
2. Investigate the influence of autophagy loss on the activity of different signalling cascades downstream of EGFR
3. Test whether these results can translate to different cell lines
4. Assay the effect of autophagy-RTK cross-talk on cell survival
5. Measure the activation and termination of EGFR signalling

13.3 Signalling From the Epidermal Growth Factor Receptor is Perturbed Upon Autophagy Ablation in Glial Cells

13.3.1 Investigation of the Influence of Autophagy on Signalling From Different RTKs

To investigate the role of autophagy in a GBM cell model, XFM/*tv-a* glial cells with combined knockdown of *Nf-1* and *Tp53* had the expression of different essential autophagy genes ablated by CRISRP/Cas9, as described in chapter 12 above. To directly assay whether receptor tyrosine kinases (RTKs) in these transformed glial cells rely on autophagy for cell signalling, the activation of Akt and ERK were

measured following cell stimulation with a variety of growth factors. Under my supervision, Rosella Fontana (a visiting student) stimulated cells for fifteen minutes with either FBS (to stimulate a variety of different RTKs), EGF (for EGFR), IGF-1 (for IGF-1R), or HGF (for c-Met), following four hours of serum withdrawal to synchronise receptors at the plasma membrane. Western blotting revealed that autophagy knockout resulted in significantly reduced the phosphorylation of Akt following stimulation with FBS, HGF, and EGF (Figure 13.3A, B, D). However, autophagy was not required for Akt signalling from IGF-1R (Figure 13.3A, D). ERK phosphorylation induced by treatment with FBS, HGF, and EGF was also marginally reduced in autophagy-deficient cells, although variability between experiments prevented statistical analyses reaching significance, except in the case of HGF treatment of sg*Atg7* #3 cells (Figure 13.3A, B, D). These blots show that autophagy is required for the maximal signalling activity of a subset of RTKs, but not IGF-1R. Importantly, these experiments were optimised such that the stimulation of each receptor provided equal activation of Akt in control cells, thereby not over-saturating the pathways or receptors and making results comparable between growth factors.

Of the RTKs tested here, EGFR is the most frequently perturbed in GBM. Therefore in exploring the mechanism by which autophagy facilitates signalling from these receptors, experiments were focussed on signalling through EGFR.

13.3.2 Atg3, Atg7, and Atg16l1 Are Required for EGFR Signalling

Data shown in Figure 13.3 utilised single-guide RNAs against *Atg7* to inhibit its expression. To check that this phenotype depends on autophagy as a pathway rather that Atg7 specifically, *Atg3* and *Atg16l1* knockout cells were also used. Each of these genes is essential for LC3 lipidation and therefore for autophagic flux. Stimulation of these cells with EGF had the same results in all these knockout lines: Atg gene expression loss resulted in reduced Akt and ERK phosphorylation (Figure 13.4). These blots therefore show that the autophagy pathway is required for signalling from EGFR.

13.3.3 Autophagy Is Required for Signalling to a Range of EGFR Downstream Targets

Stimulation of EGFR by its ligand results in the activation of a variety of downstream kinase signalling cascades, of which Akt and ERK are members. These blots have

shown that autophagy is required for the activation of these proteins, but what about the other members of these cascades and the activity of other pathways?

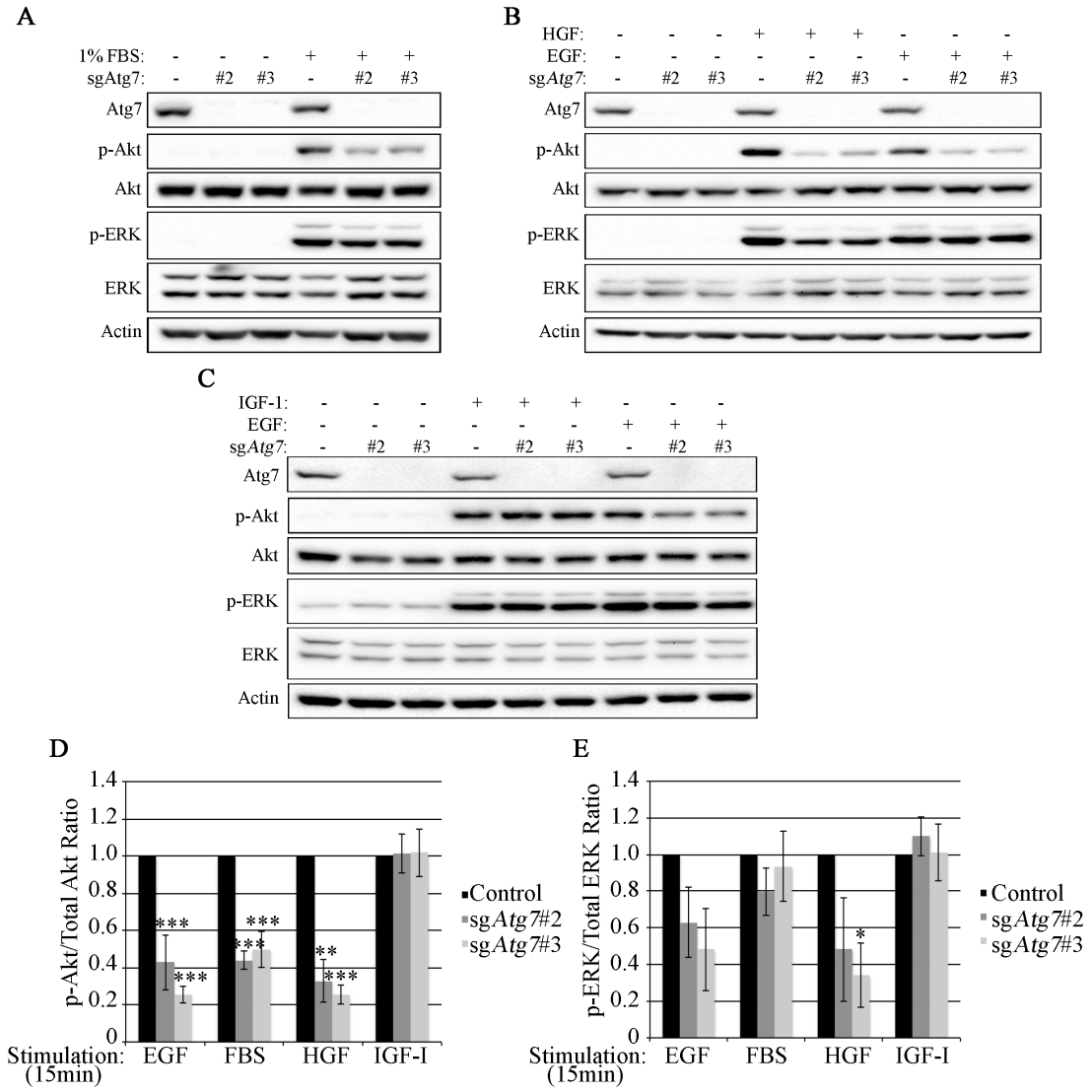

Figure 13.3 Signalling from a subset of receptor tyrosine kinases is regulated by autophagy
A-C Western blots of growth factor stimulation in XFM/*tv-a* sh*Nf-1*/sh*Tp53* glial cells with *Atg7* knockout following 4 hr serum starvation. Cells were stimulated with either 1% FBS (**A**), 2 ng/ml EGF (**B**), 0.1 ng/ml HGF (**B, C**), or 100 ng/ml IGF-I (**C**) for 15 min. **D, E** Densitometry quantification of phosphorylated and total proteins following cell stimulation with various growth factors. Graphs represent the ratio of p-Akt to total Akt (**D**) and p-ERK to total ERK (**E**), made relative to the value in control cells. n=3, error bars represent SEM, * $p<0.05$, ** $p<0.01$, *** $p<0.001$.

To undertake a more comprehensive study of protein abundances and modifications, the reverse phase protein array (RPPA) high-throughput screening platform was used. Samples consisted of Control or sg*Atg7*#3 XFM/*tv-a* sh*Nf-1*/sh*Tp53* cells that were either untreated ('10% FBS'), serum starved for four hours ('-FBS'), or serum starved for four hours then stimulated with EGF or FBS ('+EGF 15 min', '+EGF 30 min', and '+FBS 30 min'). Sample integrity and identity was then checked by Western blotting

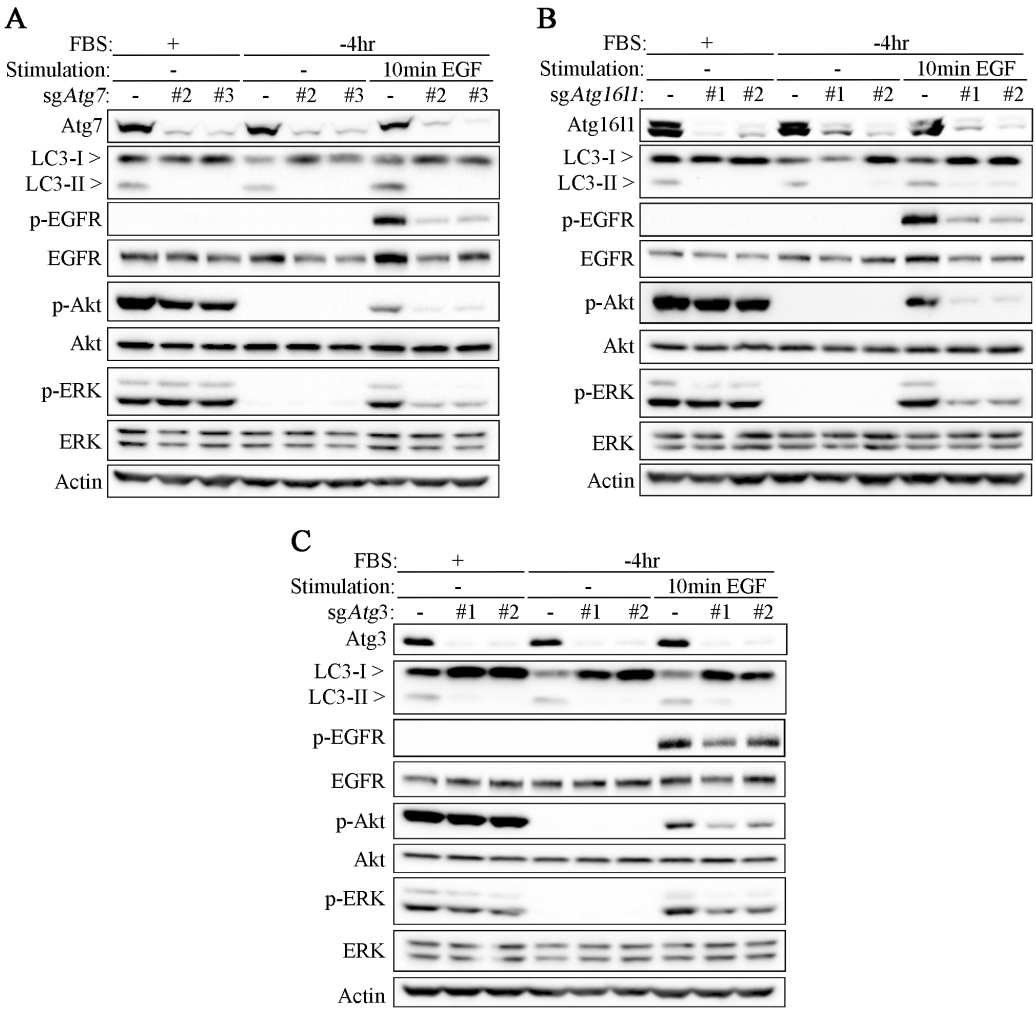

Figure 13.4 Autophagy gene expression is required for EGFR signalling activity
A-C: XFM/*tv-a* sh*Nf-1*/sh*Tp53* glial cells were serum starved for 4 hr before 15 min stimulation with 2 ng/ml EGF, then were lysed for Western blotting analysis. **A:** *Atg7* knockout cells, **B:** *Atg16l1* knockout cells, **C:** *Atg3* knockout cells. Experiments repeated at least 3 times.

before submission for processing by Kenneth McCleod at the institute's drug discovery facility (Figure 13.5A). I then analysed the results of the assay and sorted them from highest to lowest ratio of Control:sg*Atg7* signal for each protein or protein modification (Figure 13.5B, Appendix 1). This study generated a wealth of interesting data, which I shall go through here in some detail.

The top hits with the greatest fold difference of signal observed in control cells versus sg*Atg7* cells following fifteen minutes EGF stimulation are almost all constituents of PI3K/Akt, mTOR, and MAPK signalling cascades (Figure 13.5, Appendix 1). The reduction in phosphorylation upon autophagy ablation is observed at fifteen and thirty minutes of stimulation with EGF and, to a lesser extent, in some cases at thirty minutes of FBS stimulation post-starvation. Although the phosphorylation of STAT5 protein is a well-known readout of EGFR activity, its phosphorylation was not altered

here by serum starvation or EGF treatment (Appendix 1). However, its upstream regulator JAK was responsive to growth factors and did rely on autophagy for its activation, as did the other STAT proteins 1 and 6, although this was to a lesser degree than the other pathways (Appendix 1).

On the other hand, autophagy-deficient cells displayed an increase in abundance of marks that are inhibitory of the cell cycle or inducers of cell death. For example, the mark with the highest sg*Atg7*:Control ratio following serum starvation was cleaved Caspase-3, a marker of cell death induction (Figure S17.15). Furthermore, whilst the cell cycle inhibitor pRb was phosphorylated and therefore inhibited upon EGF stimulation in control cells, cells lacking Atg7 did not induce its phosphorylation, thereby keeping it in an active state that can inhibit the E2F transcription factors and repress the cell cycle (Figure S17.2). The time points measured, however, were not sufficiently long enough to allow transcription and translation of the targets of E2F, such as Cyclin-D, in EGF-stimulated control cells (Figure S17.14). The protein XIAP inhibits members of the Caspase family and in this experiment its expression was increased in control cells following thirty minutes of EGF stimulation (Appendix 1). Similarly, inhibition of the pro-apoptotic protein Bad by phosphorylation was also increased in control cells following thirty minutes of EGF stimulation (Appendix 1). Furthermore, although these cells have knockdown of Tp53 (Figure 13.5A), there still appeared to be some degree of regulation of the cell cycle inhibitor p21 (downstream target of Tp53). Following thirty minutes of EGF stimulation the levels of p21 decrease in control cells whilst remaining higher in autophagy-deficient cells (Appendix 1). This is in contrast to what has previously seen for this protein, where EGF was seen to increase p21 expression[375]. However, other factors known to regulate cell cycle or cell death were not affected, including Bcl-2; PUMA; Bim; ATM; PARP; and Bcl-x (all Appendix 1). Regarding the RTKs that lie upstream of these signalling cascades, autophagy also appears to have a role in promoting the activity of some and the expression levels of others following EGF stimulation (Table 13.1). The receptors that are influenced by autophagy loss are those that are known to cross talk with EGFR; therefore it is possible that autophagy regulates their activities following EGF stimulation via EGFR. Furthermore, FBS stimulation did not activate these receptors

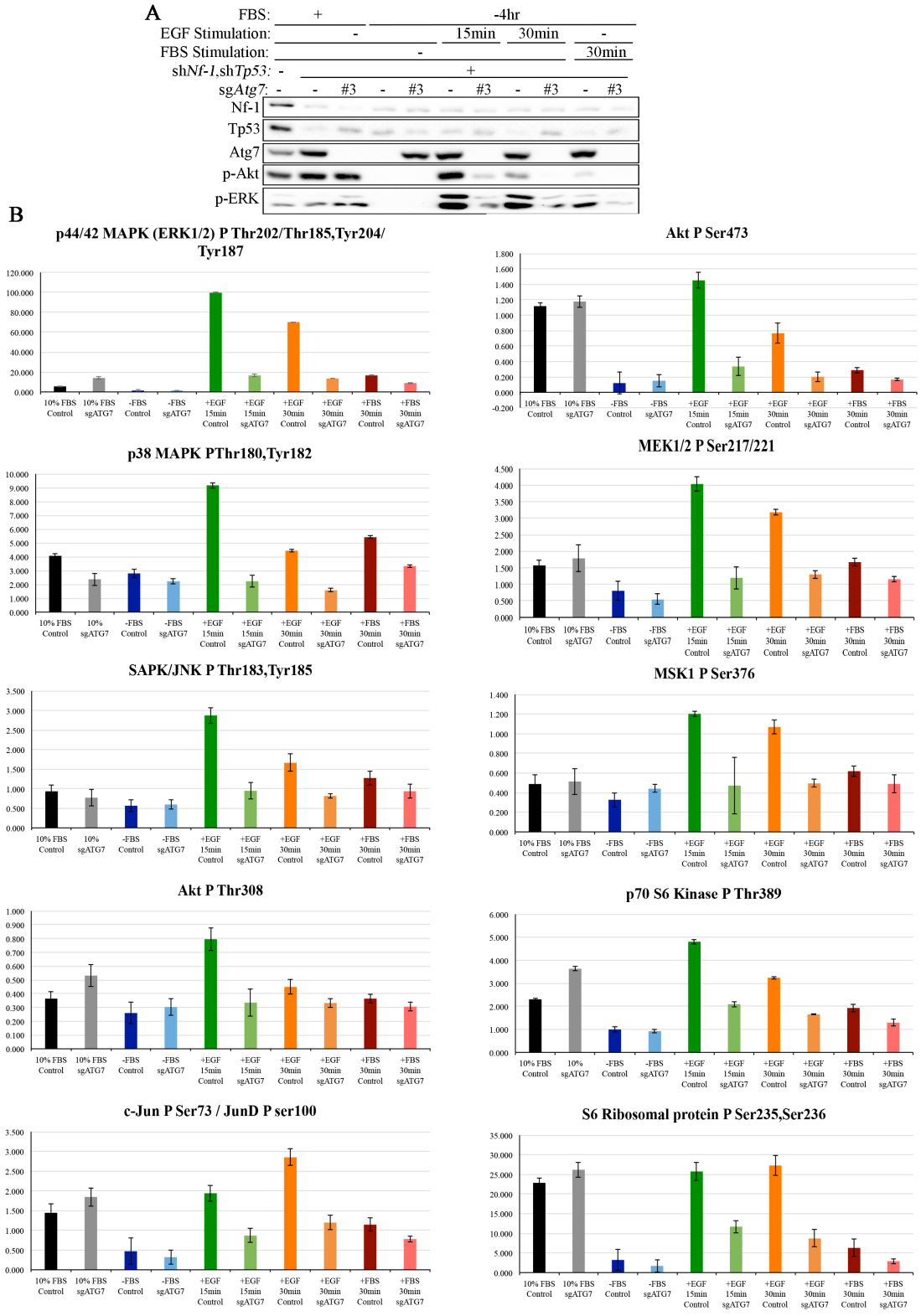

Figure 13.5 Reverse phase protein array analysis reveals Atg7 loss reduces the activity of EGFR downstream signalling cascades I

A,B: XFM/*tv-a* sh*Nf-1*/sh*Tp53* cells were serum starved 4 hr then stimulated with FBS or EGF as indicated. **A:** Western blot confirming the identity of samples submitted for RPPA analysis and validating the Akt and ERK signalling defects observed by this method, **B:** The results of the RPPA (n=1) were ordered from highest to lowest signal ratio in Control over sg*Atg7* for the condition '+EGF 15 min'. Here are shown the top eight hits from this analysis, with the rest found in Appendix 1.

Table 13.1 Summary of RPPA results for RTK abundances and activities following EGF stimulation

Receptor (+ modification)	Influence of autophagy loss		Graph in Figure
	15 min EGF	30 min EGF	
EGFR	Lower	Lower	Figure S17.1
EGFR pY1173	No change	No change	Figure S17.6
EGFR pY1086	No change	No change	Figure S17.7
Her2	Lower	Lower	Figure S17.2
Her2 pY1248, Y1173	Lower	Lower	Figure S17.4
Her3	Lower	Lower	Figure S17.5
Her3 pY1289	Lower	Lower	Figure S17.6
FLT3 pY591	Lower	Lower	Figure S17.2
IGF-1R	No change	No change	Figure S17.7
IGF-1R pY1162, Y1163	Lower	Lower	Figure S17.2
VEGFR pY1059	Lower	Lower	Figure S17.3
VEGFR pY1175	No change	Lower	Figure S17.9
PDGFR pY1021	No change	No change	Figure S17.8
PDGFR pY751	No change	Lower	Figure S17.9
Met	Lower	Lower	Figure S17.2
Met pY1349	Lower	Lower	Figure S17.3
Met pY1234	Lower	Lower	Figure S17.4

above the levels found following serum starvation, supporting the idea that their activation is via the support of EGFR activation by autophagy. Unfortunately, the antibodies for EGFR phosphorylation sites Y1086 and Y1173 were not functional in this assay however, with no increase in signal between serum starved and EGF stimulated conditions, although this is known to be induced in this cell type (Figure 13.3). Together, these RPPA results demonstrate that autophagy facilitates the activity of kinase cascades downstream of EGFR, as well as cross talk between EGFR and other RTKs, ultimately resulting in the suppression of cell cycle inhibitors and pro-death factors.

13.3.4 Autophagy Mediates EGFR in Different Cell Types

Here we have seen that autophagy is able to regulate signalling from EGFR in XFM/*tv-a* transformed with sh*Nf-1*/sh*Tp53*, which represents a model of the 'mesenchymal' and 'neural' subtypes of GBM[251]. But do other cell types also rely on autophagy for RTK signalling? To test this, CRISPR/Cas9 was used to ablate autophagy gene expression in either XFM/*tv-a* cells expressing constitutively active EGFRvIII, representing the 'classical' GBM subtype, or, in order to test this in a cell line that is far removed from GBM, mouse embryonic fibroblasts (MEFs)

Firstly, my colleague, Joanne Simpson, carried out a careful analysis of the response of XFM/*tv-a* EGFRvIII cells to either EGF or FGF ligands. When cells were

stimulated with EGF for five, ten, or fifteen minutes the phosphorylation of Akt and ERK were comparable in control and sg*Atg7* cells (Figure 13.6A). However, when EGFRvIII cells were stimulated with FGF it was clear that Atg7 was required for Akt phosphorylation (Figure 13.6B). This suggested that the effect of autophagy on RTK regulation is negated or over-powered when the receptor is constitutively active, although other receptors are still sensitive to the influence of autophagy.

To test whether this is a universal mechanism in cells, a non-glial cell model was then interrogated: mouse embryonic fibroblasts (MEFs). sg*Atg7* was introduced into these

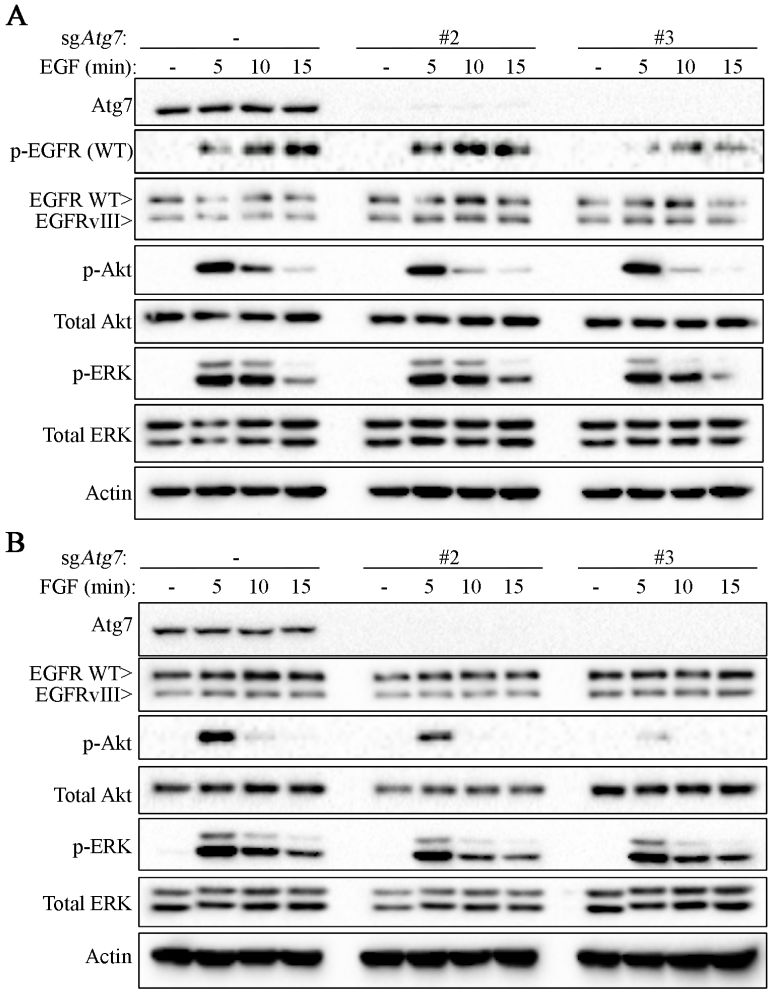

Figure 13.6 Autophagy is required for FGF-induced signalling but not EGF-induced signalling in glial cells with constitutively active EGFR
A XFM/*tv-a* EGFRvIII cells were serum starved for 4hr followed by stimulation with EGF (2 ng/ml) for the indicated amounts of time before analysis by Western blotting, **B** XFM/*tv-a* EGFRvIII cells were serum starved for 4 hr followed by stimulation with FGF (10 ng/ml) for the indicated amounts of time before analysis by Western blotting. Experiments were repeated at least 3 times.

cells then I examined the expression levels of EGFR under untreated conditions. Although in XFM/*tv-a* cells I had not observed any consistent or significant change in EGFR levels, here in MEFs it was clear that EGFR expression was greatly reduced by *Atg7* knockout (Figure 13.7A). To check that this was due to the loss of autophagic

flux rather than loss of Atg7, *Atg3* and *Atg16l1* were also knockout out from MEF cells using CRISPR/Cas9. The loss of these autophagy players also reduced the levels of EGFR under untreated conditions (Figure 13.7B, C). In glial cells, we have seen that autophagy loss impacts signal transduction to Akt and ERK following RTK activation. Does the diminished EGFR expression observed here translate into reduced signalling downstream?

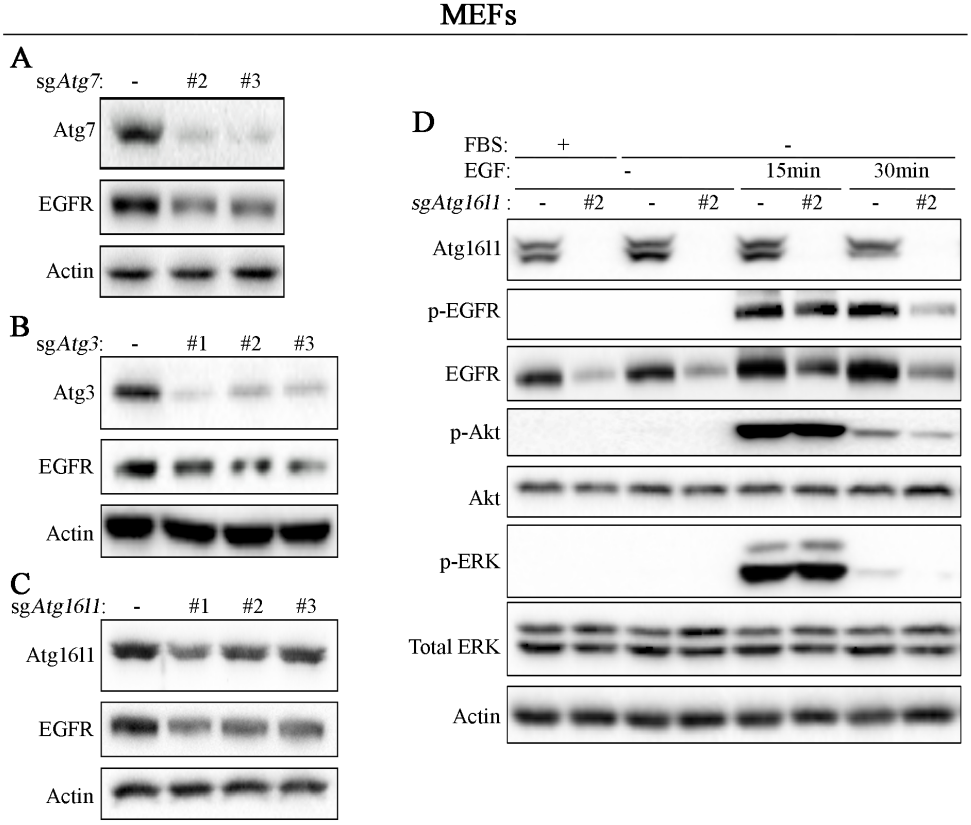

Figure 13.7 EGFR expression is reduced by autophagy knockout in MEFs
A-C: Western blotting of untreated MEF cells expressing sgRNA against *Atg7* (**A**), *Atg3* (**B**), or *Atg16l1* (**C**). **D:** Western blotting of single-clones selected from sg*Atg16l1*#2 transfected MEFs treated with 2 ng/ml EGF for 15 or 30 minutes. Experiments repeated at least 3 times.

A single-cell clone selected from sg*Atg16l1* cells by Ainara González-Cabodevilla had complete loss of Atg16l1 expression. Along with wild-type MEFs, these cells were serum-starved for four hours then treated with EGF for fifteen or thirty minutes. The results show that whilst EGFR phosphorylation and levels are reduced by Atg16l1 loss, the activation of downstream players was similar following EGF stimulation (Figure 13.7D). Therefore, in MEFs the mechanism by which autophagy regulates of EGFR appears to impact its protein levels rather than perturbing its signalling activity. Alternatively, it may also be that autophagy-deficient MEFs have

acquired an alternative mechanism to compensate for EGFR deficiency that results in similar activation of Akt and ERK.

13.3.5 Autophagy Loss De-Sensitises Transformed Glial Cells to EGF-Induced Cell Survival

When grown under normal tissue culture conditions or when starved of serum for a short period of time, the growth rates of autophagy-competent and autophagy-deficient XFM/*tv-a* sh*Nf-1*/sh*Tp53* and EGFRvIII-expressing cells are comparable. However, we have seen that the activities of key cell growth and survival regulators are severely reduced in autophagy-deficient cells following stimulation with EGF, FGF, or HGF ligands. Is the regulation of RTK signalling by autophagy important for cell fate decisions? To address this point, I cultured my cells in serum-free media for twenty-four hours, which strongly induced cell death that could be measured by propidium iodide (PI) labelling. To test the influence of autophagy on the pro-survival capacity of RTKs, the mitogens EGF and HGF were added to the media[376]. Relative PI fluorescence was then measured using a high-throughput plate reader and made relative to the total cell number, as measured by DAPI. This value of cell death/total cell number was then made relative to the value of untreated cells.

These analyses revealed that EGFRvIII and sh*Nf-1*/sh*Tp53* cells have differing requirements for autophagy. sh*Nf-1*/sh*Tp53* autophagy-competent cells experienced significantly less death when cultured with EGF or HGF than when serum starved, but autophagy-deficient cells did not, instead maintaining high levels of cell death (Figure 13.8A, B). Similarly, EGFRvIII cells control cells were able to rescue serum starvation-induced cell death when incubated with EGF or HGF (Figure 13.8A, C). However, although Atg7 loss did prevent a response to HGF, EGF-mediated rescue of cell death was autophagy-independent in this cell line. Therefore, EGFRvIII over-rides the requirement for autophagy to facilitate EGFR signalling and mediate EGF-induced cell survival. It is also interesting to note that EGFRvIII cells experienced a lessened induction of cell death, relative to sh*Nf-1*/sh*Tp53* cells, during serum starvation, which corroborates with previous data suggesting EGFRvIII acts as a cell death repressor (Figure 13.8)[377].

13.4 Autophagy Mediates Maintenance of EGFR Signalling Activity

The results presented above have shown that autophagy positively regulates signalling from EGFR following EGF stimulation. To begin to understand what affects this change, a series of studies were undertaken to investigate whether autophagy

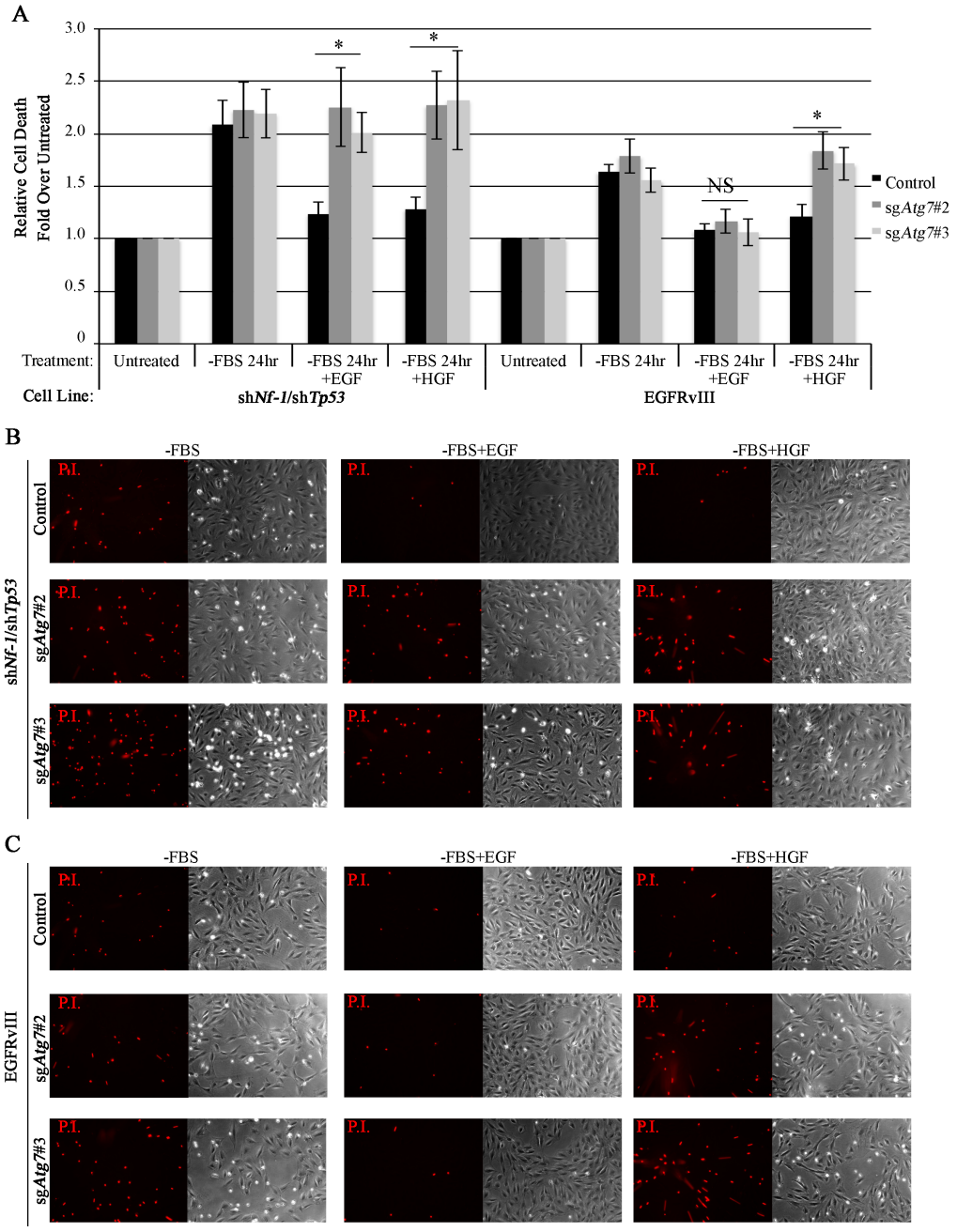

Figure 13.8 Growth factors rescue cell death induced by serum starvation in autophagy-competent cells

A Graph representing the proportion of cell death (propidium iodide) relative to cell number (DAPI) in XFM/*tv-a* glial cells transformed with either sh*Nf-1*/sh*Tp53* or EGFRvIII. Cells were either left untreated (10% FBS DMEM) or serum-starved for 24 hr, in the presence or absence of EGF (20 ng/ml) or HGF (10 ng/ml). Values made relative to that of untreated cells. **B, C** Representative images of propidium iodide staining of sh*Nf-1*/sh*Tp53* (**B**) or EGFRvIII (**C**) cell lines either left untreated (10% FBS DMEM) or serum-starved for 24 hr, in the presence or absence of EGF (20 ng/ml) or HGF (10 ng/ml). n=3, error bars represent SEM, * $p<0.05$, ** $p<0.01$, *** $p<0.001$.

influences the activation or termination of EGFR signalling.

13.4.1 Autophagy Loss Does Not Affect EGFR Degradation Rates

Autophagy is primarily a catabolic pathway in the cell that results in lysosomal degradation of various cargoes and EGFR signalling is known to be terminated at the lysosome[32,90,378,379]. Therefore, it is possible that autophagy loss influences EGFR lysosomal degradation to mediate its signalling response to EGF. Measuring EGFR levels after EGF stimulation for up to two hours in control and sg*Atg7* XFM/*tv-a* sh*Nf-1*/sh*Tp53* cells was used to test this hypothesis. Quantification of these blots reveals that EGFR degradation rates were not influenced by autophagy loss (**Error! Reference source not found.** 13.9). There was, however, a clear reduction in EGFR phosphorylation (**Error! Reference source not found.** 13.9A). Therefore, autophagy is mediating the activity of EGFR rather than its protein levels.

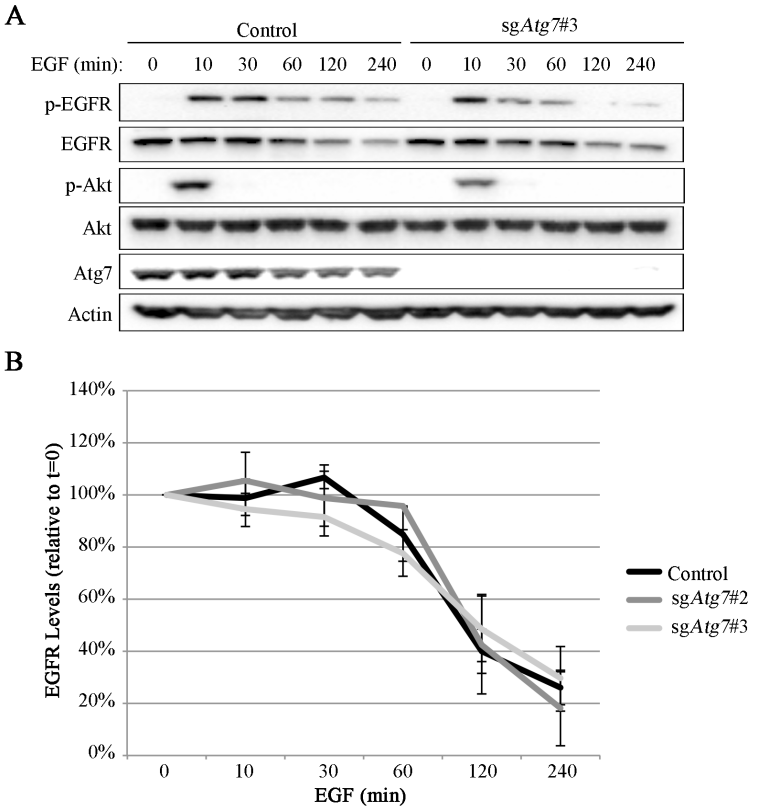

Figure 13.9 EGFR degradation rate does not rely on autophagy
A: Example Western blot of XFM/*tv-a* sh*Nf-1*/sh*Tp53* control and sg*Atg7*#2 cells stimulated with 20 ng/ml EGF for up to 2 hr, **B**: Densitometry quantifications of EGFR levels following EGF stimulation in control and Atg7 knockout cells expressed as a percentage of the start material (t= 0 min). n=3, error bars represent SEM, * $p<0.05$, ** $p<0.01$, *** $p<0.001$.

13.4.2 Autophagy Loss Shortens the Duration of EGFR Signalling But Does Not Influence EGFR Phosphorylation *in vitro*

How is autophagy mediating EGFR activity? Is it reducing its initial kinase activation or something further downstream? Short time-points of EGF stimulation were used to try to distinguish between these possibilities. Stimulation up to five minutes shows that the initial activation of EGFR and its signal transmission to Akt, as measured by their phosphorylation levels, were both functional in autophagy-deficient cells (Figure 13.10A-C). However, at time-points greater than seven minutes, EGFR and Akt phosphorylation were significantly reduced in *Atg7* knockout cells. Therefore, autophagy seems to be required for the maintenance of EGFR signalling following an initial activation peak.

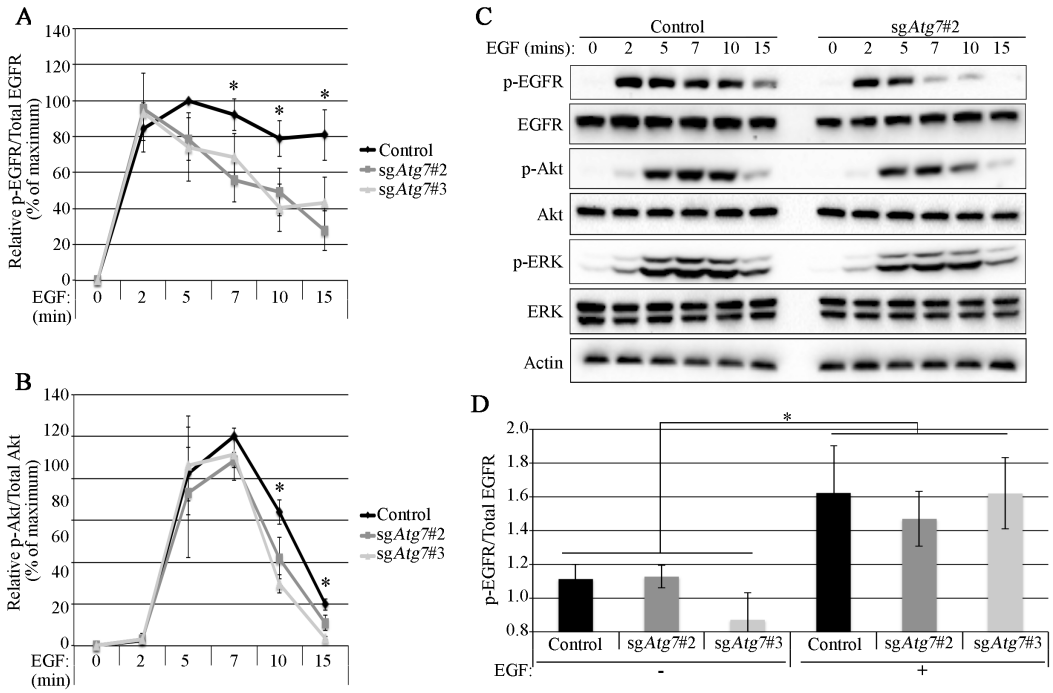

Figure 13.10 Autophagy is required to maintain EGFR and Akt phosphorylation during EGF stimulation

A-D: XFM/*tv-a* sh*Nf-1*/sh*Tp53* control and sg*Atg7* cells were serum starved 4 hr then stimulated with 2 ng/ml EGF for the indicated time points. **A, B:** Densitometry quantification of EGFR (**B**) and Akt (**C**) phosphorylation relative to their respective total protein levels, expressed as a percentage of control cell's maximum signalling time-point, **C:** Representative Western blot of control and sg*Atg7*#2 cells following different time-points of 2 ng/ml EGF stimulation, **D:** *in vitro* kinase reaction with cell lysates incubated at 30°C for 15 min in the presence or absence of 50 ng. n=3, error bars represent SEM, * $p<0.05$, ** $p<0.01$, *** $p<0.001$.

To test whether the activation of the EGFR tyrosine kinase domain is impeded autophagy-deficient cells, an *in vitro* kinase assay was undertaken. This assay was performed by lysing cells in a kinase reaction buffer then incubating at 30°C for fifteen minutes in the presence or absence of EGF. Western blotting analysis showed that the addition of EGF induced the phosphorylation EGFR equally in control and

sg*Atg7* cells (Figure 13.10D). This suggests that autophagy is likely not mediating an EGFR kinase inhibitor, but instead is regulating the maintenance of EGFR phosphorylation by another means in the cell.

13.5 Discussion

The data presented above have shown that autophagy is required to for the maximal of signalling downstream of a subset of receptor tyrosine kinases, including EGFR, in a cell model of GBM. Further study revealed that perturbed signalling as a result of autophagy gene ablation is caused by a failure to maintain EGFR phosphorylation following an initial peak in activity.

RTK signalling targets Akt and ERK were directly measured following the growth factor stimulation of EGFR and c-Met, and were found to be significantly reduced by *Atg7* knockout in XFM/*tv-a* glial cells transformed with *Nf-1* and *Tp53* knockdown. Although some reliance on autophagy has been implicated for these receptors before, this is the first study of its kind to evaluate equally ligand-stimulated RTKs under controlled conditions in the same cell line and therefore be able to directly compare downstream read-outs. In this manner, it is possible to show that whilst stimulation of Akt by EGF and HGF requires autophagy, stimulation with IGF-1 does not. In comparing autophagy-competent and -deficient cells that are stimulated with a mixture of growth factors (i.e. FBS), a requirement for autophagy to transmit general growth factor-to-Akt signalling was discovered. Furthermore, this was not specific to the expression of one autophagy regulator, but instead relied on Atg3, Atg7, and Atg16l1. Being able to demonstrate that this is a overall autophagy-dependent phenomenon is important due to evidence showing that different forms of so-called 'non-canonical autophagy' can generate autophagosome-like structures and autophagy-related endomembranes, some of which have been seen to facilitate cell signalling[170,363,380].

These findings revealed by Western blotting were followed-up and substantiated by RPPA analysis. This technique showed that signalling cascades downstream of RTKs were perturbed from source to terminus by autophagy loss, following stimulation with either EGF or FBS. Unexpectedly, there was also reliance on autophagy for crosstalk between different RTKs, including other ErbB family members and VEGFR. The activities of these pathways are important with regards to GBM as ~88% of patient tumours are seen to have aberrant activity through different RTK pathways. If the

activity of a variety of RTKs can be similarly inhibited through the targeting of a common factor (e.g. autophagy) then it may be more effective at inhibiting the pro-growth and pro-survival pathways that facilitate tumourigenesis.

In chapter 11, low nutrient conditions induced an autophagy-deficient KRas-transformed cell line to establish senescence, correlating with low Akt activity. This senescent phenotype was characterised by increased pRb activity and increased levels of the cell-cycle inhibitor p27. RPPA of EGF-stimulated cells here shows that Akt phosphorylation is lower in *Atg7* knockout cells (Figure 13.5), correlating with a reduction in pRb phosphorylation (Appendix 1, Figure S17.2), thereby permitting its activity in repressing the E2F transcription factors and inhibiting the transcription of cell-cycle progression factors. This supports the pathway hypothesised in that chapter whereby: autophagy → Akt ⊣ p27 → pRb, although in that instance autophagy was maintaining Akt activity during serum starvation, whereas here autophagy is facilitating the activation of Akt following EGF stimulation.

Upon investigating whether autophagy may be similarly required in other cellular contexts, XFM/*tv-a* cells with constitutively active EGFRvIII had *Atg7* knocked-out then were stimulated with EGF and FGF. The activation of Akt by FGF did require Atg7, similarly to the sh*Nf-1*/sh*Tp53*-transformed XFM/*tv-a* cells. However, when stimulated with EGF, an elevated and sustained response in EGFR activity was observed, regardless of autophagy status. Therefore, this mutation of EGFR that renders it constitutively active can bypass its regulation by autophagy, but retains the reliance of other RTKs on autophagy for signalling activity. This was investigated further in an *in vitro* cell death assay that measured the response of cells to EGF and HGF ligands. In sh*Nf-1*/sh*Tp53* cells, there was a reliance on autophagy to transmit pro-survival signalling from EGF and HGF during serum starvation stress, but EGFRvIII cells only relied on autophagy to transmit HGF signals, but not EGF, where Atg7 expression did not influence cell fate. Previous studies have shown that EGFRvIII signals primarily from the plasma membrane and has a low rate of endocytosis, resulting in exemption from endocytic regulation. Therefore, if autophagy mediates receptor signalling by a post-endocytosis process, then EGFRvIII would be rendered insensitive to it.

Although relatively abundant in gliomas and head and neck squamous cell carcinomas (HNSCC), the constitutively active variant III mutant is not the only EGFR perturbation that is seen in cancers. Further work regarding the role of autophagy in

EGFR signalling capacity may explore the influence of autophagy on other EGFR mutations, such as the leucine to arginine mutation observed at position 858 in many lung cancers[381]. Most frequently observed in GBM, however, is the amplification of the EGFR gene locus[251]. Therefore, testing whether autophagy can also regulate signalling from an increased number of receptors would also be of clinical concern. Results from this study suggest that oncogenic constitutive activation of EGFR may render cells insensitive to autophagic regulation of signalling pathways, but perhaps the over-expressed wild-type receptor may still be vulnerable. This represents an opportunity for personalised therapy, with different inhibitors having different efficacy between patients depending on the specific mutational landscape.

Why this modulation of RTK signalling is selective for EGFR and c-Met over IGF-1R is unclear. It may be that different regulatory mechanisms are employed for specific receptors by the cell, of which autophagy may only affect a subset. If this is the case, it is highly likely that the outcome of autophagic regulation of RTKs will vary between cell types, which have varied expression and activities of different RTKs respective to their differentiation status and tissue niche[77,367,382]. Alternatively, similarly to EGFRvIII expression, IGF-1R may have a low rate of endocytosis meaning it would not be influenced by potential endocytic regulation by autophagy.

These results in XFM/*tv-a* cells with different oncogenic drivers have highlighted that the influence of autophagy on RTKs may depend on the mutational background of the cells. Furthermore, subsequent knockout of autophagy proteins in MEFs showed that the outcome of EGFR modulation by autophagy varies between cell types. Whilst glial cells utilised autophagy for EGFR signalling regulation, in MEFs autophagy seemed instead to divert EGFR from lysosomal trafficking but not influence cell signalling. It is possible that autophagy may be acting on the same process in these disparate cell types that generates different outcomes due to the cellular connect.

But what is this mechanism? As outlined in the introduction, EGFR can be regulated either by modulation of its tyrosine kinase activity or by its endocytic trafficking. Cell lysates were tested for EGFR tyrosine kinase competency and found it to be equal in cells with or without Atg7. Regulators of the kinase domain, such as PTPs would be directly exposed to the receptor, irrespective of their cellular spatial regulation, by this method. Therefore, if they were targets of autophagic degradation and sg*Atg7* resulted in the increase of their expression levels, EGFR activation would be lower when stimulated with EGF. However, no such difference was observed in this assay.

However, it does not rule out that autophagy can regulate the spatial regulation of RTK inhibitors like PTPs.

EGFR activation by ligand binding occurs in an initial spike then is slowly dampened over the ensuing minutes by various regulatory mechanisms. To assay whether the activation of the receptor was influenced by autophagy loss, short time-points of EGF stimulation were used. It was possible to see that the peak of EGFR activation was not changed by autophagy loss then, following seven to ten minutes of stimulation, EGFR phosphorylation was reduced in autophagy-deficient cells. This is approximately within the timeframe during which EGFR recycling to the plasma membrane occurs[78]. The recycling of EGFR potentiates its signalling capacity as returning to the plasma membrane presents the receptor for another round of ligand binding to reinforce signalling pathway activity. Therefore, the recycling of EGFR may be how autophagy facilitates the maintenance of EGFR activity.

Collectively these results suggest that autophagy may be involved in the regulation of a subset of RTKs, including EGFR, which is important in maintaining their activity and, consequently, the stimulation of downstream signalling cascades. The mechanism by which autophagy regulates these signalling pathways shall be explored in the next chapter.

14 Autophagy Regulates Endosomal Dynamics and Epidermal Growth Factor Receptor Trafficking

14.1 Introduction

14.1.1 Regulation of The Endosomal System

Cells must constantly respond to the conditions in which they find themselves in order to mediate processes like proliferation, metabolism, and migration. To sense these conditions, cells can take up extracellular materials using processes like macropinocytosis, phagocytosis, clathrin-mediated endocytosis, or clathrin-independent endocytosis (see introduction 8.2.1). Although it is important to consider the other types of endocytosis, it is known that EGFR is primarily regulated by clathrin-mediated endocytosis (CME) at the low concentrations of EGF that have been used in this and the previous chapter[78,383]. Therefore, here I will focus on introducing CME.

Many of the adaptors that initiate clathrin-coated pit formation bind to the negatively charged plasma membrane that form around around clusters of activated RTKs. One such example is adaptor protein-2 (AP-2), which connects cargo (such as EGFR) and membrane lipids to multimeric clathrin to generate a nascent coat[384]. These clathrin-coated buds are then pinched off from the plasma membrane in a dynamin-mediated fashion[99]. These pre-early endosomes are signalling active, negative for phosphatidylinositol-3-phosphate (PI(3)P), and characterised by the presence of adaptor protein phosphotyrosine interacting with PH domain and leucine zipper 1 (APPL1)[82,182]. Maturation to early endosomes follows the recruitment the PI(3)P kinase complex, which is composed of PIK3C3, Beclin-1, and regulatory proteins UVRAG and Bim (Figure 14.1)[385,386]. These early endosomes then undergo a sorting process, with cargo destined for either: multivesicular bodies (MVBs) and late endosomes that fuse with the lysosome, or recycling endosomes that return to the plasma membrane. It has been suggested that although other means of endocytosis are primarily used to transport cargoes to the lysosome for degradation, CME chiefly results in sorting into the recycling route[78]. Whilst lysosomal degradation terminates signalling in a manner only replenishable by transcription and translation of new protein, recycling allows for the immediate replacement of receptors for renewed stimulation and re-enforcement of downstream signalling cascades[78,129].

During endocytic maturation steps, regulatory and scaffold factors are exchanged or modified, such as phosphatidylinositol moieties and Rab GTPases. These can act as molecular markers for each stage of the endocytic pathway:

- **Early endosomes:** PI(3)P, Rab5, EEA1
- **Late endosomes:** PI(3,5)P_2, Rab7
- **Recycling endosomes:** PI(4)P, PI(4,5)P_2, Rab4, Rab11
- **Multivesicular bodies:** PI(3)P, PI(3,5)P_2, Rab5, Rab7
- **Golgi apparatus:** PI(4)P, Rabs 1, 2, 6, 8, 9, 18
- **Plasma membrane:** PI(4,5)P_2, PI(3,4,5)P_3

Furthermore, it is possible to inhibit transition between these compartments by preventing the catalytic production of each phosphatidylinositide or recruitment of each Rab.

Whilst some RTK adaptor proteins mediate CME, others recruit initiators of signalling cascades. One such example is Grb2, which connects RTKs such as EGFR to the signalling molecule SOS that in turn activates Ras to initiate the MAPK signalling cascade[387]. Whilst CME adaptor molecules bind at the plasma membrane, signalling adaptors can also interact with RTKs after their endocytosis[388].

RTK endocytosis has been seen to have varying affects on signalling activity. Preventing endocytosis by inhibiting dynamin has produced conflicting and context-dependent results, with different reports showing that the activities of downstream signalling pathways can be promoted[389,390], inhibited[391], or unaffected[132,391,392]. Alternatively, inhibition of endosomal maturation from pre-early endosomes results in prolonged signalling capacity, suggesting progression from these vesicles has an inhibitory effect on RTK signalling[182]. Given the importance of the activity of RTK downstream signalling pathways in diseases such as cancer, there is a need for increased clarity in this field.

The signalling activity of EGFR relies on the activity of its tyrosine kinase domain, which is activated by phosphorylation and therefore can be inhibited by the action of protein phosphatases[371,393,394]. The binding of these phosphatases can occur at different stages of endocytosis including at the plasma membrane or in endosomes[395].

14.1.2 PI(3)P and the PIK3C3 Complex

As described above, early endosomes are defined by the presence of PI(3)P that then acts to recruit the effectors EEA1 and Rab5. The PIK3C3 complex catalyses the synthesis of this lipid on endosomal membranes but also it also has a parallel role in autophagosome biogenesis. The apportionment of PIK3C3 between these two functions is specified by the binding of different regulatory factors: the autophagy-specific complex sees it bound to Beclin-1, ATG14L1, and AMBRA1, whereas the

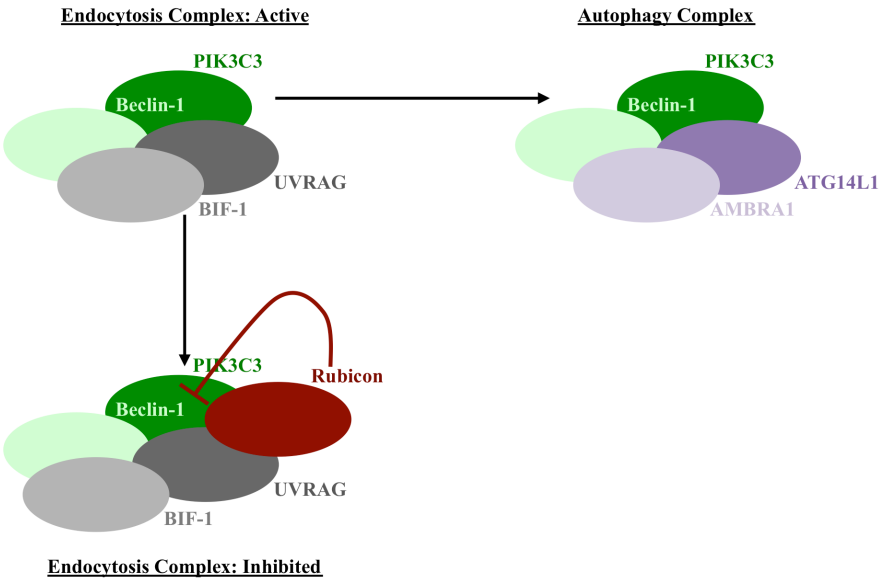

Figure 14.1 The Different Configurations of the PIK3C3/Beclin-1 Complex
Green: Core complex components PIK3C3 kinase and regulatory partner Beclin-1, **purple:** Proteins that direct PIK3C3 activity to autophagosome biogenesis, **grey:** PIK3C3 endocytic regulators, **red:** Rubicon can inhibit the activity of the PIK3C3/Beclin-1 complex

endocytosis-regulatory complex relies on binding to Beclin-1, UVRAG, and Bim1 (Figure 14.1)[25,396]. In these two different conformations, therefore, this complex lies at a nexus between autophagy and endocytic trafficking.

14.1.3 Autophagy and Endocytic Trafficking Commonalities

The PIK3C3 complex is not the only common factor between autophagy and the endocytic pathway, however. A multitude of commonalities exist between these processes including shared trafficking compartments, such as the Golgi and ER, and mutual regulators, like TRE2-BUB2-CDC16 (TBC) domain-containing RAB GTPase activating proteins (GAPs) (Figure 14.2).

TBC Rab GAPs are master endocytic regulators can interact with a multitude of essential autophagy mediators, including ATG9 and LC3[24,144,397]. The fact that LC3

and ATG9 are amongst the few known lipid-binding autophagy proteins may belie the convergence of autophagic and endocytic membranes.

Indeed, autophagy proteins have been seen to trace along several lines of endosomal traffic. For example, essential autophagy players ATG16L1 and ATG9 can interact with clathrin and AP-2, respectively, at the plasma membrane[31,398]. ATG16L1 and ATG9 can then localise to recycling endosomes upon autophagy induction, mediated, in the case of ATG9, by the activity of ULK1[24,145]. Furthermore, MVBs/late endosomes can co-localise with ATG9 upon autophagy induction, which is likewise associated with ULK1 but additionally requires PI(3)P[142]. Another connection with

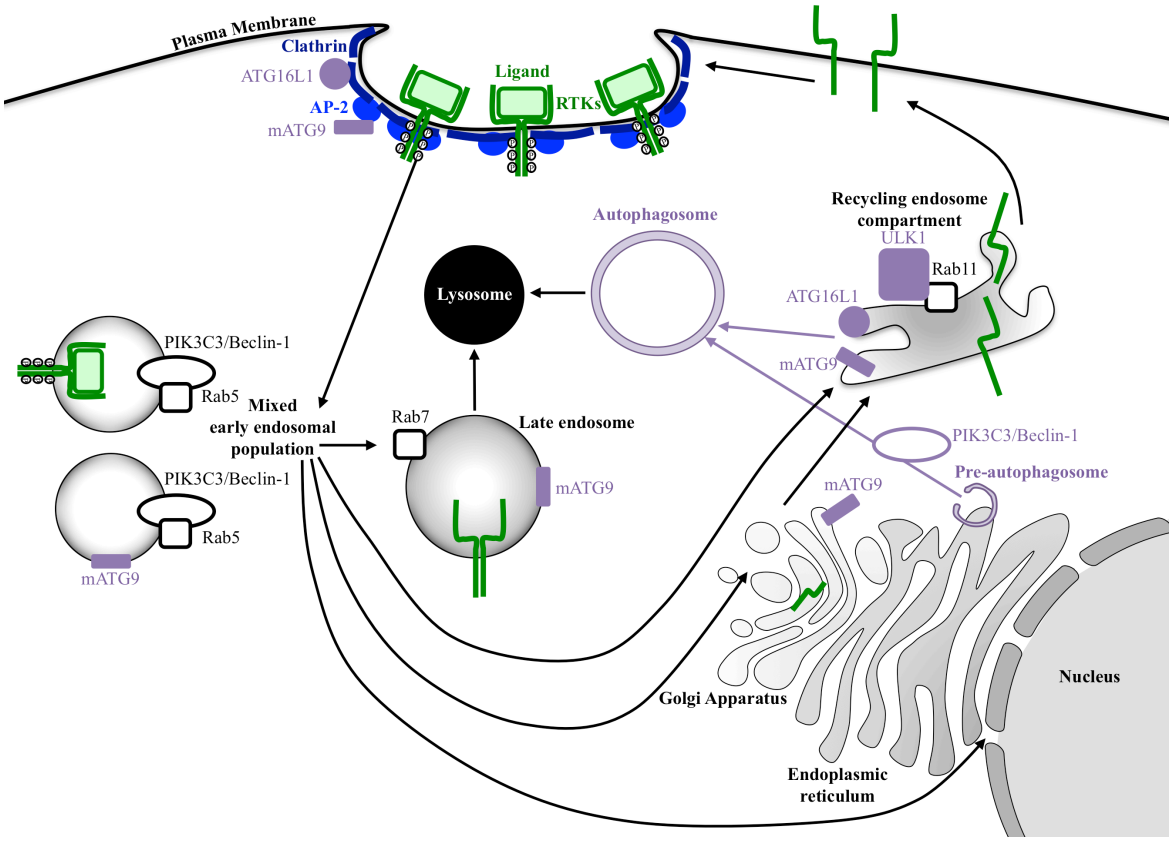

Figure 14.2 Diagram Representing a Simplified Version of the Endocytic Pathway and Where Autophagy Proteins Have Been Observed in that Pathway
Green: receptor tyrosine kinases and their ligands, **purple:** constituents of the autophagy pathway, **black/grey:** components of the endocytic pathway.

late endosome compartments is found in the fusion of autophagosomes with MVBs to form 'amphisome' structures that target to the lysosome[379].

Furthermore, by switching between its two different complexes PIK3C3 is able to provide feedback mechanisms between autophagy and RTK signalling. For example, preferential participation of PIK3C3 in autophagosome biogenesis would abrogate the addition of PI(3)P to pre-early endosomal structures, thereby holding them in a

permissive state for RTK signalling. Active RTKs then stimulate cascades that inhibit autophagy upstream, thereby making PIK3C3 complex components available to act in endosomal regulation[16,18,19]. On the other hand, RTK activity can instigate Beclin-1 post-translational modifications that inhibit that activity of the PIK3C3 complex[33,180]. Alternatively, Rubicon-mediated inhibition of PIK3C3 sequesters UVRAG from its function with HOPS in activating Rab7[181]. As the final stages of autophagy rely on Rab7, its suppression by Rubicon therefore has the potential to inhibit both RTK endocytic degradation and autophagy[181,399]. These actions of Rubicon can thereby hypothetically promote RTK signalling and reinforce inhibition of autophagic catabolism under times of nutrient availability.

14.2 Aims

Research question: How does autophagy facilitate EGFR signalling?

In the previous chapter the reliance of sustained EGFR signalling on the expression of key autophagy proteins was demonstrated. Disrupting this signalling by autophagy loss reduced the phosphorylation of Akt and ERK and lead to insensitivity to EGF-induced cell survival. The initial activation of the tyrosine kinase domain of EGFR was seen to be intact in cells and *in vitro*. Therefore, it is likely that, following its activation and endocytosis, EGFR is undergoing differential endocytic regulation. The current literature offers a complex picture of connections between autophagy and the endocytic trafficking pathways that regulate RTKs. To tease apart how autophagy facilitates the proper signalling of EGFR a series of points had to be addressed:

1. Investigate whether autophagy players regulate EGFR signalling by affecting its endocytic trafficking
2. Examine potential direct connections between autophagy proteins and EGFR or endocytic players
3. Test which endocytic regulators are disrupted by autophagy knockout
4. Finally, determine the molecular interactions by which autophagy can influence EGFR endocytic trafficking

---

14.3 Autophagy Perturbs EGFR Endocytic Trafficking

In the previous chapter it was shown that XFM/*tv-a* sh*Nf-1*/sh*Tp53* transformed glial cells require autophagy for the maintenance of signalling from EGFR after stimulation for more than ten minutes with EGF, although the initial activation of the kinase was autophagy-independent. But a question mark remained regarding how autophagy was able to effect this change in signalling. As the kinase activity of the receptor was unchanged it suggested that autophagy might act upon its regulation by endocytosis.

14.3.1 Autophagy Loss Alters EGFR Endosomal Residency

Endocytic trafficking tightly regulates EGFR signalling and to begin exploring how autophagy was influencing EGFR its localisation in different endosomal compartments was tested.

Once endocytosed, EGFR traffics to early endosomal compartments that are marked with Rab5 and EEA1. EGFR co-localisation with mCherry-tagged Rab5 and endogenous EEA1 was analysed by immunofluorescence (IF) following stimulation with EGF for either five or fifteen minutes. Image analysis showed that whilst after five minutes of stimulation there were similar amounts of EGFR in early endosomes in control of sg*Atg7* cells, by fifteen minutes there was a marked accumulation of EGFR in early endosomal vesicles in autophagy-deficient cells (Figure 14.3).

The EGF-EGFR complex that forms at the plasma membrane remains intact during its initial endocytosis and in early endosomes, but as the pH lowers during endosome maturation, the ligand detaches from its receptor[49]. Upon testing co-localisation between Alexa555-tagged EGF (denoted 555-EGF) and endogenous EGFR in these cells, it was possible to see numerous $EGFR^{+}/EGF^{-}$ vesicles in control cells. However, autophagy ablation reduced the incidence of green $EGFR^{+}/EGF^{-}$ puncta, instead showing increased yellow co-localisation between ligand and receptor, thereby suggesting that endocytic maturation was defective (Figure 14.4).

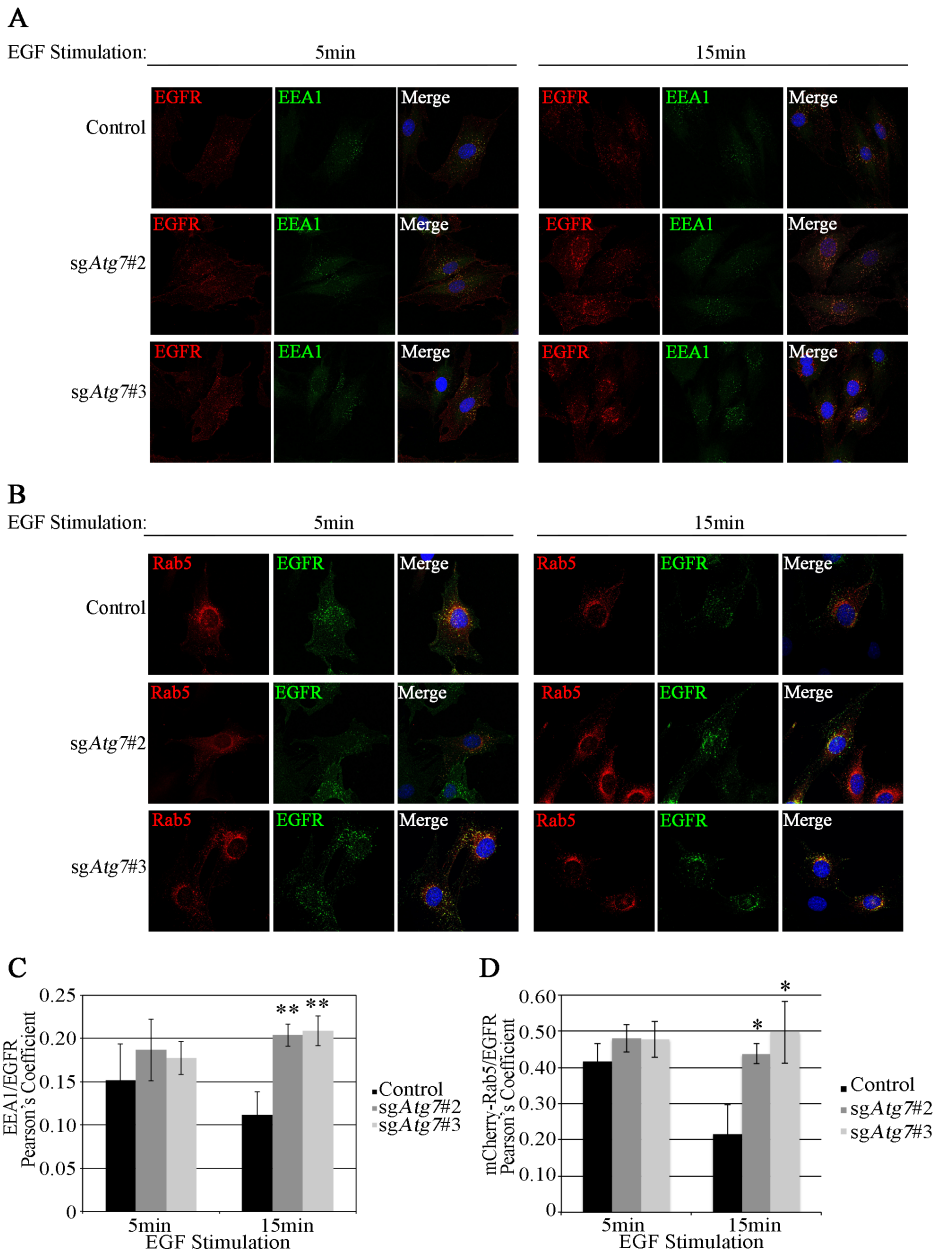

Figure 14.3 *Atg7* Knockout Cells Have an Accumulation of EGFR in Early Endosomes Following 15min of EGF Stimulation

A, B: Representative images of EGFR staining with either endogenous EEA1 (**A**) or over-expressed mCherry-Rab5 (**B**) following 5 or 15 min (20 ng/ml) EGF stimulation in XFM/*tv-a* sh*Nf-1*/sh*Tp53* cells, **C, D:** Quantification of Pearson's coefficient for EEA1/EGFR and mCherry-Rab5/EGFR colocalisation following 5 and 15 min EGF stimulation. n=3 experiments, ≥30 cells quantified per condition, error bars represent SEM, * $p<0.05$, ** $p<0.01$, *** $p<0.001$.

Early endosomes can sort cargo into late endosomes for trafficking to the lysosome for degradation. As EGFR was seen to accumulate in these early endosomes, was it possible that they were not maturing to late endosomes in autophagy-deficient cells? To investigate this, 555-EGF was applied for fifteen minutes before cells were stained for endogenous Rab5 or Rab7 to mark early and late endosomes, respectively.

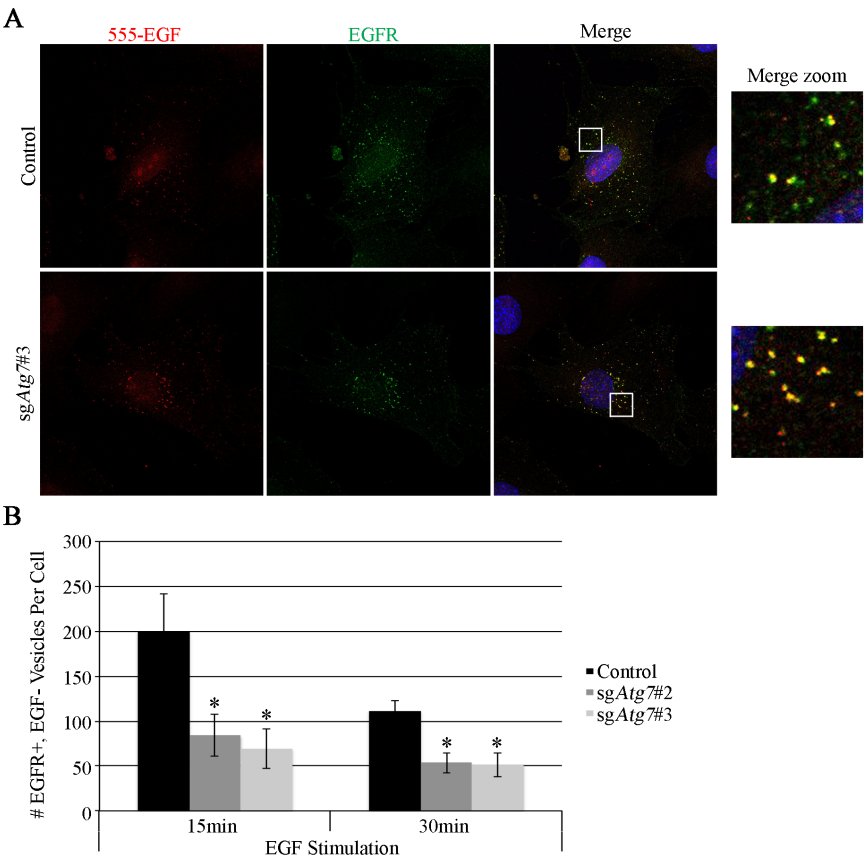

Figure 14.4 EGF/EGFR Co-localisation is Greater in *Atg7* Knockout Cells
A: Representative confocal images showing increased co-localisation between EGFR and 555-EGF in *Atg7* knockout XFM/*tv*-a sh*Nf-1*/sh*Tp53* cells (red: 555-EGF, green: EGFR, blue: DAPI), **B:** Quantification of the number of EGFR-positive, 555-EGF-negative vesicles per cell. n=3 experiments, ≥30 cells quantified per condition, error bars represent SEM, * $p<0.05$, ** $p<0.01$, *** $p<0.001$.

These images showed that EGF was able to traffic similarly to Rab7-positive late endosomes in autophagy-competent and autophagy-deficient cells, whilst confirming that EGF accumulates in Rab5-positive early endosomes when Atg7 expression is lost (Figure 14.5). This data is in line with the results from the EGFR degradation assay presented in the previous chapter: EGFR trafficking to late endosomes and its subsequent lysosomal degradation is not influenced by autophagy status.

Alternatively, EGFR can be sorted into recycling endosomes from early endosomes then returned to the plasma membrane. There are two classes of recycling endosomes, so-called ‘fast’ and ‘slow’, which are marked by Rab4 and Rab11, respectively. Although Rab4 co-localisation with EGFR was not affected by *Atg7* knockout, EGFR trafficking to Rab11-positive recycling endosomes was significantly reduced by autophagy loss (Figure 14.6). Therefore, autophagy facilitates the delivery of EGFR to recycling endosomes, correlating with an enhanced signalling capacity.

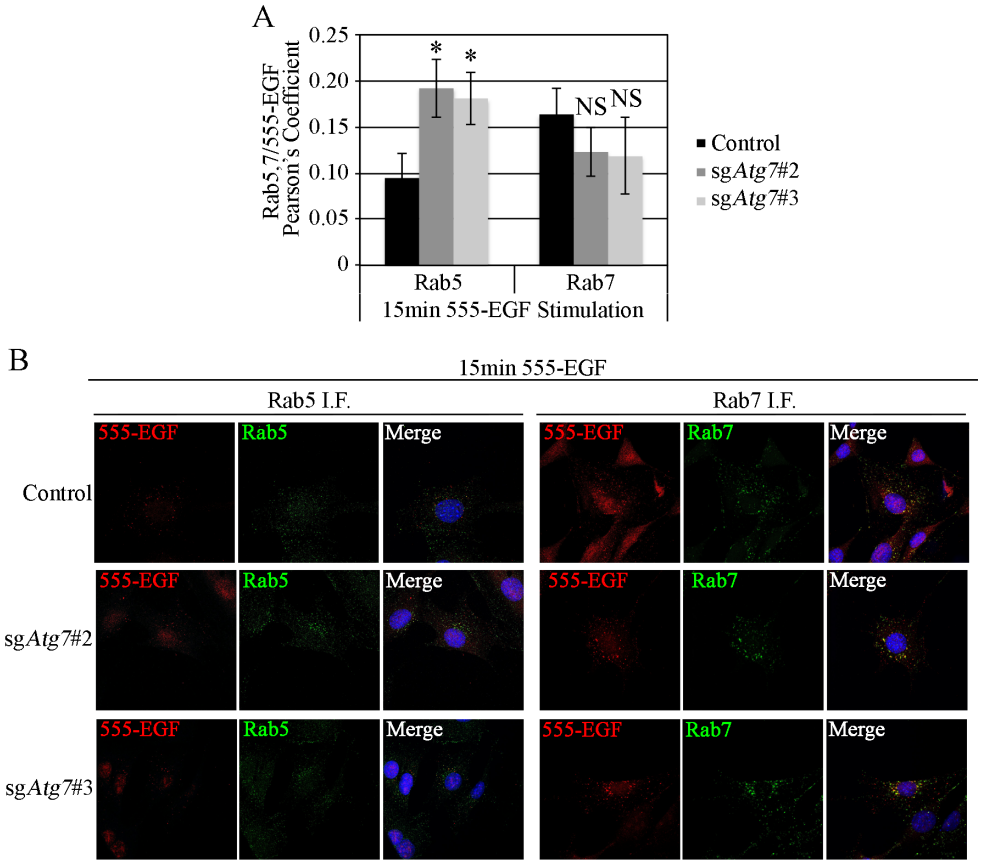

Figure 14.5 Late Endosome Trafficking of EGFR Is Not Influenced By Autophagy Loss
A: Quantification of co-localisation between endogenous Rab5 or Rab7 with 555-EGF, which was applied at 20 ng/ml for 15 min to XFM/*tv-a* sh*Nf-1*/sh*Tp53* cells , **B:** Representative images of co-localisation between 555-EGF and Rab5 or Rab7. n=3 experiments, ≥30 cells quantified per condition, error bars represent SEM, * $p<0.05$, ** $p<0.01$, *** $p<0.001$.

14.3.2 *Atg7* Knockout Results in the Accumulation of Perinuclear EGFR^{+} Vesicles

During the course of the above studies, it was clear that stimulation with EGF resulted in the accumulation of EGFR in a perinuclear region when *Atg7* was knocked out. In order to quantify this phenomenon, 'perinuclear' vesicles were defined as within a fifteen-micron radius from the centre of the nucleus. Following five minutes of EGF stimulation EGFR was evenly distributed in autophagy-competent and deficient cells whilst in the process of early endosome trafficking (Figure 14.7A). However, following fifteen minutes of EGF treatment, although EGFR was still well distributed throughout control cells, over two-thirds of EGFR was perinuclear in autophagy-deficient cells (Figure 14.7B).

Confocal live cell imaging was then used to characterise this trafficking defect. Following four hours of serum starvation, fluorescently labelled EGF (555-EGF) was applied to control or *Atg7* knockout sh*Nf-1*/sh*Tp53* cells and imaged in dimensions of

x, y, z, and time. Computational tracking of EGF-containing vesicles in this setting confirmed the fixed confocal data: autophagy loss results in the perinuclear accumulation of EGFR (representative example tracks A). There were a multitude of tracks continuously originating from the plasma membrane in control

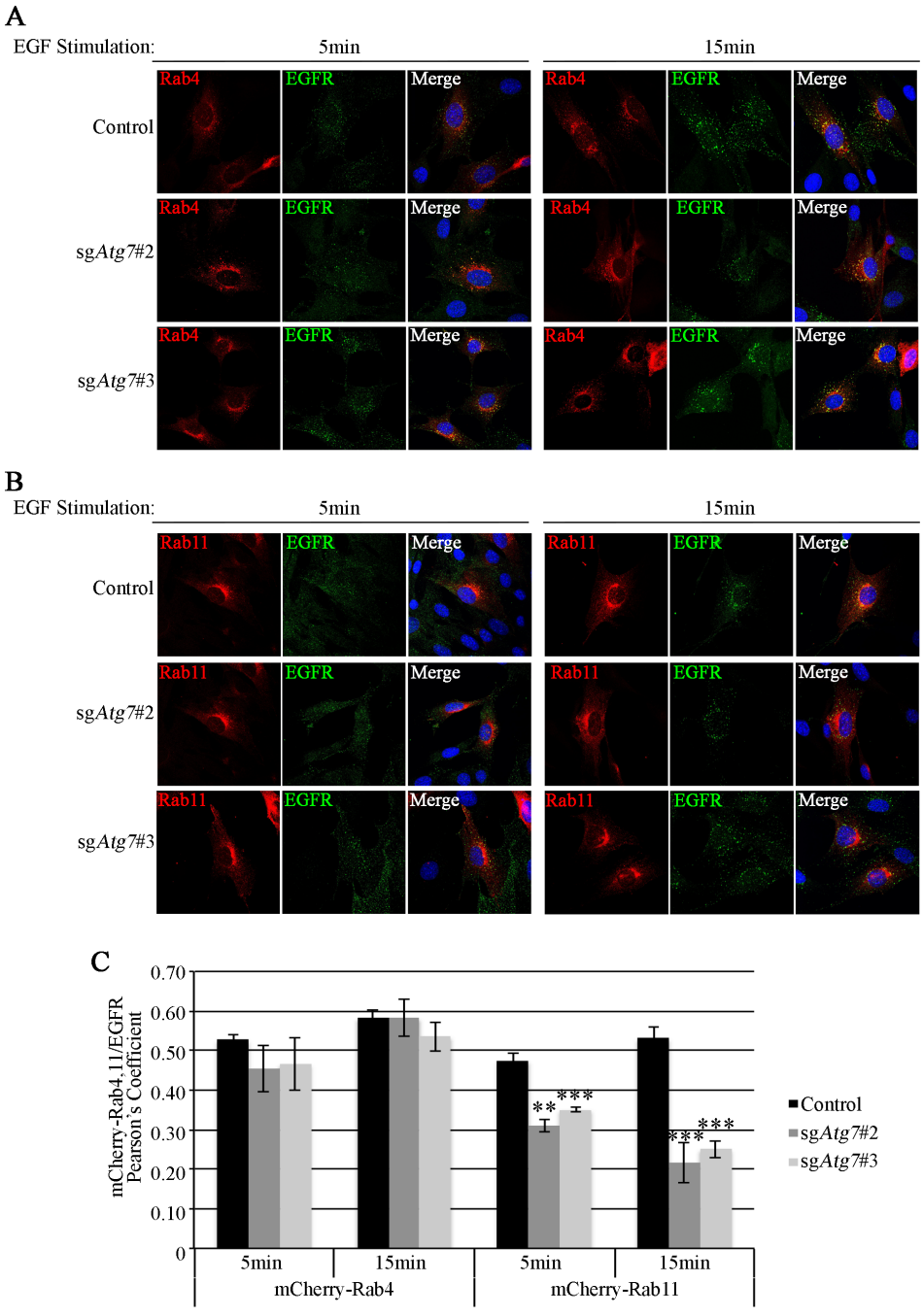

Figure 14.6 Atg7 Is Required For EGFR Trafficking to Rab11-Positive But Not Rab4-Positive Recycling Endosomes

A, B: Representative images of EGFR staining with mCherry-Rab4 (**A**) or mCherry-Rab11 (**B**) following 5 or 15 min (20 ng/ml) EGF stimulation in XFM/*tv-a* sh*Nf-1*/sh*Tp53* cells , **C:** Quantification of Pearson's coefficient for EGFR with mCherry-Rab4/Rab11 colocalisation following 5 and 15 min EGF stimulation. n=3 experiments, ≥30 cells quantified per condition, error bars represent SEM, * $p<0.05$, ** $p<0.01$, *** $p<0.001$.

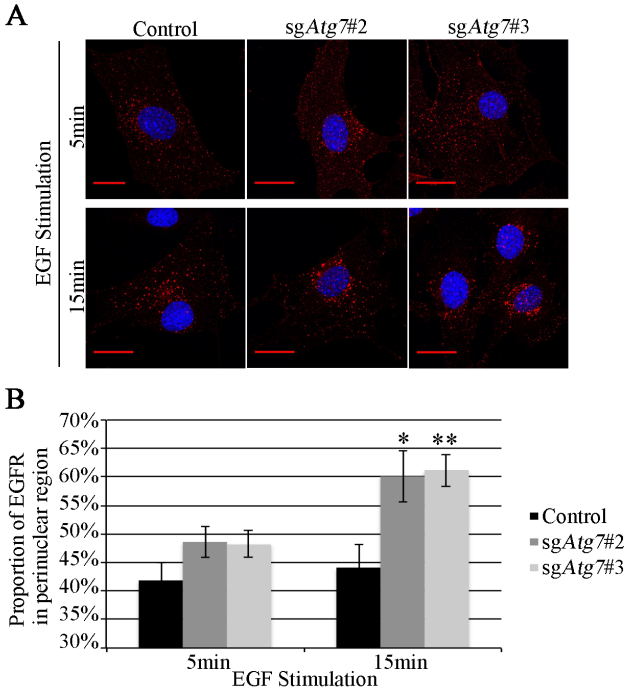

Figure 14.8 EGFR Accumulates in a Perinuclear Region of *Atg7* Knockout Cells
A: Representative images showing that after 5 min EGF stimulation (20 ng/ml) control and *Atg7* knockout XFM/*tv-a* sh*Nf-1*/sh*Tp53* cells show similar EGFR staining pattern but by 15 min *Atg7* knockout cells accumulate perinuclear EGFR, scale bars=20 µm, **B** Quantification of EGFR staining within 15 µm of the centre of the nucleus at 5 and 15 min EGF stimulation. n=3 experiments, ≥30 cells quantified per condition, error bars represent SEM, * $p<0.05$, ** $p<0.01$

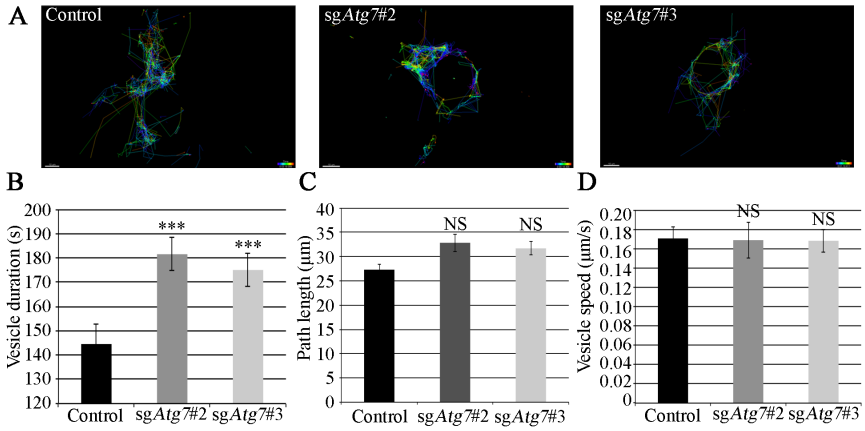

Figure 14.7 Live Cell Imaging Reveals Autophagy Facilitates EGF$^+$ Vesicle Dynamics
A: Representative rainbow-coded tracks of 555-EGF$^+$ vesicles in XFM/*tv-a* sh*Nf-1*/sh*Tp53* cells over time generated in Imaris, where t=0 is purple and the end of the experiment is red, **B-D:** 555-EGF$^+$ vesicle tracks were analysed by Imaris software for duration (**B**), distance travelled (**C**), and speed (**D**). n=3 experiments, ≥30 cells quantified per condition, error bars represent SEM, * $p<0.05$, ** $p<0.01$, *** $p<0.001$.

cells, whilst autophagy-deficient cells EGF maintained a continuous circumnavigation of the nucleus (Figure 14.8). Furthermore, quantification of these tracks showed that each EGF$^+$ vesicle has an increased duration when *Atg7* is knocked-out (Figure 14.8B). This suggests that EGF is most likely still bound to its receptor in early endosomes, rather than becoming dissociated and degraded, leaving EGFR free to return to the plasma membrane for renewed activation. This did not, however,

influence the speed at which vesicles moved or how far they travelled, perhaps indicating that the association between EGFR and the cytoskeleton is not affected (Figure 14.8C, D). Therefore, autophagy loss results in perturbed EGFR trafficking by preventing proper sorting into Rab11-positive recycling endosomes, instead causing its accumulation in early endosomes clustered close to the nucleus.

14.3.3 EGFR Endosome-Plasma Membrane Recycling Is Facilitated By Autophagy

Does this disruption of Rab11-positive endosomes in autophagy-deficient cells impact the plasma membrane recycling of EGFR? EGFR was still seen to traffic to Rab4-positive 'fast' recycling endosomes, which may be able to compensate for the defects in Rab11 traffic. To assay whether EGFR recycling is affected, a cell-surface biotinylation-based method was utilised to track receptors following endocytosis (Figure 14.9). Following four hours of serum starvation, cell-surface proteins (e.g. EGFR) were conjugated to biotin on ice. Negative controls were generated by immediately stripping off this biotin label with a reducing solution on ice.

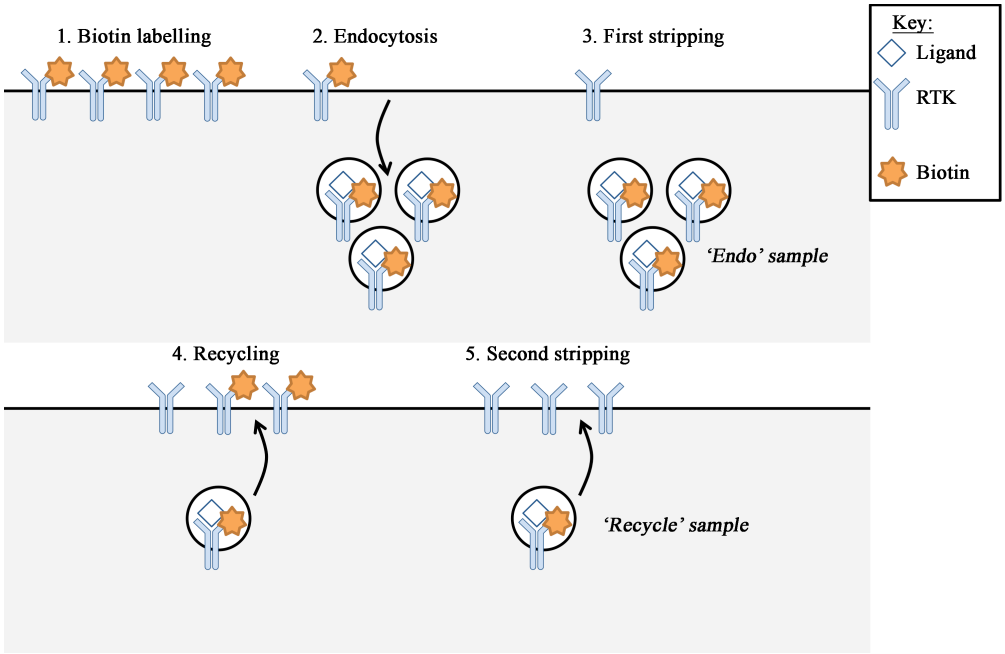

Figure 14.9 Diagram of Biotinylation Recycling Assay

Alternatively, 'endocytosis' and 'recycling' samples were incubated at 37°C for fifteen minutes with EGF to induce EGFR uptake before any non-endocytosed cell-surface biotin label was then removed on ice. 'Endocytosis' samples were then lysed. 'Recycling' samples were subjected to an additional round of fifteen minutes 37°C incubation with EGF, then were stripped for a final time. Thus, only protein that was

endocytosed would retain its biotin label in 'endocytosis' samples, and only endocytosed but not recycled protein would be labelled in 'recycling' samples. Pull-down of biotin using streptavidin then allowed the relative quantities of biotinylated EGFR to be determined.

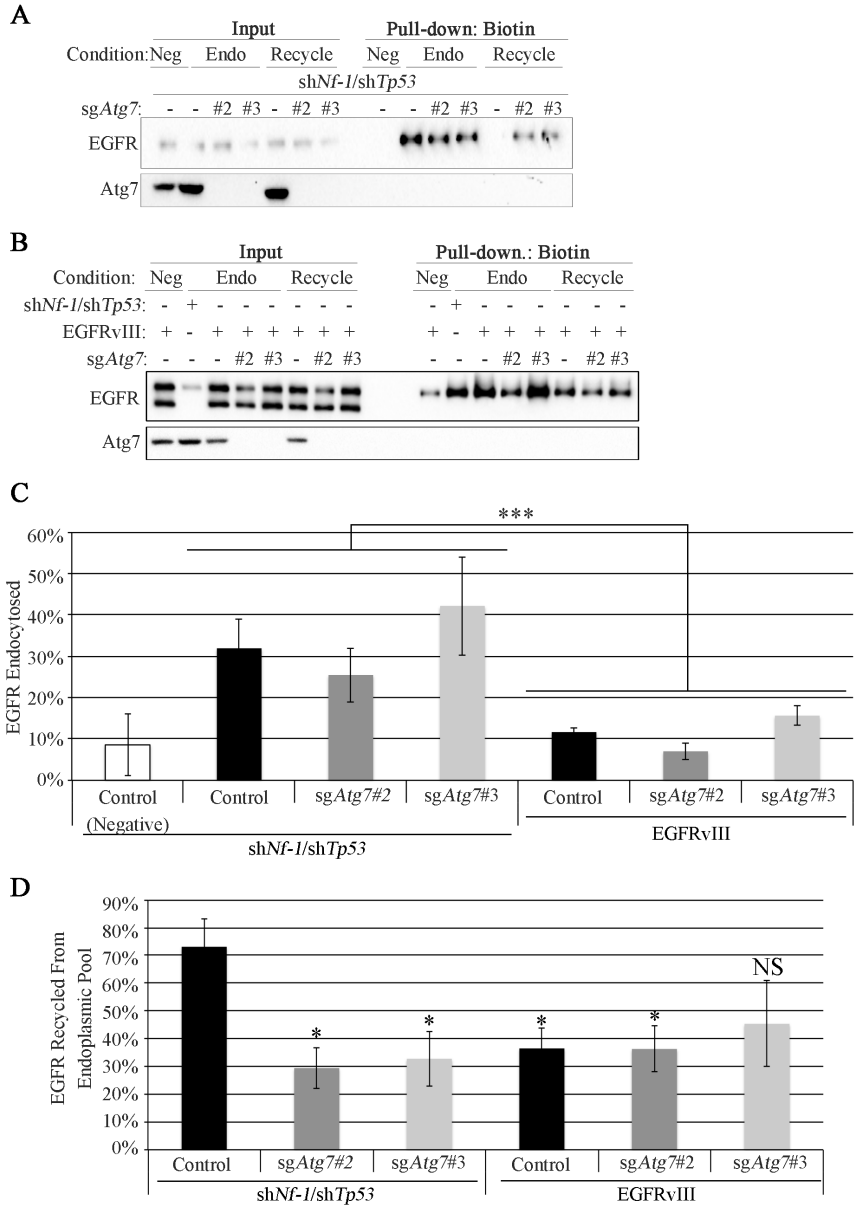

Figure 14.10 Expression of EGFRvIII and Atg7 Influences EGFR Endocytosis and Recycling Rates
A, **B:** Western blots of the biotinylation recycling assay in shNf-1/shTp53 (**A**) and EGFRvIII-expressing (**B**) XFM/tv-a glial cells. Cell-surface proteins were labelled with biotin then treated with either: surface biotin stripping buffer directly (*Neg*); EGF (2ng/ml) at 37°C 15 min and then stripping buffer (*Endo*); or EGF at 37°C 15 min, then stripping buffer, then EGF at 37°C 15 min, and then stripping buffer (*Recycle*), **C, D:** Graphs representing the percentage of endocytosed biotin-labelled EGFR (**C**) and quantity of endocytosed EGFR that is recycled to the plasma membrane (**D**). n=3, error bars represent SEM, * $p<0.05$, ** $p<0.01$, *** $p<0.001$.

XFM/*tv-a* sh*Nf-1*/sh*Tp53* cells were treated as described above, then inputs and biotin pull-downs analysed by Western blotting. Firstly, we can see that the endocytosis rate

of EGFR is comparable in cells with or without Atg7 expression (Figure 14.10A, C). In comparing the protein that has been endocytosed to that which remains internalised after recycling is permitted, we can determine the relative recycling rate of EGFR in each cell line. In control cells, approximately three-quarters of EGFR was recycled back to the plasma membrane, leaving little biotin signal detected by Western blot (Figure 14.10A, D). However, a significant proportion of internalised EGFR remained in *Atg7* knockout cells. Therefore, defective delivery of EGFR to Rab11-positive recycling endosomes does actually prevent its efficient recycling to the plasma membrane. The small proportion of EGFR that was recycled in cells without Atg7 (~30%) may be attributed to recycling via Rab4-positive recycling endosomes.

Atg7 was a useful control protein in this experiment: it confirmed the knockout efficiency in these cells as well as acting as a negative control. Atg7 is a cytoplasmic protein and therefore it should not be labelled with biotin and should not bind to the streptavidin beads. Indeed, pull-downs were clean of Atg7 signal, confirming the stringency of the pull-down conditions (Figure 14.10A, B).

In the previous chapter it was seen that although sh*Nf-1*/sh*Tp53* cells relied on autophagy for EGFR signalling, EGFRvIII-expressing cells did not. To explore this difference, EGFRvIII cells were tested for the rate of EGFR endocytosis and recycling. Due to the deletion of extracellular domains that confers the oncogenicity of this mutant, EGFRvIII was not able to be biotinylated. Therefore, here the influence of EGFRvIII on the wild-type receptor was assayed. As shown in chapter 12, EGFRvIII expression stabilises the wild-type receptor and this was seen again here, with sh*Nf-1*/sh*Tp53* cells expressing less EGFR.

However, when EGF was applied, the quantity of endocytosed EGFR was similar between these cell lines (Figure 14.10B, C). Therefore, the fraction of wild-type receptor that was endocytosed was reduced in EGFRvIII-expressing cells, consistent with previous studies that showed EGFRvIII stabilises wild-type EGFR at the plasma membrane. Furthermore, wild-type EGFR that was taken up in EGFRvIII cells had a poor rate of recycling to the plasma membrane, and instead primarily remained internalised (Figure 14.10B, D). Autophagy did not influence the rate of endocytosis or recycling in these cells.

14.3.4 *Atg7* Knockout Reduces the Quantity of EGF Ligand Taken Up By Cells

The recycling rate of EGFR has been seen to regulate the activity of downstream signalling cascades, most likely through the continued exposure of the receptor to additional ligand for continuous stimulation. If this were true, there would be a greater influx of EGF in recycling-competent than in recycling-defective cells. To test this in cells with or without Atg7, 555-EGF (whose fluorescence is stable at low pH) was

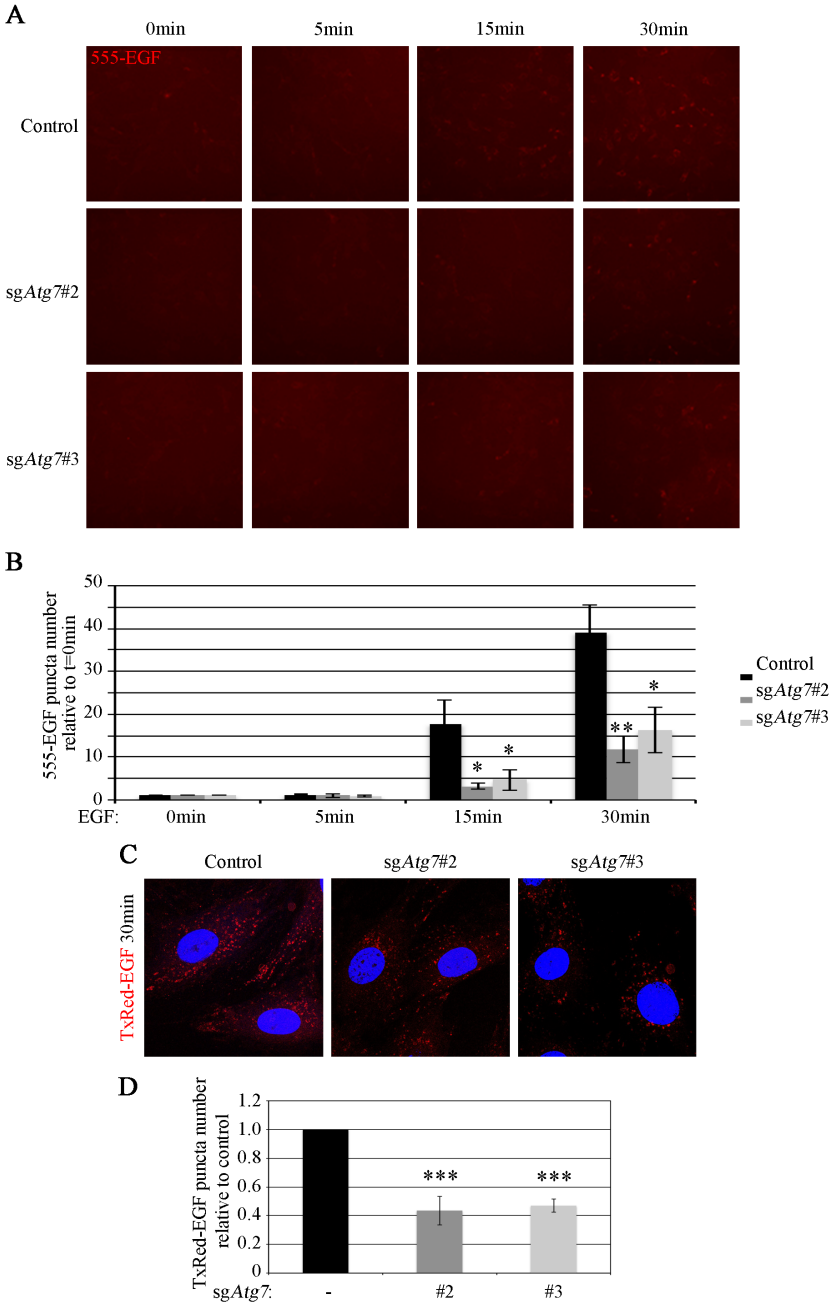

Figure 14.11 Autophagy Loss Reduces Uptake of Fluorescent EGF
20ng/ml of either Alexa555-EGF (555-EGF: **A**, **B**) or TexasRed-EGF (TxRed-EGF: **C**, **D**) was applied to XFM/*tv-a* sh*Nf-1*/sh*Tp53* cells. **A**: Representative images from ImageXpress high-throughput microscope after 0, 5, 15, or 30 min 555-EGF, **B**: Quantification of 555-EGF fluorescence relative to cell number (DAPI), expressed as fold increase over background fluorescence levels (t=0 min), **C**: Representative confocal images of cells treated with TxRed-EGF for 30 min, **D**: Quantification of TxRed-EGF punta per cell, relative to the value in control cells. n=3 experiments, ≥30 cells quantified per condition, error bars represent SEM, * $p<0.05$, ** $p<0.01$, *** $p<0.001$.

applied to cells for different lengths of time and then fluorescence signal was measured relative to cell number using high-throughput microscopy. These low magnification images show that control cells amass a large quantity of 555-EGF after thirty minutes of treatment, whilst autophagy-deficient cells take up less (Figure 14.11A, B). To confirm the results obtained using the high-throughput method, cells were again treated with fluorescent EGF but were imaged instead by confocal microscopy. It was even more apparent at this magnification that autophagy-deficient cells had fewer EGF vesicles than control cells following thirty minutes of stimulation (Figure 14.11C, D). When considered in light of the trafficking data shown above, diminished uptake of EGF ligand in autophagy-deficient cells can be attributed to reduced EGFR recycling.

14.3.5 Nuclear Translocation of EGFR Requires Autophagy

EGFR is not just transported through the cytoplasm of the cell; however, it can also be translocated to the nucleus[50]. Once in the nucleus it can co-operate with various transcription factors, such as STAT3, STAT5, or E2F1, to promote the expression of a variety of proteins that promote cell growth and survival, as well as regulating chromatin components[51,52]. Autophagy has been seen here to regulate endosomal trafficking of EGFR and therefore its nuclear translocation was also investigated. Cells were fractionated with increasing detergent stringency to separate 'cytoplasmic', 'membrane', and 'nuclear' matter. Western blotting of these fractions showed that under serum starvation conditions, there was a larger quantity of nuclear-localised EGFR in control cells than in Atg7-deficient cells (Figure 14.12). Thirty

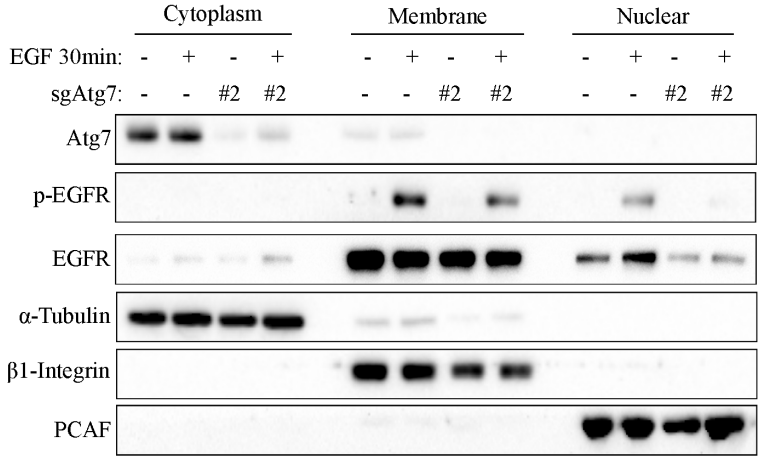

Figure 14.12 Autophagy is Required for Nuclear Localisation of EGFR
Western blotting analysis of cellular fractionation into cytoplasmic (marked by α-tubulin), membrane (β1-integrin), and nuclear (PCAF) fractions, showing an accumulation of active EGFR in the nucleus only in control, not *Atg7* knockout, XFM/*tv-a* sh*Nf-1*/sh*Tp53* cells following 30 min of EGF treatment (20 ng/ml) after 4 hr serum starvation. Experiment repeated at least 3 times.

minutes of EGF treatment resulted in EGFR phosphorylation in the membrane fraction that was reduced by Atg7 loss, consistent with findings from the previous chapter. Furthermore, although this stimulation induced elevated EGFR translocation to the nucleus in control cells, this was not seen in cells lacking Atg7. This experiment presents a novel role for autophagy in promoting the nuclear translocation of EGFR to the nucleus, where is known to promote cell survival and proliferation.

14.3.6 The Interacting Partners of EGFR Are Altered in *Atg7* Knockout Cells

As autophagy loss induces a significant redistribution of EGFR, I became intrigued to find out whether this results in a change in the EGFR interactome. To investigate this, cells were treated with EGF for thirty minutes before they were lysed, EGFR was

Table 14.1 Mass Spectrometry Top Ten Hits Enriched in Control Over Autophagy-Deficient Cells

Hits were identified by a greater than two fold enrichment of control samples over both sg*Atg7*#2 and sg*Atg7*#3 from triplicate samples and student's T-Test value of less than 0.05.

Gene Name	**Protein Name**	**Function Summary** ***(based on information from uniprot.org)***
Egfr	Epidermal growth factor receptor	Bait
Arpc3	Actin-related protein 2/3 complex subunit 3	Involved in actin polymerisation associated with endosomal fission, specifically in association with the retromer.
Sec61g	Protein transport protein Sec61 subunit gamma	Necessary for protein translocation in the endoplasmic reticulum
Zfp91	E3 ubiquitin-protein ligase ZFP91	Atypical E3 ubiquitin-protein ligase that mediates 'Lys-63'-linked ubiquitination of MAP3K14/NIK. May also play an important role in cell proliferation and/or anti-apoptosis
Usp7	Ubiquitin carboxyl-terminal hydrolase 7	Hydrolase that deubiquitinates target proteins such as FOXO4, p53/TP53, MDM2, ERCC6, DNMT1, UHRF1, PTEN and DAXX.
Mob4	MOB-like protein phocein	May play a role in membrane trafficking, specifically in membrane budding reactions
Lrp1b	Low-density lipoprotein receptor-related protein 1B	Cell surface protein that binds and internalizes ligands in the process of receptor-mediated endocytosis
Ap2a2	AP-2 complex subunit alpha-2	Component of the adaptor protein complex 2 (AP-2), involved in clathrin-dependent endocytosis, destined for fusion with the early endosome. Potentially mediates an interaction between clathrin and ATG16L1 in the context of membrane recruitment for autophagosomes
Cttnbp2nl	CTTNBP2 N-terminal-like protein	Binds protein phosphatase 2A (prevents EGF-induced EGFR degradation & sustains EGF-mediated signalling)
Anxa2	Annexin A2	Calcium-regulated membrane-binding regulated by anionic phospholipids. May cross-link plasma membrane phospholipids with the cytoskeleton and be involved with exocytosis.
Pip5k1a	Phosphatidylinositol 4-phosphate 5-kinase type-1 alpha	Catalyses the phosphorylation of phosphatidylinositol 4-phosphate (PtdIns4P) to form phosphatidylinositol 4,5-bisphosphate (PtdIns(4,5)P2)

immunoprecipitated, and the resulting binding partners were analysed by the IGMM mass spectrometry facility. Several known EGFR-interacting proteins were equally enriched in control and knockout cells, such as Grb2, and, importantly, binding of EGFR kinase inhibitors, such as Mig6, were not altered by autophagy loss (Figure 14.13A). However, several hits were identified as selectively enriched in control cells over both *Atg7* knockout cell lines (Table 14.1). After discounting unlikely candidates, the top ten remaining hits were subjected to GO term analysis of reactome pathways that revealed a common pattern of interactors that were depleted by autophagy loss (Table 14.2). Intriguingly, this evaluation flagged several phosphatidylinositol (PI) regulatory processes as the most over-represented in the dataset. It is known that the conversion of PI species characterises the different stages of endocytic trafficking.

Table 14.2 GO Term Pathway Analysis of Top Ten Mass Spectrometry Hits

Reactome pathways	Total Number of Proteins in Pathway	# Mass Spec Hits in Pathway	Expected	Over Enriched?	Fold Enrichment	Raw P-value	False Discovery Rate
Synthesis of PIPs at the plasma membrane	34	2	0.02	+	> 100	1.13E-04	9.03E-03
PI5P, PP2A and IER3 regulate PI3K/AKT signalling	78	3	0.04	+	85.62	5.46E-06	8.26E-03
PI metabolism	57	2	0.03	+	78.11	3.06E-04	1.32E-02
L1CAM interactions	67	2	0.03	+	66.45	4.19E-04	1.63E-02
PIP3 activates AKT signalling	102	3	0.05	+	65.48	1.19E-05	2.01E-03
PI3K/AKT activation	105	3	0.05	+	63.61	1.30E-05	1.96E-03
GAB1 signallosome	105	3	0.05	+	63.61	1.30E-05	1.79E-03
Clathrin-mediated endocytosis	111	3	0.05	+	60.17	1.53E-05	1.93E-03
Role of LAT2/NTAL/LAB on calcium mobilization	111	3	0.05	+	60.17	1.53E-05	1.78E-03
Cargo recognition for clathrin-mediated endocytosis	77	2	0.03	+	57.82	5.49E-04	2.08E-02
Signalling by EGFR	300	3	0.13	+	22.26	2.79E-04	1.36E-02
Membrane trafficking	440	3	0.2	+	15.18	8.45E-04	3.04E-02
Vesicle-mediated transport	470	3	0.21	+	14.21	1.02E-03	3.60E-02

It was also seen that deletion of *Atg7* reduced the binding of EGFR with known players in endocytosis (e.g. AP-2) and regulators of recycling endosome traffic (e.g. Annexin-A2, PI4P5K). However, STRING analysis was not able to identify one

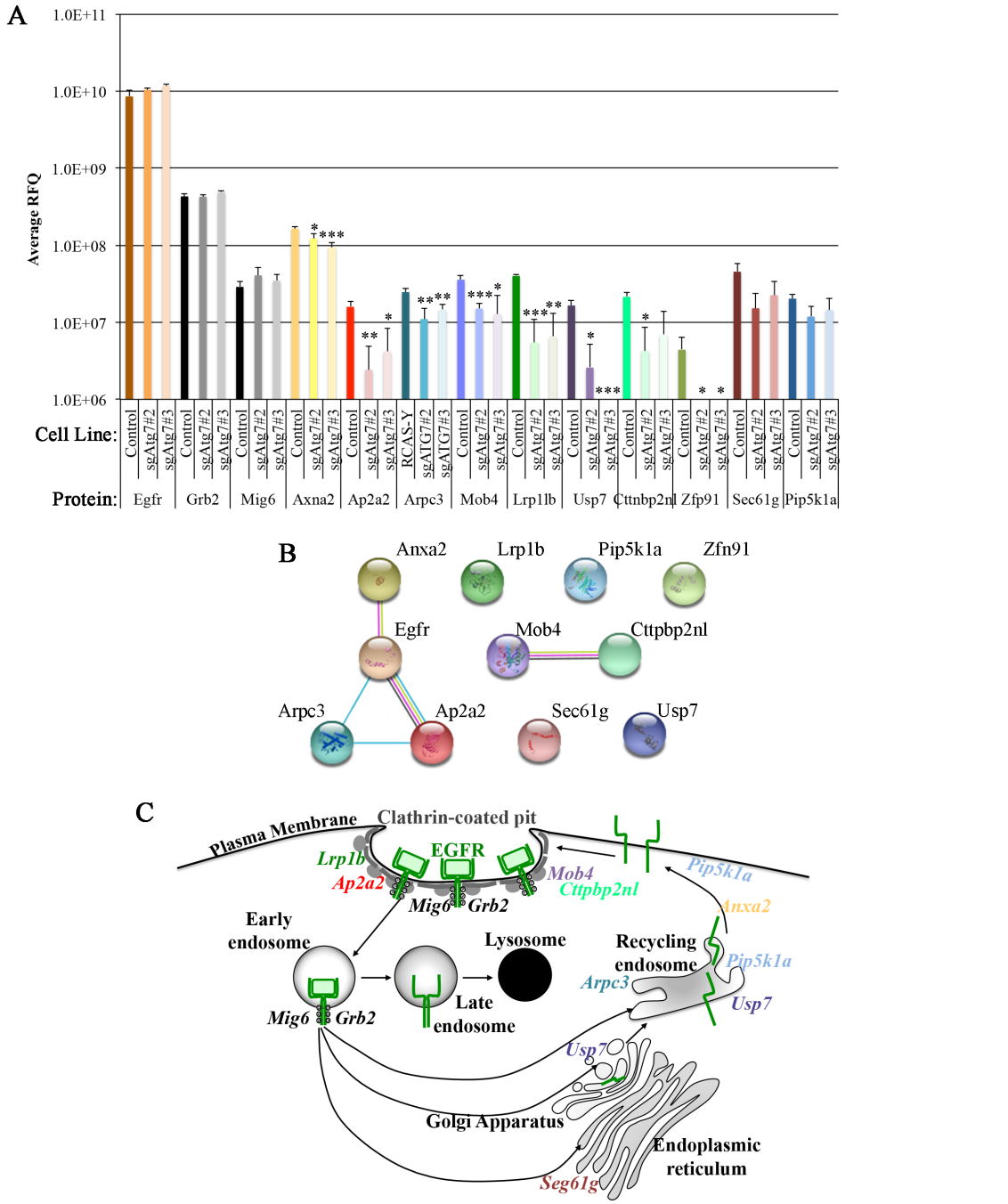

Figure 14.13 Autophagy Loss Alters the EGFR Interactome
A: Graphs representing protein relative abundance as measured by label-free quantification (LFQ) mass spectrometry analysis of EGFR I.P.s from XFM/*tv-a* sh*Nf-1*/sh*Tp53* control and *Atg7* knockout cell lines, with LFQ given on a $\log_{10}$ scale. Colour coding refers to part **N** of the figure, whereas black/grey coding designated for proteins with no enrichment in control over autophagy-deficient samples, **B:** STRING analysis of the top ten hits enriched in control samples over *Atg7* knockout, **C:** Schematic simplified diagram of the endocytic pathway labelled with mass spectrometry hits lost in autophagy knockout cells. n=3, error bars represent SEM, * p<0.05, ** p<0.01, *** p<0.001.

particular complex that is disrupted by Atg7 loss (Figure 14.13B). The loss of binding of some endocytic regulators, such AP-2, is likely due to the stalling of EGFR in early endosomes in *Atg7* knockout cells thereby preventing its binding to players at the plasma membrane. These data are in agreement with EGF uptake analyses that suggest the reduced flux of EGFR to the plasma membrane in knockout cells dampens EGF/EGFR endocytosis rate. Other players which are known to act at the plasma membrane, such as Mig6 and Grb2, were not seen to be influenced by autophagy loss, likely because they actually also bind to EGFR throughout its passage through to early endosomes[14,24] (Figure 14.13C).

Collectively, these analyses show that autophagy loss results in the abrogation of EGFR binding to certain initiators of endocytosis, recycling endosome mediators, and PI-regulators.

14.3.7 Inhibitors of Vesicular Processes Can Mimic Autophagy Loss

EGFR activity is regulated is by its endocytic trafficking that can direct it either through recycling endosomes back to the plasma membrane or to the lysosome for degradation. If autophagy is mediating EGFR activity by its endocytic trafficking, using inhibitors of different stages of endocytosis should mimic or oppose autophagy knockout. To test this, inhibitors were used against dynamin (Dynasore), lysosomal/vesicle acidification (Bafilomycin A1), or PI(3)P production (PIK3C3 inhibitor) in sh*Nf-1*/sh*Tp53* control cells.

Bafilomycin A1 inhibits the final step of autophagosome degradation in the lysosome, and therefore might be expected to mimic the loss of autophagic flux caused when Atg7 is deleted. However, inhibition of vesicle acidification resulted in an increase of EGFR activity following EGF stimulation, as measured by EGFR and Akt phosphorylation, possibly attributable to the lack of EGFR regulation by degradation (Figure 14.14A). EGFR induction was also enhanced by treatment with Dynasore. Inhibiting dynamin prevents the pinching off of clathrin-coated pits, thereby holding EGFR at the plasma membrane in the clusters that are formed prior to endocytosis. Therefore, EGFR is not endocytosed and instead remains active at the plasma membrane where is can signal to Akt. However, inhibition of PIK3C3 diminished signalling from EGFR following EGF stimulation, mimicking *Atg7* knockout. PI(3)P is essential for both the formation of early endosomes and in autophagosome biogenesis, as evidenced here in the reduction of LC3-II when its production is

inhibited. Therefore, this inhibitor is unable to distinguish whether EGFR activity is being regulated by the influences of either autophagy or endosomal trafficking. The evidence presented thus far has indicated that autophagy plays a role in regulating the endocytic trafficking of EGFR. Furthermore, a mutant of EGFR with a reduced rate of endocytosis is insensitive to the influence of autophagy. To confirm this, *Atg7*

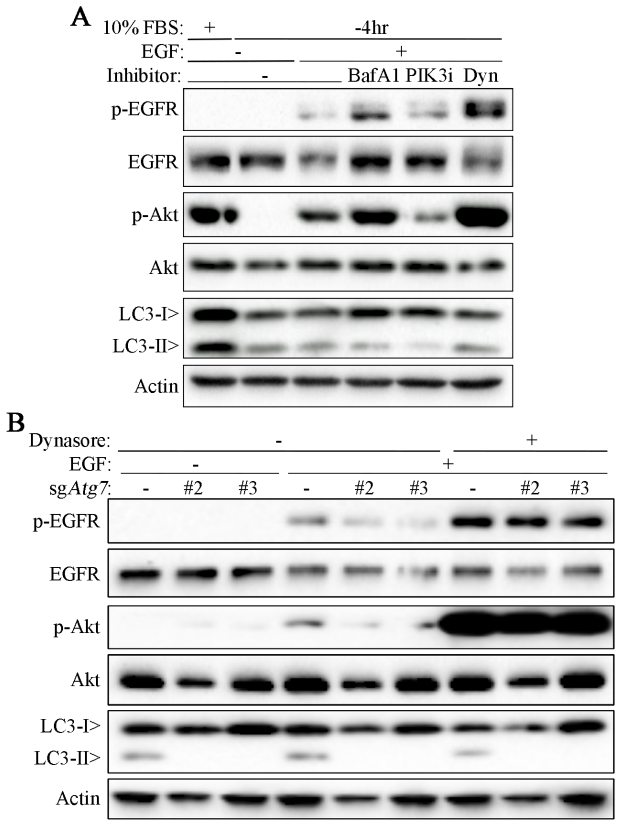

Figure 14.14 The Influence of *Atg7* Knockout on EGFR Can Be Mimicked By PIK3C3 Inhibition and Rescued By Inhibiting Endocytosis
A: XFM/*tv-a* sh*Nf-1*/sh*Tp53* cells were starved of serum for 4 hr then treated with 20 ng/ml EGF alone or in combination with either 20 μM Bafilomycin A1, 10 μM PIK3C3, or 30 μM Dynasore for 30 min, before analysing by Western blot, **B:** XFM/*tv-a* sh*Nf-1*/sh*Tp53* control and sg*Atg7* cells were serum starved for 4 hr then stimulated with 20 ng/ml EGF for 30 min with or without 30 μM Dynasore. Experiments repeated at least 3 times.

knockout cells were treated with Dynasore to inhibit CME. Western blotting showed that the influence of autophagy loss on EGFR signalling could indeed be bypassed by holding EGFR at the plasma membrane (Figure 14.14B). Therefore, autophagy influences EGFR signalling subsequent to its endocytosis.

14.4 Homeostasis of the Endosomal System Relies on Autophagy

The above microscopic analyses regarding the influence of autophagy proteins on EGFR trafficking suggest that there is a direct interplay between these two processes. However, the precise molecular disturbances caused by Atg7 loss to perturb the

endocytic pathway are not clear. To try to address this, I undertook a series of experiments to characterise the disruption in endosomal maturation.

14.4.1 Electron Microscopy Reveals Endosomal Compartments are Perturbed By Autophagy Loss

Thus far, the majority of the experiments utilising imaging methods have been targeted to look at specific proteins as a read-out for the status of different endocytic compartments. To take a step back and view the wider situation in the cell, transmission electron microscopy was employed. Inspection of Atg7-deficient cells showed a striking disruption in two key aspects of the endosomal system. Firstly, there was a significant increase in the number of multivesicular bodies (MVBs: Figure 14.15A, C). These bodies are so named because they are composed of a number of distinct vesicles enclosed within a single larger structure. These are known trafficking sites for EGFR en route to the lysosome for degradation, particularly after stimulation with high levels of EGF[2,54]. Secondly, the average area of the endosome or endosome-like vesicles was more than doubled by *Atg7* knockout (Figure 14.15B, C). Therefore, autophagy loss has a significant impact on the regulation of the endosomal system.

14.4.2 EGFR Does Not Accumulate in Multivesicular Bodies in *Atg7* Knockout Cells

Electron microscopy demonstrated that Atg7-deficient cells have dramatically more MVBs than control cells. Previous studies have shown that MVBs can fuse with autophagosomes to generate 'amphisome' structures that are destined for the lysosome. Alternatively, MVBs have also been seen to have a role in exocytosis[40,55–57]. Given the documented targeting of EGFR to MVBs, I was interested to understand whether autophagy may be regulating EGFR plasma membrane recycling via MVB structures. Using GFP-tagged CD63 as a marker of MVBs, EGF-induced trafficking of EGFR to MVBs was measured in control and autophagy-deficient cells. The formation of large MVBs was promoted in autophagy-deficient cells, confirming the observations from the electron microscope (Figure 14.16A). Furthermore, there was an increased co-localisation between EGFR and CD63 in *Atg7* knockout cells (Figure 14.16B). However, inspection of the images shows that the vast majority of EGFR is not in fact localised in these MVBs (Figure 14.16C). Instead, earlier IF studies demonstrate EGFR is primarily located in early endosomes when Atg7 is lost.

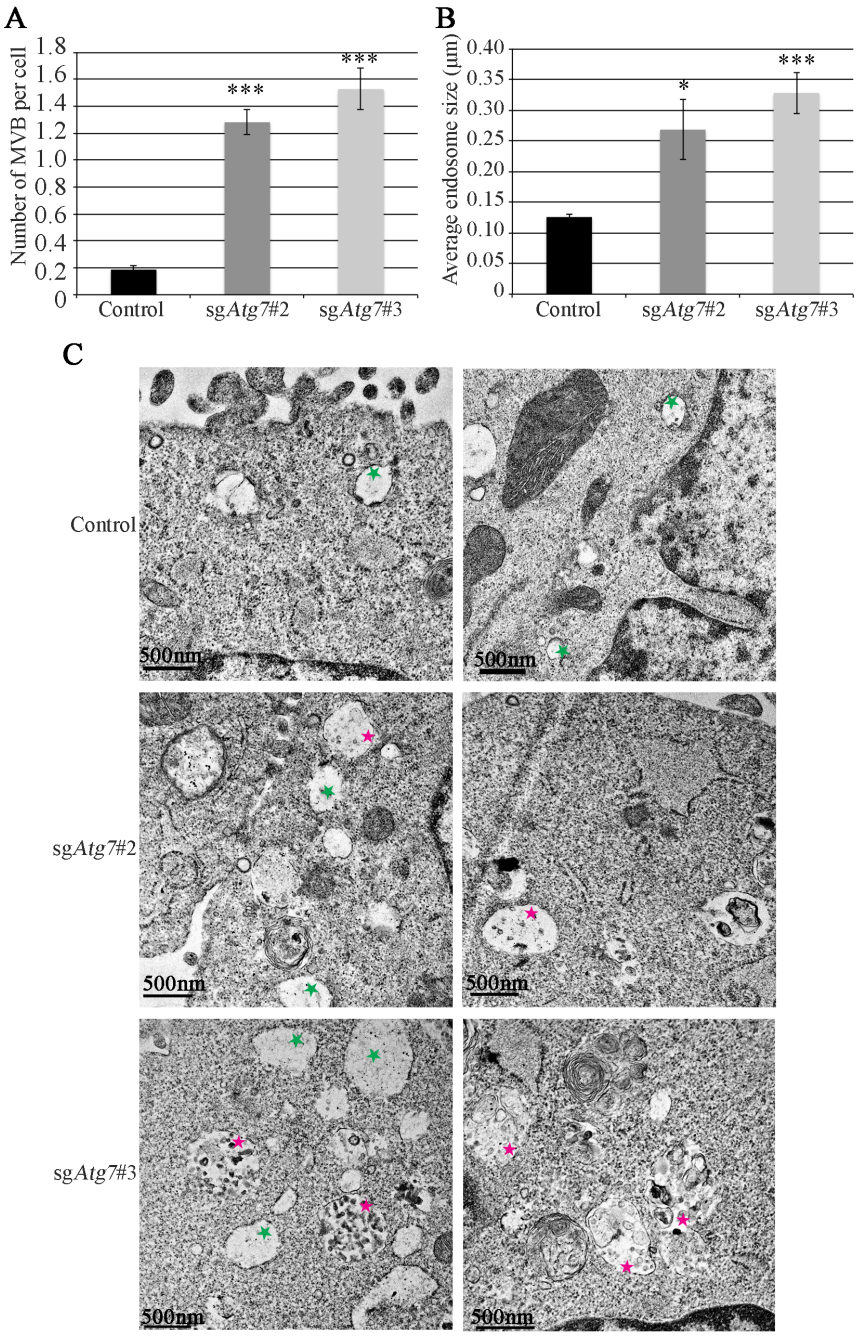

Figure 14.15 Transmission Electron Microscope Analyses of Autophagy-Deficient Cells Show Disruption of Endosomal Compartments
XFM/*tv-a* sh*Nf-1*/sh*Tp53* cells with *Atg7* knockout were serum starved for 4hr then stimulated with 2 ng/ml EGF for 15 min before fixation and sectioning for electron microscope analysis.
A: Quantification of the number of multivesicular bodies (MVBs) per cell, **B:** Quantification of endosomal vesicle size, **C:** Representative images showing endosomal (green stars) and MVB (pink stars) disruption by Atg7 loss. 3 technical replicates, 1 biological replicate, error bars represent SEM, * $p<0.05$, ** $p<0.01$, *** $p<0.001$.

Therefore, it can be surmised that the increase in MVBs is a side effect of autophagy loss, but not the cause of EGFR trafficking disruption.

14.4.3 Autophagy-Deficient Cells Have Increased Endosomal Phosphatidylinositol-3-Phosphate

Evidence from these experiments has connected autophagy with the regulation of early endosomes and MVBs. All three of these vesicular structures rely on the lipid phosphatidylinositol-3-phosphate (PI(3)P) to form[5,26,58,59]. Therefore, might the deregulation of early endosomes and MVBs caused by autophagy loss be attributable to PI(3)P disruption?

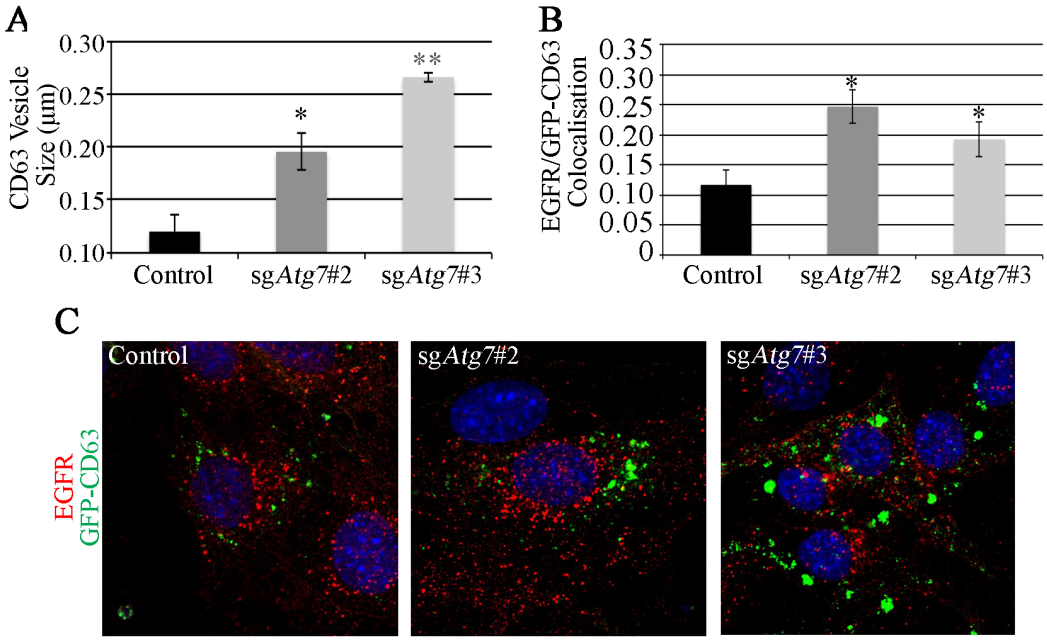

Figure 14.16 Autophagy-Deficient Cells Accumulate Large CD63-Positive Vesicles
XFM/*tv-a* sh*Nf-1*/sh*Tp53* cells expressing GFP-CD63 were serum starved for 4hr then stimulated with 2 ng/ml EGF 15 min. Cells were then stained for EGFR. **A:** CD63-positive vesicles are larger in *Atg7* knockout cells, **B:** CD63-positive vesicles co-localise more with EGFR in *Atg7* knockout cells, **C:** Representative images of GFP-CD63 expressing cells co-localising with EGFR. n=3 experiments, ≥30 cells quantified per condition, error bars represent SEM, * $p<0.05$, ** $p<0.01$, *** $p<0.001$.

The overexpression of fluorescently tagged PI(3)P-binding domains in cells can perturb normal trafficking processes. Therefore, a technique was used to detect levels of PI(3)P whereby cells that were permeabilised by liquid nitrogen and fixed with PFA were then incubated with a recombinantly expressed Alexa488-tagged FYVE domain ('PI(3)P probe')[60]. As in all of the assays outlined above, cells were serum starved for four hours then stimulated with EGF. In sh*Nf-1*/sh*Tp53* XFM/*tv-a* glial cells the knockout of either *Atg7* or *Atg16l1* resulted in a striking increase in the levels of PI(3)P (Figure 14.17A,E). As loss of these downstream autophagy players may be causing an accumulation of $PI(3)P^{+}$ autophagosome precursor structures, the endosomal localisation of this lipid was tested with concurrent EEA1 staining. This showed that loss of these essential autophagy proteins causes an increase specifically

in early endosomal PI(3)P (Figure 14.17C,E). The specificity of this probe was confirmed using an inhibitor of PIK3C3, 3-methyladenine (3-MA), which reduced PI(3)P levels and prevented its co-localisation with EEA1.

The majority of the experiments investigating EGFR trafficking regulation by autophagy in this study have utilised XFM/*tv-a* sh*Nf-1*/sh*Tp53* cells. However, in the previous chapter we saw that EGFR in mouse embryonic fibroblasts (MEFs) also relies on autophagy. The phenotype observed was slightly different, however, with EGFR expression, but not signalling capacity, significantly reduced by autophagy loss. Application of the PI(3)P probe in these MEF cells shows that *Atg7* knockout also increases the endosomal levels of this lipid in an alternative cell line (Figure 14.17B,D,F).

Therefore, loss of expression of essential autophagy genes results in a marked increase in the levels of PI(3)P at early endosomes in two distinct mouse cell lines. Whilst in glial cells this results in perturbed signalling from EGFR, in MEFs EGFR experiences increased lysosomal targeting.

14.4.4 Autophagy Does Not Influence PIK3C3 Catalytic Activity

Autophagy and early endosomes share a common essential kinase player: PIK3C3. This kinase produces PI(3)P that acts as a docking site for downstream effectors in both of these pathways. The PIK3C3 complex has different regulatory players depending on whether it is functioning in an autophagic (Atg14l1^{+}) or endocytic (UVRAG^{+}) capacity[7]. One player that is common between these complexes is Beclin-1. Therefore, to test whether the knockout of downstream autophagy players Atg7 and Atg16l1 influences the formation of either of these complexes, Beclin-1 was immunoprecipitated from cells and its binding partners were interrogated. Post-translational modification of Beclin-1 by EGFR has been seen to regulate the kinase complex and direct its activity[33]. Therefore, it was isolated from either serum-starved cells or cells that were serum-starved then treated with EGF.

However, co-immunoprecipitation of components from these complexes was not changed by either treatment with EGF or *Atg7* knockout (Figure 14.18A). Binding of Rubicon, which inhibits the endocytic complex, was also not altered. This was confirmed by the reciprocal immunoprecipitation of PIK3C3 itself and testing for binding partner configuration. The binding of known partners of PIK3C3, UVRAG, and Beclin-1, were not changed by Atg7 loss, but an exciting novel association was

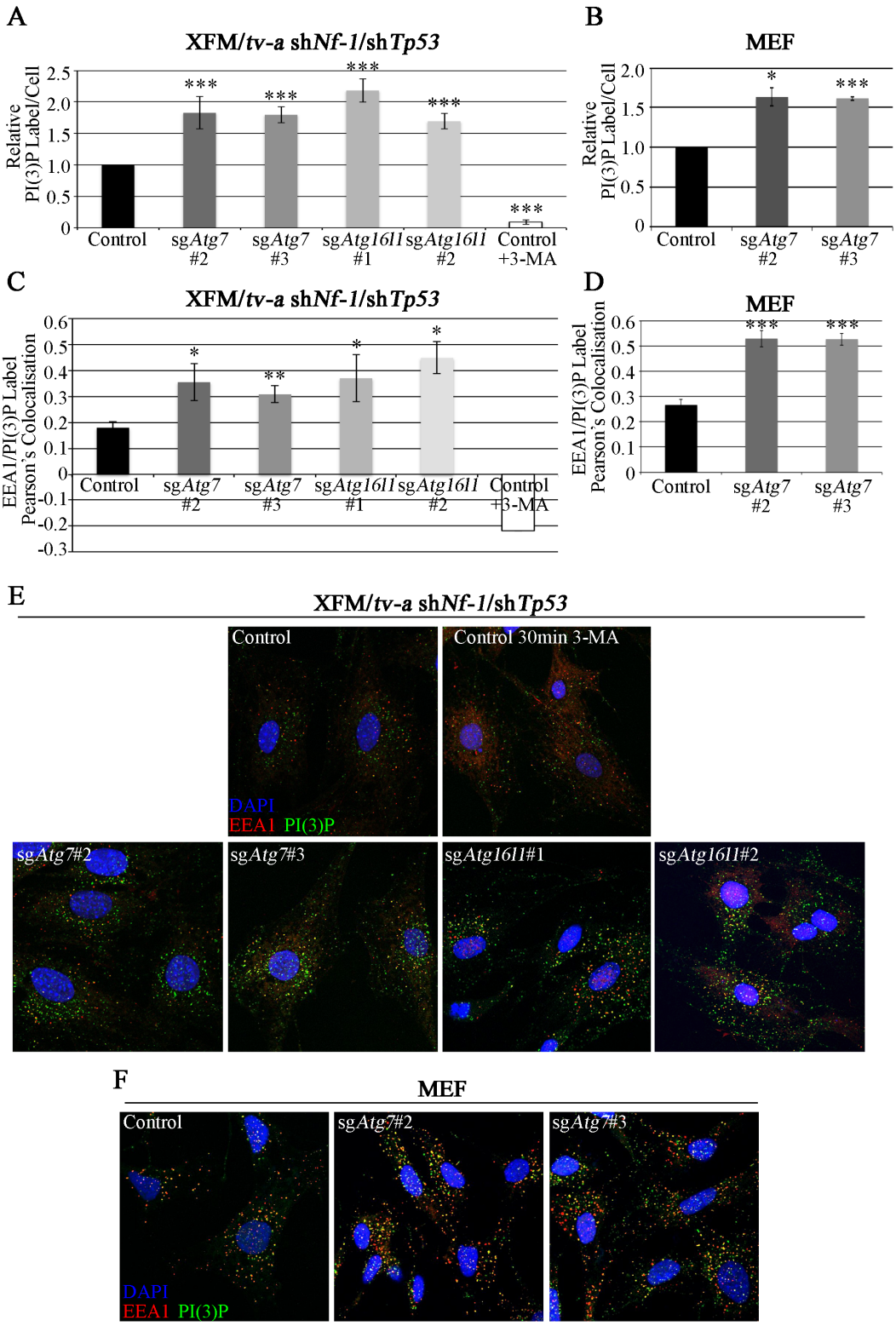

Figure 14.17 Autophagy Loss Increases Levels of Early Endosomal PI(3)P
Control, sg*Atg7*, or sg*Atg16l1* cells were serum starved 4hr then stimulated with EGF 15 min (with or without 30 min 3-MA pre-treatment) before probing for PI(3)P and EEA1.
A, B: Quantification of the number of PI(3)P label per cell, made relative to control autophagy-competent cells for either sh*Nf-1*/sh*Tp53* XFM/*tv-a* glial cells (**A**) or MEFs (**B**), **C, D:** Pearson's coefficient for co-localisation between PI(3)P probe and EEA1 in sh*Nf-1*/sh*Tp53* (**C**) and MEF (**D**) cells, **E, F:** Representative images of EEA1 and PI(3)P staining in sh*Nf-1*/sh*Tp53* (**E**) and MEF (**F**) cells. n=3 experiments, ≥30 cells quantified per condition, error bars represent SEM, * $p<0.05$, ** $p<0.01$, *** $p<0.001$.

uncovered with Atg16l1 (Figure 14.18B-E). As this is only observed when *Atg7* is knocked-out, it is suggestive that this may only be a very transient or weak binding under autophagy-competent circumstances. Upon probing for Atg16l1 in the input, it was clear that it is severely destabilised when not in its complex with Atg5 and Atg12 in Atg7-deficient cells. The binding of WIPI2 was also tested. WIPI2 is a PI(3)P-binding autophagy protein and an interacting partner of Atg16l1 and therefore might bridge a PIK3C3-Atg16l1 association. However, it was not detected in the PIK3C3 immunoprecipitation.

To investigate the importance of the interaction of Atg16l1 with PIK3C3, *Atg16l1* knockout cell lysates were subjected to PIK3C3 immunoprecipitation. However, this did not change the co-immunoprecipitation of either Beclin-1 or UVRAG (Figure 14.18F). Therefore, Atg16l1 is not mediating the formation of the PIK3C3 complex.

To understand whether the Atg16l1-PIK3C3 association relies on Atg7 or on autophagic flux, full length or an Atg5 binding-deficient (autophagy defective 'Δ5') mutant of Atg16l1 were re-expressed in *Atg16l1* knockout cells. However, due to the constitutive expression of sgRNA and Cas9 enzyme in XFM/*tv-a* cells, it is not possible to use re-expression constructs of Atg16l1. Consequently, MEFs were used to re-express Atg16l1 where the knockout of Atg16l1 was carried out using transient sgRNA/Cas9 expression vectors. This mutant should recapitulate Atg7 deletion, as Atg7 facilitates Atg16l1 conjugation to Atg5. However, Atg16l1 was not detected above levels of background non-specific binding to PIK3C3 in either full length or Δ5 Atg16l1 lysates (Figure 14.18G). Therefore, the stabilised association of Atg16l1 with PIK3C3 that was observed may either be specific to glial cells or only occur in the context of Atg7 loss. However, it is clear that autophagy status does not influence the composition of either autophagy or endocytosis complexes of PIK3C3. Although known binding partners are not changed, it is possible that the loss of autophagy positively impacts the activity of the endocytic PIK3C3 complex by another means, such as post-translational modifications, resulting in an increase of PI(3)P. To analyse whether this is the case, PIK3C3 isolated from control or *Atg7* knockout cells was used in an *in vitro* kinase reaction with phosphatidylinositol (PI). The PI(3)P produced by these reactions was then detected by an ELISA-like method.

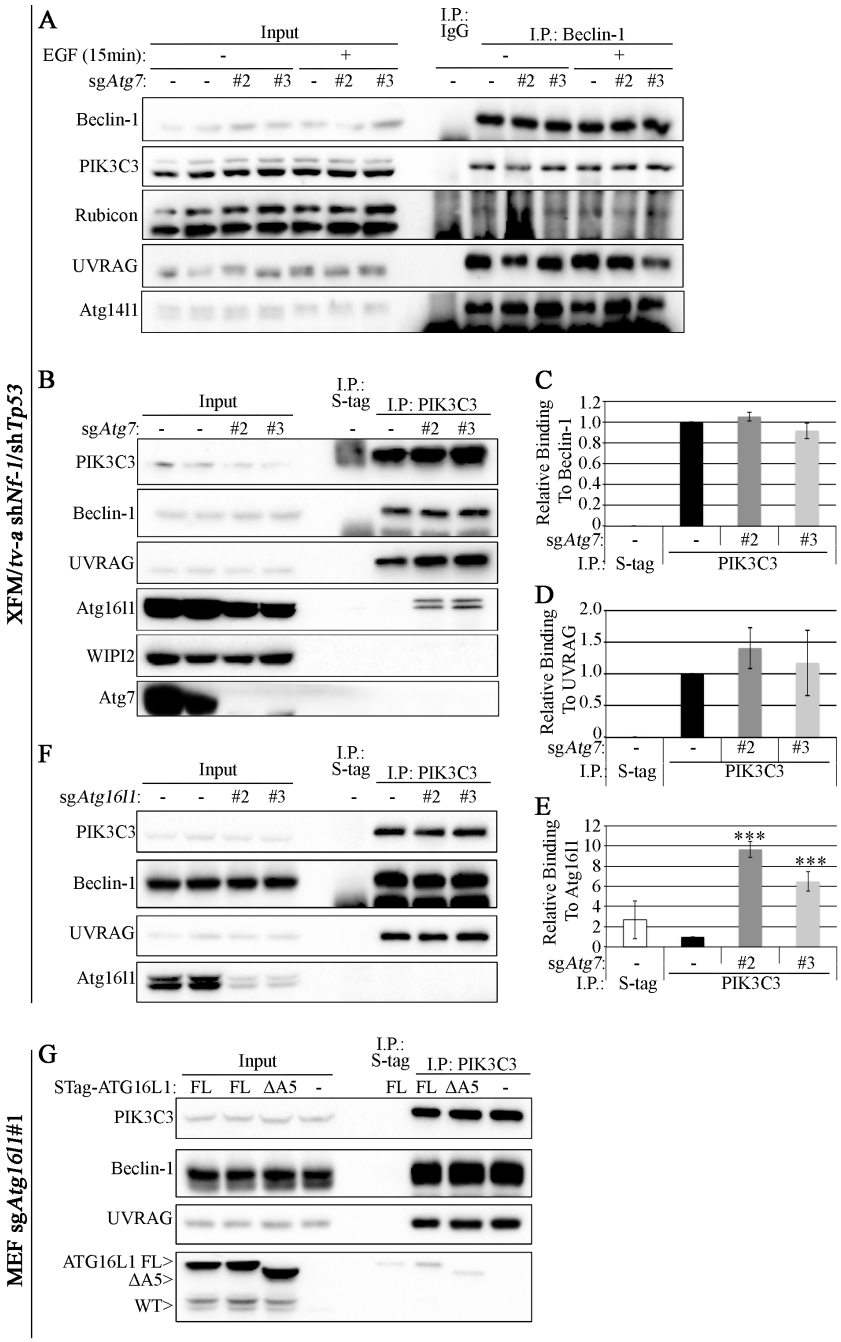

Figure 14.18 Compositions of PIK3C3/Beclin-1 Complexes are Not Changed By Atg7 Loss, But Does Reveal an Association with Atg16l1
Cells were serum starved for 4 hr then stimulated with 2 ng/ml EGF for 15 min before lysis and immunoprecipitation. **A:** Beclin-1 immunoprecipitation from *Atg7* knockout sh*Nf-1*/sh*Tp53* XFM/*tv-a* glial cells, **B:** PIK3C3 immunoprecipitation from *Atg7* knockout sh*Nf-1*/sh*Tp53* cells XFM/*tv-a*, **C-E:** Quantification of co-immunoprecipitation of different PIK3C3 binding partners in XFM/*tv-a* cells, proportionate to their input, expressed relative to the binding observed in control cells, **F:** PIK3C3 immunoprecipitation from *Atg16l1* knockout sh*Nf-1*/sh*Tp53* cells, **G:** PIK3C3 immunoprecipitation from *Atg16l1* knockout MEFs re-expressing either full length (FL) or Atg5 binding-deficient mutant (Δ5) Atg16l1. n=3, error bars represent SEM, * p<0.05, ** p<0.01, *** p<0.001.

Interpolation from the resulting standard curve (Figure 14.19A) revealed that, rather than increasing its activity, *Atg7* knockout actually marginally reduced PIK3C3-catalysed production of PI(3)P (Figure 14.19B). However, it is difficult to interpret

these results without further positive and negative controls, such as active recombinant enzyme and chemical inhibition of PIK3C3 (e.g. 3-MA), respectively. Also, although within the range of the standard controls for the assay, the PI(3)P conversion rate was quite low in this assay, suggesting some component may not be optimal. Additionally, it is possible that the process of PIK3C3 isolation disrupts its possible misregulation in *Atg7* knockout cells, such as spatial regulatory mechanisms or a weak interacting partner.

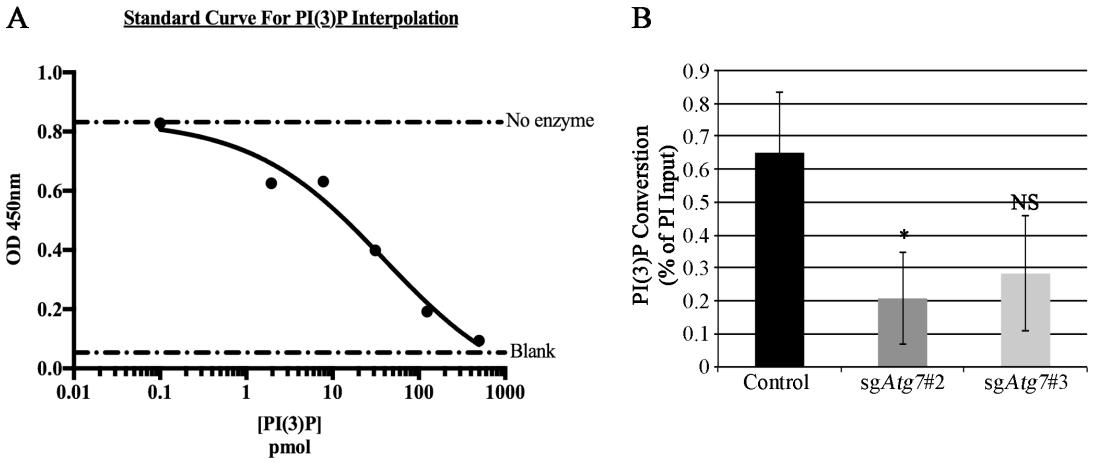

Figure 14.19 Atg7 Marginally Inhibits PIK3C3 Catalytic Activity
A: Standard curve of PI(3)P levels in XFM/*tv-a* sh*Nf-1*/sh*Tp53* read by Echelon's PIK3C3 ELISA kit, **B:** Interpolation and data analysis allows inference of percentage of PI substrate converted to PI(3)P. n=3, error bars represent SEM, * p<0.05, ** p<0.01, *** p<0.001.

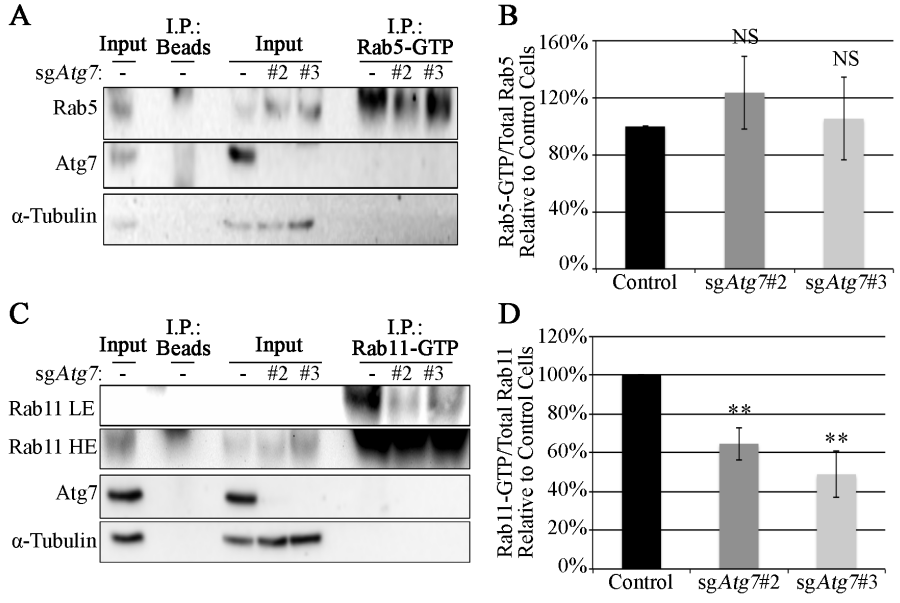

Figure 14.20 Autophagy Loss Reduces Rab11, But Not Rab5, Activity
A, C: Western blots of Rab5-GTP (**A**) and Rab11-GTP (**C**) immunoprecipitation from sh*Nf-1*/sh*Tp53* XFM/*tv-a* control and *Atg7* knockout cells that were serum starved 4 hr then stimulated 2 ng/ml EGF 15 min (low exposure =LE, high exposure= HE), **B, D:** Quantification of the proportion of GTP- bound Rab5 (**B**) and Rab11 (**D**) levels, expressed relative to that of control cells. n=3, error bars represent SEM, * p<0.05, ** p<0.01, *** p<0.001.

14.4.5 Autophagy Loss Reduces Rab11 Activity

If the levels of PI(3)P are increased by autophagy loss but the production of PI(3)P is not influenced, then it stands to reason that the subsequent consumption of PI(3)P may instead be perturbed. In recycling endosome formation, early endosomal PI(3)P is first dephosphorylated to PI. Then it is phosphorylated at the 4' by PI4K before a second phosphorylation at the 5', likely in anticipation of fusion with the PI(4,5)P_2-enriched plasma membrane. This lipid switch occurs in parallel with the loss of Rab5 and the addition of Rab11 GTPases. To assay whether autophagy loss influences the activity of these proteins, immunoprecipitation of specifically the GTP-bound active forms of Rabs were performed from lysates of control and *Atg7* knockout cells treated with EGF. Rab5-GTP levels were marginally, but not significantly, higher in autophagy-deficient cells (Figure 14.20A, B). Conversely, Rab11-GTP levels were significantly reduced when Atg7 expression was lost (Figure 14.20C, D). This

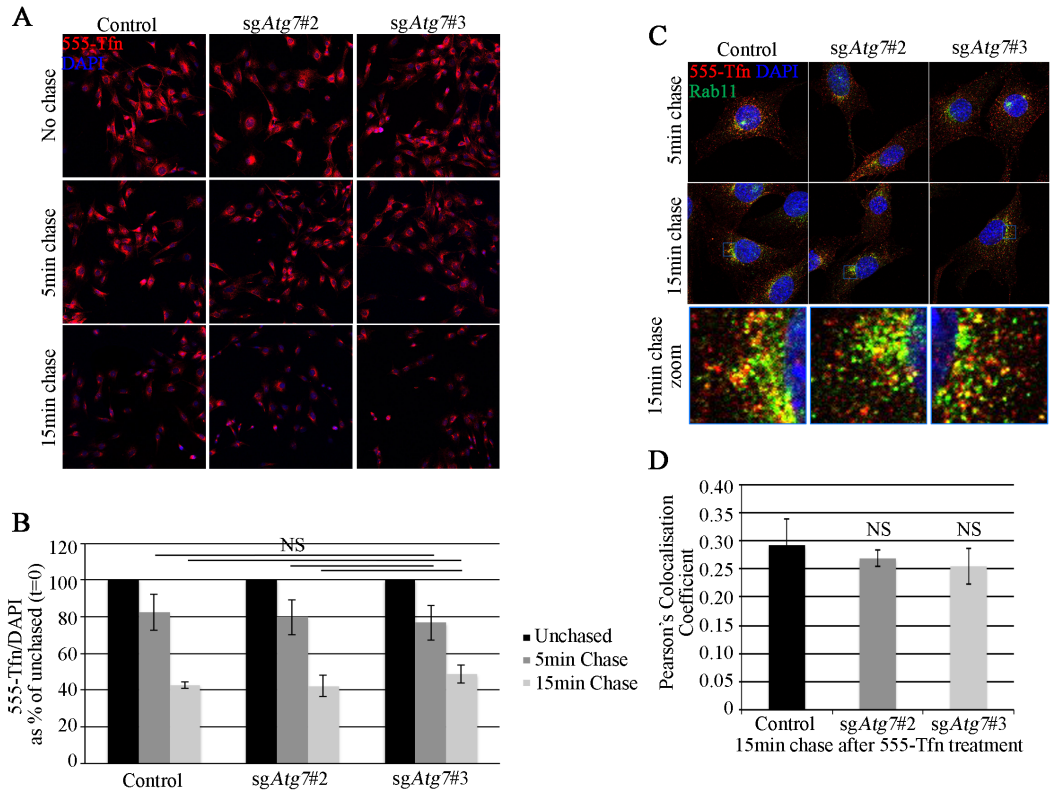

Figure 14.21 Autophagy Status Does Not Influence Transferrin Receptor Recycling
A-D: 555-Tfn was applied to sh*Nf-1*/sh*Tp53* XFM/*tv-a* cells with or without sg*Atg7* for 15 min then chased with media without Tfn for 5 or 15 min. **A:** Representative low magnification images of 555-Tfn levels following -Tfn chase, **B:** Quantification of 555-Tfn levels per cell, relative to levels before chasing with -Tfn media (i.e. t=0 is 100%), **C:** Co-localisation between 555-Tfn and endogenous Rab11 is maximised following 15 min chase with -Tfn media as 555-Tfn is localised to recycling endosomes, **D:** Quantification of Pearson's coefficient between 555-Tfn and Rab11 following 15 min chase with -Tfn media. n=3 experiments, ≥30 cells quantified per condition, error bars represent SEM, non-significant (NS): p>0.05

suggests that the defective processing of PI(3)P in autophagy-deficient cells results in a failure to engage the recruitment of Rab11.

The archetypal recycled protein is the transferrin receptor (TfnR). Following the binding of Tfn ligand, endocytosed TfnR has a very low rate of targeting to late endosomes and is instead constitutively recycled via Rab11-positive endosomes to the plasma membrane. To test whether autophagy influences all Rab11 recycling endosome traffic, the recycling rate of TfnR was investigated. Unlike EGFR, which detaches from EGF during endosomal sorting, TfnR remains bound to Tfn during endocytosis and recycling then releases it into the extracellular space. Following a pulse with fluorescently labelled Tfn ligand (Alexa555-Tfn, denoted 555-Tfn), cells were chased with media without ligand to allow the expulsion of Tfn, meaning that a slower recycling rate would correspond to greater levels of 555-Tfn in the cell.

However, analysis showed that cells with or without Atg7 expression were able to recycle TfnR at comparable rates (Figure 14.21A,B). To confirm that this was by the known Rab11-mediated recycling route, 555-Tfn was co-localised with endogenous Rab11. The Pearson's coefficient between these two vesicles was similar between control and sg*Atg7* cells (Figure 14.21C,D). Therefore, autophagy does not regulate the trafficking of all cargoes through Rab11-positive recycling endosomes, only a subset including EGFR.

14.5 Autophagy Players Localise to Early Endosomes

These results have shown that knockout of autophagy players, such as *Atg3*, *Atg7*, and *Atg16l1*, reduces signalling from EGFR and results in stalled EGFR trafficking from perinuclear early endosomes. But do autophagy players directly interact with the endosomal pathway and EGFR to affect this change? To investigate this, a series of microscopic analyses were undertaken.

14.5.1 Live Imaging of EGF and Autophagy Players Reveals Their Transient Association

To capture any potentially transient associations between autophagy and endosomes, direct interrogation of autophagy players and EGFR trafficking was undertaken using confocal live-cell imaging. GFP-tagged essential autophagy players LC3 and Atg16l1 were stably expressed in cells, which were then serum starved for four hours then

stimulated with Alexa555-tagged EGF (555-EGF). Full co-localisation was not observed between EGF and either of these proteins, but instead a transient contact was detected (Figure 14.22A,B). A 'kiss-and-run' style of association occurred for approximately 155 seconds between GFP-LC3 and 555-EGF, but only 86 seconds between GFP-Atg16l1 and 555-EGF, which might be suggestive of the mechanism of association (Figure 14.22C). LC3 recruitment to pre-autophagosomal membranes occurs upon its conjugation to phosphatidylethanolamine, which is catalysed by

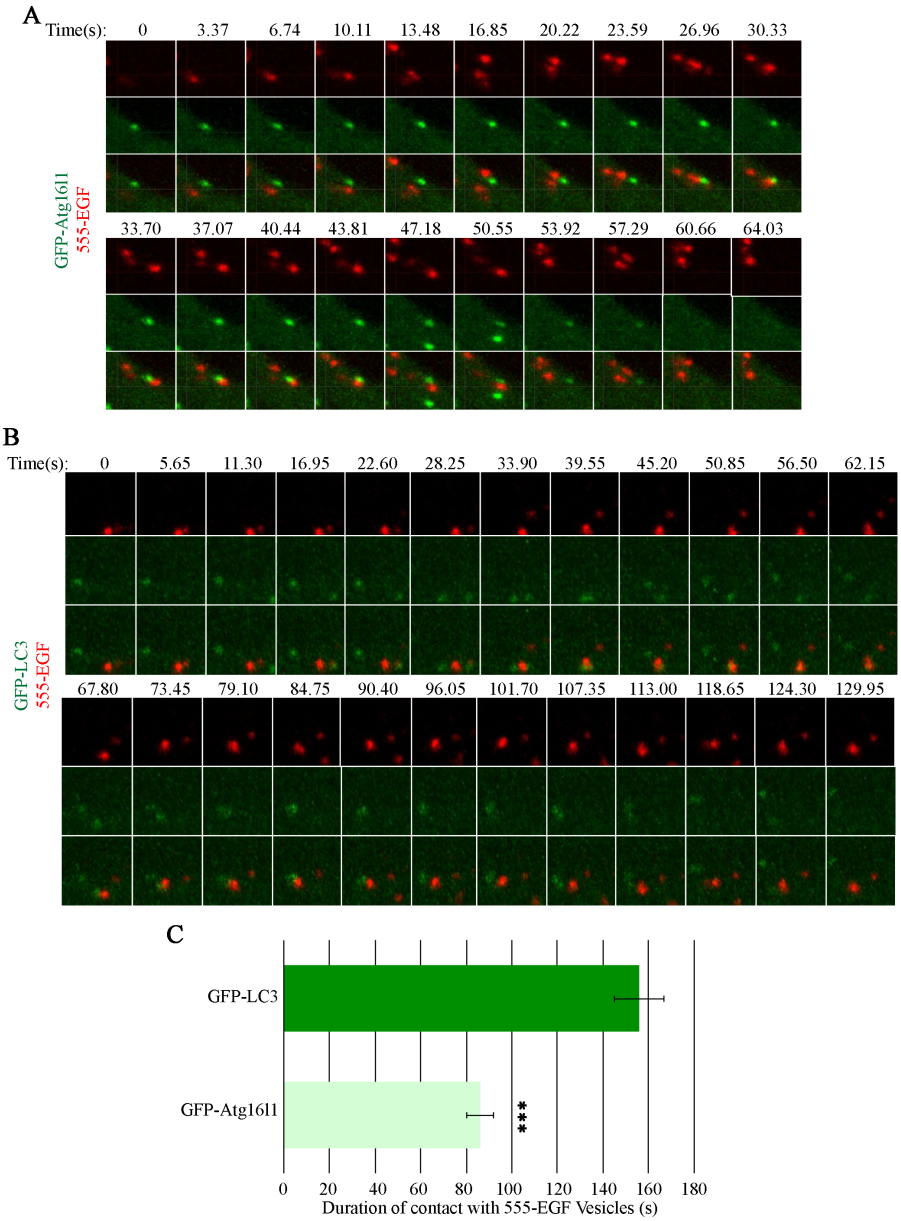

Figure 14.22 Live Imaging of GFP-Tagged Autophagy Players and 555-EGF Trafficking Reveals a Transient Association

A, B: Representative time lapses of puncta from 555-EGF-treated GFP-Atg16l1 (**A**) and GFP-LC3 (**B**) XFM/*tv-a* sh*Nf-1*/sh*Tp53* cells, **C:** Bar graph showing that GFP-LC3 puncta contact 555-EGF for longer than GFP-Atg16l1. n=3 experiments, ≥75 events quantified per condition, error bars represent SEM, * $p<0.05$, ** $p<0.01$, *** $p<0.001$.

various ATG proteins, including Atg16l1. LC3 then remains on autophagosomes during their expansion/formation and until their fusion with the lysosome. As LC3 is associated with EGF for longer than Atg16l1, it implies EGF^+ vesicles are recruited for longer than just the LC3 lipidation step. Furthermore, following its association with EGF, Atg16l1 converts from its punctate localisation to becoming diffuse in the cell (Figure 14.22A), whilst LC3 remains in puncta after contact with EGF (Figure 14.22B). Together, this implies that autophagosome biogenesis may occur following contact with EGF^+ structures.

14.5.2 Imaging Interactions Between Autophagy Proteins and Endosomes By Structured Illumination Microscopy

This association was then viewed in more detail using high-resolution structured illumination microscopy (SIM). This provided greater clarity in showing that EGFR

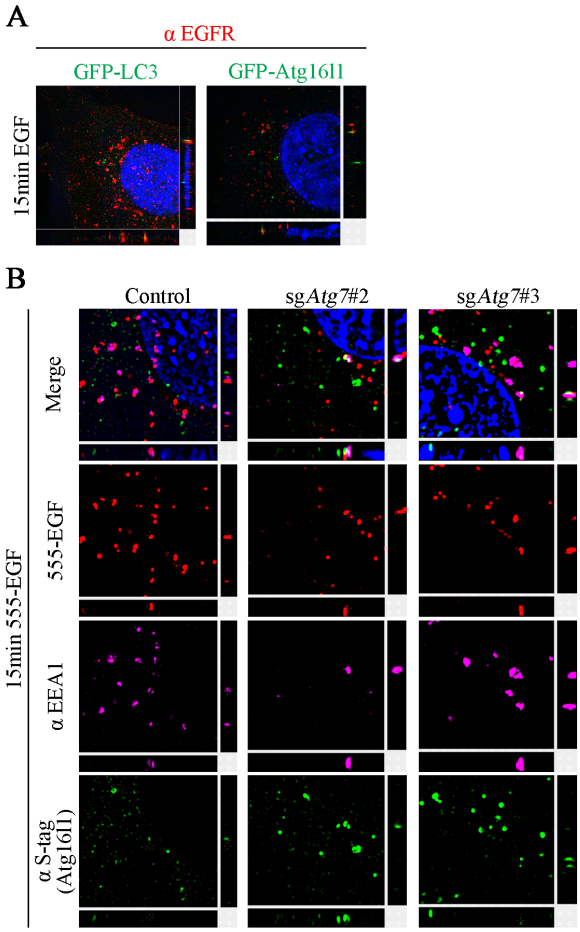

Figure 14.23 Structured Illumination Microscopy (SIM) of Endosomal and Autophagy Structures
A: XFM/*tv-a* sh*Nf-1*/sh*Tp53* cells expressing either GFP-LC3 or GFP-Atg16l1 were serum starved for 4 hr then stimulated for 15 min with 20 ng/ml EGF then stained for EGFR, **B:** XFM/*tv-a* sh*Nf-1*/sh*Tp53* cells overexpressing S-tagged Atg16l1 were serum starved for 4 hr then stimulated with 20 ng/ml 555-EGF 15 min before staining for EEA1 and S-tag. Experiment repeated 3 times.

was truly contacting, but did not co-localising with, GFP-LC3 and GFP-Atg16l1, as detected by IF following fifteen minutes of EGF stimulation (Figure 14.23A). If these structures are becoming associated but not directly binding one another, then what was actually providing the connection? It has been previously seen that Atg16l1 is trafficked through the endosomal system and that endosomes can contribute to autophagosome biogenesis[36,53]. As autophagy has been shown here to regulate early endosomes it is possible that they might provide the link between autophagy players and EGFR. To test this, cells stimulated with 555-EGF for fifteen minutes were prepared for SIM analysis by staining for Atg16l1 and EEA1. The resulting images show that $EEA1^+$ vesicles do in fact provide a link between autophagy and EGF^+ structures and these hybrid compartments are stabilised by loss of Atg7 (Figure 14.23B).

14.5.3 Weak Localisation of Atg16l1 and WIPI2 at Early Endosomes is Stabilised by Atg7 Loss or Chemical Disruption of Endosomes

The above studies have revealed a weak or transient interaction between autophagy proteins and early endosomes in untreated autophagy-competent cells and an early endosomal defect in autophagy-deficient cells. This therefore raises the question of whether autophagy proteins can directly play a role in regulating early endosomal homeostasis. To interrogate this possibility, the localisation of autophagy proteins to endosomes was tested under different conditions.

Confirming the findings from live cell imaging and SIM, confocal microscopy of autophagy-competent cells revealed a poor co-localisation between Atg16l1 and EEA1 (Figure 14.24A). However, as Atg7 loss had been seen to disrupt different endosomal structures, I hypothesised that any potential weak or transient interaction of upstream autophagy players at early endosomes may be captured in Atg7-deficient cells. Indeed, in *Atg7* knockout cells there is a strong co-localisation between Atg16l1 and EEA1 (Figure 14.24A,C). Furthermore, quantification of the size of early endosomes that co-localised with Atg16l1 shows that they have a larger area than that of the population of $EEA1^+$ vesicles as a whole, irrespective of cell line (Figure 14.24B). This suggests that autophagy could have a role either in regulation of endosomal size by facilitating an early to recycling endosomal switch that occurs in larger ‘sorting endosomes’ or autophagy proteins may be specifically targeted to

perturbed endosomes for degradation. This goes hand-in-hand with the EM data in section 14.4.1, which showed that Atg7 loss increased endosomal size.

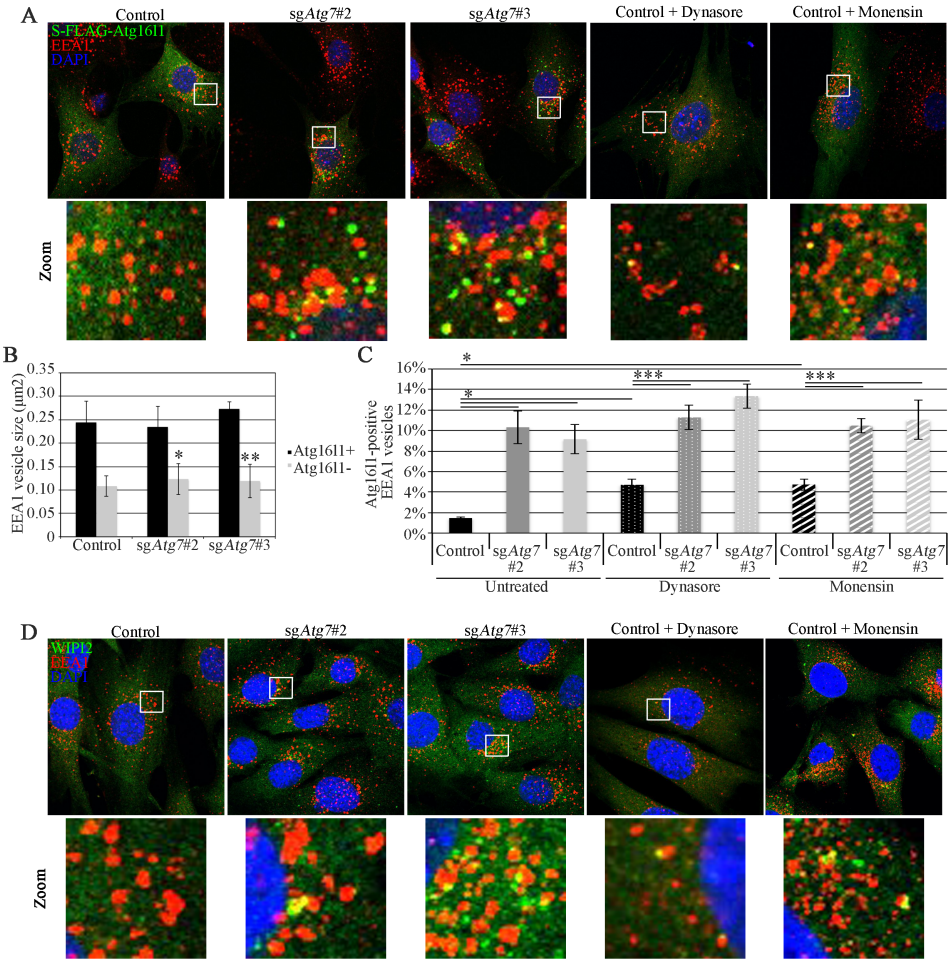

Figure 14.24 Atg16l1 and WIPI2 are Targeted to Early Endosomes When Atg7 Expression is Lost and Atg16l1$^+$ Early Endosomes Are Larger Than The General Endosomal Population
A: Representative images of EEA1 and Atg16l1 co-localisation in serum starved XFM/*tv-a* sh*Nf-1*/sh*Tp53* cells with or without Atg7 expression or treated for 1 hr with 100 µM monensin or 50 µM Dynasore, **B:** Quantification of the size of EEA1$^+$ vesicles that co-localise with Atg16l1 compared to the average vesicle size of the total EEA1 population, **C:** Quantification of the percentage of Atg16l1$^+$ early endosomes in control and *Atg7* knockout cells that were either untreated or treated for 1hr with monensin or Dynasore, **D:** Representative images of EEA1 and WIPI2 co-localisation in serum starved XFM/*tv-a* sh*Nf-1*/sh*Tp53* cells with or without Atg7 expression or treated for 1 hr with 100 µM monensin or 50 µM Dynasore. n=3 experiments, ≥30 cells quantified per condition, error bars represent SEM, * $p<0.05$, ** $p<0.01$, *** $p<0.001$.

To chemically mimic the effect of *Atg7* knockout on endocytic trafficking, inhibitors of different endosomal functions were employed. Prior to immunofluorescence staining against Atg16l1 and EEA1, cells were treated with either monensin, which inhibits the generation of a proton gradient over endosomal membranes and thereby prevents recycling endosome traffic, or Dynasore, which inhibits the pinching off of recycling endosomes that is mediated by dynamin. Interestingly, preventing the early to recycling endosome transition with either of these compounds induces the

localisation of Atg16l1 to early endosomes (Figure 14.24A,C). This localisation was less than that observed for *Atg7* knockout cells, possibly due to the cumulative effects that occur during successive passages.

It has been previously observed that lipidation of LC3 can occur on single-membrane vesicles, known as 'LC3-associated phagocytosis' (LAP)[400]. This non-canonical form of autophagy occurs independent of the upstream regulator WIPI2 and so to determine whether the targeting of Atg16l1 to early endosomes is part of a LAP-like process the co-localisation of EEA1 with WIPI2 was tested. However, WIPI2 was similarly targeted to early endosomes, suggesting a canonical autophagic process (Figure 14.24D).

14.5.4 Markers of Endosomal Damage Localise to Early Endosomes in *Atg7* Knockout Cells

The localisation of these autophagy players at endosomes under conditions of endosomal disruption suggests that the autophagy machinery may target endosomes for degradation. By extension, the accumulation of Atg16l1 and WIPI2 at early endosomes in Atg7-deficient cells may represent stalled pre-autophagosomal structures that are endeavouring to encapsulate endosomes. Interestingly, the targeting of similar single-membrane vesicles for autophagic degradation has been described previously in response to bacterial infection[58]. In this regard, when *Salmonella* attempts to escape its vacuole in order to propagate, β-galactosides on the inner surface of the vesicle membrane become exposed to the cytoplasm. These are then recognised by the β-galactoside-binding lectins galectins-3, -8, and -9 and recruit active phosphorylated TANK-binding kinase 1 (p-TBK1). Galectin-8 was found to be the player required for the selective clearance of *Salmonella* by autophagy via its interaction with NDP52 that then recruits LC3C[59]. Conversely, the exact mechanisms by which p-TBK1 is able to mediate autophagosome biogenesis, for xenophagy or under other circumstances, are currently unclear. To investigate whether the same machinery is targeting early endosomes in the context of this study, the co-localisation between these upstream autophagy regulators with EEA1 was tested. Accumulations of p-TBK1 puncta were observed in Atg7-deficient cells and, excitingly, these almost exclusively localised to early endosomes (Figure 14.25A).

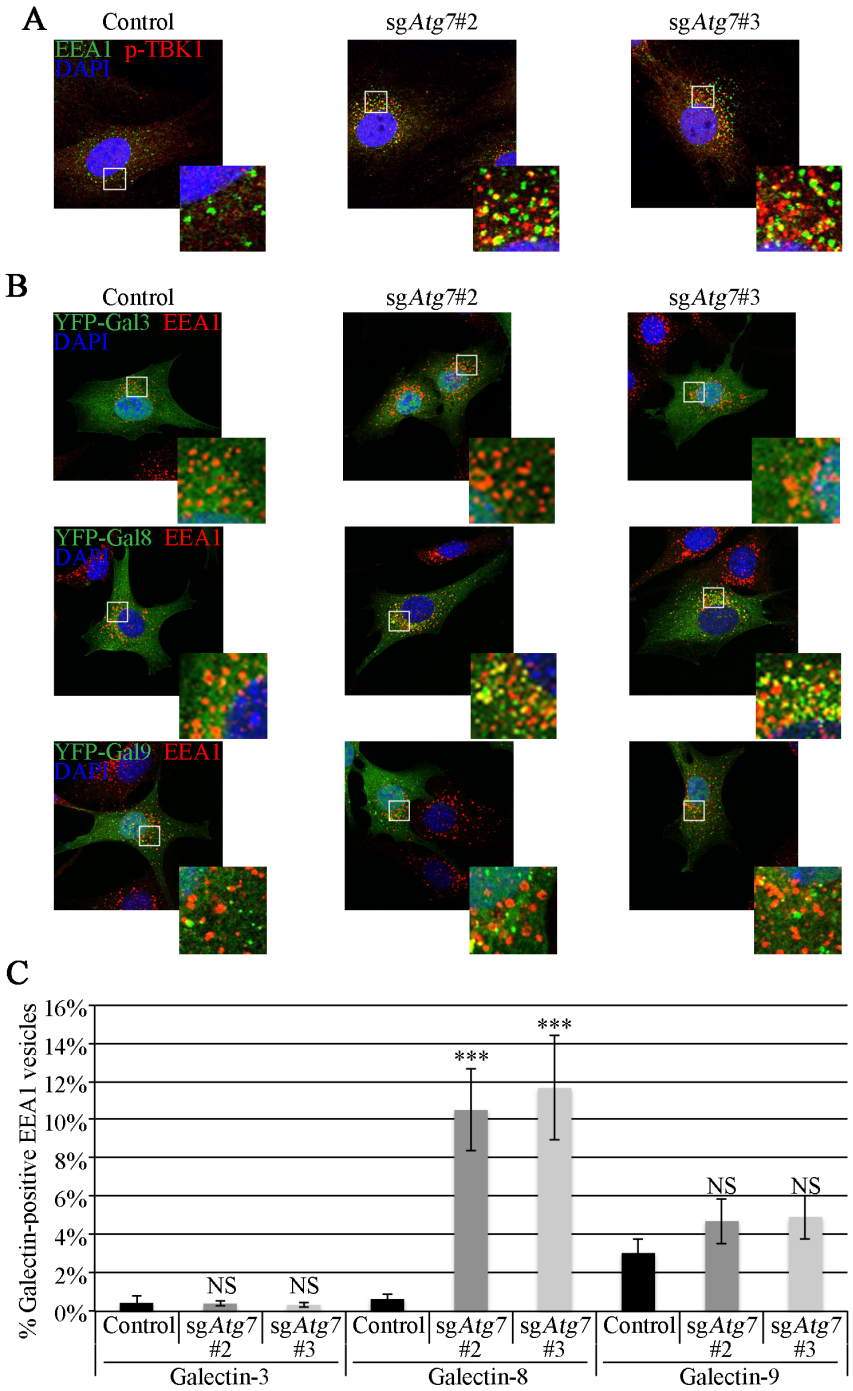

Figure 14.25 Markers of Selective Autophagy are Targeted to Early Endosomes in *Atg7* Knockout Cells

A: Representative images of XFM/*tv-a* sh*Nf-1*/sh*Tp53* control and *Atg7* knockout cells that were serum starved 4 hr before staining against endogenous EEA1 and p-TBK1, **B:** Representative images taken from XFM/*tv-a* sh*Nf-1*/sh*Tp53* control and *Atg7* knockout cells that were transfected with YFP-Galectin-3, -8, or -9 constructs 24 hr prior to 4 hr of serum starvation followed by staining for EEA1, **C:** Quantification of the experiment outlines in part **B**. n=3 experiments, ≥30 cells quantified per condition, error bars represent SEM, * $p<0.05$, ** $p<0.01$, *** $p<0.001$.

Further to this, YFP-tagged galectins were over-expressed in control and sg*Atg7* cells and their co-localisation with EEA1 was examined. Unlike results gleaned from galectin co-localisation with *Salmonella*, only galectin-8 exhibited an Atg7-dependent accumulation on these vesicles (Figure 14.25B, C). Some co-localisation between galectin-9 and EEA1 occurred but this was not increased upon Atg7 loss, suggesting it may not be part of the mechanism by which early endosomes are targeted by autophagy. Likewise, galectin-3 was ruled out as it had minimal co-localisation with EEA1 in either control of *Atg7* knockout cells. This therefore led me to hypothesise that the autophagy machinery is recruited to early endosomes via a p-TBK1/galectin-8-regulated mechanism.

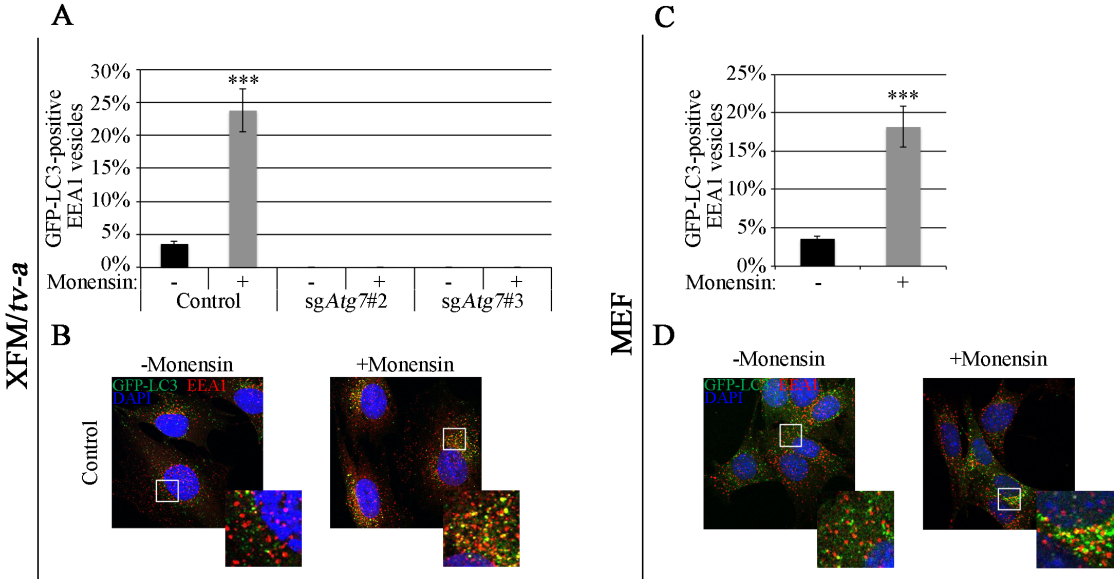

Figure 14.26 GFP-LC3 is Targeted to Early Endosomes Upon Monensin Treatment
The percentage of GFP-LC3 positive EEA1 vesicles were quantified in XFM/*tv-a* sh*Nf-1*/sh*Tp53* cells (**A**) and MEF cells (**C**) that were either serum starved 4 hr (-monensin) or serum starved 4 hr with 1 hr treatment 100 μM monensin. Representative images (green: GFP-LC3, red: EEA1) of untreated or monensin treated XFM/*tv-a* sh*Nf-1*/sh*Tp53* (**B**) and MEF (**D**) are shown with overlaid panels of zoom areas. n=3 experiments, ≥30 cells quantified per condition, error bars represent SEM, * p<0.05, ** p<0.01, *** p<0.001.

14.5.5 Early Endosomes are Targeted to Autophagosomes Upon Monensin Treatment

As galectin-8 recognises damaged endosomes and the chemical disruption of endosomes had been seen to recruitment of autophagy players, I hypothesised that autophagy may selectively degrade damaged early endosomes, thereby maintaining the health of the endosomal system. To test whether autophagosomes are indeed generated at early endosomes, targeted damage of early endosomes was induced using monensin and recruitment of GFP-LC3 was monitored. A striking increase in LC3 punctuation was observed upon monensin treatment, which was predominantly

localised to early endosomes (Figure 14.26). This was observed in both XFM/*tv-a* sh*Nf-1*/sh*Tp53* and MEF cells, but, as expected, did not occur in Atg7-deficient cells. Alongside the previous results, this data suggests that autophagy selectively targets early endosomes, or parts of early endosomes, when they are damaged and inhibiting this process by knocking out *Atg7* results in perturbed and dysfunctional endosomes.

14.6 Discussion

Previous studies have shown that signalling from certain RTKs, such as EGFR and c-Met, relies on the expression of different autophagy proteins and that autophagy proteins can be localised to different endosomal compartments [170,171,174]. However, the reasons behind these connections are largely unknown. During the course of the experiments described above, it was discovered that EGFR signalling relies on the mediation of its plasma membrane recycling by autophagy. Autophagy promotes the EGFR early-to-recycling endosome maturation step without influencing its degradation. Inhibition of this maturation step by the loss of autophagy results in the perinuclear accumulation of EGFR, defects in its nuclear translocation, and reduced uptake of its ligand. Knockout of *Atg7* results in the accumulation of upstream autophagy players at early endosomes, correlating with increased endosomal vesicle size and elevated levels of the lipid PI(3)P. Further investigation revealed that selective targeting of damaged early endosomes by autophagy is critical for endosomal homeostasis. This is required for EGFR trafficking to Rab11-positive recycling endosomes and its subsequent return to the plasma membrane.

Recent reports have suggested that signalling from the RTK c-Met and EGF-mediated activation of ERK occurs on LC3-positive so-called 'autophagy-related endomembranes'[170,174]. Here, although relying on autophagy protein expression for signalling activity, EGFR was not seen to fully co-localise with autophagy players. Instead, Atg16l1 and LC3 had a juxta-EGFR localisation following EGF stimulation. This occurred in a transient manner and was seen in fact to be bridged by early endosomal membranes. Therefore, EGFR was still occupying canonical endosomal vesicles but was experiencing a brief association with autophagy proteins. Given that LC3 contacted these endosomal points for longer than Atg16l1, it is plausible that they represent sites of autophagosome biogenesis. The duration of these puncta also correlate well with the approximate 2-5 minute window estimated by others for autophagosome formation[13,153]. Subsequent studies revealed that upstream autophagy

players strongly localised to early endosomes when Atg7 was lost. Together, these data suggest that autophagosomes form at early endosomes containing EGFR.

The regulation of endosomes by autophagy also appears to be critical for the nuclear translocation of EGFR. This may contribute to the autophagy-mediated EGF-induced promotion of cell survival during serum starvation that was documented in the earlier chapter. Whilst the signalling cascades triggered by EGFR activity can instigate changes in transcription and cell cycle regulators, recent studies have also outlined a key role for EGFR itself as a co-transcriptional regulator of cell survival genes, particularly during times of stress[135,137]. Therefore, in addition to the known roles of autophagy in cell health promotion during stress, here we see that it can facilitate EGFR nuclear translocation to aid cell survival.

Atg7 knockout increased the vesicular co-localisation between EGF and EGFR and lengthened the duration of EGF^{+} puncta during live imaging. These represent early endosomal populations that were seen to accumulate in a perinuclear region. Mass spectrometry revealed that certain EGFR interacting partners were altered upon *Atg7* knockout. Complexes such as CME regulator AP-2, and ER-related proteins Sec61 and Arp2/3 exhibited reduced binding to EGFR, suggesting that loss of autophagy sequesters EGFR from these sites. However, other known interactors were not affected by autophagy loss, such as Grb2. This adaptor connects EGFR to SOS, and so positively regulates Ras signalling from both the plasma membrane and early endosomes[387,388,401]. This seemingly conflicts with data presented in the previous chapter that showed autophagy loss reduced the activity of the downstream Ras target, ERK. If Grb2 adaptor binding was similar with or without autophagy, how can ERK phosphorylation be lower? One explanation might be that ERK can also be activated by Ras-GTP via the PI3K/Akt signalling axis[402–404]. Therefore, the reduced Akt signalling in autophagy knockout cells that is caused by restriction of EGFR in early endosomes may prevent the full activation of ERK, despite Grb2/SOS/Ras activity.

The GO term reactome pathway analysis undertaken on the mass spectrometry hits highlighted a defect in PI metabolism pathway components in autophagy-deficient cells. This is given credence by the striking increase in the levels of the lipid PI(3)P at early endosomes following the loss of Atg7 and Atg16l1 in glial cells, as well as in *Atg7* knockout MEFs. This suggests that autophagy loss is somehow disturbing the regulation of this lipid. However, the interactions of known regulatory partners of PI generating enzyme PIK3C3 were not influenced by autophagy loss and neither was its

in vitro catalytic efficiency. In fact, rather than increasing PIK3C3 activity, autophagy loss actually slightly diminished it. This may be a form of feedback inhibition instigated by PI(3)P accumulation in these cells. Therefore, these results suggest that it is the maturation from early endosomes and the processing of PI(3)P are defective in autophagy-deficient cells, rather than excessive synthesis.

Interestingly, loss of Atg7 resulted in the co-immunoprecipitation of PIK3C3 with Atg16l1. This experiment was carried out under conditions of low detergent, however, with cell lysis buffer containing just 0.8% CHAPS. Therefore, the integrity of some biological membranes can be retained, suggesting that this binding may be indirect and occur over a membrane. Moreover, Atg16l1 is enriched at early endosomes, where the PIK3C3 functions, in Atg7-deficient cells. Therefore, it is possible that, instead of a direct interaction between PIK3C3 and Atg16l1, the abrogation of autophagy results in the accumulation of Atg16l1 at early endosomal membranes that can then be isolated by PIK3C3 immunoprecipitation.

In contrast to previous reports, Atg16l1 was not seen to traffic to Rab11-positive recycling endosomal populations in either control or *Atg7* knockout cells (data not shown)[31,152]. This was elucidated using both stable overexpression and endogenous staining of Atg16l1, whereas previous studies have primarily focussed on overexpression vectors. Additionally, a more recent study uncovered that transiently overexpressed Atg16l1 can be aberrantly targeted to recycling endosomes, but the endogenous protein is not prone to do so[154]. Therefore, my results regarding Atg16l1 targeting to early rather than recycling endosomes agree with the finding of some groups but not with others. It is possible that this may demonstrate that the trafficking of this protein is cell type dependent.

Instead, an alternative connection between autophagy and recycling endosomes was seen in this study: autophagy facilitated the sorting of EGFR into recycling endosomes. However, it did not regulate transferrin receptor (TfnR) recycling rates or its co-localisation with Rab11. Therefore, autophagy appears to be able to regulate the efficient sorting of a subset of receptors. This is supported by the observation that autophagy loss reduces the overall levels of active Rab11-GTP by approximately 45% but not completely. This evidence shows that other factors or mechanisms are at play that can mediate Rab11-positive recycling endosome formation for different factions of receptors, such as TfnR.

Investigation of the wider status of the endocytic system by electron microscopy revealed that disruption of early endosome maturation and PI(3)P levels by autophagy loss results in larger vesicle size and elevated formation of multivesicular bodies (MVBs). However, EGFR was not significantly trafficked to these MVBs upon autophagy inhibition suggesting that their production may be a secondary effect, potentially indirectly promoted by the elevated PI(3)P levels[405].

Moreover, enlarged early endosomal size may be attributable to increased PI(3)P as the homotypic fusion of early endosomes requires by EEA1, which binds PI(3)P[83]. Therefore, the increase in PI(3)P levels may result in promotion of early endosomal fusion. Immunofluorescence (IF) studies revealed that early endosomes have a larger size when co-localised with Atg16l1, thereby implicating this autophagy protein in the regulation of PI(3)P and endosomal homeostasis. However, these proposals are based on correlative evidence. To demonstrate that excess PI(3)P drives the formation of MVBs in autophagy-deficient cells, PI(3)P synthesis could be inhibited before undertaking EM or IF studies. Indeed it is possible that autophagy loss may instead be preventing the clearance of MVBs rather than promoting their formation as autophagosome-MVB fusion products, amphisomes, are known to be directed to the lysosome for degradation. Further study is required to clarify this point.

Work outlined here has shown that the autophagy players Atg16l1 and WIPI2 target early endosomes and these associations can be clearly captured when autophagosome formation is prevented by *Atg7* knockout. Furthermore, inducing endosomal disruption using monensin results in the recruitment of not only Atg16l1 and WIPI2 but also, in autophagy-competent cells, LC3. This therefore suggests that endosomes are likely to be selective targets for autophagic degradation. Upstream, this is seen to mediated by galectin-8 and TBK1, which have previously been described to recruit the autophagy machinery to damaged endomembranes in the context of xenophagy[58]. Here we observe a parallel process under homeostatic conditions, where the autophagy machinery appears to be important in the targeting of damaged early endosomes (as induced with monensin or Dynasore and were found to accumulate in Atg7-deficient cells). Taken together with the data outlined above, preventing the targeting of endomembranes by autophagy can lead to the accumulation of PI(3)P-positive early endosomes. However, in light of these findings many questions are raised, some of which I shall outline here.

Firstly, although these data uncover the targeting of early endosomes by the autophagy machinery, I have not demonstrated that autophagy actually degrades damaged endomembranes. To do this, it would be necessary to induce endomembrane damage then either show the localisation of early endosomal markers at the lysosome or demonstrate that the protein levels of these markers are reduced by Western blotting. Although we see accumulations of early endosomal lipid PI(3)P when autophagy is inhibited, currently we cannot be certain that early endosomes are actually degraded by autophagy.

It is also unclear how endomembranes are damaged under normal conditions to require their selective removal. In the case of escaping bacteria, it is known that damage is induced by type III secretion systems, and that endolysosomal membrane damage can occur as a result of mineral crystals such as silica[58,65]. Here it is seen that inhibiting the formation of a proton gradient (monensin) or preventing dynamin-mediated scission of budding vesicles (Dynasore) can result in the recruitment of autophagy players such as Atg16l1. These are quite disparate cues- what do they converge on? Do they result in membrane stress and rupture to be recognised by galectin-8? If so, might disruption of these processes in untreated cells be the cause of the membrane damage that fails to be cleared in *Atg7* knockout cells?

Furthermore, the role of TBK1 in mediating targeted autophagy remains somewhat elusive, with its upstream regulators and downstream targets not completely understood. This kinase has been seen to be required for the efficient recruitment of autophagy adaptors such as Optineurin and NDP52 to targeted cargoes, such as mitochondria or bacteria[56,61]. What adaptor protein might be responsible for early endosome membrane targeting in this study? If it were a comparable system to that for *Salmonella* clearance, it would be reasonable to suggest that it may be NDP52, which can bind galectin-8, co-ordinate TBK1 recruitment, and bind to LC3. However, this remains to be tested.

Additionally, how can stalled canonical autophagosome biogenesis be distinguished from the targeting of endosomes by autophagy? It has previously been described that components of the COPI 'coatomer', which is required for Golgi-to-ER transport, are required for autophagosome maturation and depletion of these components induces LC3 co-localisation with early endosomal EEA1[406]. Might the loss of Atg7 or treatment with monensin or Dynasore actually be inhibiting autophagosome formation? To test this, a more targeted sterile rupture of early endosomes could be

achieved using an osmotic disruption method, which has been previously described[58]. If these membranes also co-localise with autophagy players, I would suggest that they are indeed being targeted by autophagy rather than acting as a membrane source for autophagosome biogenesis.

Alternatively, the expression of the upstream damage recognition players could be inhibited and the consequential recruitment of the LC3 lipidation machinery tested. This is indeed how I aim to conclude this study; currently I am working to generate CRISPR/Cas9 constructs against galectin-8 and TBK1. The loss of these proteins would be hypothesised to prevent the recruitment of the autophagy machinery to early endosomes. This would therefore support a cascade of recruitment from damage recognition (galectin-8) and autophagy adaptor stimulation (TBK1) to recruitment of LC3 lipidation machinery (e.g. Atg16l1). Importantly, I will also test the influence of the knockout of these players on EGFR phosphorylation and signalling. However, many other avenues remain to be explored, particularly with regards to specificity of the endomembrane cargo.

Together, the studies outlined above clearly demonstrate a key role for autophagy in facilitating the endocytic recycling of EGFR. Further results suggest this is promoted by autophagic clearance of perturbed early endosomes that thereby maintains endosomal homeostasis and allows progression of specific cargoes, such as EGFR, from $PI(3)P^+/EEA1^+$ early endosomes to $Rab11^+$ recycling endosomes. Functional autophagy consequently promotes RTK signalling, EGFR nuclear translocation, and cell survival induced by EGF.

15 Final Discussion

Throughout the course of this project I have endeavoured to elucidate whether autophagy can promote pro-growth properties of glioblastoma multiforme (GBM). The results gleaned during the course of experiments outlined above have uncovered a novel role for autophagy in regulating oncogenic receptor tyrosine kinase signalling. By delving into the cellular trafficking pathways that regulate such signalling it was possible to show that autophagy players are important in maintaining early endosomal function. These findings related back to my earlier work that showed that autophagy is important for oncogenic phenotypes of GBM cell line and mouse models. Here I shall discuss these results in the context of the existing literature, the relative problems and pitfalls of the experimental techniques, and how this work may be built upon in the future.

15.1 Endosomal Regulation by Autophagy Proteins

Endocytosis and autophagy are both vesicular trafficking mechanisms that regulate the abundance and activities of a variety of different cellular regulators. These pathways share a variety of common regulators, from lipid modifiers like phosphatidylinositol-3-kinase complex 3 (PIK3C3) to activators of Rab small GTPases. Several groups have described the localisation of autophagy proteins at different endosomal compartments and endosomal trafficking destinations, such as the Golgi. Whilst the contribution of these compartments to autophagosome biogenesis is beginning to be understood, the influence of autophagy proteins on the endosomal system is not known. By using a variety of microscopy analyses, here I have been able to show that inhibition of autophagic flux by genetic ablation of Atg7 expression results in a significant disruption of endosomal homeostasis. Specifically, the loss of autophagy results in more multivesicular bodies (MVBs) and perturbs the maturation of early to recycling endosomes. Molecularly, this correlates with an increase in phosphatidylinositol-3-phosphate (PI(3)P) levels and the accumulation of autophagy proteins at early endosomes.

15.1.1 Atg16l1 Localisation to Early Endosomes

How does this fit into the larger picture of the endocytic and autophagy pathways? The plasma membrane and endosomal compartments have been shown to significantly contribute to autophagosome biogenesis, with certain autophagy players

localising there before re-distribution to pre-autophagosomal structures[24,31,32,44]. For example, Atg16l1 has been described to localise to recycling endosomal compartments[31,146]. However, during the course of the studies undertaken here in glial cells, I was unable to replicate this result, instead finding that this essential autophagy protein primarily tends to localise to early endosomes, particularly when recycling endosome formation was disrupted either chemically (monensin or Dynasore) or genetically (Atg7 loss). Further, a recent study reported in the *Autophagy* journal suggested that Atg16l1 targeting to recycling endosomes was only possible when transiently overexpressed Atg16l1 aberrantly targets there, but is not a common event for the endogenous protein[154].

These findings are interesting when considering that Atg16l1 can interact with the endocytic regulator clathrin-heavy chain at the plasma membrane: how does Atg16l1 traffic from the plasma membrane to endosomes and on to autophagosomes? And therefore, by inhibiting autophagic flux in this study am I capturing an otherwise transient or minute intermediate of Atg16l1 transport? Current standard immunofluorescence techniques rely on a significant enrichment of a protein at a certain subcellular locale for detection above diffuse/background staining and therefore the trafficking of a small subset of protein cannot be detected, perhaps explaining why other groups have not observed Atg16l1 at early endosomes. By inhibiting its use in autophagy by deleting Atg7, we accumulate Atg16l1 at early endosomes to sufficient levels for detection by immunofluorescence staining. Alternatively, it is possible that Atg16l1 is targeted to early endosomes in Atg7-deficient cells by virtue of a perturbation of the properties of those endosomes, like increased PI(3)P levels or changes in membrane curvature. I have shown that Atg16l1 localises specifically to larger EEA1-positive early endosomes, and that this correlates with an increase in PI(3)P levels. Unpublished evidence from our laboratory group demonstrates that Atg16l1 can bind lipid moieties, with a specificity for PI(3)P (generated by Leo Dudley and Ainara González-Cabodevilla, data not shown here). Therefore, my data co-localising Atg16l1 with EEA1 may represent targeting of Atg16l1 to enlarged early endosomal compartments that have elevated PI(3)P.

It is interesting to consider the purpose of Atg16l1 trafficking through the endosomal system, however, not just with regards to regulation of endocytic trafficking but when considering autophagic flux. For instance, autophagy proteins at endosomes may act as sensors for extracellular conditions – might the presence of Atg16l1 act as a sensor

of growth factor signalling? For example, under starved conditions Atg16l1 might be targeted to sites of autophagosome formation, whilst under fed conditions, when there is less demand for autophagy, it might transport via early endosomes to the lysosome. Alternatively, the localisation of autophagy players at early endosomes may indicate that autophagosome biogenesis requires membrane sourced from the endocytic pathway. Whilst these hypotheses are intriguing, further investigation suggested that Atg16l1 and other autophagy proteins are likely to be targeted to early endosomes as part of another mechanism, as described below.

15.1.2 Autophagy Targets Early Endosomes For Degradation

Although traditionally believed to be a largely random bulk degradation pathway, the discovery of multiple mechanisms that regulate the targeting of autophagy machinery to specific cargoes in a closely regulated manner has shown it to be a highly specialised degradation process. In particular, the targeting of organelles, such as the ER or mitochondria, by autophagy has garnered much attention in recent years[60,66,70,407–409]. Functionally, the selective clearance of damaged organelles, or parts of organelles, has is seen to be important for their overall function and consequently the maintenance of cell fitness[60,69,410]. Excitingly, for the first time here we show that autophagy proteins can also selectively target early endosomes. However, the work undertaken here has not shown that autophagosomes actually deliver these structures to the lysosome for degradation. As discussed in section 14.6, further experimentation is required to verify the final steps in this pathway.

Early endosomal targeting seems to occur constitutively in cells as the loss of Atg7 results in the accumulation of autophagy regulators, such as Atg16l1 and WIPI2, at early endosomesunder untreated conditions. However, it is likely to occur at a low level under basal conditions, as the co-localisation of these players with EEA1 in unstimulated autophagy-competent cells is infrequent. Instead, for significant Atg16l1-EEA1 co-localisation in wild-type cells, endosomal stress had to be induced using monensin and Dynasore, which disrupt membrane potential and prevent the dynamin-mediated budding off from vesicles from endosomes, respectively.

15.1.2.1 How Does Endomembrane Damage Occur?

Further investigation revealed that perturbed early endosomes are targeted by galectin-8, which recognises galactosides on the luminal face of endomembranes, and phosphorylated TBK1, which is known to function as part of the innate immune

response[58,411]. However, it is unclear how endomembrane damage might occur under basal conditions and accrue in Atg7-deficient cells. One possibility is that membrane remodelling processes that are undertaken as vesicles bud off from endosomes induce membrane stress and rupture that needs to then be cleared. This is supported by the localisation of Atg16l1 and WIPI2 to early endosomes following Dynasore treatment, which is known to cause elongated enlarged endosomes (as shown here and elsewhere[412,413]) and therefore could alter endosomal membrane integrity by increasing its curvature. Alternatively, the osmotic imbalance or disruption of the pH gradient over the endosomal membrane may result in membrane rupture and galectin-8 recruitment. These perturbations are induced by monensin, the application of which resulted in the co-localisation of EEA1 with Atg16l1, WIPI2, and LC3.

Further study to understand the exact cause of this damage is challenging due to the difficulty in controlling for the multitude of factors that can regulate early endosomes and can compensate for their disruption. A targeted approach would be required to test specific hypotheses and candidate processes.

15.1.2.2 Selectivity of Autophagic Endosomal Targeting

Deciphering the cause of this membrane disruption might also help address another question: why early endosomes? Several other endosomal types exist in the cell, yet early endosomes seem to be specifically targeted by the autophagy machinery in Atg7-deficient and monensin- or Dynasore-treated cells. Why do these factors not also induce late or recycling endosomal degradation? It is possible this selectivity is due to the enrichment of PI(3)P at early endosomes – a lipid known to be essential for autophagosome biogenesis by recruiting key factors including WIPI2[414], DFCP1[415], and Atg16l1 (unpublished data from our laboratory).

It is also conceivable that targeting early endosomes over other forms is the most efficient means of controlling membrane quality throughout the endocytic system as other endosomes are derived from early endosomes. In one model, cargoes can be sorted into subdomains in a so-called ‘sorting endosome’ that then bud off as late or recycling endosomes[416–418]. Therefore, ensuring early endosome membranes are intact would promote the membrane integrity of any subsequent daughter vesicles. In the course of these experiments we have seen that loss of autophagic endosomal homeostasis does indeed perturb recycling endosome traffic, either by hindrance of formation or an inability to properly mature into $Rab11^{+}$ recycling endosomes.

Therefore, it seems that maintaining endomembrane integrity is important for recycling endosome function. Conversely, ensuring late endosomal membranes are intact is a relatively futile task as they are destined to imminently fuse with the lysosome and be degraded.

15.1.3 Multivesicular Bodies are Elevated in Autophagy-Deficient Cells

As well as defects in early endosomes, immunofluorescence and electron microscopy revealed that Atg7-deficient cells have a striking increase in the numbers of MVBs. It has been known that endosomal structures such as MVBs can fuse with autophagic vesicles to mediate their degradation[90]. Therefore, the increased incidence of MVBs in autophagy-deficient cells may be as a result of one of two factors: either the increased formation promoted by elevated PI(3)P-positive early endosomes, or defective clearance of MVBs via autophagosome-fused intermediate structures called amphisomes[419,420].

Although the work undertaken here is unable to resolve whether it is the synthesis or degradation of MVBs that is influenced, it would be possible to address this point by acutely inhibiting these processes. One means of doing this may be by using PI3KC3 inhibitors, like SAR405, to prevent PI(3)P synthesis and thereby abrogate the recruitment of the ESCRT complex to form MVBs[91]. The degradation rate of MVB structures could then be monitored in autophagy-competent and autophagy-deficient cells whilst preventing any fresh synthesis.

In the light of the data gathered during this study, however, I would hypothesise that rather than blocking in their degradation, autophagy loss seems instead to result in the accumulation of PI(3)P at early endosomes that would promote MVB formation. To test this, blocking lysosomal function, such as by using bafilomycin A1, could inhibit MVB degradation and so the subsequent formation rate of MVBs could be calculated.

Although not explored extensively in the context of this study, MVBs are known to be important organelles for several cellular processes, such as dampening RTK signalling and exosome release, which have been seen to have a role a wide-range of pathologies including cancer and neurodegeneration[421–423]. Therefore, the impact of autophagy loss on MVB biology warrants further investigation.

15.1.4 Autophagy Regulates the Trafficking of EGFR to the Nucleus

Away from endosomal vesicles, autophagy has been seen to be required for the homeostasis of and trafficking of various cellular components to organelles like the

Golgi and mitochondria. Trafficking of receptor tyrosine kinases to the nucleus is thought to occur via early endosomes that either sends cargo retrograde via the Golgi/ER or even by direct fusion with the nuclear envelope. Previous work has shown that autophagic flux is required for the trafficking of EGFR to mitochondria and here we have demonstrated that expression of Atg7 is required for EGFR trafficking to a nuclear marker-containing fraction of cell lysate[176]. However, whether this fraction represents solely the nuclear fraction was not proven- it was isolated by removing 'cytosolic' and 'membrane' fractions by increasing detergent stringency, leaving only constituents that are not soluble in 1% NP-40 but are soluble in RIPA buffer. Whilst lacking the membrane marker β1-integrin and enriched in the nuclear protein PCAF, the presence of other contaminating organelles, such as ER or Golgi, was not investigated. As the function of nuclear EGFR is known to be a potent driver of cell survival/growth but ER/Golgi-resident EGFR is not known to have a function, distinguishing these possibilities is would be important in determining whether this function of autophagy truly mediates nuclear EGFR.

The nuclear localisation of EGFR is induced by its ligand-mediated activation[137]. Therefore, it is not clear whether the defect in EGFR nuclear translocation is due to the reduced EGFR activity or perturbed early endosome function or maturation. Alas, there is not enough currently known about the mechanism of plasma membrane-to-nucleus trafficking mechanisms for molecules such as RTKs or integrins to be able to dissect this phenomenon easily[108,109,135].

Once in the nucleus, EGFR has been described to act as a co-transcriptional activator by binding to other transcription factors, such as STAT3, to initiate the expression of proliferative genes, such as c-Myc[424]. It would be interesting to test whether the apparent requirement for autophagy for EGFR nuclear translocation influences its ability to act as a co-transcriptional activator. In this scenario, the expression of gene products such as c-Myc, Cyclin-D, iNOS, and STAT1 could be measured by quantitative reverse transcription PCR (qRT-PCR) in autophagy-competent or -deficient cells that are or are not stimulated with EGF for different time-points[135].

15.1.5 Autophagic RTK Endocytic Regulation is Selective

This study has used EGFR trafficking as a model marker for the impact of autophagy on endocytic trafficking proficiency as a whole. However, we (and others[170,171]) have also seen that whilst this phenomenon also holds true for other RTKs, like c-Met,

others do not rely on autophagy for maximal signalling activity, such as IGF-1R. Alternatively, the transferrin receptor (TfnR) is a well-known model for Rab11-mediated endocytic recycling but its endocytosis, recycling rate, and Rab11 colocalisation were unaffected by loss of Atg7 expression, suggesting Rab11-positive recycling endosomes were functional.

How can we align these data with those from experiments demonstrating the recycling via Rab11-positive and maximal signalling activity of some RTKs relies on autophagy? It has long been postulated that not all RTKs are handled equally by endosomes: whilst some seem to preferentially signal from the plasma membrane others can signal in endosomes, and although RTKs such as Trk kinases are preferentially recycled, others, like PDGFR are sorted to the lysosome[117,425–427]. What dictates these specificities is currently unknown and constitutes a field of active research. These RTK regulatory mechanisms are generally considered to be specific to cell type and likely help establish lineage-specific properties. Here we may suggest that glial cells have a high reliance on plasma membrane-localised EGFR that is maintained by Rab11-mediated recycling routes, whereas IGF-1R may either be directly sent to the lysosome, internalised at a reduced rate, signal from endosomes, or returned to the plasma membrane preferentially via Rab4-regulated 'fast' recycling endosomes. This would be an interesting point to pursue through further experiments localising IGF-1R to different endocytic compartments and utilising a cell surface biotinylation recycling assay, as described in section 14.3.3. Alternatively, these differences may be attributable to discrepancies in the efficiency of receptor sorting to Rab11-positive recycling endosomes that depends on autophagy. This, indeed, would be the most likely explanation of why the TfnR is recycled at a similar rate in autophagy-competent and autophagy-deficient cells: whilst TfnR is able to be sorted properly, EGFR, which has a drastically different set of binding partners and ubiquitination marks, is unable to be correctly sorted.

To explore the importance of autophagy in endocytic trafficking and EGFR signalling, here I have manipulated the expression of three genes (*Atg3*, *Atg7*, and *Atg16l1*) that are essential for autophagy. Whilst these proteins are known to function in both canonical and so-called 'non-canonical' autophagy, other autophagy players, such as Atg13, have only been documented to participate in canonical autophagosome biogenesis[428–431]. To explore the possibility that this is a non-canonical autophagosomal process it would be necessary to ablate expression of Atg13 in these

cells and then assay the signalling response to EGF and the recycling capability of EGFR.

On the other hand, an alternative form of LC3 lipidation has been described to occur on single membrane vesicles called LC3-associated phagocytosis (LAP)[400]. However, as this process is WIPI2-independent, the co-localisation of WIPI2 with EEA1 observed here argues against the phenomenon observed here being LAP. To conclusively test this, however, a mutant of Atg16l1 has been described that can function in canonical autophagy but is unable to target to sites of LAP[400]. Therefore, the targeting of this mutant to early endosomal membranes would demonstrate that this is not LAP but rather a canonical form of autophagy.

15.2 Autophagy as a Modulator of Receptor Tyrosine Kinase Signalling

It is known that the endocytic trafficking of RTKs is a critical regulator of their activity. Indeed, the studies undertaken here show that the perturbation of endocytic homeostasis in autophagy-deficient cells correlates with an inability to maintain maximal signalling capacity, which is attributed to reduced plasma membrane recycling. Furthermore, Atg7 loss results in inhibition of EGFR nuclear translocation, where it is known to carry out a function as a co-transcriptional activator[135,137]. Here I shall put this in the context of data gathered in chapters 11 and 12, as well as with regards to what has been described previously in the field. Additionally, I shall discuss some of the technical considerations when interpreting cellular signalling data.

15.2.1 The Interpretation of Signalling Data

In chapter 13 I uncovered a role for autophagy in promoting signalling from EGFR, specifically to Akt and ERK that lie in the interconnected PI3K/mTOR and MAPK cascades, respectively. Although these are both well-known read-outs of EGFR activity, interestingly I found a particularly striking defect in Akt signalling but a mild or inconsistent perturbation in ERK, as evidenced by the larger error bars in the quantification for p-ERK ratios. This may be due to the possibility of ERK to be stimulated from early endosomes, whereas Akt is widely believed to be primarily activated at the plasma membrane, where its upstream activator PI3K resides[130–134]. Subsequent endocytic trafficking studies showed that EGFR was stalled in early

endocytic compartments in *Atg7* knockout cells and therefore was sequestered from being able to activate Akt but ERK signalling may still be possible. These findings highlight the importance of utilising more than one read-out of RTK activity to be able to clearly understand whether a process of interest is capable of influencing signalling. However, by the low-throughput process of Western blotting I was only able to investigate these two players whereas EGFR is known to signal to a wide variety of downstream pathways including JAK/STAT[77,432].

To test whether Atg7 loss also impacted these pathways I employed RPPA, which can measure the phosphorylation and total levels of proteins and thereby infer their activity. This demonstrated that in fact autophagy was important for the activation all known EGF-stimulated pathways. However, this technique is not without its limitations. For example, it is highly dependent on the accuracy of the RPPA robot in spotting protein lysates on slides as well as the specificity of the antibody of interest.

As an illustration of this point, whilst Western blotting (confirmed with two different antibodies) showed that EGFR levels were not altered by *Atg7* knockout, RPPA indicated reduced expression of the protein. However, due to time limitations, this experiment was only repeated once and therefore this study should only be considered as preliminary data indicating a wide-ranging effect of autophagy on EGFR signalling output. To further confirm this finding, RPPA would need to be repeated and key pathways checked by Western blotting.

Furthermore, in section 13.3.5, cell death during prolonged serum starvation with or without growth factor co-culture was used as a read-out of RTK activity. However, other outputs, including proliferation rate and expression of co-transcriptional targets are also frequently used in the field to measure the activity of RTKs. In order to more comprehensively test the cellular impact of autophagy loss on RTK activity, these factors should also be tested following growth factor stimulation. Additionally, although unfortunately outside the scope of the present study, RTK activity could be measured *in vivo*. This could be achieved by immunohistochemical staining of against phosphorylated forms of proteins such as EGFR and ERK in tumours with or without autophagy protein expression, or by checking for the presence of RTKs in the nucleus of tumour cells.

15.2.2 Cell Line Specificity of the Effect Autophagy on RTK Signalling

It is also of interest to understand whether autophagy is engaged in the quality control of early endosomes in other cell types.

I observed that autophagy has differing effects on the RTK EGFR according to cell line. Whilst in XFM/*tv-a* glial cells EGFR steady-state levels were found to be similar but its recycling rate and downstream signalling activities were abrogated by Atg7 loss, in MEF cells signalling in response to EGF stimulation was unaffected but overall expression levels of the receptor were significantly reduced. Encouragingly, this fits with data previously reported for EGFR levels in MEF cells with autophagy loss[52,433]. However, thus far, the cause of these differences has not been resolved. I propose that early endosomal defects that accumulate following autophagy loss result in a cell-type specific effect on EGFR. Whilst in glial cells the recycling route of EGFR is inhibited but degradation is unchanged, in MEFs when the receptor is unable to be recycled it is preferentially targeted via late endosomes to the lysosome. Studies of the endocytic pathway undertaken in both cell lines (e.g. elevated PI(3)P levels and early endosomal targeting by LC3) yielded similar results, supporting the notion that this mechanism may be common between different cell lines. However, more extensive testing is required to confirm this.

Furthermore, I observed conflicting results of ERK and Akt phosphorylation following EGF stimulation in MEF and XFM/*tv-a* cells. It is possible that this is due to their capacities for RTK signalling from early endosomes. Conflicting evidence regarding the stimulation of downstream signalling from early endosomes has been widely discussed[77,82,130–133]. Studies undertaken here have shown that EGFR accumulates in $PI(3)P^{+}$ early endosomes when autophagy is lost- a compartment that has been suggested to be signalling defective. However, EGF stimulation of MEFs generated similar levels of Akt and ERK phosphorylation. This may be because EGFR activity is not in fact inhibited in this compartment in MEFs and therefore its accumulation there instead of its recycling to the plasma membrane does not impact the signalling output. To test this hypothesis, immunofluorescence against phospho-ERK or -Akt and intracellular EGFR puncta could be undertaken. If true, in XFM/*tv-a* cells there would be little co-localisation expected whilst in MEFs a strong co-localisation may be found.

However, both XFM/*tv-a* and MEFs are mouse-derived cell lines so to be able to assess the potential importance of this process in GBM oncogenicity it would be

necessary to repeat several key findings in a human-derived GBM model cell line. Additionally, it would be fascinating to test this mechanism *in vivo*, perhaps by utilising the GFP-LC3 mouse.

15.2.3 Autophagy and RTK Signalling as Regulators of Senescence

As outlined in chapter 11, the prolonged culture of XFM/*tv-a* KRas cells in low serum conditions caused sh*Atg7* cells to undergo p27/pRB-mediated senescence. In a parallel experiment, whilst autophagy-competent cells were able to maintain strong Akt and ERK signalling in low serum or oxygen conditions, Atg7-deficient cells were unable to so. Might these two observations be linked? And might they relate to the reduction RTK signalling capacity described in chapter 13?

RTKs like EGFR are known to promote cell survival during stressful conditions, such as low oxygen[326,434–436]. Lying downstream of EGFR lie Akt and ERK, which are here seen to have reduced activation in sh*Atg7* cells. This may impact the susceptibility of these cells to senesce as Akt acts as a negative regulator of p27, a key cell cycle inhibitor and senescence modulator[212–214]. Therefore, a pathway may be envisaged in which autophagy promotes EGFR endocytic trafficking and signalling under conditions of low serum or oxygen, thereby maintaining Akt activity and keeping p27 at bay to prevent the induction of senescence. To understand whether this mechanism might be occurring in these cells, chemical inhibitors of Akt and EGFR could be employed, which should mimic the senescent phenotype observed in Atg7-deficient cells. This finding could have an impact on a number of fields, including development, cancer, and ageing[344,437,438].

15.3 Autophagy as a Regulator of Glioblastoma: An Opportunity for Therapeutic Intervention?

The results gleaned here from *in vitro* GBM model cell line models have elucidated a role for autophagy in maintaining signalling frequently found to be oncogenic in this aggressive brain cancer. But how useful is this information in the clinical setting?

15.3.1 Autophagy as an Inhibitor of Resistance and Recurrence

Throughout the course of this work I have assayed the influence of autophagy on the oncogenic properties of glial cells. However, the greatest challenge in treating patients is the recurrence of the tumour. Although I have not directly investigated the importance of autophagy following radiotherapeutic or chemotherapeutic insults, the

results gleaned can be interpreted in the context of known drivers of tumour resistance.

For example, nuclear EGFR is believed to drive resistance to therapies, particularly with regards to GBM and in section 14.3.5 I demonstrated that the nuclear translocation of this receptor is significantly inhibited in Atg7-deficient cells[135,359]. Therefore, autophagy may promote resistance to therapies by facilitating EGFR trafficking to the nucleus. Alternatively, I found that the influence of Atg7 loss on signalling and wild-type EGFR trafficking can be overridden by the presence of the constitutively active EGFRvIII mutant which is found in approximately 23% of GBM cases[251]. This variant is also known to support the nuclear functions of EGFR[347,439]. Therefore any potential influence of autophagy on the signalling or nuclear translocation of EGFR would be overcome in cells expressing this mutant receptor. This result argues for the need for a personalised approach when targeting autophagy in GBM, as it may not be efficacious in patients with EGFRvIII mutation.

15.3.2 Targeting Autophagy as a Broad-Range RTK Inhibitor in GBM

How might we go about targeting autophagy in GBM? And what factors would need to be considered in light of the results gleaned here?

One of the major considerations for any GBM therapeutic is the low permeability of the blood-brain barrier and the difficulty in penetrating completely through the tumour mass. Therefore, producing an efficacious concentration of an autophagy inhibitor in GBM tumours would require a potent and specific compound. Currently, the only clinically available inhibitors of autophagy are not specific to autophagy and have not been able to achieve high enough concentrations to properly inhibit the pathway in patients[288]. More specific compounds are in high demand in a clinical as well as basic research capacity. Some interesting compounds are starting to be developed in this regard, such as the ATG4B inhibitor NSC185058 which was used to target autophagy in combination with radiotherapy treatment in a GBM model[40]. However, further work is required to develop such compounds and provide options for trials in patients.

In the meantime, of the genetic tools available to specifically target the autophagy pathway shRNA is likely to be the best representation of the situation in tumours, where there is unlikely to be a complete loss of protein function upon the application of an inhibitor. Therefore, although a quick and useful tool in the laboratory,

CRISRP/Cas9-mediated knockout may not be an accurate prediction of the effect of an autophagy inhibitor. Additionally, shRNAs in the RCAS/*tv-a* mouse model were constitutively expressed to a high level to achieve a very effective knockdown of autophagy gene expression, and so also be not be a good representation of a therapeutic agent. However, rapid advancements in the CRISPR/Cas9 field are raising the possibility of utilising this tool in the clinic[440,441]. If this technique can be developed in GBM, the direct targeting of autophagy players could be achieved. However, unlike acute treatment with a selective chemical inhibitor, the delivery of these agents would have to be targeted to tumour cells as studies in mice have shown that the systemic irreversible loss of autophagy causes a multitude of issues, including neurodegeneration and susceptibility to infection[6,200].

The results gleaned here also highlight a potential pitfall in targeting autophagy to simultaneously inhibit a variety of RTKs. Although several RTKs, such as EGFR and c-Met, are reliant on autophagy to achieve maximal signalling, others are not, such as IGF-1R and EGFRvIII. Therefore, as has been documented previously for targeted RTK inhibitors, a compensatory upregulation of non-inhibited receptors might make an autophagy inhibitor ineffectual as a treatement due to being prone to resistance and relapse[442,443]. However, a therapeutic window to increase patient survival may exist for those with tumours addicted to signalling from an RTK that is modulated by autophagy, thereby providing an opportunity to employ a personalised medicine approach.

Furthermore, a number of reports are coming through that autophagy proteins can actively participate in cellular processes independently of their canonical function in the autophagy as a catabolic pathway. This includes regulating mitochondrial function, endocytic trafficking, and supporting RTK signalling, as also described here[146,170,173,444]. Therefore, even inhibition a single autophagy player to inhibit autophagy might be complicated by its role in an additional process.

15.4 Conclusion and Graphical Abstract

As a whole, the results of these studies highlight autophagy as an exciting therapeutic target in GBM. Initial experiments showed that this pathway is critical for tumour formation in a mouse model of GBM due to its ability to maintain pro-growth signalling pathway activity and inhibit senescence. Further work demonstrated that autophagy supports signalling and cell survival during anchorage loss, a key feature of oncogenic transformation. Finally, work focussing on EGFR has demonstrated that autophagy is able to directly regulate homeostasis of the endocytic system. This promotes efficient EGFR recycling to the plasma membrane to consequentially maintain maximal signalling and cell survival.

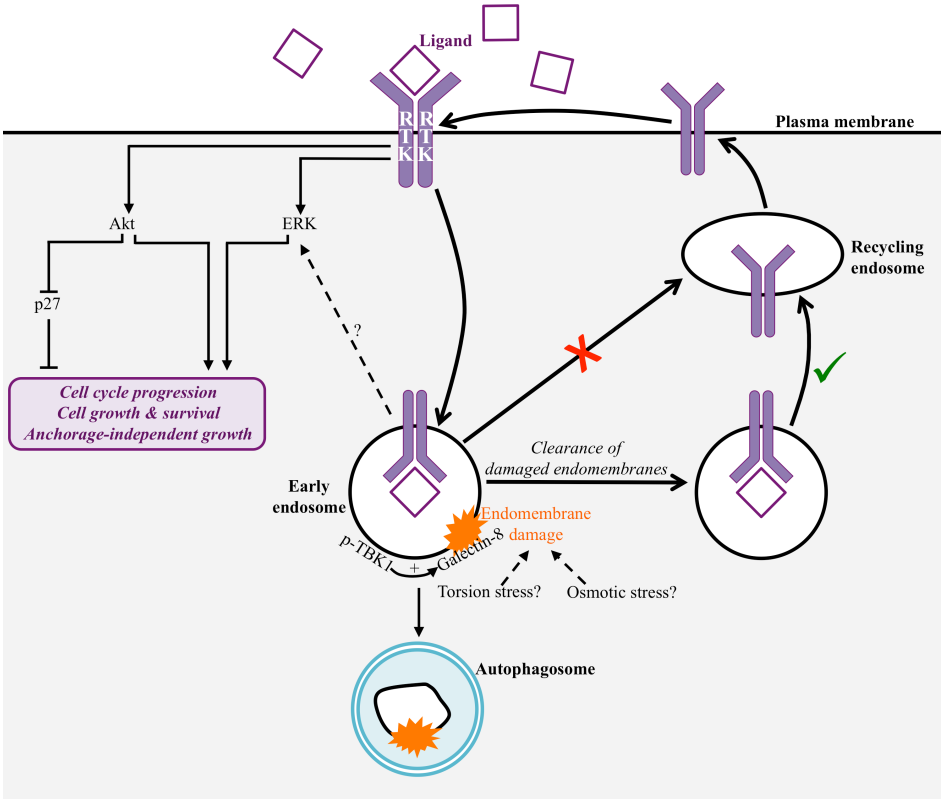

Figure 15.1 Graphical Abstract
Early endosomal membrane damage is recognised by galectin-8 and p-TBK1. Removal of such damage is important for the early-to-recycling endosome switch to mediate the recycling of RTKs, such as EGFR. This facilitates their downstream signalling to PI3K/Akt and ERK/MAPK pathways that promote cell growth, survival, and anchorage-independent growth, whilst suppressing senescence.

16 Bibliography

1. De Duve, C. The lysosome. *Sci. Am.* **208,** 64–72 (1963).
2. Cuervo, A. M. & Wong, E. Chaperone-mediated autophagy: roles in disease and aging. *Cell Res.* **24,** 92–104 (2014).
3. Li, W., Li, J. & Bao, J. Microautophagy: lesser-known self-eating. *Cell. Mol. Life Sci.* **69,** 1125–1136 (2012).
4. Kuma, A. *et al.* The role of autophagy during the early neonatal starvation period. *Nature* **432,** 1032–1036 (2004).
5. Menzies, F. M., Fleming, A. & Rubinsztein, D. C. Compromised autophagy and neurodegenerative diseases. *Nat. Rev. Neurosci.* **16,** 345–357 (2015).
6. Hara, T. *et al.* Suppression of basal autophagy in neural cells causes neurodegenerative disease in mice. *Nature* **441,** 885–889 (2006).
7. White, E. & DiPaola, R. S. The Double-Edged Sword of Autophagy Modulation in Cancer. *Clin. Cancer Res.* **15,** 5308–5316 (2009).
8. Tsukada, M. & Ohsumi, Y. Isolation and characterization of autophagy-defective mutants of *Saccharomyces cerevisiae*. *FEBS Lett.* **333,** 169–174 (1993).
9. Takeshige, K. Autophagy in yeast demonstrated with proteinase-deficient mutants and conditions for its induction. *J. Cell Biol.* **119,** 301–311 (1992).
10. Tooze, S. A. & Dikic, I. Autophagy Captures the Nobel Prize. *Cell* **167,** 1433–1435 (2016).
11. Klionsky, D. J. *et al.* Guidelines for the use and interpretation of assays for monitoring autophagy (3rd edition). *Autophagy* **12,** 1–222 (2016).
12. Biazik, J., Ylä-Anttila, P., Vihinen, H., Jokitalo, E. & Eskelinen, E.-L. Ultrastructural relationship of the phagophore with surrounding organelles. *Autophagy* **11,** 439–451 (2015).
13. Axe, E. L. *et al.* Autophagosome formation from membrane compartments enriched in phosphatidylinositol 3-phosphate and dynamically connected to the endoplasmic reticulum. *J. Cell Biol.* **182,** 685–701 (2008).
14. Sabatini, D. M. Twenty-five years of mTOR: Uncovering the link from nutrients to growth. *Proc. Natl. Acad. Sci. U. S. A.* **114,** 11818–11825 (2017).
15. Zoncu, R. *et al.* mTORC1 Senses Lysosomal Amino Acids Through an Inside-Out Mechanism That Requires the Vacuolar H+-ATPase. *Science* **334,** 678–683 (2011).
16. Hosokawa, N. *et al.* Nutrient-dependent mTORC1 Association with the ULK1-Atg13-FIP200 Complex Required for Autophagy. *Mol. Biol. Cell* **20,** 1981–1991 (2009).
17. Lee, E.-J. & Tournier, C. The requirement of uncoordinated 51-like kinase 1 (ULK1) and ULK2 in the regulation of autophagy. *Autophagy* **7,** 689–695 (2011).
18. Ganley, I. G. *et al.* ULK1.ATG13.FIP200 complex mediates mTOR signaling and is essential for autophagy. *J. Biol. Chem.* **284,** 12297–12305 (2009).
19. Jung, C. H. *et al.* ULK-Atg13-FIP200 complexes mediate mTOR signaling to the autophagy machinery. *Mol. Biol. Cell* **20,** 1992–2003 (2009).
20. Garami, A. *et al.* Insulin Activation of Rheb, a Mediator of mTOR/S6K/4E-BP Signaling, Is Inhibited by TSC1 and 2. *Mol. Cell* **11,** 1457–1466 (2003).
21. Long, X., Lin, Y., Ortiz-Vega, S., Yonezawa, K. & Avruch, J. Rheb Binds and Regulates the mTOR Kinase. *Curr. Biol.* **15,** 702–713 (2005).

22. Sancak, Y. *et al.* Ragulator-Rag Complex Targets mTORC1 to the Lysosomal Surface and Is Necessary for Its Activation by Amino Acids. *Cell* **141,** 290–303 (2010).
23. Manifava, M. *et al.* Dynamics of mTORC1 activation in response to amino acids. *eLife* **5,** (2016).
24. Longatti, A. *et al.* TBC1D14 regulates autophagosome formation via Rab11- and ULK1-positive recycling endosomes. *J. Cell Biol.* **197,** 659–675 (2012).
25. Itakura, E., Kishi, C., Inoue, K. & Mizushima, N. Beclin 1 forms two distinct phosphatidylinositol 3-kinase complexes with mammalian Atg14 and UVRAG. *Mol. Biol. Cell* **19,** 5360–5372 (2008).
26. Hamasaki, M. *et al.* Autophagosomes form at ER–mitochondria contact sites. *Nature* **495,** 389–393 (2013).
27. Matsunaga, K. *et al.* Autophagy requires endoplasmic reticulum targeting of the PI3-kinase complex via Atg14L. *J. Cell Biol.* **190,** 511–521 (2010).
28. Rostislavleva, K. *et al.* Structure and flexibility of the endosomal Vps34 complex reveals the basis of its function on membranes. *Science* **350,** aac7365–aac7365 (2015).
29. Polson, H. E. J. *et al.* Mammalian Atg18 (WIPI2) localizes to omegasome-anchored phagophores and positively regulates LC3 lipidation. *Autophagy* **6,** 506–522 (2010).
30. Nascimbeni, A. C., Codogno, P. & Morel, E. *Autophagy* 1–11 (2017). doi:10.1080/15548627.2017.1341465
31. Puri, C., Renna, M., Bento, C. F., Moreau, K. & Rubinsztein, D. C. Diverse autophagosome membrane sources coalesce in recycling endosomes. *Cell* **154,** 1285–1299 (2013).
32. Lamb, C. A., Yoshimori, T. & Tooze, S. A. The autophagosome: origins unknown, biogenesis complex. *Nat. Rev. Mol. Cell Biol.* **14,** 759–774 (2013).
33. Wei, Y. *et al.* EGFR-mediated Beclin 1 phosphorylation in autophagy suppression, tumor progression, and tumor chemoresistance. *Cell* **154,** 1269–1284 (2013).
34. Kabeya, Y. LC3, a mammalian homologue of yeast Apg8p, is localized in autophagosome membranes after processing. *EMBO J.* **19,** 5720–5728 (2000).
35. Li, M. *et al.* Kinetics Comparisons of Mammalian Atg4 Homologues Indicate Selective Preferences toward Diverse Atg8 Substrates. *J. Biol. Chem.* **286,** 7327–7338 (2011).
36. Nakatogawa, H., Ishii, J., Asai, E. & Ohsumi, Y. Atg4 recycles inappropriately lipidated Atg8 to promote autophagosome biogenesis. *Autophagy* **8,** 177–186 (2012).
37. Fujita, N. *et al.* An Atg4B Mutant Hampers the Lipidation of LC3 Paralogues and Causes Defects in Autophagosome Closure. *Mol. Biol. Cell* **19,** 4651–4659 (2008).
38. Scherz-Shouval, R. *et al.* Reactive oxygen species are essential for autophagy and specifically regulate the activity of Atg4. *EMBO J.* **26,** 1749–1760 (2007).
39. Pérez-Pérez, M. E., Zaffagnini, M., Marchand, C. H., Crespo, J. L. & Lemaire, S. D. The yeast autophagy protease Atg4 is regulated by thioredoxin. *Autophagy* **10,** 1953–1964 (2014).
40. Huang, T. *et al.* MST4 Phosphorylation of ATG4B Regulates Autophagic Activity, Tumorigenicity, and Radioresistance in Glioblastoma. *Cancer Cell* **32,** 840-855.e8 (2017).

41. Gammoh, N., Florey, O., Overholtzer, M. & Jiang, X. Interaction between FIP200 and ATG16L1 distinguishes ULK1 complex–dependent and –independent autophagy. *Nat. Struct. Mol. Biol.* **20,** 144–149 (2012).
42. Nath, S. *et al.* Lipidation of the LC3/GABARAP family of autophagy proteins relies on a membrane-curvature-sensing domain in Atg3. *Nat. Cell Biol.* **16,** 415–424 (2014).
43. Hanada, T. *et al.* The Atg12-Atg5 Conjugate Has a Novel E3-like Activity for Protein Lipidation in Autophagy. *J. Biol. Chem.* **282,** 37298–37302 (2007).
44. Ravikumar, B., Moreau, K., Jahreiss, L., Puri, C. & Rubinsztein, D. C. Plasma membrane contributes to the formation of pre-autophagosomal structures. *Nat. Cell Biol.* **12,** 747–757 (2010).
45. Itakura, E., Kishi-Itakura, C. & Mizushima, N. The Hairpin-type Tail-Anchored SNARE Syntaxin 17 Targets to Autophagosomes for Fusion with Endosomes/Lysosomes. *Cell* **151,** 1256–1269 (2012).
46. Webb, J. L., Ravikumar, B. & Rubinsztein, D. C. Microtubule disruption inhibits autophagosome-lysosome fusion: implications for studying the roles of aggresomes in polyglutamine diseases. *Int. J. Biochem. Cell Biol.* **36,** 2541–2550 (2004).
47. Gao, J., Langemeyer, L., Kuemmel, D., Reggiori, F. & Ungermann, C. Molecular mechanism to target the endosomal Mon1-Ccz1 GEF complex to the pre-autophagosomal structure. *eLife* **7,** (2018).
48. Reggiori, F. & Ungermann, C. Autophagosome Maturation and Fusion. *J. Mol. Biol.* **429,** 486–496 (2017).
49. McEwan, D. G. *et al.* PLEKHM1 Regulates Autophagosome-Lysosome Fusion through HOPS Complex and LC3/GABARAP Proteins. *Mol. Cell* **57,** 39–54 (2015).
50. Liu, R., Zhi, X. & Zhong, Q. ATG14 controls SNARE-mediated autophagosome fusion with a lysosome. *Autophagy* **11,** 847–849 (2015).
51. Tan, X., Thapa, N., Liao, Y., Choi, S. & Anderson, R. A. PtdIns(4,5)P2 signaling regulates ATG14 and autophagy. *Proc. Natl. Acad. Sci.* **113,** 10896–10901 (2016).
52. Tsuboyama, K. *et al.* The ATG conjugation systems are important for degradation of the inner autophagosomal membrane. *Science* **354,** 1036–1041 (2016).
53. Yoshimori, T. Autophagy: a regulated bulk degradation process inside cells. *Biochem. Biophys. Res. Commun.* **313,** 453–458 (2004).
54. Mostowy, S. *et al.* p62 and NDP52 Proteins Target Intracytosolic *Shigella* and *Listeria* to Different Autophagy Pathways. *J. Biol. Chem.* **286,** 26987–26995 (2011).
55. Geisler, S. *et al.* PINK1/Parkin-mediated mitophagy is dependent on VDAC1 and p62/SQSTM1. *Nat. Cell Biol.* **12,** 119–131 (2010).
56. Wild, P. *et al.* Phosphorylation of the Autophagy Receptor Optineurin Restricts Salmonella Growth. *Science* **333,** 228–233 (2011).
57. Dupont, N. *et al.* Shigella Phagocytic Vacuolar Membrane Remnants Participate in the Cellular Response to Pathogen Invasion and Are Regulated by Autophagy. *Cell Host Microbe* **6,** 137–149 (2009).
58. Thurston, T. L. M., Wandel, M. P., von Muhlinen, N., Foeglein, Á. & Randow, F. Galectin 8 targets damaged vesicles for autophagy to defend cells against bacterial invasion. *Nature* **482,** 414–418 (2012).
59. von Muhlinen, N. *et al.* LC3C, bound selectively by a noncanonical LIR motif in NDP52, is required for antibacterial autophagy. *Mol. Cell* **48,** 329–342 (2012).

60. Kim, I., Rodriguez-Enriquez, S. & Lemasters, J. J. Selective degradation of mitochondria by mitophagy. *Arch. Biochem. Biophys.* **462,** 245–253 (2007).
61. Heo, J.-M., Ordureau, A., Paulo, J. A., Rinehart, J. & Harper, J. W. The PINK1-PARKIN Mitochondrial Ubiquitylation Pathway Drives a Program of OPTN/NDP52 Recruitment and TBK1 Activation to Promote Mitophagy. *Mol. Cell* **60,** 7–20 (2015).
62. Lücking, C. B. *et al.* Association between Early-Onset Parkinson's Disease and Mutations in the *Parkin* Gene. *N. Engl. J. Med.* **342,** 1560–1567 (2000).
63. Aits, S. & Jaattela, M. Lysosomal cell death at a glance. *J. Cell Sci.* **126,** 1905–1912 (2013).
64. Hung, Y.-H., Chen, L. M.-W., Yang, J.-Y. & Yang, W. Y. Spatiotemporally controlled induction of autophagy-mediated lysosome turnover. *Nat. Commun.* **4,** 2111 (2013).
65. Maejima, I. *et al.* Autophagy sequesters damaged lysosomes to control lysosomal biogenesis and kidney injury. *EMBO J.* **32,** 2336–2347 (2013).
66. Radulovic, M. *et al.* ESCRT-mediated lysosome repair precedes lysophagy and promotes cell survival. (2018). doi:10.1101/313866
67. Wyant, G. A. *et al.* NUFIP1 is a ribosome receptor for starvation-induced ribophagy. *Science* eaar2663 (2018). doi:10.1126/science.aar2663
68. Grumati, P. *et al.* Full length RTN3 regulates turnover of tubular endoplasmic reticulum via selective autophagy. *eLife* **6,** (2017).
69. Smith, M. D. *et al.* CCPG1 Is a Non-canonical Autophagy Cargo Receptor Essential for ER-Phagy and Pancreatic ER Proteostasis. *Dev. Cell* (2017). doi:10.1016/j.devcel.2017.11.024
70. Khaminets, A. *et al.* Regulation of endoplasmic reticulum turnover by selective autophagy. *Nature* **522,** 354–358 (2015).
71. Sandilands, E. *et al.* Autophagic targeting of Src promotes cancer cell survival following reduced FAK signalling. *Nat. Cell Biol.* **14,** 51–60 (2011).
72. Taguchi, K. *et al.* Keap1 degradation by autophagy for the maintenance of redox homeostasis. *Proc. Natl. Acad. Sci.* **109,** 13561–13566 (2012).
73. Harris, J. *et al.* Autophagy Controls IL-1β Secretion by Targeting Pro-IL-1β for Degradation. *J. Biol. Chem.* **286,** 9587–9597 (2011).
74. Xu, S.-W. *et al.* Autophagic degradation of epidermal growth factor receptor in gefitinib-resistant lung cancer by celastrol. *Int. J. Oncol.* **49,** 1576–1588 (2016).
75. Cossart, P. & Helenius, A. Endocytosis of viruses and bacteria. *Cold Spring Harb. Perspect. Biol.* **6,** (2014).
76. Foley, K., Boguslavsky, S. & Klip, A. Endocytosis, recycling, and regulated exocytosis of glucose transporter 4. *Biochemistry (Mosc.)* **50,** 3048–3061 (2011).
77. Lemmon, M. A. & Schlessinger, J. Cell signaling by receptor tyrosine kinases. *Cell* **141,** 1117–1134 (2010).
78. Sigismund, S. *et al.* Clathrin-mediated internalization is essential for sustained EGFR signaling but dispensable for degradation. *Dev. Cell* **15,** 209–219 (2008).
79. Ford, M. G. J. *et al.* Curvature of clathrin-coated pits driven by epsin. *Nature* **419,** 361–366 (2002).
80. Lundmark, R. & Carlsson, S. R. Driving membrane curvature in clathrin-dependent and clathrin-independent endocytosis. *Semin. Cell Dev. Biol.* **21,** 363–370 (2010).
81. Zhu, G. *et al.* Structure of the APPL1 BAR-PH domain and characterization of its interaction with Rab5. *EMBO J.* **26,** 3484–3493 (2007).

82. Zoncu, R. *et al.* A Phosphoinositide Switch Controls the Maturation and Signaling Properties of APPL Endosomes. *Cell* **136,** 1110–1121 (2009).
83. Simonsen, A. *et al.* EEA1 links PI(3)K function to Rab5 regulation of endosome fusion. *Nature* **394,** 494–498 (1998).
84. Worby, C. A. & Dixon, J. E. Sorting out the cellular functions of sorting nexins. *Nat. Rev. Mol. Cell Biol.* **3,** 919–931 (2002).
85. Schink, K. O., Tan, K.-W. & Stenmark, H. Phosphoinositides in Control of Membrane Dynamics. *Annu. Rev. Cell Dev. Biol.* **32,** 143–171 (2016).
86. Vanlandingham, P. A. & Ceresa, B. P. Rab7 Regulates Late Endocytic Trafficking Downstream of Multivesicular Body Biogenesis and Cargo Sequestration. *J. Biol. Chem.* **284,** 12110–12124 (2009).
87. Rink, J., Ghigo, E., Kalaidzidis, Y. & Zerial, M. Rab Conversion as a Mechanism of Progression from Early to Late Endosomes. *Cell* **122,** 735–749 (2005).
88. Jefferies, H. B. J. *et al.* A selective PIKfyve inhibitor blocks PtdIns(3,5)P2 production and disrupts endomembrane transport and retroviral budding. *EMBO Rep.* **9,** 164–170 (2008).
89. Ikonomov, O. C., Sbrissa, D. & Shisheva, A. Mammalian Cell Morphology and Endocytic Membrane Homeostasis Require Enzymatically Active Phosphoinositide 5-Kinase PIKfyve. *J. Biol. Chem.* **276,** 26141–26147 (2001).
90. Futter, C. E. Multivesicular endosomes containing internalized EGF-EGF receptor complexes mature and then fuse directly with lysosomes. *J. Cell Biol.* **132,** 1011–1023 (1996).
91. Katzmann, D. J., Stefan, C. J., Babst, M. & Emr, S. D. Vps27 recruits ESCRT machinery to endosomes during MVB sorting. *J. Cell Biol.* **162,** 413–423 (2003).
92. Williams, R. L. & Urbé, S. The emerging shape of the ESCRT machinery. *Nat. Rev. Mol. Cell Biol.* **8,** 355–368 (2007).
93. Marat, A. L. & Haucke, V. Phosphatidylinositol 3-phosphates-at the interface between cell signalling and membrane traffic. *EMBO J.* **35,** 561–579 (2016).
94. De Duve, C. & Wattiaux, R. Functions of lysosomes. *Annu. Rev. Physiol.* **28,** 435–492 (1966).
95. Forgac, M. Structure and Properties of the Vacuolar H+ ATPases. *J. Biol. Chem.* **274,** 12951–12954 (1999).
96. Eskelinen, E.-L. Roles of LAMP-1 and LAMP-2 in lysosome biogenesis and autophagy. *Mol. Aspects Med.* **27,** 495–502 (2006).
97. Ullrich, O. Rab11 regulates recycling through the pericentriolar recycling endosome. *J. Cell Biol.* **135,** 913–924 (1996).
98. Chen, W., Feng, Y., Chen, D. & Wandinger-Ness, A. Rab11 Is Required for Trans-Golgi Network-to-Plasma Membrane Transport and a Preferential Target for GDP Dissociation Inhibitor. *Mol. Biol. Cell* **9,** 3241–3257 (1998).
99. Ferguson, S. M. & De Camilli, P. Dynamin, a membrane-remodelling GTPase. *Nat. Rev. Mol. Cell Biol.* **13,** 75–88 (2012).
100. van Dam, E. M. Dynamin-dependent Transferrin Receptor Recycling by Endosome-derived Clathrin-coated Vesicles. *Mol. Biol. Cell* **13,** 169–182 (2002).
101. Henmi, Y. *et al.* PtdIns4KII generates endosomal PtdIns(4)P and is required for receptor sorting at early endosomes. *Mol. Biol. Cell* **27,** 990–1001 (2016).
102. Ketel, K. *et al.* A phosphoinositide conversion mechanism for exit from endosomes. *Nature* **529,** 408–412 (2016).

103. Seaman, M. N. J. Cargo-selective endosomal sorting for retrieval to the Golgi requires retromer. *J. Cell Biol.* **165,** 111–122 (2004).
104. Small, S. A. & Petsko, G. A. Retromer in Alzheimer disease, Parkinson disease and other neurological disorders. *Nat. Rev. Neurosci.* **16,** 126 (2015).
105. Burda, P. Retromer function in endosome-to-Golgi retrograde transport is regulated by the yeast Vps34 PtdIns 3-kinase. *J. Cell Sci.* **115,** 3889–3900 (2002).
106. Arighi, C. N., Hartnell, L. M., Aguilar, R. C., Haft, C. R. & Bonifacino, J. S. Role of the mammalian retromer in sorting of the cation-independent mannose 6-phosphate receptor. *J. Cell Biol.* **165,** 123–133 (2004).
107. Lo, H.-W. *et al.* Nuclear-cytoplasmic transport of EGFR involves receptor endocytosis, importin β1 and CRM1. *J. Cell. Biochem.* **98,** 1570–1583 (2006).
108. Chaumet, A. *et al.* Nuclear envelope-associated endosomes deliver surface proteins to the nucleus. *Nat. Commun.* **6,** (2015).
109. Chen, M.-K. & Hung, M.-C. Proteolytic cleavage, trafficking, and functions of nuclear receptor tyrosine kinases. *FEBS J.* **282,** 3693–3721 (2015).
110. Downward, J., Parker, P. & Waterfield, M. D. Autophosphorylation sites on the epidermal growth factor receptor. *Nature* **311,** 483–485 (1984).
111. Eck, M. J., Dhe-Paganon, S., Trüb, T., Nolte, R. T. & Shoelson, S. E. Structure of the IRS-1 PTB Domain Bound to the Juxtamembrane Region of the Insulin Receptor. *Cell* **85,** 695–705 (1996).
112. Vainshtein, I., Kovacina, K. S. & Roth, R. A. The insulin receptor substrate (IRS)-1 pleckstrin homology domain functions in downstream signaling. *J. Biol. Chem.* **276,** 8073–8078 (2001).
113. Skolnik, E. Y. *et al.* The SH2/SH3 domain-containing protein GRB2 interacts with tyrosine-phosphorylated IRS1 and Shc: implications for insulin control of ras signalling. *EMBO J.* **12,** 1929–1936 (1993).
114. Bae, Y. S. *et al.* Epidermal Growth Factor (EGF)-induced Generation of Hydrogen Peroxide: ROLE IN EGF RECEPTOR-MEDIATED TYROSINE PHOSPHORYLATION. *J. Biol. Chem.* **272,** 217–221 (1997).
115. Lee, S.-R., Kwon, K.-S., Kim, S.-R. & Rhee, S. G. Reversible Inactivation of Protein-tyrosine Phosphatase 1B in A431 Cells Stimulated with Epidermal Growth Factor. *J. Biol. Chem.* **273,** 15366–15372 (1998).
116. Haj, F. G. Imaging Sites of Receptor Dephosphorylation by PTP1B on the Surface of the Endoplasmic Reticulum. *Science* **295,** 1708–1711 (2002).
117. Haglund, K. *et al.* Multiple monoubiquitination of RTKs is sufficient for their endocytosis and degradation. *Nat. Cell Biol.* **5,** 461–466 (2003).
118. Huang, F., Kirkpatrick, D., Jiang, X., Gygi, S. & Sorkin, A. Differential Regulation of EGF Receptor Internalization and Degradation by Multiubiquitination within the Kinase Domain. *Mol. Cell* **21,** 737–748 (2006).
119. Sigismund, S. *et al.* Threshold-controlled ubiquitination of the EGFR directs receptor fate. *EMBO J.* **32,** 2140–2157 (2013).
120. Alessi, D. R. *et al.* Characterization of a 3-phosphoinositide-dependent protein kinase which phosphorylates and activates protein kinase Bα. *Curr. Biol.* **7,** 261–269 (1997).
121. Hresko, R. C. & Mueckler, M. mTOR·RICTOR Is the Ser 473 Kinase for Akt/Protein Kinase B in 3T3-L1 Adipocytes. *J. Biol. Chem.* **280,** 40406–40416 (2005).

122. Sarbassov, D. D., Guertin, D. A., Ali, S. M. & Sabatini, D. M. Phosphorylation and Regulation of Akt/PKB by the Rictor-mTOR Complex. *Science* **307,** 1098 (2005).
123. Sarbassov, D. D. *et al.* Prolonged Rapamycin Treatment Inhibits mTORC2 Assembly and Akt/PKB. *Mol. Cell* **22,** 159–168 (2006).
124. Inoki, K., Li, Y., Zhu, T., Wu, J. & Guan, K.-L. TSC2 is phosphorylated and inhibited by Akt and suppresses mTOR signalling. *Nat. Cell Biol.* **4,** 648–657 (2002).
125. Downward, J. Targeting RAS signalling pathways in cancer therapy. *Nat. Rev. Cancer* **3,** 11–22 (2003).
126. Hancock, J. F., Magee, A. I., Childs, J. E. & Marshall, C. J. All ras proteins are polyisoprenylated but only some are palmitoylated. *Cell* **57,** 1167–1177 (1989).
127. Kim, E. K. & Choi, E.-J. Pathological roles of MAPK signaling pathways in human diseases. *Biochim. Biophys. Acta BBA - Mol. Basis Dis.* **1802,** 396–405 (2010).
128. Rodriguez-Viciana, P. *et al.* Phosphatidylinositol-3-OH kinase direct target of Ras. *Nature* **370,** 527–532 (1994).
129. Roepstorff, K. *et al.* Differential Effects of EGFR Ligands on Endocytic Sorting of the Receptor. *Traffic* **10,** 1115–1127 (2009).
130. Sorkin, A. & von Zastrow, M. Signal transduction and endocytosis: close encounters of many kinds. *Nat. Rev. Mol. Cell Biol.* **3,** 600–614 (2002).
131. Wang, Y., Pennock, S., Chen, X. & Wang, Z. Endosomal Signaling of Epidermal Growth Factor Receptor Stimulates Signal Transduction Pathways Leading to Cell Survival. *Mol. Cell. Biol.* **22,** 7279–7290 (2002).
132. Garay, C. *et al.* Epidermal growth factor-stimulated Akt phosphorylation requires clathrin or ErbB2 but not receptor endocytosis. *Mol. Biol. Cell* **26,** 3504–3519 (2015).
133. Gao, X. *et al.* PI3K/Akt signaling requires spatial compartmentalization in plasma membrane microdomains. *Proc. Natl. Acad. Sci.* **108,** 14509–14514 (2011).
134. Schenck, A. *et al.* The Endosomal Protein Appl1 Mediates Akt Substrate Specificity and Cell Survival in Vertebrate Development. *Cell* **133,** 486–497 (2008).
135. Brand, T. M. *et al.* Nuclear EGFR as a molecular target in cancer. *Radiother. Oncol.* **108,** 370–377 (2013).
136. Liccardi, G., Hartley, J. A. & Hochhauser, D. EGFR Nuclear Translocation Modulates DNA Repair following Cisplatin and Ionizing Radiation Treatment. *Cancer Res.* **71,** 1103–1114 (2011).
137. Lin, S.-Y. *et al.* Nuclear localization of EGF receptor and its potential new role as a transcription factor. *Nat. Cell Biol.* **3,** 802–808 (2001).
138. Wang, Y.-N. *et al.* The Translocon Sec61β Localized in the Inner Nuclear Membrane Transports Membrane-embedded EGF Receptor to the Nucleus. *J. Biol. Chem.* **285,** 38720–38729 (2010).
139. Du, Y. *et al.* Syntaxin 6-mediated Golgi translocation plays an important role in nuclear functions of EGFR through microtubule-dependent trafficking. *Oncogene* **33,** 756–770 (2014).
140. Wang, Y.-N. *et al.* COPI-mediated retrograde trafficking from the Golgi to the ER regulates EGFR nuclear transport. *Biochem. Biophys. Res. Commun.* **399,** 498–504 (2010).

141. Wang, Y.-N. *et al.* Membrane-bound Trafficking Regulates Nuclear Transport of Integral Epidermal Growth Factor Receptor (EGFR) and ErbB-2. *J. Biol. Chem.* **287,** 16869–16879 (2012).
142. Young, A. R. J. *et al.* Starvation and ULK1-dependent cycling of mammalian Atg9 between the TGN and endosomes. *J. Cell Sci.* **119,** 3888–3900 (2006).
143. Yamamoto, H. *et al.* Atg9 vesicles are an important membrane source during early steps of autophagosome formation. *J. Cell Biol.* **198,** 219–233 (2012).
144. Popovic, D. & Dikic, I. TBC1D5 and the AP2 complex regulate ATG9 trafficking and initiation of autophagy. *EMBO Rep.* **15,** 392–401 (2014).
145. Zhou, C. *et al.* Regulation of mATG9 trafficking by Src- and ULK1-mediated phosphorylation in basal and starvation-induced autophagy. *Cell Res.* **27,** 184–201 (2017).
146. He, S. *et al.* PtdIns(3)P-bound UVRAG coordinates Golgi–ER retrograde and Atg9 transport by differential interactions with the ER tether and the beclin 1 complex. *Nat. Cell Biol.* **15,** 1206–1219 (2013).
147. Søreng, K. *et al.* SNX18 regulates ATG9A trafficking from recycling endosomes by recruiting Dynamin-2. *EMBO Rep.* e44837 (2018). doi:10.15252/embr.201744837
148. Popovic, D. *et al.* Rab GTPase-activating proteins in autophagy: regulation of endocytic and autophagy pathways by direct binding to human ATG8 modifiers. *Mol. Cell. Biol.* **32,** 1733–1744 (2012).
149. Itoh, T., Kanno, E., Uemura, T., Waguri, S. & Fukuda, M. OATL1, a novel autophagosome-resident Rab33B-GAP, regulates autophagosomal maturation. *J. Cell Biol.* **192,** 839–853 (2011).
150. Carroll, B. *et al.* The TBC/RabGAP Armus Coordinates Rac1 and Rab7 Functions during Autophagy. *Dev. Cell* **25,** 15–28 (2013).
151. Roy, S., Leidal, A. M., Ye, J., Ronen, S. M. & Debnath, J. Autophagy-Dependent Shuttling of TBC1D5 Controls Plasma Membrane Translocation of GLUT1 and Glucose Uptake. *Mol. Cell* **67,** 84-95.e5 (2017).
152. Knævelsrud, H. *et al.* Membrane remodeling by the PX-BAR protein SNX18 promotes autophagosome formation. *J. Cell Biol.* **202,** 331–349 (2013).
153. Puri, C. *et al.* The RAB11A-Positive Compartment Is a Primary Platform for Autophagosome Assembly Mediated by WIPI2 Recognition of PI3P-RAB11A. *Dev. Cell* **45,** 114-131.e8 (2018).
154. Li, J., Chen, Z., Stang, M. T. & Gao, W. Transiently expressed ATG16L1 inhibits autophagosome biogenesis and aberrantly targets RAB11-positive recycling endosomes. *Autophagy* **13,** 345–358 (2017).
155. Morozova, K. *et al.* Annexin A2 promotes phagophore assembly by enhancing Atg16L+ vesicle biogenesis and homotypic fusion. *Nat. Commun.* **6,** (2015).
156. Wei, Y. *et al.* EGFR-Mediated Beclin 1 Phosphorylation in Autophagy Suppression, Tumor Progression, and Tumor Chemoresistance. *Cell* **154,** 1269–1284 (2013).
157. Chukkapalli, S. *et al.* Role of the EphB2 receptor in autophagy, apoptosis and invasion in human breast cancer cells. *Exp. Cell Res.* **320,** 233–246 (2014).
158. Kandouz, M., Haidara, K., Zhao, J., Brisson, M.-L. & Batist, G. The EphB2 tumor suppressor induces autophagic cell death via concomitant activation of the ERK1/2 and PI3K pathways. *Cell Cycle* **9,** 398–407 (2010).
159. Schmukler, E., Shai, B., Ehrlich, M. & Pinkas-Kramarski, R. Neuregulin Promotes Incomplete Autophagy of Prostate Cancer Cells That Is Independent of mTOR Pathway Inhibition. *PLoS ONE* **7,** e36828 (2012).

160. Hansen, K. *et al.* Autophagic cell death induced by TrkA receptor activation in human glioblastoma cells. *J. Neurochem.* **0,** 259–75 (2007).
161. Han, J. *et al.* Autophagy induced by AXL receptor tyrosine kinase alleviates acute liver injury via inhibition of NLRP3 inflammasome activation in mice. *Autophagy* **12,** 2326–2343 (2016).
162. Domigan, C. K. *et al.* Autocrine VEGF maintains endothelial survival through regulation of metabolism and autophagy. *J. Cell Sci.* **128,** 2236–2248 (2015).
163. Wang, J. *et al.* A Non-canonical MEK/ERK Signaling Pathway Regulates Autophagy via Regulating Beclin 1. *J. Biol. Chem.* **284,** 21412–21424 (2009).
164. Tan, X., Thapa, N., Sun, Y. & Anderson, R. A. A kinase-independent role for EGF receptor in autophagy initiation. *Cell* **160,** 145–160 (2015).
165. Settembre, C. *et al.* TFEB links autophagy to lysosomal biogenesis. *Science* **332,** 1429–1433 (2011).
166. Zhao, J. *et al.* FoxO3 coordinately activates protein degradation by the autophagic/lysosomal and proteasomal pathways in atrophying muscle cells. *Cell Metab.* **6,** 472–483 (2007).
167. Mammucari, C. *et al.* FoxO3 controls autophagy in skeletal muscle in vivo. *Cell Metab.* **6,** 458–471 (2007).
168. Settembre, C. *et al.* A lysosome-to-nucleus signalling mechanism senses and regulates the lysosome via mTOR and TFEB. *EMBO J.* **31,** 1095–1108 (2012).
169. You, L. *et al.* The role of STAT3 in autophagy. *Autophagy* **11,** 729–739 (2015).
170. Barrow-McGee, R. *et al.* Beta 1-integrin-c-Met cooperation reveals an inside-in survival signalling on autophagy-related endomembranes. *Nat. Commun.* **7,** 11942 (2016).
171. Lampada, A. *et al.* mTORC1-independent autophagy regulates receptor tyrosine kinase phosphorylation in colorectal cancer cells via an mTORC2-mediated mechanism. *Cell Death Differ.* **24,** 1045–1062 (2017).
172. Li, J. *et al.* Autophagy-dependent generation of Axin2+ cancer stem-like cells promotes hepatocarcinogenesis in liver cirrhosis. *Oncogene* **36,** 6725–6737 (2017).
173. Murrow, L., Malhotra, R. & Debnath, J. ATG12–ATG3 interacts with Alix to promote basal autophagic flux and late endosome function. *Nat. Cell Biol.* **17,** 300–310 (2015).
174. Martinez-Lopez, N., Athonvarangkul, D., Mishall, P., Sahu, S. & Singh, R. Autophagy proteins regulate ERK phosphorylation. *Nat. Commun.* **4,** (2013).
175. Jones, S., Cunningham, D. L., Rappoport, J. Z. & Heath, J. K. The non-receptor tyrosine kinase Ack1 regulates the fate of activated EGFR by inducing trafficking to the p62/NBR1 pre-autophagosome. *J. Cell Sci.* **127,** 994–1006 (2014).
176. Yue, X. *et al.* Mitochondrially localized EGFR is subjected to autophagic regulation and implicated in cell survival. *Autophagy* **4,** 641–649 (2008).
177. Yao, Y. *et al.* Mitochondrially localized EGFR is independent of its endocytosis and associates with cell viability. *Acta Biochim. Biophys. Sin.* **42,** 763–770 (2010).
178. Hanahan, D. & Weinberg, R. A. Hallmarks of Cancer: The Next Generation. *Cell* **144,** 646–674 (2011).
179. Liang, X. H. *et al.* Induction of autophagy and inhibition of tumorigenesis by beclin 1. *Nature* **402,** 672–676 (1999).
180. Wang, R. C. *et al.* Akt-Mediated Regulation of Autophagy and Tumorigenesis Through Beclin 1 Phosphorylation. *Science* **338,** 956–959 (2012).

181. Sun, Q., Westphal, W., Wong, K. N., Tan, I. & Zhong, Q. Rubicon controls endosome maturation as a Rab7 effector. *Proc. Natl. Acad. Sci.* **107,** 19338–19343 (2010).
182. Rohatgi, R. A. *et al.* Beclin 1 regulates growth factor receptor signaling in breast cancer. *Oncogene* **34,** 5352–5362 (2015).
183. Wei, H. *et al.* Suppression of autophagy by FIP200 deletion inhibits mammary tumorigenesis. *Genes Dev.* **25,** 1510–1527 (2011).
184. Huo, Y. *et al.* Autophagy Opposes p53-Mediated Tumor Barrier to Facilitate Tumorigenesis in a Model of PALB2-Associated Hereditary Breast Cancer. *Cancer Discov.* **3,** 894–907 (2013).
185. Strohecker, A. M. & White, E. Autophagy promotes *Braf* ^{V600E} -driven lung tumorigenesis by preserving mitochondrial metabolism. *Autophagy* **10,** 384–385 (2014).
186. Xie, X., Koh, J. Y., Price, S., White, E. & Mehnert, J. M. Atg7 Overcomes Senescence and Promotes Growth of BrafV600E-Driven Melanoma. *Cancer Discov.* **5,** 410–423 (2015).
187. Perera, R. M. *et al.* Transcriptional control of autophagy-lysosome function drives pancreatic cancer metabolism. *Nature* **524,** 361–365 (2015).
188. Galavotti, S. *et al.* The autophagy-associated factors DRAM1 and p62 regulate cell migration and invasion in glioblastoma stem cells. *Oncogene* **32,** 699–712 (2013).
189. Costa, J. R., Prak, K., Aldous, S., Gewinner, C. A. & Ketteler, R. Autophagy gene expression profiling identifies a defective microtubule-associated protein light chain 3A mutant in cancer. *Oncotarget* **7,** (2016).
190. Young, A. R. J. *et al.* Autophagy mediates the mitotic senescence transition. *Genes Dev.* **23,** 798–803 (2009).
191. Lenain, C., Gusyatiner, O., Douma, S., van den Broek, B. & Peeper, D. S. Autophagy-mediated degradation of nuclear envelope proteins during oncogene-induced senescence. *Carcinogenesis* **36,** 1263–1274 (2015).
192. Yoo, B. H. *et al.* Oncogenic RAS-induced downregulation of ATG12 is required for survival of malignant intestinal epithelial cells. *Autophagy* 1–18 (2017). doi:10.1080/15548627.2017.1370171
193. Rubinstein, A. D., Eisenstein, M., Ber, Y., Bialik, S. & Kimchi, A. The Autophagy Protein Atg12 Associates with Antiapoptotic Bcl-2 Family Members to Promote Mitochondrial Apoptosis. *Mol. Cell* **44,** 698–709 (2011).
194. Wang, Y. *et al.* Autophagic activity dictates the cellular response to oncogenic RAS. *Proc. Natl. Acad. Sci.* **109,** 13325–13330 (2012).
195. Lock, R. *et al.* Autophagy facilitates glycolysis during Ras-mediated oncogenic transformation. *Mol. Biol. Cell* **22,** 165–178 (2011).
196. Yang, S. *et al.* Pancreatic cancers require autophagy for tumor growth. *Genes Dev.* **25,** 717–729 (2011).
197. Guo, J. Y. *et al.* Activated Ras requires autophagy to maintain oxidative metabolism and tumorigenesis. *Genes Dev.* **25,** 460–470 (2011).
198. Karsli-Uzunbas, G. *et al.* Autophagy Is Required for Glucose Homeostasis and Lung Tumor Maintenance. *Cancer Discov.* **4,** 914–927 (2014).
199. Newman, A. C., Kemp, A. J., Drabsch, Y., Behrends, C. & Wilkinson, S. Autophagy acts through TRAF3 and RELB to regulate gene expression via antagonism of SMAD proteins. *Nat. Commun.* **8,** (2017).

200. Guo, J. Y. *et al.* Autophagy suppresses progression of K-ras-induced lung tumors to oncocytomas and maintains lipid homeostasis. *Genes Dev.* **27,** 1447–1461 (2013).
201. Rosenfeldt, M. T. *et al.* p53 status determines the role of autophagy in pancreatic tumour development. *Nature* **504,** 296–300 (2013).
202. Serrano, M., Lin, A. W., McCurrach, M. E., Beach, D. & Lowe, S. W. Oncogenic ras Provokes Premature Cell Senescence Associated with Accumulation of p53 and p16INK4a. *Cell* **88,** 593–602 (1997).
203. Brugarolas, J. *et al.* Radiation-induced cell cycle arrest compromised by p21 deficiency. *Nature* **377,** 552–557 (1995).
204. Alexander, K. & Hinds, P. W. Requirement for p27(KIP1) in retinoblastoma protein-mediated senescence. *Mol. Cell. Biol.* **21,** 3616–3631 (2001).
205. Ji, P. *et al.* An Rb-Skp2-p27 Pathway Mediates Acute Cell Cycle Inhibition by Rb and Is Retained in a Partial-Penetrance Rb Mutant. *Mol. Cell* **16,** 47–58 (2004).
206. Lane, D. P. Cancer. p53, guardian of the genome. *Nature* **358,** 15–16 (1992).
207. Sionov, R. V. & Haupt, Y. The cellular response to p53: the decision between life and death. *Oncogene* **18,** 6145–6157 (1999).
208. Bunz, F. Requirement for p53 and p21 to Sustain G2 Arrest After DNA Damage. *Science* **282,** 1497–1501 (1998).
209. Henley, S. A. & Dick, F. A. The retinoblastoma family of proteins and their regulatory functions in the mammalian cell division cycle. *Cell Div.* **7,** 10 (2012).
210. Weinberg, R. A. The retinoblastoma protein and cell cycle control. *Cell* **81,** 323–330 (1995).
211. Chicas, A. *et al.* Dissecting the unique role of the retinoblastoma tumor suppressor during cellular senescence. *Cancer Cell* **17,** 376–387 (2010).
212. Fujita, N., Sato, S., Katayama, K. & Tsuruo, T. Akt-dependent Phosphorylation of p27 ^{Kip1} Promotes Binding to 14-3-3 and Cytoplasmic Localization. *J. Biol. Chem.* **277,** 28706–28713 (2002).
213. Liang, J. *et al.* PKB/Akt phosphorylates p27, impairs nuclear import of p27 and opposes p27-mediated G1 arrest. *Nat. Med.* **8,** 1153–1160 (2002).
214. Shin, I. *et al.* PKB/Akt mediates cell-cycle progression by phosphorylation of p27Kip1 at threonine 157 and modulation of its cellular localization. *Nat. Med.* **8,** 1145–1152 (2002).
215. Ogawara, Y. *et al.* Akt Enhances Mdm2-mediated Ubiquitination and Degradation of p53. *J. Biol. Chem.* **277,** 21843–21850 (2002).
216. Rufini, A., Tucci, P., Celardo, I. & Melino, G. Senescence and aging: the critical roles of p53. *Oncogene* **32,** 5129–5143 (2013).
217. Lee, B. Y. *et al.* Senescence-associated β-galactosidase is lysosomal β-galactosidase. *Aging Cell* **5,** 187–195 (2006).
218. Zhang, R., Chen, W. & Adams, P. D. Molecular dissection of formation of senescence-associated heterochromatin foci. *Mol. Cell. Biol.* **27,** 2343–2358 (2007).
219. Di Micco, R. *et al.* Oncogene-induced senescence is a DNA damage response triggered by DNA hyper-replication. *Nature* **444,** 638–642 (2006).
220. Fagagna, F. d'Adda di *et al.* A DNA damage checkpoint response in telomere-initiated senescence. *Nature* **426,** 194–198 (2003).

221. Acosta, J. C. *et al.* A complex secretory program orchestrated by the inflammasome controls paracrine senescence. *Nat. Cell Biol.* **15,** 978–990 (2013).
222. Gao, W., Shen, Z., Shang, L. & Wang, X. Upregulation of human autophagy-initiation kinase ULK1 by tumor suppressor p53 contributes to DNA-damage-induced cell death. *Cell Death Differ.* **18,** 1598–1607 (2011).
223. Kang, C. *et al.* The DNA damage response induces inflammation and senescence by inhibiting autophagy of GATA4. *Science* **349,** 5612–5612 (2015).
224. Kroemer, G. & Levine, B. Autophagic cell death: the story of a misnomer. *Nat. Rev. Mol. Cell Biol.* **9,** 1004–1010 (2008).
225. White, E. Deconvoluting the context-dependent role for autophagy in cancer. *Nat. Rev. Cancer* **12,** 401–410 (2012).
226. Frisch, S. M. & Ruoslahti, E. Integrins and anoikis. *Curr. Opin. Cell Biol.* **9,** 701–706 (1997).
227. Freedman, V. Cellular tumorigenicity in nude mice: Correlation with cell growth in semi-solid medium. *Cell* **3,** 355–359 (1974).
228. Debnath, J. *et al.* The role of apoptosis in creating and maintaining luminal space within normal and oncogene-expressing mammary acini. *Cell* **111,** 29–40 (2002).
229. Reginato, M. J. *et al.* Integrins and EGFR coordinately regulate the pro-apoptotic protein Bim to prevent anoikis. *Nat. Cell Biol.* **5,** 733–740 (2003).
230. Reginato, M. J. *et al.* Bim regulation of lumen formation in cultured mammary epithelial acini is targeted by oncogenes. *Mol. Cell. Biol.* **25,** 4591–4601 (2005).
231. Jia, J. *et al.* Epithelial mesenchymal transition is required for acquisition of anoikis resistance and metastatic potential in adenoid cystic carcinoma. *PloS One* **7,** e51549 (2012).
232. Derksen, P. W. B. *et al.* Somatic inactivation of E-cadherin and p53 in mice leads to metastatic lobular mammary carcinoma through induction of anoikis resistance and angiogenesis. *Cancer Cell* **10,** 437–449 (2006).
233. Kumar, S. *et al.* A Pathway for the Control of Anoikis Sensitivity by E-Cadherin and Epithelial-to-Mesenchymal Transition. *Mol. Cell. Biol.* **31,** 4036–4051 (2011).
234. Dunn, S. E. *et al.* A dominant negative mutant of the insulin-like growth factor-I receptor inhibits the adhesion, invasion, and metastasis of breast cancer. *Cancer Res.* **58,** 3353–3361 (1998).
235. Kwon, O.-J. *et al.* Increased Notch signalling inhibits anoikis and stimulates proliferation of prostate luminal epithelial cells. *Nat. Commun.* **5,** (2014).
236. Carduner, L. *et al.* Cell cycle arrest or survival signaling through αv integrins, activation of PKC and ERK1/2 lead to anoikis resistance of ovarian cancer spheroids. *Exp. Cell Res.* **320,** 329–342 (2014).
237. Braunholz, D. *et al.* Spheroid Culture of Head and Neck Cancer Cells Reveals an Important Role of EGFR Signalling in Anchorage Independent Survival. *PLOS ONE* **11,** e0163149 (2016).
238. Yu, M. *et al.* RNA sequencing of pancreatic circulating tumour cells implicates WNT signalling in metastasis. *Nature* **487,** 510–513 (2012).
239. Schafer, Z. T. *et al.* Antioxidant and oncogene rescue of metabolic defects caused by loss of matrix attachment. *Nature* **461,** 109–113 (2009).
240. Grassian, A. R., Metallo, C. M., Coloff, J. L., Stephanopoulos, G. & Brugge, J. S. Erk regulation of pyruvate dehydrogenase flux through PDK4 modulates cell proliferation. *Genes Dev.* **25,** 1716–1733 (2011).

241. Davison, C. A. *et al.* Antioxidant enzymes mediate survival of breast cancer cells deprived of extracellular matrix. *Cancer Res.* **73,** 3704–3715 (2013).
242. Jiang, L. *et al.* Reductive carboxylation supports redox homeostasis during anchorage-independent growth. *Nature* **532,** 255–258 (2016).
243. De Luca, A. *et al.* Mitochondrial biogenesis is required for the anchorage-independent survival and propagation of stem-like cancer cells. *Oncotarget* **6,** 14777–14795 (2015).
244. Fung, C., Lock, R., Gao, S., Salas, E. & Debnath, J. Induction of autophagy during extracellular matrix detachment promotes cell survival. *Mol. Biol. Cell* **19,** 797–806 (2008).
245. Onodera, J. & Ohsumi, Y. Autophagy Is Required for Maintenance of Amino Acid Levels and Protein Synthesis under Nitrogen Starvation. *J. Biol. Chem.* **280,** 31582–31586 (2005).
246. Florey, O., Kim, S. E., Sandoval, C. P., Haynes, C. M. & Overholtzer, M. Autophagy machinery mediates macroendocytic processing and entotic cell death by targeting single membranes. *Nat. Cell Biol.* **13,** 1335–1343 (2011).
247. Overholtzer, M. & Brugge, J. S. The cell biology of cell-in-cell structures. *Nat. Rev. Mol. Cell Biol.* **9,** 796–809 (2008).
248. Krajcovic, M., Krishna, S., Akkari, L., Joyce, J. A. & Overholtzer, M. mTOR regulates phagosome and entotic vacuole fission. *Mol. Biol. Cell* **24,** 3736–3745 (2013).
249. Polley, M.-Y. C. *et al.* Conditional Probability of Survival in Patients With Newly Diagnosed Glioblastoma. *J. Clin. Oncol.* **29,** 4175–4180 (2011).
250. Tanaka, S., Louis, D. N., Curry, W. T., Batchelor, T. T. & Dietrich, J. Diagnostic and therapeutic avenues for glioblastoma: no longer a dead end? *Nat. Rev. Clin. Oncol.* **10,** 14–26 (2012).
251. Verhaak, R. G. W. *et al.* Integrated Genomic Analysis Identifies Clinically Relevant Subtypes of Glioblastoma Characterized by Abnormalities in PDGFRA, IDH1, EGFR, and NF1. *Cancer Cell* **17,** 98–110 (2010).
252. Hambardzumyan, D., Amankulor, N. M., Helmy, K. Y., Becher, O. J. & Holland, E. C. Modeling Adult Gliomas Using RCAS/t-va Technology. *Transl. Oncol.* **2,** 89–95 (2009).
253. Bao, S. *et al.* Glioma stem cells promote radioresistance by preferential activation of the DNA damage response. *Nature* **444,** 756–760 (2006).
254. Fu, J. *et al.* Glioblastoma stem cells resistant to temozolomide-induced autophagy. *Chin. Med. J. (Engl.)* **122,** 1255–1259 (2009).
255. Beier, D., Schulz, J. B. & Beier, C. P. Chemoresistance of glioblastoma cancer stem cells–much more complex than expected. *Mol Cancer* **10,** 128–139 (2011).
256. Cheng, L., Bao, S. & Rich, J. N. Potential therapeutic implications of cancer stem cells in glioblastoma. *Biochem. Pharmacol.* **80,** 654–665 (2010).
257. Clarke, J., Butowski, N. & Chang, S. Recent advances in therapy for glioblastoma. *Arch. Neurol.* **67,** 279–283 (2010).
258. van den Bent, M. J. *et al.* Randomized Phase II Trial of Erlotinib Versus Temozolomide or Carmustine in Recurrent Glioblastoma: EORTC Brain Tumor Group Study 26034. *J. Clin. Oncol.* **27,** 1268–1274 (2009).
259. Prados, M. D. *et al.* Phase II Study of Erlotinib Plus Temozolomide During and After Radiation Therapy in Patients With Newly Diagnosed Glioblastoma Multiforme or Gliosarcoma. *J. Clin. Oncol.* **27,** 579–584 (2008).

260. Wen, P. Y. Phase I/II Study of Imatinib Mesylate for Recurrent Malignant Gliomas: North American Brain Tumor Consortium Study 99-08. *Clin. Cancer Res.* **12,** 4899–4907 (2006).
261. Günes, C. & Rudolph, K. L. The Role of Telomeres in Stem Cells and Cancer. *Cell* **152,** 390–393 (2013).
262. Viale, A. *et al.* Cell-cycle restriction limits DNA damage and maintains self-renewal of leukaemia stem cells. *Nature* **457,** 51–56 (2009).
263. Roesch, A. *et al.* A Temporarily Distinct Subpopulation of Slow-Cycling Melanoma Cells Is Required for Continuous Tumor Growth. *Cell* **141,** 583–594 (2010).
264. Shay, J. W. & Bacchetti, S. A survey of telomerase activity in human cancer. *Eur. J. Cancer Oxf. Engl. 1990* **33,** 787–791 (1997).
265. Murat, A. *et al.* Stem cell–related "self-renewal" signature and high epidermal growth factor receptor expression associated with resistance to concomitant chemoradiotherapy in glioblastoma. *J. Clin. Oncol.* **26,** 3015–3024 (2008).
266. Li, Z. *et al.* Hypoxia-Inducible Factors Regulate Tumorigenic Capacity of Glioma Stem Cells. *Cancer Cell* **15,** 501–513 (2009).
267. Qin, J. *et al.* Hypoxia-inducible factor 1 alpha promotes cancer stem cells-like properties in human ovarian cancer cells by upregulating SIRT1 expression. *Sci. Rep.* **7,** (2017).
268. Zhang, C. *et al.* Hypoxia induces the breast cancer stem cell phenotype by HIF-dependent and ALKBH5-mediated m ^{6} A-demethylation of NANOG mRNA. *Proc. Natl. Acad. Sci.* **113,** E2047–E2056 (2016).
269. Conley, S. J. *et al.* Antiangiogenic agents increase breast cancer stem cells via the generation of tumor hypoxia. *Proc. Natl. Acad. Sci.* **109,** 2784–2789 (2012).
270. Hu, Y.-L. *et al.* Hypoxia-Induced Autophagy Promotes Tumor Cell Survival and Adaptation to Antiangiogenic Treatment in Glioblastoma. *Cancer Res.* **72,** 1773–1783 (2012).
271. Mazure, N. M. & Pouysségur, J. Hypoxia-induced autophagy: cell death or cell survival? *Curr. Opin. Cell Biol.* **22,** 177–180 (2010).
272. Mizushima, N. & Komatsu, M. Autophagy: renovation of cells and tissues. *Cell* **147,** 728–741 (2011).
273. Wu, X. *et al.* Autophagy regulates Notch degradation and modulates stem cell development and neurogenesis. *Nat. Commun.* **7,** 10533 (2016).
274. Mortensen, M. *et al.* The autophagy protein Atg7 is essential for hematopoietic stem cell maintenance. *J. Exp. Med.* **208,** 455–467 (2011).
275. Salemi, S., Yousefi, S., Constantinescu, M. A., Fey, M. F. & Simon, H.-U. Autophagy is required for self-renewal and differentiation of adult human stem cells. *Cell Res.* **22,** 432–435 (2012).
276. Nager, M. *et al.* Inhibition of WNT-CTNNB1 signaling upregulates SQSTM1 and sensitizes glioblastoma cells to autophagy blockers. *Autophagy* 01–40 (2018). doi:10.1080/15548627.2017.1423439
277. Fodde, R. & Brabletz, T. Wnt/β-catenin signaling in cancer stemness and malignant behavior. *Curr. Opin. Cell Biol.* **19,** 150–158 (2007).
278. Lei, Y. *et al.* Targeting autophagy in cancer stem cells as an anticancer therapy. *Cancer Lett.* **393,** 33–39 (2017).
279. Holland, E. C. & Varmus, H. E. Basic fibroblast growth factor induces cell migration and proliferation after glia-specific gene transfer in mice. *Proc. Natl. Acad. Sci. U. S. A.* **95,** 1218–1223 (1998).

280. Dai, C. *et al.* PDGF autocrine stimulation dedifferentiates cultured astrocytes and induces oligodendrogliomas and oligoastrocytomas from neural progenitors and astrocytes in vivo. *Genes Dev.* **15,** 1913–1925 (2001).
281. Holland, E. C. *et al.* Combined activation of Ras and Akt in neural progenitors induces glioblastoma formation in mice. *Nat. Genet.* **25,** 55–57 (2000).
282. Hu, X. *et al.* mTOR Promotes Survival and Astrocytic Characteristics Induced by Pten/Akt Signaling in Glioblastoma. *Neoplasia* **7,** 356–368 (2005).
283. Ozawa, T. *et al.* Most Human Non-GCIMP Glioblastoma Subtypes Evolve from a Common Proneural-like Precursor Glioma. *Cancer Cell* **26,** 288–300 (2014).
284. Holland, E. C., Hively, W. P., DePinho, R. A. & Varmus, H. E. A constitutively active epidermal growth factor receptor cooperates with disruption of G1 cell-cycle arrest pathways to induce glioma-like lesions in mice. *Genes Dev.* **12,** 3675–3685 (1998).
285. Ravi, R. *et al.* Regulation of tumor angiogenesis by p53-induced degradation of hypoxia-inducible factor 1alpha. *Genes Dev.* **14,** 34–44 (2000).
286. Yoshii, S. R. *et al.* Systemic Analysis of Atg5 -Null Mice Rescued from Neonatal Lethality by Transgenic ATG5 Expression in Neurons. *Dev. Cell* **39,** 116–130 (2016).
287. Galluzzi, L., Bravo-San Pedro, J. M., Levine, B., Green, D. R. & Kroemer, G. Pharmacological modulation of autophagy: therapeutic potential and persisting obstacles. *Nat. Rev. Drug Discov.* **16,** 487–511 (2017).
288. Rosenfeld, M. R. *et al.* A phase I/II trial of hydroxychloroquine in conjunction with radiation therapy and concurrent and adjuvant temozolomide in patients with newly diagnosed glioblastoma multiforme. *Autophagy* **10,** 1359–1368 (2014).
289. Bevan, A. P. *et al.* Chloroquine Extends the Lifetime of the Activated Insulin Receptor Complex in Endosomes. *J. Biol. Chem.* **272,** 26833–26840 (1997).
290. Eng, C. H. *et al.* Macroautophagy is dispensable for growth of KRAS mutant tumors and chloroquine efficacy. *Proc. Natl. Acad. Sci.* **113,** 182–187 (2016).
291. Maycotte, P. *et al.* Chloroquine sensitizes breast cancer cells to chemotherapy independent of autophagy. *Autophagy* **8,** 200–212 (2012).
292. Chude, C. I. & Amaravadi, R. K. Targeting Autophagy in Cancer: Update on Clinical Trials and Novel Inhibitors. *Int. J. Mol. Sci.* **18,** (2017).
293. Petherick, K. J. *et al.* Pharmacological inhibition of ULK1 kinase blocks mammalian target of rapamycin (mTOR)-dependent autophagy. *J. Biol. Chem.* **290,** 11376–11383 (2015).
294. Ronan, B. *et al.* A highly potent and selective Vps34 inhibitor alters vesicle trafficking and autophagy. *Nat. Chem. Biol.* **10,** 1013 (2014).
295. Wu, Y.-T. *et al.* Dual Role of 3-Methyladenine in Modulation of Autophagy via Different Temporal Patterns of Inhibition on Class I and III Phosphoinositide 3-Kinase. *J. Biol. Chem.* **285,** 10850–10861 (2010).
296. Fan, Q.-W. *et al.* Akt and autophagy cooperate to promote survival of drug-resistant glioma. *Sci. Signal.* **3,** ra81 (2010).
297. Katayama, M., Kawaguchi, T., Berger, M. S. & Pieper, R. O. DNA damaging agent-induced autophagy produces a cytoprotective adenosine triphosphate surge in malignant glioma cells. *Cell Death Differ.* **14,** 548–558 (2007).
298. Wu, W. *et al.* Aldehyde dehydrogenase 1A3 (ALDH1A3) is regulated by autophagy in human glioblastoma cells. *Cancer Lett.* **417,** 112–123 (2018).

299. Huang, E. H. *et al.* Aldehyde Dehydrogenase 1 Is a Marker for Normal and Malignant Human Colonic Stem Cells (SC) and Tracks SC Overpopulation during Colon Tumorigenesis. *Cancer Res.* **69,** 3382–3389 (2009).
300. Lomonaco, S. L. *et al.* The induction of autophagy by γ-radiation contributes to the radioresistance of glioma stem cells. *Int. J. Cancer* **125,** 717–722 (2009).
301. Lee, C. *et al.* Polo-Like Kinase 1 Inhibition Kills Glioblastoma Multiforme Brain Tumor Cells in Part Through Loss of SOX2 and Delays Tumor Progression in Mice. *STEM CELLS* **30,** 1064–1075 (2012).
302. Bachoo, R. M. *et al.* Epidermal growth factor receptor and Ink4a/Arf: Convergent mechanisms governing terminal differentiation and transformation along the neural stem cell to astrocyte axis. *Cancer Cell* **1,** 269–277 (2002).
303. Bruggeman, S. W. M. *et al.* Bmi1 Controls Tumor Development in an Ink4a/Arf-Independent Manner in a Mouse Model for Glioma. *Cancer Cell* **12,** 328–341 (2007).
304. Bulstrode, H. *et al.* Elevated FOXG1 and SOX2 in glioblastoma enforces neural stem cell identity through transcriptional control of cell cycle and epigenetic regulators. *Genes Dev.* **31,** 757–773 (2017).
305. Engedal, N. *et al.* Modulation of intracellular calcium homeostasis blocks autophagosome formation. *Autophagy* **9,** 1475–1490 (2013).
306. Creedon, H. *et al.* Identification of novel pathways linking epithelial-to-mesenchymal transition with resistance to HER2-targeted therapy. *Oncotarget* **7,** 11539–11552 (2016).
307. Guha, A., Feldkamp, M. M., Lau, N., Boss, G. & Pawson, A. Proliferation of human malignant astrocytomas is dependent on Ras activation. *Oncogene* **15,** 2755–2765 (1997).
308. Uhrbom, L., Kastemar, M., Johansson, F. K., Westermark, B. & Holland, E. C. Cell Type-Specific Tumor Suppression by *Ink4a* and *Arf* in Kras-Induced Mouse Gliomagenesis. *Cancer Res.* **65,** 2065–2069 (2005).
309. Wiese, C. *et al.* Nestin expression-a property of multi-lineage progenitor cells? *Cell. Mol. Life Sci. CMLS* **61,** 2510–2522 (2004).
310. Young, A. R. J. *et al.* Autophagy mediates the mitotic senescence transition. *Genes Dev.* **23,** 798–803 (2009).
311. Yang, Z. & Klionsky, D. J. Mammalian autophagy: core molecular machinery and signaling regulation. *Curr. Opin. Cell Biol.* **22,** 124–131 (2010).
312. Azad, M. B. *et al.* Hypoxia induces autophagic cell death in apoptosis-competent cells through a mechanism involving BNIP3. *Autophagy* **4,** 195–204 (2008).
313. Levine, B. Autophagy in cell death: an innocent convict? *J. Clin. Invest.* **115,** 2679–2688 (2005).
314. Yu, L. Regulation of an ATG7-beclin 1 Program of Autophagic Cell Death by Caspase-8. *Science* **304,** 1500–1502 (2004).
315. Zhang, H. *et al.* Mitochondrial Autophagy Is an HIF-1-dependent Adaptive Metabolic Response to Hypoxia. *J. Biol. Chem.* **283,** 10892–10903 (2008).
316. Dupont, N. *et al.* Autophagy-based unconventional secretory pathway for extracellular delivery of IL-1β: Autophagy-based unconventional secretory pathway. *EMBO J.* **30,** 4701–4711 (2011).
317. Canman, C. E. *et al.* Activation of the ATM Kinase by Ionizing Radiation and Phosphorylation of p53. *Science* **281,** 1677–1679 (1998).
318. Suzuki, K. *et al.* Radiation-induced senescence-like growth arrest requires TP53 function but not telomere shortening. *Radiat. Res.* **155,** 248–253 (2001).

319. Hayflick, L. The limited in vitro lifetime of human diploid cell strains. *Exp. Cell Res.* **37,** 614–636 (1965).
320. Narita, M. *et al.* Spatial coupling of mTOR and autophagy augments secretory phenotypes. *Science* **332,** 966–970 (2011).
321. Xie, X., Koh, J. Y., Price, S., White, E. & Mehnert, J. M. Atg7 Overcomes Senescence and Promotes Growth of BrafV600E-Driven Melanoma. *Cancer Discov.* **5,** 410–423 (2015).
322. García-Prat, L. *et al.* Autophagy maintains stemness by preventing senescence. *Nature* **529,** 37–42 (2016).
323. Jacinto, E. *et al.* SIN1/MIP1 Maintains rictor-mTOR Complex Integrity and Regulates Akt Phosphorylation and Substrate Specificity. *Cell* **127,** 125–137 (2006).
324. Du, J. *et al.* PI3K and ERK-Induced Rac1 Activation Mediates Hypoxia-Induced HIF-1α Expression in MCF-7 Breast Cancer Cells. *PLoS ONE* **6,** e25213 (2011).
325. Kwon, D. S. *et al.* Signal transduction of MEK/ERK and PI3K/Akt activation by hypoxia/reoxygenation in renal epithelial cells. *Eur. J. Cell Biol.* **85,** 1189–1199 (2006).
326. Zhong, H. *et al.* Modulation of hypoxia-inducible factor 1alpha expression by the epidermal growth factor/phosphatidylinositol 3-kinase/PTEN/AKT/FRAP pathway in human prostate cancer cells: implications for tumor angiogenesis and therapeutics. *Cancer Res.* **60,** 1541–1545 (2000).
327. Mazure, N. M., Chen, E. Y., Laderoute, K. R. & Giaccia, A. J. Induction of vascular endothelial growth factor by hypoxia is modulated by a phosphatidylinositol 3-kinase/Akt signaling pathway in Ha-ras-transformed cells through a hypoxia inducible factor-1 transcriptional element. *Blood* **90,** 3322–3331 (1997).
328. Wilkinson, S., O'Prey, J., Fricker, M. & Ryan, K. M. Hypoxia-selective macroautophagy and cell survival signaled by autocrine PDGFR activity. *Genes Dev.* **23,** 1283–1288 (2009).
329. Rzymski, T. *et al.* Regulation of autophagy by ATF4 in response to severe hypoxia. *Oncogene* **29,** 4424–4435 (2010).
330. Brugarolas, J. Regulation of mTOR function in response to hypoxia by REDD1 and the TSC1/TSC2 tumor suppressor complex. *Genes Dev.* **18,** 2893–2904 (2004).
331. Soeda, A. *et al.* Hypoxia promotes expansion of the CD133-positive glioma stem cells through activation of HIF-1α. *Oncogene* **28,** 3949–3959 (2009).
332. Majmundar, A. J., Wong, W. J. & Simon, M. C. Hypoxia-Inducible Factors and the Response to Hypoxic Stress. *Mol. Cell* **40,** 294–309 (2010).
333. Mizushima, N. Autophagy: process and function. *Genes Dev.* **21,** 2861–2873 (2007).
334. Hurford, R. K., Cobrinik, D., Lee, M. H. & Dyson, N. pRB and p107/p130 are required for the regulated expression of different sets of E2F responsive genes. *Genes Dev.* **11,** 1447–1463 (1997).
335. Chen, D. S. & Mellman, I. Oncology Meets Immunology: The Cancer-Immunity Cycle. *Immunity* **39,** 1–10 (2013).
336. Hambardzumyan, D., Parada, L. F., Holland, E. C. & Charest, A. Genetic modeling of gliomas in mice: New tools to tackle old problems. *Glia* **59,** 1155–1168 (2011).

337. Qin, L., Wang, Z., Tao, L. & Wang, Y. ER stress negatively regulates AKT/TSC/mTOR pathway to enhance autophagy. *Autophagy* **6,** 239–247 (2010).
338. Nakahira, K. *et al.* Autophagy proteins regulate innate immune responses by inhibiting the release of mitochondrial DNA mediated by the NALP3 inflammasome. *Nat. Immunol.* **12,** 222–230 (2011).
339. Cheng, M. *et al.* The p21(Cip1) and p27(Kip1) CDK 'inhibitors' are essential activators of cyclin D-dependent kinases in murine fibroblasts. *EMBO J.* **18,** 1571–1583 (1999).
340. Kohn, A. D., Takeuchi, F. & Roth, R. A. Akt, a Pleckstrin Homology Domain Containing Kinase, Is Activated Primarily by Phosphorylation. *J. Biol. Chem.* **271,** 21920–21926 (1996).
341. Kuilman, T., Michaloglou, C., Mooi, W. J. & Peeper, D. S. The essence of senescence. *Genes Dev.* **24,** 2463–2479 (2010).
342. Baker, D. J. *et al.* Clearance of p16Ink4a-positive senescent cells delays ageing-associated disorders. *Nature* **479,** 232–236 (2011).
343. Xue, W. *et al.* Senescence and tumour clearance is triggered by p53 restoration in murine liver carcinomas. *Nature* **445,** 656–660 (2007).
344. Loaiza, N. & Demaria, M. Cellular senescence and tumor promotion: Is aging the key? *Biochim. Biophys. Acta BBA - Rev. Cancer* **1865,** 155–167 (2016).
345. Ouchi, R., Okabe, S., Migita, T., Nakano, I. & Seimiya, H. Senescence from glioma stem cell differentiation promotes tumor growth. *Biochem. Biophys. Res. Commun.* **470,** 275–281 (2016).
346. Nogueira, L. *et al.* Blockade of the NFκB pathway drives differentiating glioblastoma-initiating cells into senescence both in vitro and in vivo. *Oncogene* **30,** 3537–3548 (2011).
347. Gan, H. K., Cvrljevic, A. N. & Johns, T. G. The epidermal growth factor receptor variant III (EGFRvIII): where wild things are altered. *FEBS J.* **280,** 5350–5370 (2013).
348. Galli, R. *et al.* Isolation and characterization of tumorigenic, stem-like neural precursors from human glioblastoma. *Cancer Res.* **64,** 7011–7021 (2004).
349. Pollard, S. M. *et al.* Glioma Stem Cell Lines Expanded in Adherent Culture Have Tumor-Specific Phenotypes and Are Suitable for Chemical and Genetic Screens. *Cell Stem Cell* **4,** 568–580 (2009).
350. Günther, H. S. *et al.* Glioblastoma-derived stem cell-enriched cultures form distinct subgroups according to molecular and phenotypic criteria. *Oncogene* **27,** 2897–2909 (2008).
351. Lee, J. *et al.* Tumor stem cells derived from glioblastomas cultured in bFGF and EGF more closely mirror the phenotype and genotype of primary tumors than do serum-cultured cell lines. *Cancer Cell* **9,** 391–403 (2006).
352. Bischof, J. *et al.* Cancer stem cells: The potential role of autophagy, proteolysis, and cathepsins in glioblastoma stem cells. *Tumor Biol.* **39,** 101042831769222 (2017).
353. Gomez-Roman, N., Stevenson, K., Gilmour, L., Hamilton, G. & Chalmers, A. J. A novel 3D human glioblastoma cell culture system for modeling drug and radiation responses. *Neuro-Oncol.* now164 (2016). doi:10.1093/neuonc/now164
354. Batra, S. K. *et al.* Epidermal growth factor ligand-independent, unregulated, cell-transforming potential of a naturally occurring human mutant EGFRvIII gene. *Cell Growth Differ. Mol. Biol. J. Am. Assoc. Cancer Res.* **6,** 1251–1259 (1995).

355. Stockhausen, M.-T., Kristoffersen, K., Stobbe, L. & Poulsen, H. S. Differentiation of glioblastoma multiforme stem-like cells leads to downregulation of EGFR and EGFRvIII and decreased tumorigenic and stem-like cell potential. *Cancer Biol. Ther.* **15,** 216–224 (2014).
356. Matsubara, S. *et al.* mTOR plays critical roles in pancreatic cancer stem cells through specific and stemness-related functions. *Sci. Rep.* **3,** (2013).
357. Hwang, W. *et al.* SNAIL Regulates Interleukin-8 Expression, Stem Cell–Like Activity, and Tumorigenicity of Human Colorectal Carcinoma Cells. *Gastroenterology* **141,** 279-291.e5 (2011).
358. Mani, S. A. *et al.* The Epithelial-Mesenchymal Transition Generates Cells with Properties of Stem Cells. *Cell* **133,** 704–715 (2008).
359. Fan, Q.-W. *et al.* EGFR Phosphorylates Tumor-Derived EGFRvIII Driving STAT3/5 and Progression in Glioblastoma. *Cancer Cell* **24,** 438–449 (2013).
360. Huang, H.-J. S. *et al.* The Enhanced Tumorigenic Activity of a Mutant Epidermal Growth Factor Receptor Common in Human Cancers Is Mediated by Threshold Levels of Constitutive Tyrosine Phosphorylation and Unattenuated Signaling. *J. Biol. Chem.* **272,** 2927–2935 (1997).
361. Schmidt, M. H. H., Furnari, F. B., Cavenee, W. K. & Bogler, O. Epidermal growth factor receptor signaling intensity determines intracellular protein interactions, ubiquitination, and internalization. *Proc. Natl. Acad. Sci.* **100,** 6505–6510 (2003).
362. Biagioni, A. *et al.* Type II CRISPR/Cas9 approach in the oncological therapy. *J. Exp. Clin. Cancer Res.* **36,** (2017).
363. Nishida, Y. *et al.* Discovery of Atg5/Atg7-independent alternative macroautophagy. *Nature* **461,** 654–658 (2009).
364. Robinson, M. J., Stippec, S. A., Goldsmith, E., White, M. A. & Cobb, M. H. A constitutively active and nuclear form of the MAP kinase ERK2 is sufficient for neurite outgrowth and cell transformation. *Curr. Biol. CB* **8,** 1141–1150 (1998).
365. Goberdhan, D. C. I., Wilson, C. & Harris, A. L. Amino Acid Sensing by mTORC1: Intracellular Transporters Mark the Spot. *Cell Metab.* **23,** 580–589 (2016).
366. Jewell, J. L., Russell, R. C. & Guan, K.-L. Amino acid signalling upstream of mTOR. *Nat. Rev. Mol. Cell Biol.* **14,** 133–139 (2013).
367. Real, F. X. *et al.* Expression of epidermal growth factor receptor in human cultured cells and tissues: relationship to cell lineage and stage of differentiation. *Cancer Res.* **46,** 4726–4731 (1986).
368. Larsen, A. K., Ouaret, D., El Ouadrani, K. & Petitprez, A. Targeting EGFR and VEGF(R) pathway cross-talk in tumor survival and angiogenesis. *Pharmacol. Ther.* **131,** 80–90 (2011).
369. Spurrier, B., Ramalingam, S. & Nishizuka, S. Reverse-phase protein lysate microarrays for cell signaling analysis. *Nat. Protoc.* **3,** 1796–1808 (2008).
370. Gallagher, R. I. & Espina, V. Reverse Phase Protein Arrays: Mapping the Path Towards Personalized Medicine. *Mol. Diagn. Ther.* **18,** 619–630 (2014).
371. Ullrich, A. & Schlessinger, J. Signal transduction by receptors with tyrosine kinase activity. *Cell* **61,** 203–212 (1990).
372. Fraser, J., Cabodevilla, A. G., Simpson, J. & Gammoh, N. Interplay of autophagy, receptor tyrosine kinase signalling and endocytic trafficking. *Essays Biochem.* **61,** 597–607 (2017).

373. Wu, H.-B. *et al.* Autophagy-induced KDR/VEGFR-2 activation promotes the formation of vasculogenic mimicry by glioma stem cells. *Autophagy* **13,** 1528–1542 (2017).
374. Singh, V. *et al.* Mycobacterium tuberculosis-driven targeted recalibration of macrophage lipid homeostasis promotes the foamy phenotype. *Cell Host Microbe* **12,** 669–681 (2012).
375. Cao, L. *et al.* Epidermal growth factor induces cell cycle arrest and apoptosis of squamous carcinoma cells through reduction of cell adhesion. *J. Cell. Biochem.* **77,** 569–583 (2000).
376. Henson, E. S. & Gibson, S. B. Surviving cell death through epidermal growth factor (EGF) signal transduction pathways: Implications for cancer therapy. *Cell. Signal.* **18,** 2089–2097 (2006).
377. Luwor, R. B. *et al.* The tumor-specific de2–7 epidermal growth factor receptor (EGFR) promotes cells survival and heterodimerizes with the wild-type EGFR. *Oncogene* **23,** 6095–6104 (2004).
378. Levkowitz, G. *et al.* Ubiquitin ligase activity and tyrosine phosphorylation underlie suppression of growth factor signaling by c-Cbl/Sli-1. *Mol. Cell* **4,** 1029–1040 (1999).
379. Fader, C. M. & Colombo, M. I. Autophagy and multivesicular bodies: two closely related partners. *Cell Death Differ.* **16,** 70–78 (2009).
380. Codogno, P., Mehrpour, M. & Proikas-Cezanne, T. Canonical and non-canonical autophagy: variations on a common theme of self-eating? *Nat. Rev. Mol. Cell Biol.* **13,** 7–12 (2012).
381. Paez, J. G. EGFR Mutations in Lung Cancer: Correlation with Clinical Response to Gefitinib Therapy. *Science* **304,** 1497–1500 (2004).
382. Annerén, C. Tyrosine kinase signalling in embryonic stem cells. *Clin. Sci.* **115,** 43–55 (2008).
383. Sigismund, S. *et al.* Clathrin-independent endocytosis of ubiquitinated cargos. *Proc. Natl. Acad. Sci.* **102,** 2760–2765 (2005).
384. Jackson, L. P. *et al.* A Large-Scale Conformational Change Couples Membrane Recruitment to Cargo Binding in the AP2 Clathrin Adaptor Complex. *Cell* **141,** 1220–1229 (2010).
385. Liang, C. *et al.* Beclin1-binding UVRAG targets the class C Vps complex to coordinate autophagosome maturation and endocytic trafficking. *Nat. Cell Biol.* **10,** 776–787 (2008).
386. Morris, D. H., Yip, C. K., Shi, Y., Chait, B. T. & Wang, Q. J. Beclin 1-Vps34 complex architecture: Understanding the nuts and bolts of therapeutic targets. *Front. Biol.* **10,** 398–426 (2015).
387. Rozakis-Adcock, M., Fernley, R., Wade, J., Pawson, T. & Bowtell, D. The SH2 and SH3 domains of mammalian Grb2 couple the EGF receptor to the Ras activator mSos1. *Nature* **363,** 83–85 (1993).
388. Sorkin, A., McClure, M., Huang, F. & Carter, R. Interaction of EGF receptor and Grb2 in living cells visualized by fluorescence resonance energy transfer (FRET) microscopy. *Curr. Biol.* **10,** 1395–1398 (2000).
389. Gong, C. *et al.* Dynamin2 downregulation delays EGFR endocytic trafficking and promotes EGFR signaling and invasion in hepatocellular carcinoma. *Am. J. Cancer Res.* **5,** 702–713 (2015).
390. Al-Akhrass, H. *et al.* Sortilin limits EGFR signaling by promoting its internalization in lung cancer. *Nat. Commun.* **8,** (2017).

391. Sadowski, Ł. *et al.* Dynamin Inhibitors Impair Endocytosis and Mitogenic Signaling of PDGF: Dynamin Inhibitors in Endocytosis and Signaling of PDGF. *Traffic* **14,** 725–736 (2013).
392. Omerovic, J., Hammond, D. E., Prior, I. A. & Clague, M. J. Global snapshot of the influence of endocytosis upon EGF receptor signaling output. *J. Proteome Res.* **11,** 5157–5166 (2012).
393. Östman, A., Hellberg, C. & Böhmer, F. D. Protein-tyrosine phosphatases and cancer. *Nat. Rev. Cancer* **6,** 307–320 (2006).
394. Tonks, N. K. Protein tyrosine phosphatases: from genes, to function, to disease. *Nat. Rev. Mol. Cell Biol.* **7,** 833–846 (2006).
395. Ying, H. *et al.* Mig-6 controls EGFR trafficking and suppresses gliomagenesis. *Proc. Natl. Acad. Sci.* **107,** 6912–6917 (2010).
396. Matsunaga, K. *et al.* Two Beclin 1-binding proteins, Atg14L and Rubicon, reciprocally regulate autophagy at different stages. *Nat. Cell Biol.* **11,** 385–396 (2009).
397. Kern, A., Dikic, I. & Behl, C. The integration of autophagy and cellular trafficking pathways via RAB GAPs. *Autophagy* **11,** 2393–2397 (2015).
398. Amaya, C., Fader, C. M. & Colombo, M. I. Autophagy and proteins involved in vesicular trafficking. *FEBS Lett.* **589,** 3343–3353 (2015).
399. Jager, S. Role for Rab7 in maturation of late autophagic vacuoles. *J. Cell Sci.* **117,** 4837–4848 (2004).
400. Fletcher, K. *et al.* The WD40 domain of ATG16L1 is required for its non-canonical role in lipidation of LC3 at single membranes. *EMBO J.* **37,** e97840 (2018).
401. Buday, L. & Downward, J. Epidermal growth factor regulates p21ras through the formation of a complex of receptor, Grb2 adapter protein, and Sos nucleotide exchange factor. *Cell* **73,** 611–620 (1993).
402. Miller, K. A. *et al.* Oncogenic Kras Requires Simultaneous PI3K Signaling to Induce ERK Activation and Transform Thyroid Epithelial Cells In vivo. *Cancer Res.* **69,** 3689–3694 (2009).
403. Ebi, H. *et al.* PI3K regulates MEK/ERK signaling in breast cancer via the Rac-GEF, P-Rex1. *Proc. Natl. Acad. Sci.* **110,** 21124–21129 (2013).
404. Diaz-Flores, E. *et al.* PLC- and PI3K Link Cytokines to ERK Activation in Hematopoietic Cells with Normal and Oncogenic Kras. *Sci. Signal.* **6,** ra105–ra105 (2013).
405. Futter, C. E., Collinson, L. M., Backer, J. M. & Hopkins, C. R. Human VPS34 is required for internal vesicle formation within multivesicular endosomes. *J. Cell Biol.* **155,** 1251–1264 (2001).
406. Razi, M., Chan, E. Y. W. & Tooze, S. A. Early endosomes and endosomal coatomer are required for autophagy. *J. Cell Biol.* **185,** 305–321 (2009).
407. Buchan, J. R., Kolaitis, R.-M., Taylor, J. P. & Parker, R. Eukaryotic Stress Granules Are Cleared by Autophagy and Cdc48/VCP Function. *Cell* **153,** 1461–1474 (2013).
408. van Zutphen, T. *et al.* Lipid droplet autophagy in the yeast *Saccharomyces cerevisiae*. *Mol. Biol. Cell* **25,** 290–301 (2014).
409. Till, A., Lakhani, R., Burnett, S. F. & Subramani, S. Pexophagy: The Selective Degradation of Peroxisomes. *Int. J. Cell Biol.* **2012,** 1–18 (2012).
410. Strohecker, A. M. *et al.* Autophagy Sustains Mitochondrial Glutamine Metabolism and Growth of BrafV600E-Driven Lung Tumors. *Cancer Discov.* **3,** 1272–1285 (2013).

411. Fitzgerald, K. A. *et al.* IKKε and TBK1 are essential components of the IRF3 signaling pathway. *Nat. Immunol.* **4,** 491–496 (2003).
412. Rowland, A. A., Chitwood, P. J., Phillips, M. J. & Voeltz, G. K. ER Contact Sites Define the Position and Timing of Endosome Fission. *Cell* **159,** 1027–1041 (2014).
413. Derivery, E. *et al.* The Arp2/3 Activator WASH Controls the Fission of Endosomes through a Large Multiprotein Complex. *Dev. Cell* **17,** 712–723 (2009).
414. Dooley, H. C. *et al.* WIPI2 Links LC3 Conjugation with PI3P, Autophagosome Formation, and Pathogen Clearance by Recruiting Atg12–5-16L1. *Mol. Cell* **55,** 238–252 (2014).
415. Hayashi-Nishino, M. *et al.* A subdomain of the endoplasmic reticulum forms a cradle for autophagosome formation. *Nat. Cell Biol.* **11,** 1433–1437 (2009).
416. Xie, S. *et al.* The endocytic recycling compartment maintains cargo segregation acquired upon exit from the sorting endosome. *Mol. Biol. Cell* **27,** 108–126 (2016).
417. Dunn, K. W. Delivery of ligands from sorting endosomes to late endosomes occurs by maturation of sorting endosomes. *J. Cell Biol.* **117,** 301–310 (1992).
418. Ren, M. *et al.* Hydrolysis of GTP on rab11 is required for the direct delivery of transferrin from the pericentriolar recycling compartment to the cell surface but not from sorting endosomes. *Proc. Natl. Acad. Sci.* **95,** 6187–6192 (1998).
419. Gordon, P. B. & Seglen, P. O. Prelysosomal convergence of autophagic and endocytic pathways. *Biochem. Biophys. Res. Commun.* **151,** 40–47 (1988).
420. Fernandez-Borja, M. *et al.* Multivesicular body morphogenesis requires phosphatidyl-inositol 3-kinase activity. *Curr. Biol.* **9,** 55–58 (1999).
421. Denzer, K., Kleijmeer, M. J., Heijnen, H. F., Stoorvogel, W. & Geuze, H. J. Exosome: from internal vesicle of the multivesicular body to intercellular signaling device. *J. Cell Sci.* **113,** 3365 (2000).
422. Cocucci, E. & Meldolesi, J. Ectosomes and exosomes: shedding the confusion between extracellular vesicles. *Trends Cell Biol.* **25,** 364–372 (2015).
423. Filimonenko, M. *et al.* Functional multivesicular bodies are required for autophagic clearance of protein aggregates associated with neurodegenerative disease. *J. Cell Biol.* **179,** 485–500 (2007).
424. Jaganathan, S. *et al.* A Functional Nuclear Epidermal Growth Factor Receptor, Src and Stat3 Heteromeric Complex in Pancreatic Cancer Cells. *PLoS ONE* **6,** e19605 (2011).
425. Chen, Z.-Y. A Novel Endocytic Recycling Signal Distinguishes Biological Responses of Trk Neurotrophin Receptors. *Mol. Biol. Cell* **16,** 5761–5772 (2005).
426. Miaczynska, M., Pelkmans, L. & Zerial, M. Not just a sink: endosomes in control of signal transduction. *Curr. Opin. Cell Biol.* **16,** 400–406 (2004).
427. von Zastrow, M. & Sorkin, A. Signaling on the endocytic pathway. *Curr. Opin. Cell Biol.* **19,** 436–445 (2007).
428. Martinez, J. *et al.* Molecular characterization of LC3-associated phagocytosis reveals distinct roles for Rubicon, NOX2 and autophagy proteins. *Nat. Cell Biol.* **17,** 893–906 (2015).
429. Kim, S. E. & Overholtzer, M. Autophagy proteins regulate cell engulfment mechanisms that participate in cancer. *Semin. Cancer Biol.* **23,** 329–336 (2013).

430. Florey, O., Gammoh, N., Kim, S. E., Jiang, X. & Overholtzer, M. V-ATPase and osmotic imbalances activate endolysosomal LC3 lipidation. *Autophagy* **11,** 88–99 (2015).
431. Sanjuan, M. A. *et al.* Toll-like receptor signalling in macrophages links the autophagy pathway to phagocytosis. *Nature* **450,** 1253–1257 (2007).
432. Blume-Jensen, P. & Hunter, T. Oncogenic kinase signalling. *Nature* **411,** 355–365 (2001).
433. Ebner, P. *et al.* The IAP family member BRUCE regulates autophagosome–lysosome fusion. *Nat. Commun.* **9,** 599 (2018).
434. Alvarez-Tejado, M. *et al.* Hypoxia Induces the Activation of the Phosphatidylinositol 3-Kinase/Akt Cell Survival Pathway in PC12 Cells: PROTECTIVE ROLE IN APOPTOSIS. *J. Biol. Chem.* **276,** 22368–22374 (2001).
435. Chen, Y. *et al.* Tyrosine kinase receptor EGFR regulates the switch in cancer cells between cell survival and cell death induced by autophagy in hypoxia. *Autophagy* **12,** 1029–1046 (2016).
436. Wang, Y. *et al.* Hypoxia promotes ligand-independent EGF receptor signaling via hypoxia-inducible factor-mediated upregulation of caveolin-1. *Proc. Natl. Acad. Sci. U. S. A.* **109,** 4892–4897 (2012).
437. Storer, M. *et al.* Senescence Is a Developmental Mechanism that Contributes to Embryonic Growth and Patterning. *Cell* **155,** 1119–1130 (2013).
438. Childs, B. G., Durik, M., Baker, D. J. & van Deursen, J. M. Cellular senescence in aging and age-related disease: from mechanisms to therapy. *Nat. Med.* **21,** 1424 (2015).
439. Padfield, E., Ellis, H. P. & Kurian, K. M. Current Therapeutic Advances Targeting EGFR and EGFRvIII in Glioblastoma. *Front. Oncol.* **5,** (2015).
440. Tang, L. *et al.* CRISPR/Cas9-mediated gene editing in human zygotes using Cas9 protein. *Mol. Genet. Genomics* **292,** 525–533 (2017).
441. Cornu, T. I., Mussolino, C. & Cathomen, T. Refining strategies to translate genome editing to the clinic. *Nat. Med.* **23,** 415 (2017).
442. Chen, Y. & Fu, L. Mechanisms of acquired resistance to tyrosine kinase inhibitors. *Acta Pharm. Sin. B* **1,** 197–207 (2011).
443. Huang, L. & Fu, L. Mechanisms of resistance to EGFR tyrosine kinase inhibitors. *Acta Pharm. Sin. B* **5,** 390–401 (2015).
444. Radoshevich, L. *et al.* ATG12 conjugation to ATG3 regulates mitochondrial homeostasis and cell death. *Cell* **142,** 590–600 (2010).

17 Appendix

Appendix 1: Additional Quantifications of Reverse Phase Protein Array Data
Continuation from Chapter X where XFM sh*Nf-1*/sh*Tp53* cells were either left untreated or subjected to serum starvation for 4hr followed by 20ng/ml EGF stimulation or 1% FBS stimulation for 15/30min The results of the RPPA were ordered from highest to lowest signal ratio in Control over sg*Atg7* for the condition '+EGF 15min'.

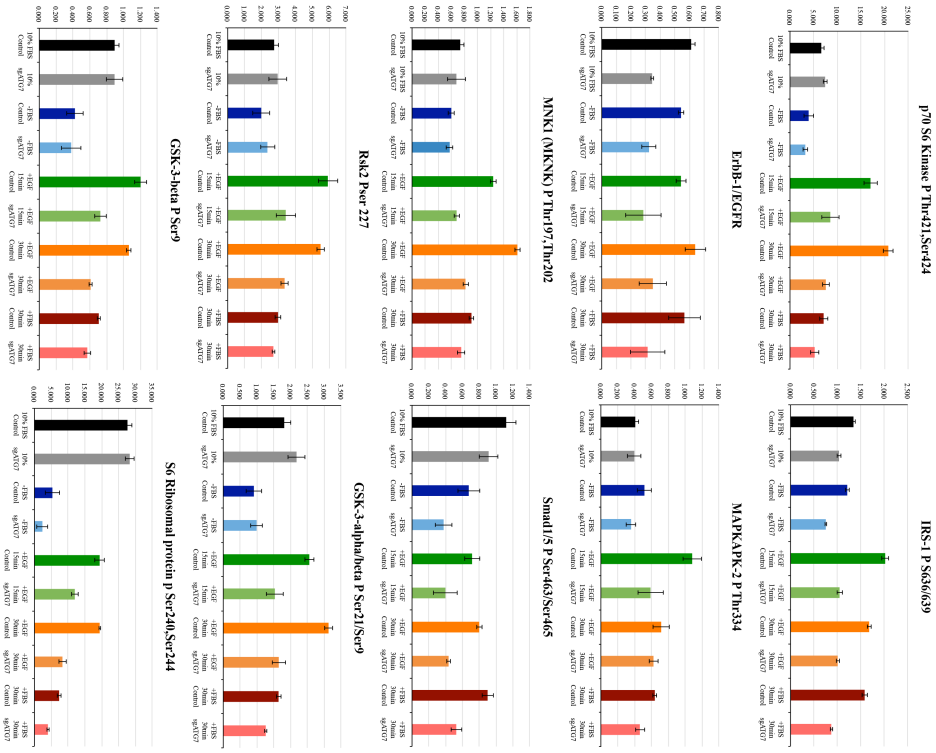

Figure S17.1 Reverse Phase Protein Array Analysis Reveals Atg7 Loss Reduces the Activity of EGFR Downstream Signalling Cascades II

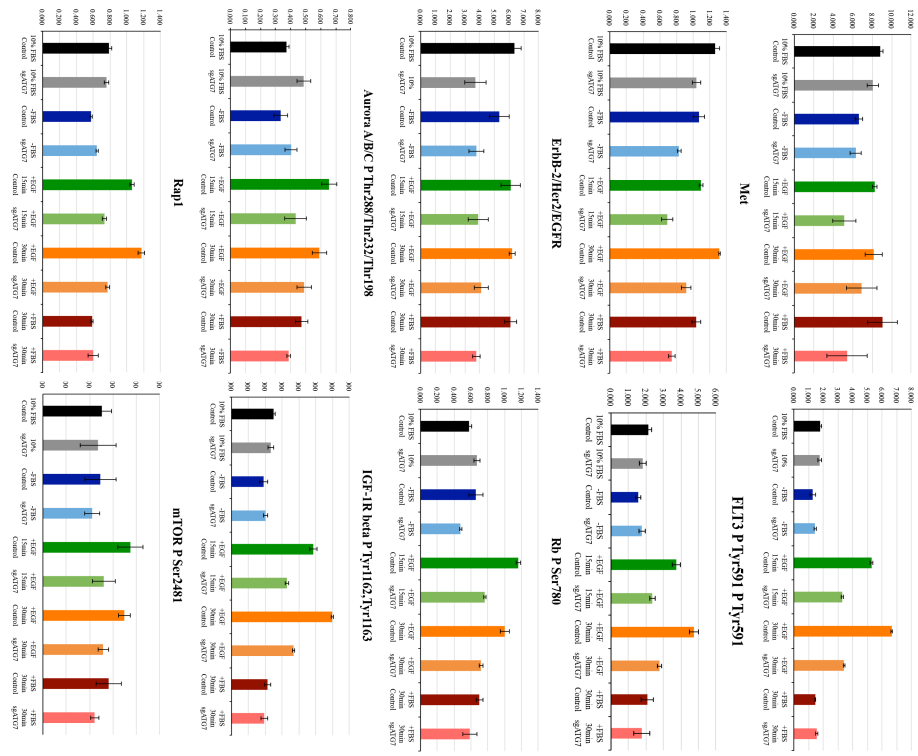

Figure S17.2 Reverse Phase Protein Array Analysis Reveals Atg7 Loss Reduces the Activity of EGFR Downstream Signalling Cascades III

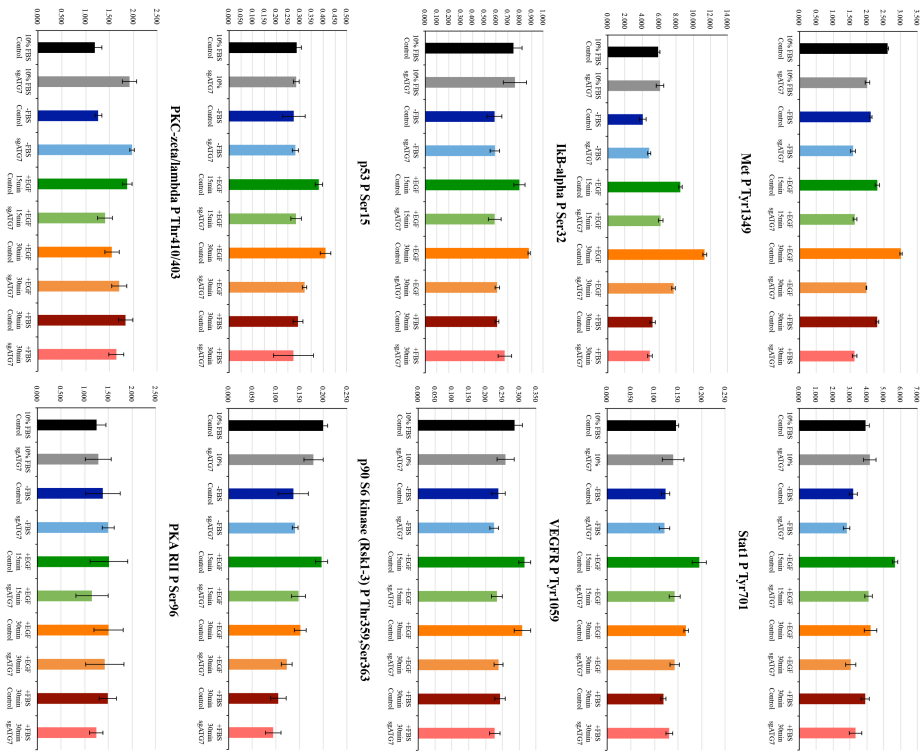

Figure S17.3 Reverse Phase Protein Array Analysis Reveals Atg7 Loss Reduces the Activity of EGFR Downstream Signalling Cascades IV

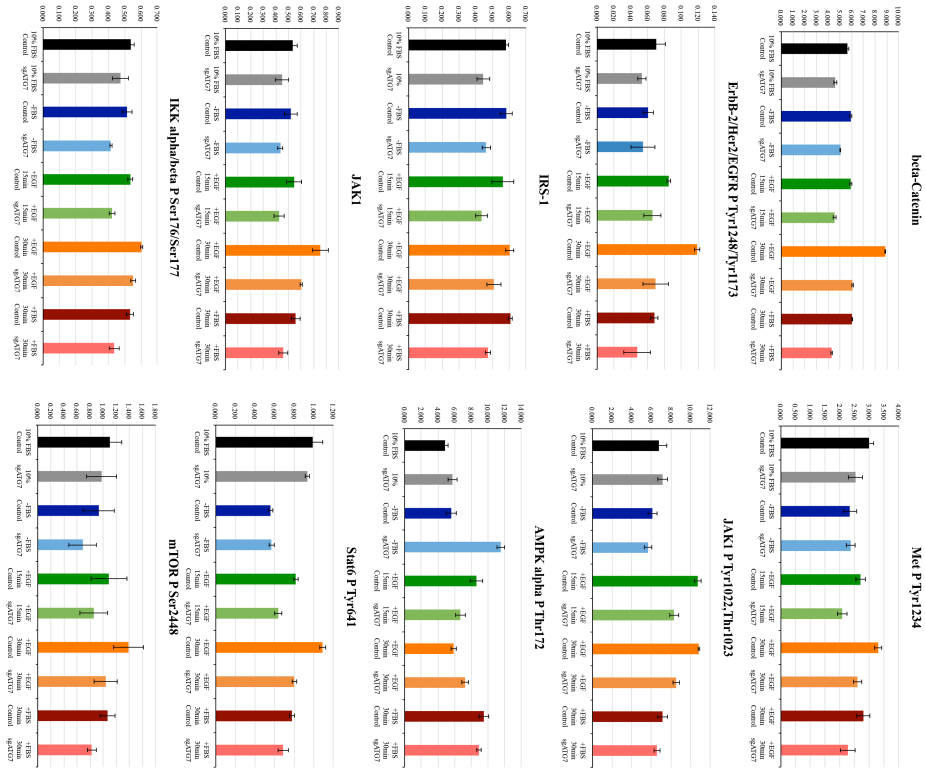

Figure S17.4 Reverse Phase Protein Array Analysis Reveals Atg7 Loss Reduces the Activity of EGFR Downstream Signalling Cascades

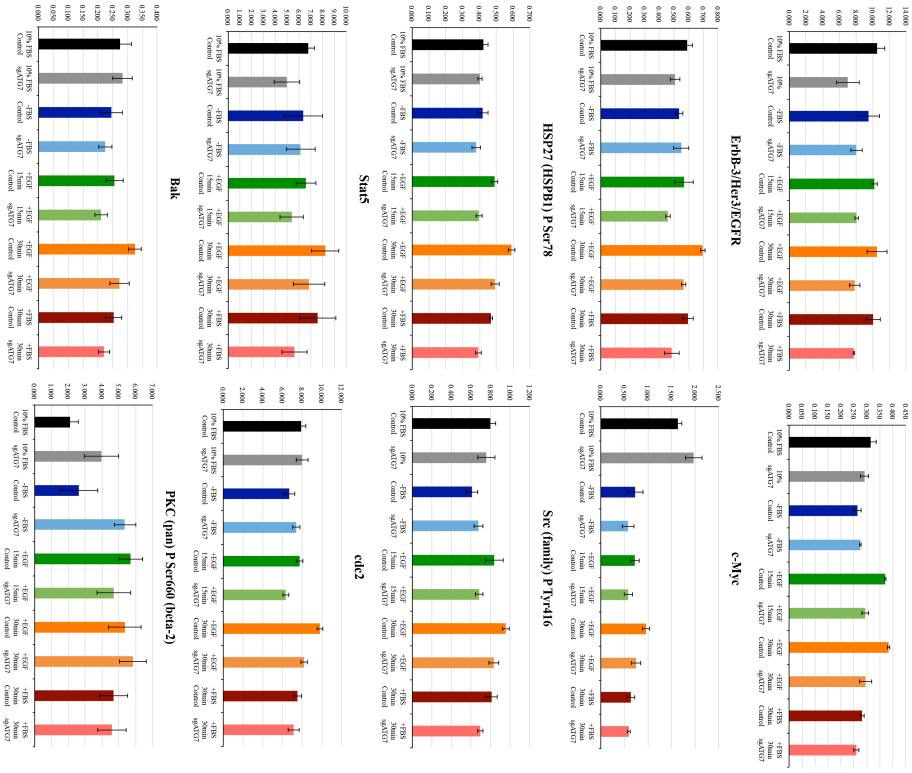

Figure S17.5 Reverse Phase Protein Array Analysis Reveals Atg7 Loss Reduces the Activity of EGFR Downstream Signalling Cascades VI

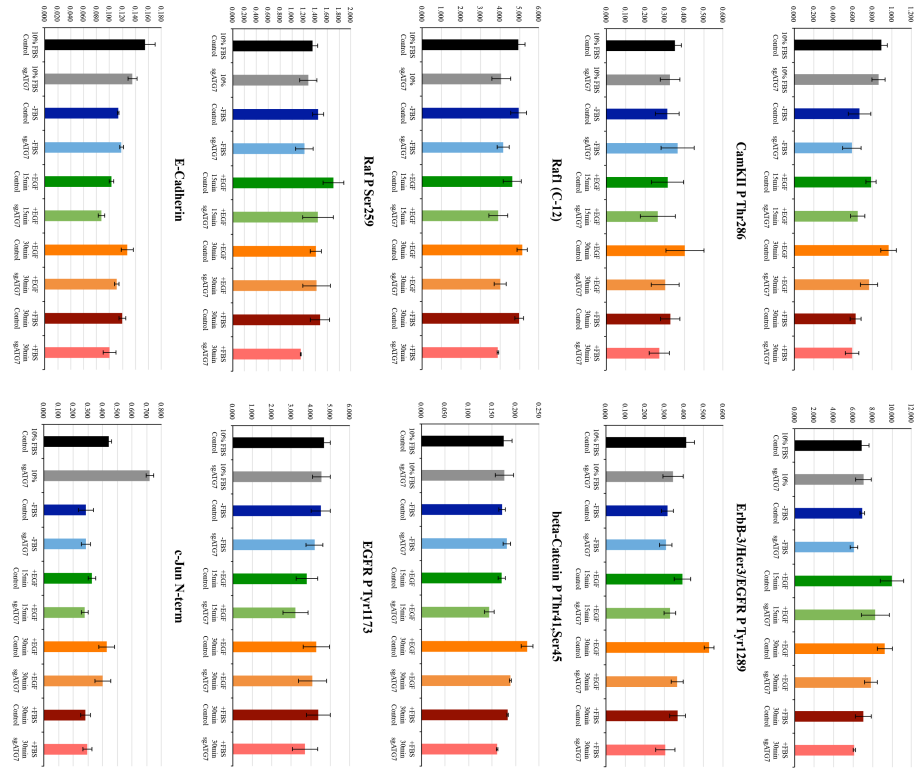

Figure S17.6 Reverse Phase Protein Array Analysis Reveals Atg7 Loss Reduces the Activity of EGFR Downstream Signalling Cascades VII

Figure S17.7 Reverse Phase Protein Array Analysis Reveals Atg7 Loss Reduces the Activity of EGFR Downstream Signalling Cascades VIII

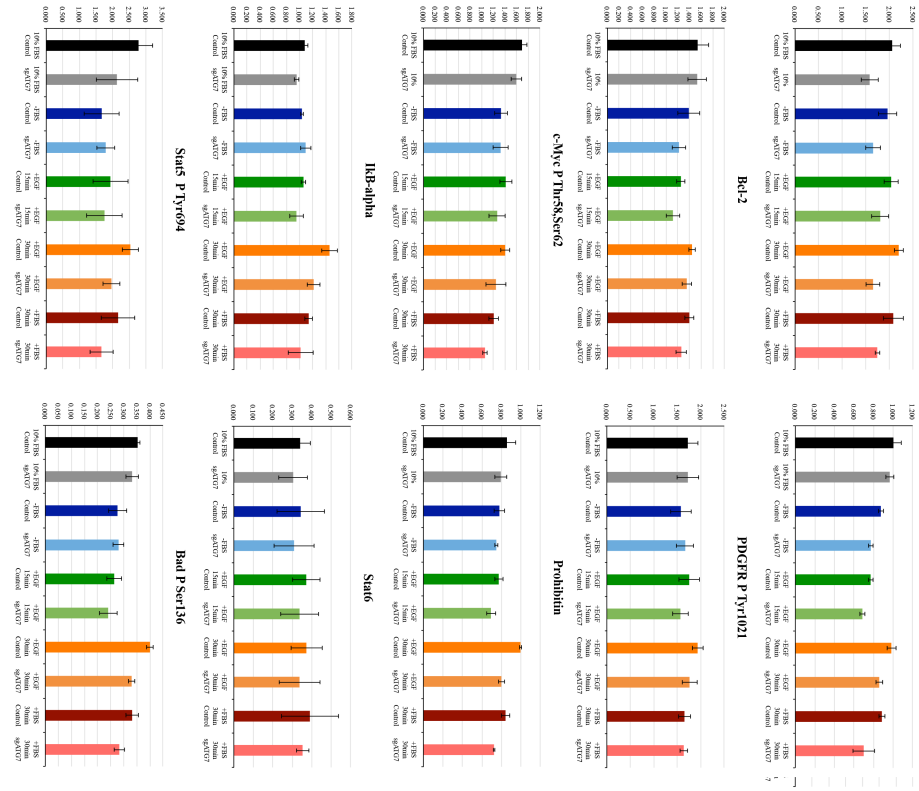

Figure S17.8 Reverse Phase Protein Array Analysis Reveals Atg7 Loss Reduces the Activity of EGFR Downstream Signalling Cascades IX

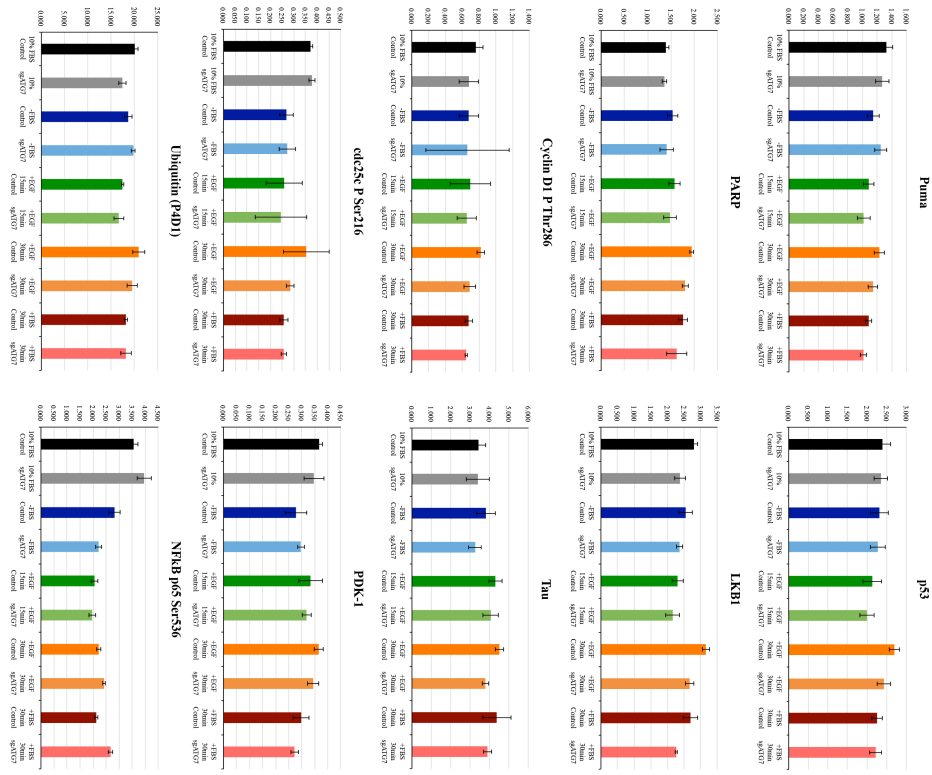

Figure S17.9 Reverse Phase Protein Array Analysis Reveals Atg7 Loss Reduces the Activity of EGFR Downstream Signalling Cascades X.

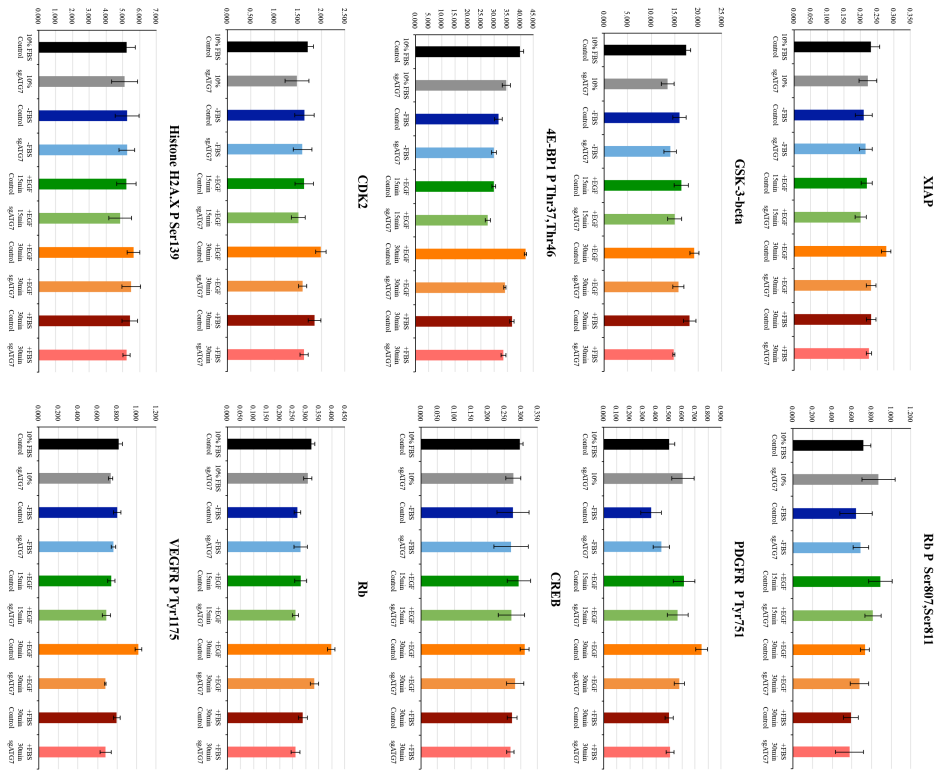

Figure S17.10 Reverse Phase Protein Array Analysis Reveals Atg7 Loss Reduces the Activity of EGFR Downstream Signalling Cascades XI

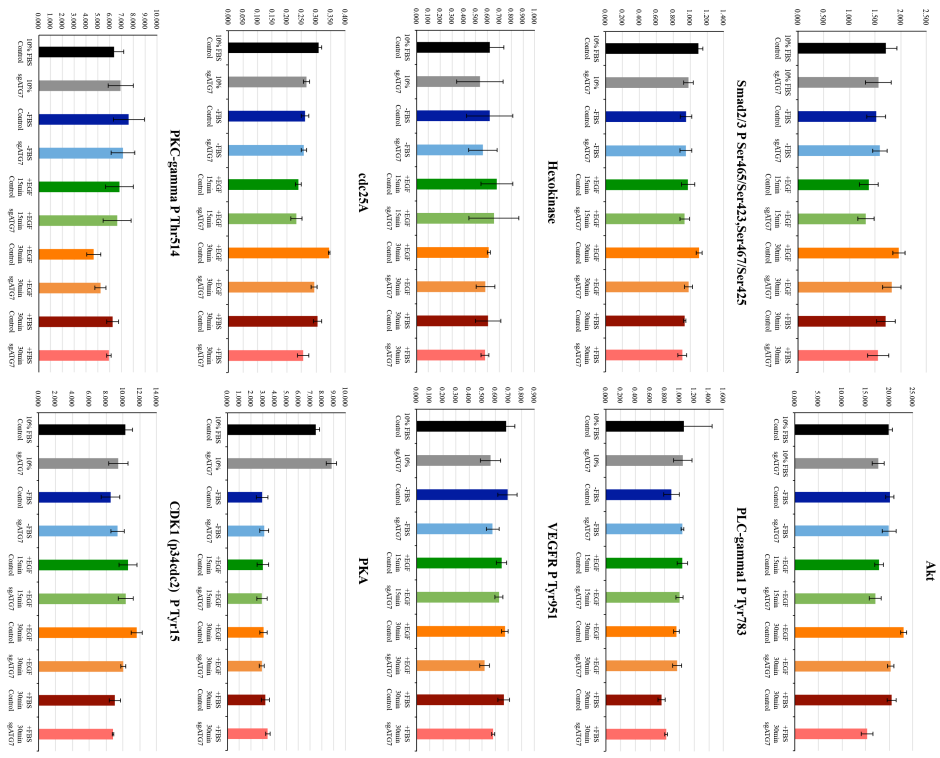

Figure S17.11 Reverse Phase Protein Array Analysis Reveals Atg7 Loss Reduces the Activity of EGFR Downstream Signalling Cascades XII

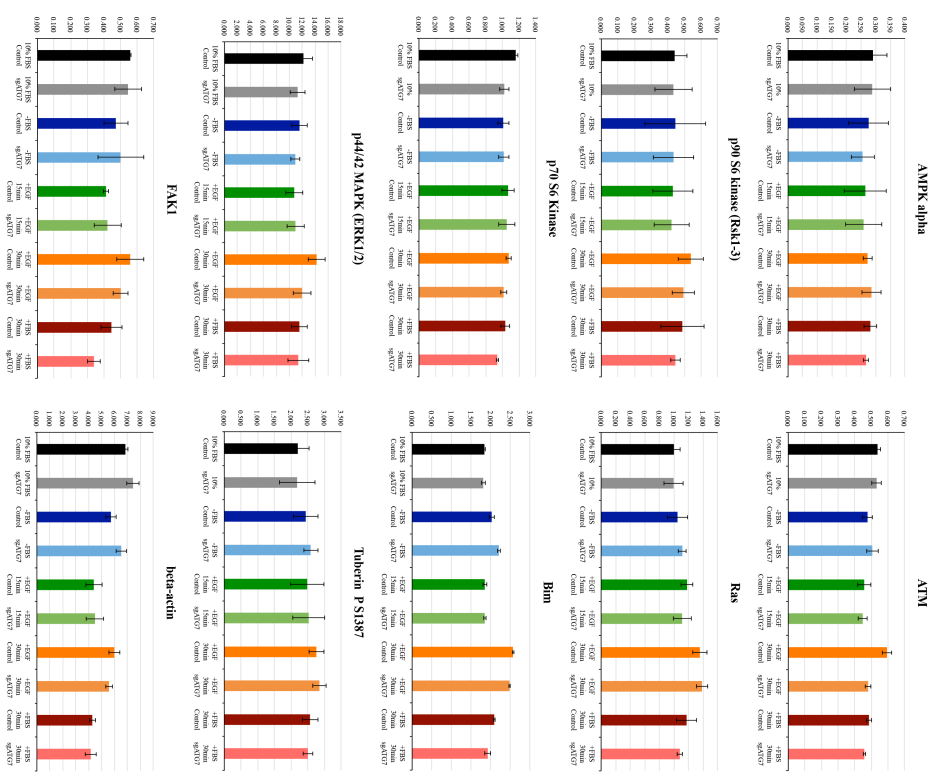

Figure S17.12 Reverse Phase Protein Array Analysis Reveals Atg7 Loss Reduces the Activity of EGFR Downstream Signalling Cascades XIII

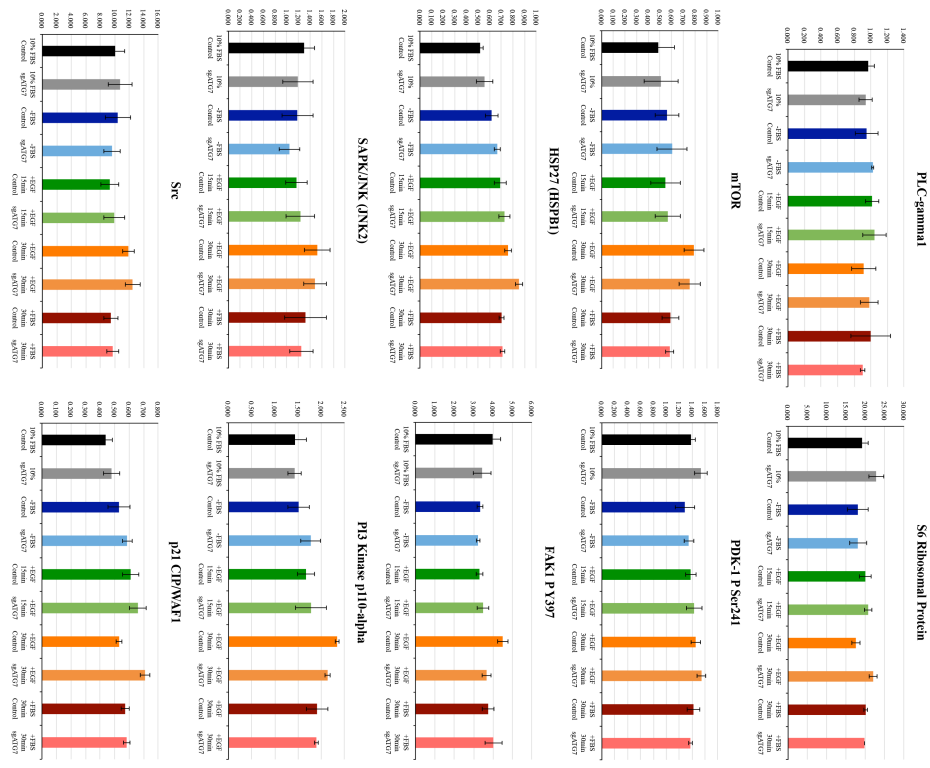

Figure S17.13 Reverse Phase Protein Array Analysis Reveals Atg7 Loss Reduces the Activity of EGFR Downstream Signalling Cascades XIV

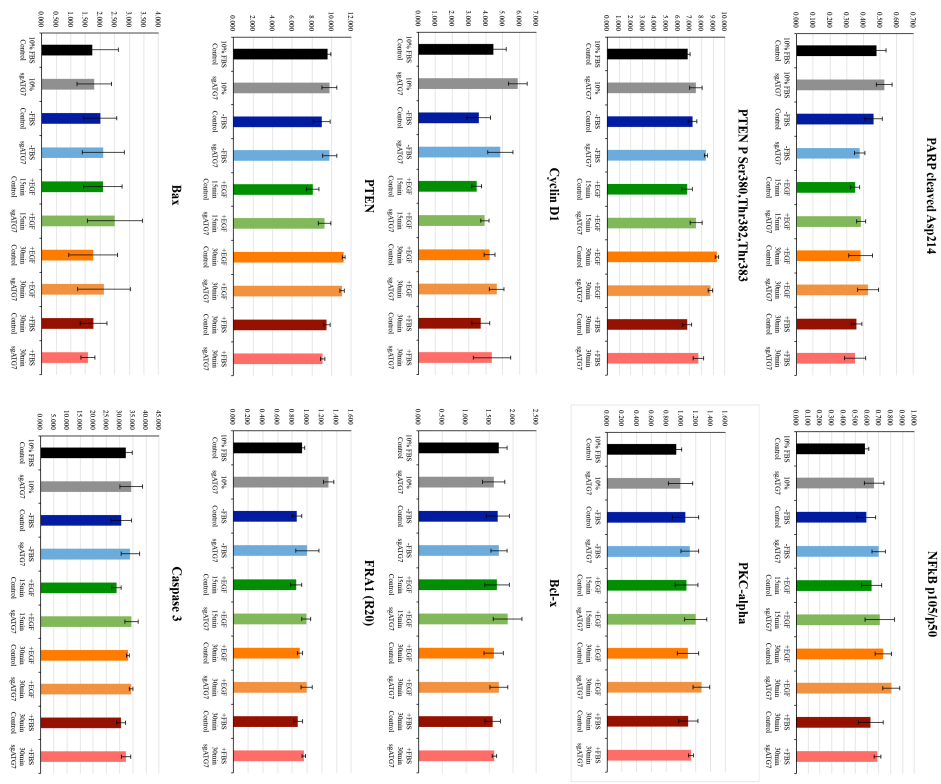

Figure S17.14 Reverse Phase Protein Array Analysis Reveals Atg7 Loss Reduces the Activity of EGFR Downstream Signalling Cascades XV

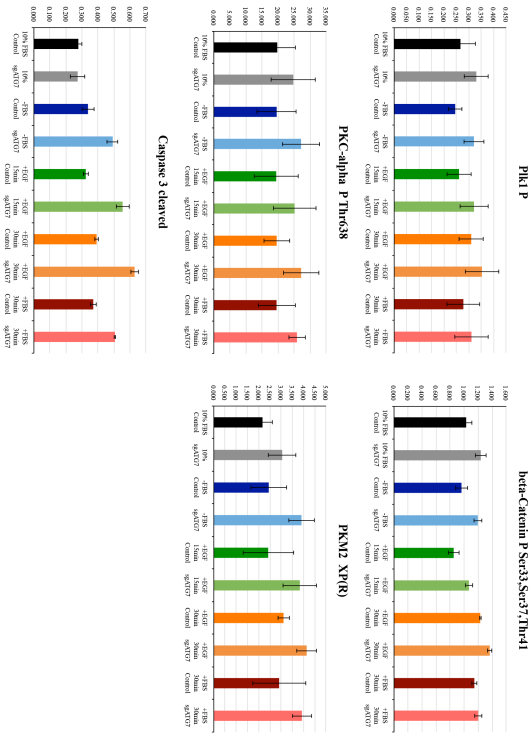

Figure S17.15 Reverse Phase Protein Array Analysis Reveals Atg7 Loss Reduces the Activity of EGFR Downstream Signalling Cascades XVI